LA--11124-PR

DE88 002998

Physics Division Progress Report

January 1, 1984--September 30, 1986

Compiled by
William E. Keller

Los Alamos National Laboratory
Los Alamos, New Mexico 87545

CONTENTS

PHYSICS DIVISION PROGRESS REPORT
January 1, 1984–September 30, 1986

Compiled by

William E. Keller

ABSTRACT

This report provides brief accounts of significant progress in development activities and research results achieved by Physics Division personnel during the period January 1, 1984, through September 31, 1986. These efforts are representative of the three main areas of experimental research and development in which the Physics Division serves Los Alamos National Laboratory's and the Nation's needs in defense and basic sciences: 1) defense physics, including the development of diagnostic methods for weapons tests, weapon-related high-energy-density physics, and programs supporting the Strategic Defense Initiative; 2) laser physics and applications, especially to high-density plasmas; and 3) fundamental research in nuclear and particle physics, condensed-matter physics, and biophysics. Throughout the report, emphasis is placed on the design, construction, and application of a variety of advanced, often unique, instruments and instrument systems that maintain the Division's position at the leading edge of research and development in the specific fields germane to its mission. Most of these projects involve close interaction and cooperation with other Laboratory organizations, and many involve the same kind of collaboration with other laboratories. A sampling of experimental systems of particular interest would include the relativistic electron-beam accelerator and its applications to high-energy-density plasmas; pulsed-power facilities; directed energy weapon devices such as free-electron lasers and neutral-particle-beam accelerators; high-intensity ultraviolet and x-ray beam lines at the National Synchrotron Light Source (at Brookhaven National Laboratory); the Aurora KrF ultraviolet laser system for projected use as an inertial fusion driver; an antiproton physics facility at CERN; and several beam developments at the Los Alamos Meson Physics Facility for studying nuclear, condensed-matter, and biological physics, highlighted by progress in establishing the Los Alamos Neutron Scattering Center. After October 1, 1986, a reorganization within the Laboratory resulted in the transfer of laser construction operations out of the Physics Division; nevertheless, the Division retained most of its laser physics activities. Some ramifications of the reorganization are described in this report.

I. INTRODUCTION

The mission of the Physics Division is to generate ideas, knowledge, and technology in critical areas of physics in order to identify and establish a foundation for both current and long-term defense and energy concepts by

- coupling basic and applied physics research in support of national security interests; and
- undertaking research at the forefronts of physics with emphasis on long-term goals, high risks, and multidisciplinary approaches.

The Division's goals are to

- understand the physics of nuclear weapons, inertial fusion, directed energy, and related areas and to develop appropriate resources needed to perform innovative experiments at the frontiers of these areas;
- investigate the basic properties of nuclear interactions, condensed matter, and high-energy-density systems with a view toward identifying new technologies or approaches applicable to new Laboratory directions;
- identify new areas of physics research to which the unique capabilities of the Division may be applied.

The Physics Division pursues its goals by

- establishing and maintaining a scientific environment that promotes creativity, innovation, and technical excellence;
- fostering dialogue within the Division and the physics community, with emphasis on the prompt dissemination and publication of research results, in order to realize the synergistic benefits of our diverse research interests;
- encouraging the professional development of each member of the Division.

This annual report covers the period October 1, 1985, to September 30, 1986, but it also provides information about earlier periods not covered in previous progress reports. Several significant changes in the Division's organization became effective on October 1, 1986. These changes are described at the end of this section. The following are brief summaries of the activities and responsibilities of the organization as constituted during the reporting period. The corresponding organization chart is given in Fig. I-1.

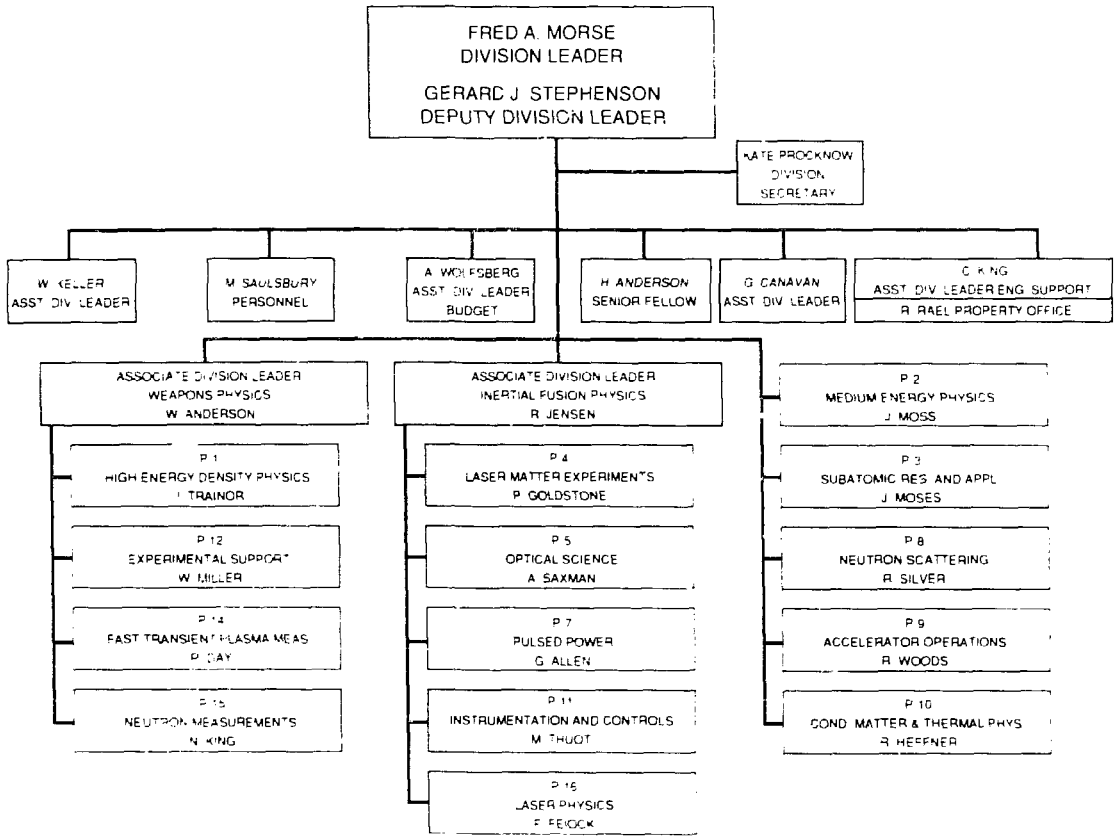

Fig. I-1. Physics Division organization, October 1, 1985-September 30, 1986.

P-1—High-Energy-Density Physics; James Trainor, Group Leader.

This group is responsible for research in high-energy plasma physics. Resources include a very-high-brightness relativistic electron beam, a Z-pinch apparatus, and a capacitor bank used as an energy source for many experiments requiring voltages and currents measured in units of 10^6 volts and amperes. Currently, programmatic efforts include a high-frequency microwave source and opening-switch work for application to large, explosively driven, collapsing cylinders that generate very high-energy plasmas. With P-16, P-1 is developing a high-brightness laser source that now provides 10^{17} W/cm^2 or 5×10^9 V/cm on target for the study of atomic physics in highly stripped ions. The development of the source undertaken this year will increase the laser's power by a factor of 30. In a joint project with P-14 and CLS Division, P-1 is using the source for atomic physics research.

P-2—Medium-Energy Physics; Joel Moss, Group Leader.

Group P-2 conducts experimental research into issues of quantum chromodynamics (QCD). Members of this group are currently using the accelerator beams at the Los Alamos Meson Physics Facility (LAMPF), the European laboratory for particle physics (CERN) in Geneva, Lawrence Berkeley Laboratory (LBL), Brookhaven National Laboratory (BNL), and Fermilab. The fine detector technology they have developed for their research has led to programmatic support of the neutral particle beam strategic defense initiative (SDI) efforts.

P-3—Subatomic and Research Applications; John Moses, Group Leader.

This diverse group is involved in programmatic and basic research in several low-energy nuclear physics arenas. It has a strong capability in reaction cross-section measurement. Much of the work is devoted to reactions below 20 MeV for fusion studies, but these researchers often use the full LAMPF energy of 800 MeV for other studies. A world-class tritium beta-decay experiment aimed at determining the mass of the neutrino has yielded data consistent with zero electron neutrino mass but giving within 98% certainty a mass less than 30 eV. Programmatic efforts range from a high-priority SDI concept to the study of how nuclei can be "pumped" to higher states, in a controlled way, as a primary step in the development of a gamma-ray laser.

P-4—Fusion Experiments and Diagnostics; Philip Goldstone, Group Leader.

Group P-4 is responsible for all experiments performed at the business end of the krypton fluoride (KrF) laser we call Aurora. This laser provides a 5- to 10-kJ pulse in the ultraviolet. Experiments deal with inertial confinement fusion (ICF) capsule performance, hydrodynamics, and some surface studies.

P-5—Optical Science and Engineering (now CLS-8); Albert Saxman, Group Leader.

The common thread in the diverse projects of P-5 is outstanding optics engineering and physics. This group supports laser programs, Department of Defense programs, the ICF program, and a host of others.

P-7—Laser Pulse Power Systems (now CLS-7); Garry Allen, Group Leader.

The pulsed power engineering and research group supports the neutral particle beam effort and the laser ICF program. To a lesser extent, members are involved in the special isotope separation project and in an induction linac design for a heavy ion beam ICF project at LBL.

P-8—Neutron-Scattering Group (now Los Alamos Neutron Scattering Center, or LANSCE); Richard Silver, Group Leader.

Researchers in P-8 are responsible for developing the neutron-scattering facility and the instrumentation for a research program in condensed-matter physics. Working closely with the Accelerator Technology (AT) and Meson Physics (MP) Divisions, the group is responsible for the proton storage ring (PSR), which enhances by many orders of magnitude the neutron flux at P-8's instruments. P-8 works closely with P-9.

P-9—IBF/LANSCE/WNR (now Ion-Beam Facility); Richard Woods, Group Leader.

This group develops, operates, and maintains the two Van de Graaff accelerators at the Ion-Beam Facility (IBF) and the data and beam delivery systems at the Weapons Neutron Research (WNR) and P-8 target facilities at LANSCE.

P-10—Condensed-Matter and Thermal Physics; Robert Heffner, Group Leader.

Group P-10 conducts a variety of studies in solid-state physics, with an emphasis on materials subjected to extreme conditions of temperature and pressure. P-10 delineates the physics of materials exhibiting competition, at the ground state, among such phenomena as superconductivity, various types of magnetic order, and spin- and charge-density waves. Of particular interest is a class of materials called heavy fermion compounds, which display complex behavior at the ground state. Other large efforts are devoted to the study of novel heat engines and of nonlinear phenomena in model hydrodynamic systems.

P-11—Laser Instrumentation and Controls (now AT-8).

This group, whose specialty is control engineering, was transferred to AT Division early in FY86.

P-12—Mechanical Engineering (now MEE-12); Bill Miller, Group Leader.

P-12 provides mechanical engineering support for the Division and for projects elsewhere in the Laboratory. Primarily, the group supports ICF, neutral particle beam (NPB), and Nevada Test Site (NTS) experiments. Members of this group have developed considerable expertise at using and applying computer-aided design systems.

P-14—Fast Transient Plasma Measurements; Robert Day, Group Leader.

High-speed measurements of gamma and x-ray fluence and spectra on weapon experiments at NTS are the specialty of this group. P-14 is also developing a strong research capability in atomic physics, principally at the Brookhaven National Synchrotron light source, and contributes substantially to the SDI programs.

P-15—Neutron Measurement; Nicholas King, Group Leader.

This group shares responsibility with P-14 for measurements and experiments at NTS. Here, the emphasis is on measurements of neutron fluence and spectra and imaging of laser beam geometries. P-15 also participates in the SDI effort. Studies in reaction nuclear physics and antiproton physics dominate the group's research interests.

P-16—Laser Physics and Applications (now CLS-9); Frank Feiock, Group Leader.

The primary mission of this laser science group is to conduct research aimed at gaining an understanding of the kinetics of gas lasers, amplifier physics, and optics/gain issues. Members are principally involved in SDI projects, in the development of the KrF laser for ICF, and in the development of the KrF bright source.

P-DO—Physics Division Office; Fred Morse, Division Leader.

The administrative functions of the Division Office are shown in Fig. I-1. Some research is carried out in P-DO owing to lack of a group home for fledgling projects. A biophysics program is one such effort.

Changes in the organization of the Division were effective on October 1, 1986. Groups P-5, P-7, and P-16 joined other laser groups to form a new Chemistry and Laser Science Division. The only remnant of the ICF program in the Physics Division is in P-4, where the group is using the laser for experiments in basic physics. This group's charter has been formally expanded to enable members to do weapon physics as well as ICF target physics with the Aurora laser beam and to propose other physics experiments for which Aurora would be appropriate.

A second change, but within the division, combined the support efforts of Groups P-9 and P-8 at the neutron-scattering center. The resulting entity was named the Los Alamos Neutron Scattering Center. Roger Pynn will be the director of LANSCE.

A third change was the transfer of researchers from the Materials Science and Technology (MST) Division to Group P-10. This welcome addition significantly strengthened our capability in condensed-matter physics research.

Finally, Group P-12 has joined a new division called Mechanical and Electrical Engineering.

The organization of the Physics Division as it appeared just after the period covered in this report is shown in Fig. I-2.

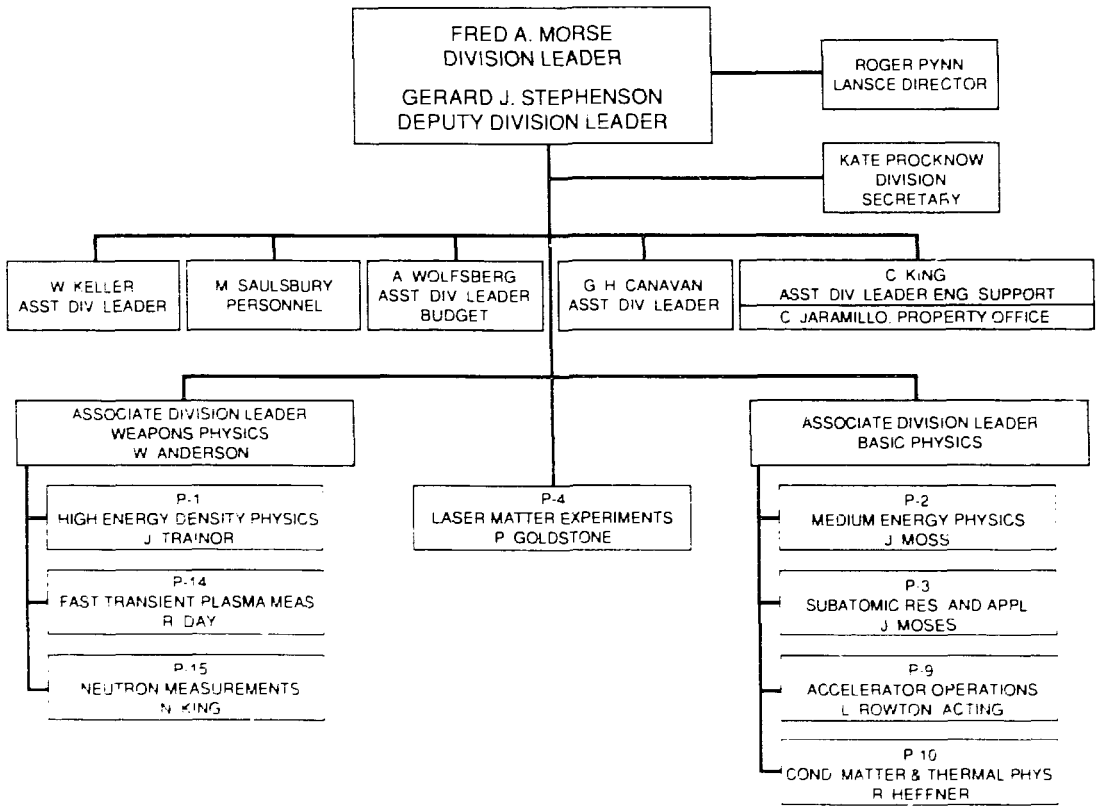

Fig. I-2. Physics Division organization as of October 1, 1986.

II. WEAPONS PHYSICS

INTRODUCTION

The Weapons Physics groups are responsible for the prompt measurement of the characteristics and performance of nuclear weapon test devices at NTS, for conducting experiments in new weapons concepts, and for making fundamental weapons physics measurements. The expertise in these groups is also applied to the exploration of physics problems in other pure fusion programs. Experimental tasks are characterized by high-speed measurements of high-power systems: characteristic times are 0.1 ns to 10 ms, and characteristic energies range from megajoules to many terajoules. The experiments require spectrally, temporally, and spatially resolved measurements of x rays, gamma rays, and neutrons.

Tests in the past year addressed both fundamental physics and weapons physics issues. In a collaborative effort with X Division, for example, we designed an experiment to measure the scattering length of the neutron-neutron interaction. The unique experimental capabilities of P-15 and the high neutron intensities obtained from underground nuclear tests made such a measurement feasible.

Electro-optic techniques continue to have an important and growing application in our weapons diagnostic effort. We routinely use fiber-optic strands in complex experiments performed on underground weapons tests. Glass fibers are used as high-frequency signal conductors and, in bundles, as optical image transfer systems for high-energy-resolution, time-resolved x-ray and gamma-ray spectroscopy.

Our unique measurement capabilities continue to be applied to other programs, such as the Laboratory's inertial-confinement-fusion program and the neutral-particle-beam diagnostic efforts.

DEVELOPMENT OF WEAPONS TEST DIAGNOSTICS

Electro-Optics Research and Development (P-15)

High-resolution imaging—spectral, temporal, and spatial—of x-ray, γ-ray, and neutron sources is essential to the acquisition of meaningful weapon diagnostic data. Electro-optic techniques, involving fiber-optic arrays, streak cameras, optical shutters, and various other imaging devices, are continually being improved to meet the vigorous demands of weapon device testing. Some important recent efforts toward satisfying those needs are summarized in this section.

Radiation Effects on Video Images. Because video images from new silicon-based television (TV) images used on several PINEX events have been contaminated with radiation-induced random speckling (stars) or background buildup, we have conducted experiments 1) to compare the relative radiation sensitivities of several TV images with Sb_2S_3 vidicons (our standard diagnostic for radiation imaging experiments) to determine whether any one offers greater radiation immunity than the others, with equal or better sensitivity to visible light; 2) to identify reaction thresholds for given sensor types in order to specify shielding; and 3) to understand the physics involved when pixel excitation occurs.

Imagers tested included the following:

1. vidicon-type sensors with the following target materials: Sb_2S_3 photoconductors I, II, and IV; silicon diode matrix; saticon (Se + Te + As); Newvicon (ZnSe); Pasecon (CdSe); Plumbicon; and Leddicon (PbO);
2. silicon-based solid-state arrays including charge-coupled devices (CCDs), charge-injection devices (CIDs), and photodiode arrays (PDAs); and
3. S-20 photoemissive image intensifiers including silicon-intensified-target vidicons (SITVs), proximity-focused microchannel plate tubes (MCPTs), and streak tubes. Where possible, similar samples from different manufacturers were tested to determine typical performances for given targets.

The radiation sources provided fluxes and fluences at levels that generally produced only transient effects, although some semipermanent damage was noted for CCDs. These sources were the following:

1. Continuous fluxes of 1.25-MeV and 662-keV γ-rays from isotopic sources ^{60}Co and ^{137}Cs, respectively. The maximum dose rates available were 77 R/s from ^{60}Co and 0.34 R/s from ^{137}Cs.
2. Bursts of bremsstrahlung photons, 1 to 80 ns in duration (average energies in the 3- to 4-MeV range), produced by bombarding a 0.125-cm-thick tungsten target with 8- to 12-MeV electrons from a linac.
3. A continuous flux of fission neutrons from ^{252}Cf (4×10^7 n/s at the source).
4. Microsecond-duration ($\sim$1 to $\sim$10 μs) bursts of 14-MeV neutrons from a D-T sealed-tube generator with a maximum fluence of $\sim 1.8 \times 10^7$ n/cm^2/pulse.
5. Van de Graaff accelerators producing monoenergetic neutrons in the range of 400 keV to 10 MeV using Li^7 (p,n) and H(T,n) reactions to study Si(n,p) and Si(n,α) reactions in the silicon-based imagers. For neutron energies below 1.3 MeV, dc irradiations were made with maximum fluxes of $\sim 5 \times 10^7$ n/cm^2/s. At higher energies, pulsed irradiations were made with neutron fluences of $\sim 3 \times 10^5$ n/cm^2/pulse, produced by gating the accelerator beam for $\sim$2ms (Fig. II-1).

All sensors show gamma sensitivity. Uniform buildup of background increases linearly with absorbed dose. Most sensitive are the image intensifiers that show a gain behavior for γ-ray flux similar to that for visible light flux, indicating that the dominant γ-ray effect is to cause photoemission from the S-20 photocathode. Reverse-biasing the photocathodes or eliminating the accelerating voltages virtually eliminates γ-induced signal. For nonintensified images, CCDs are most sensitive and Sb_2S_3 vidicons are least sensitive. A dose rate of $\sim$54 R/s produces signal-to-noise ratios (S/N) of 93/1, 65/1, 50/1, and 1.5/1 from SITVs, MCPTs, CCDs, and Sb_2S_3 vidicons, respectively. Some Sb_2S_3 vidicons are even less sensitive, producing an unmeasurable signal at 77 rads/s.

The expected number of individual interactions from silicon neutron cross-section calculations agrees well (within experimental accuracy and limited statistics available) with observed counts of affected pixels for all silicon imagers. Again, CCDs are the most sensitive imagers ($\geq$1135 interactions from 4.5×10^6 n/cm^2).

Characterization of New Focus-Projection-Scan (FPS) Vidicons for PINEX Imaging Applications. The possibility of losing our main source of FPS vidicons, General Electric Co. (GE), as a consequence of the proposed merger of GE and RCA Corporation, prompted us to investigate and develop alternative FPS vidicon sources. Several domestic and foreign manufacturers were funded to develop prototype FPS vidicons with targets similar to those available from GE and with alternative targets. Our primary interest was to find an alternative manufacturer for type 7803 Sb_2S_3 vidicons. A secondary interest was to identify targets with superior electro-optic performance and equal or improved radiation immunity.

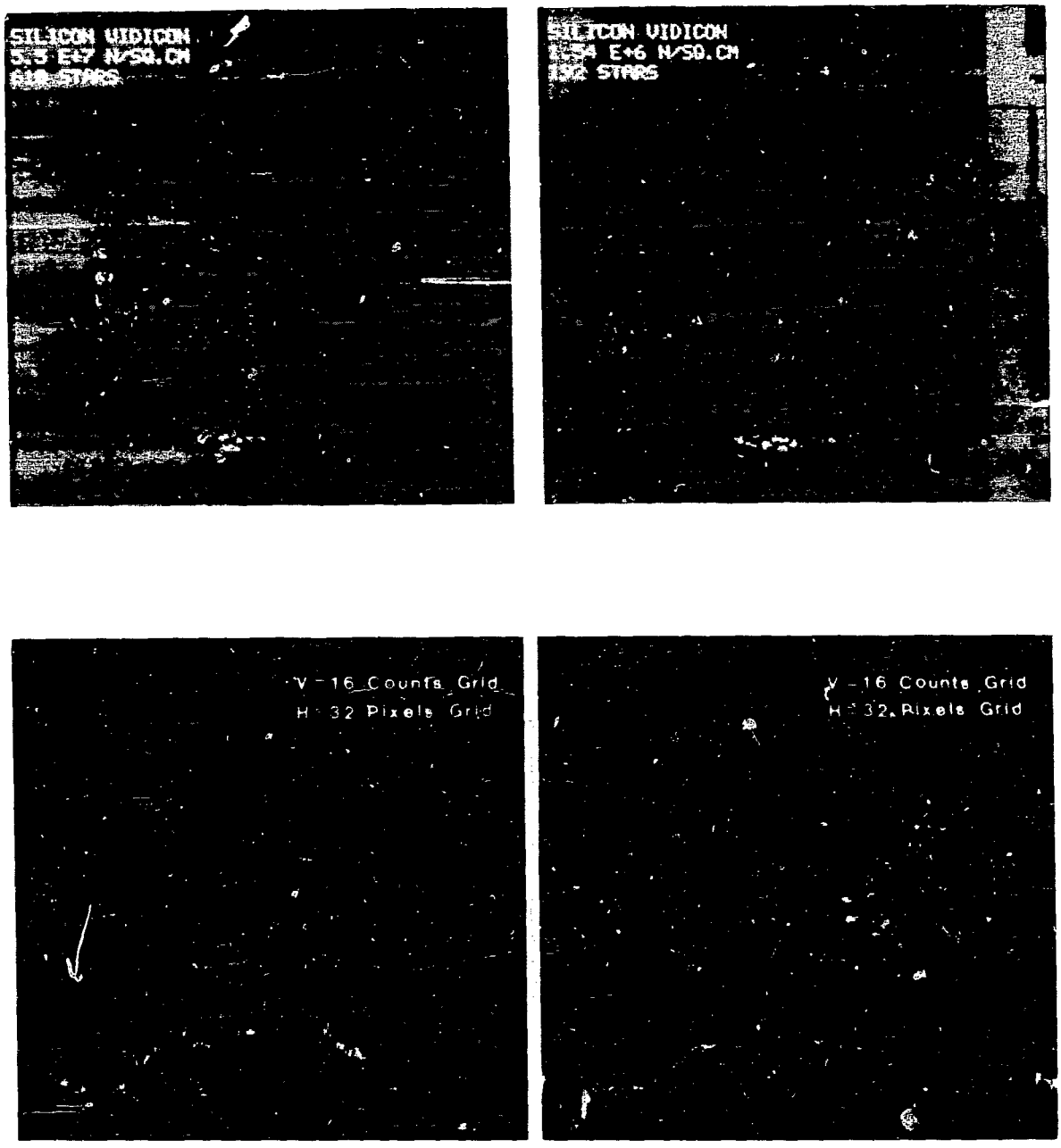

Fig. II-1. Neutron-induced stars in silicon vidicon at two dose levels. Note that background is unaffected at these doses.

For all tests of FPS tubes we used a single-field, fast-readout TV camera (Xedar Model XS-503) with 256 active scanlines in 3.2 ms. We employed only pulsed light sources (100 ps to 5 μs full width at half maximum [FWHM]) at selected wavelengths to determine transient responses to spectra used in field applications. These sources included NE-102 fluors with peak emission at 430 nm and P-20 phosphors with a 560-nm peak.

Target selection included Sb_2S_3, silicon, and saticon from Thomson-CSF; Sb_2S_3 and silicon from English Electric Valve; Sb_2S_3 and Pasecon from Heimann-MII; and Sb_2S_3, Newvicon, and Plumbicon from Amperex. We characterized the photoconductive lag and spectral responsivity of several vidicons from each manufacturer and found that both Amperex and Thomson-CSF produce Sb_2S_3 vidicons whose performance in these areas is equal to that of the GE vidicons.

For the targets, PbO photoconductors appear to be the best choice, inasmuch as they exhibit higher quantum efficiency and faster response time than do Sb_2S_3 photoconductors. Newvicon targets also performed well, but they are not available in fiber-optic versions required for coupling to image intensifiers.

High-Gain Silicon Target Streak Tube with High-Speed, High-Resolution FPS Vidicon Readout. Higher gain and resolution than can be obtained with standard streak-tube systems are required for Nevada Test Site diagnostics. To meet both requirements we have designed a prototype streak tube, incorporating the streak and readout functions in one envelope and thereby minimizing photon-to-charge transformations as well as eliminating external coupling losses. The design includes an SITV tube with streak plates and an FPS TV readout (Fig. II-2). Demagnifying electron optics (m = 0.63) in the image section map the 40-mm-diameter photocathode image on a 25-mm-diameter silicon target, where gains $\geq 10^3$ are achieved with an accelerating voltage of only 10 kV. This value is compared with the much lower gains (~50) at much higher voltages (~30 kV) reported for streak tubes with phosphor screens. The high spatial resolution (~30 lp/mm), variable scan formats, and high-speed electrostatic deflection (250-mm^2 areas are routinely rastered with 256 scan lines in 1.6 ms) available from the FPS readout add versatility. In addition, the nearly instantaneous response of silicon is a considerable improvement over the exponentially decaying persistence for the transient illumination characteristic of the phosphor.

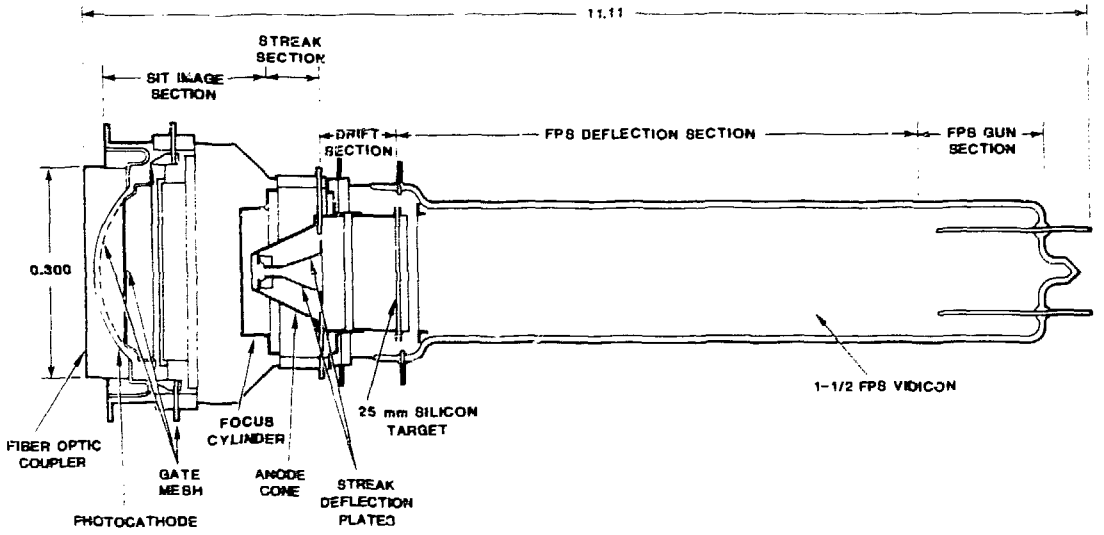

Fig. II-2. Cross-section drawing of SITV streak tube.

Preliminary data show that the new tube has static limiting spatial resolution in excess of 800 TV lines/picture height.

Stripline Microchannel Plate Intensifier Shutters for Subnanosecond Gating Applications. The need for optical shutters with speeds in the 700-ps to 1.5-ns range for time-resolved PINEX (TRP) measurements motivated us to design a stripline version of the standard night-vision goggle design (gate speeds of 2.5 to 5 ns) currently used in weapons testing diagnostics.

Because gating times of microchannel plates (MCPs) are proportional to the product of the photocathode sheet resistance and the gate (photocathode-to-microchannel plate gap) capacitance, gate speeds were improved by using nickel undercoating instead of the chromium normally used. The nickel provided ~94 Ω/sq at 50% transmission compared with 10^3 Ω/sq for the chromium. A second modification involved doubling the photocathode-to-microchannel plate gap at the perimeter to reduce the total input gate capacitance from a typical value of ~33 pf to ~22 pf. The center gap remains fixed at ~0.021 cm (~10 pf) as required for proximity focusing between the photocathode and the MCP. The reduced perimeter capacitance requires less charge from the gate pulse, resulting in a more efficient interface to the external gate pulse generators.

A final modification introduced wide tabs to the photocathode and the MCP input and output perimeters, as opposed to the normal wire lead connections used in the standard MCPT. This modification improves the high-frequency performance of the MCPT. In one of the new MCPTs, tabs are introduced on two sides of the MCPT (180° apart), one for the gate input and the other for the output termination. On another, three tabs are introduced (120° apart) to enable us to experiment with dual gate inputs while terminating the third tab position. Gate boards were developed for each of the MCPTs to impedance-match them for the inherent photocathode impedance of ~12.5 Ω to a 50-Ω gate generator system. The impedance matching is incorporated in the stripline geometry of the gate boards.

Gate speeds of 500 ps have been measured for the two-tab stripline design. Distributed rather than bulk properties were observed with lateral rather than radial propagation of the gate-voltage wave form, as shown in Fig. II-3. For this design, when driven in nonstripline configuration, the tubes show non-irising during turn-on (irising is typical for the nonstripline MCPTs); but they also do not show lateral propagation. Instead, they uniformly turn on early over the total photocathode area.

Prototypes from ITT and Philips (represented by Amperex Corp. in the U.S.) have been successfully fabricated and tested. This design has now been finalized for use in TRPs in weapon tests. Several units have been field-tested on two PINEX events.

Ultraviolet TV Camera for Hydrogen Flame Detection. National Aeronautics and Space Administration (NASA) officials at Cape Kennedy asked us to develop a TV system capable of detecting the invisible fires from hydrogen burning in the atmosphere. (Apparently, hydrogen fires associated with fuel leaks in NASA's space shuttle have gone undetected until materials that burn with the emission of visible light are ignited.) NASA first approached industry (GE and ITT Corp.), but was referred to us because of our expertise in using ultraviolet (UV) imaging for recording Cerenkov radiation.

After measuring the spectral emission from hydrogen burning in the atmosphere, both at Los Alamos and at sea level at Cape Kennedy, we decided to use the 310-nm line instead of the infrared (IR) lines because other IR sources, such as heat, could be present during shuttle launch phases. Because of the high concentration of UV light from ambient atmospheric conditions, we selected two narrow-band filters centered on the hydrogen 310-nm line and used quartz-faceplate MCPT intensifiers to provide gain for the attenuated flame signal. We employed background subtraction to further enhance the flame's image.

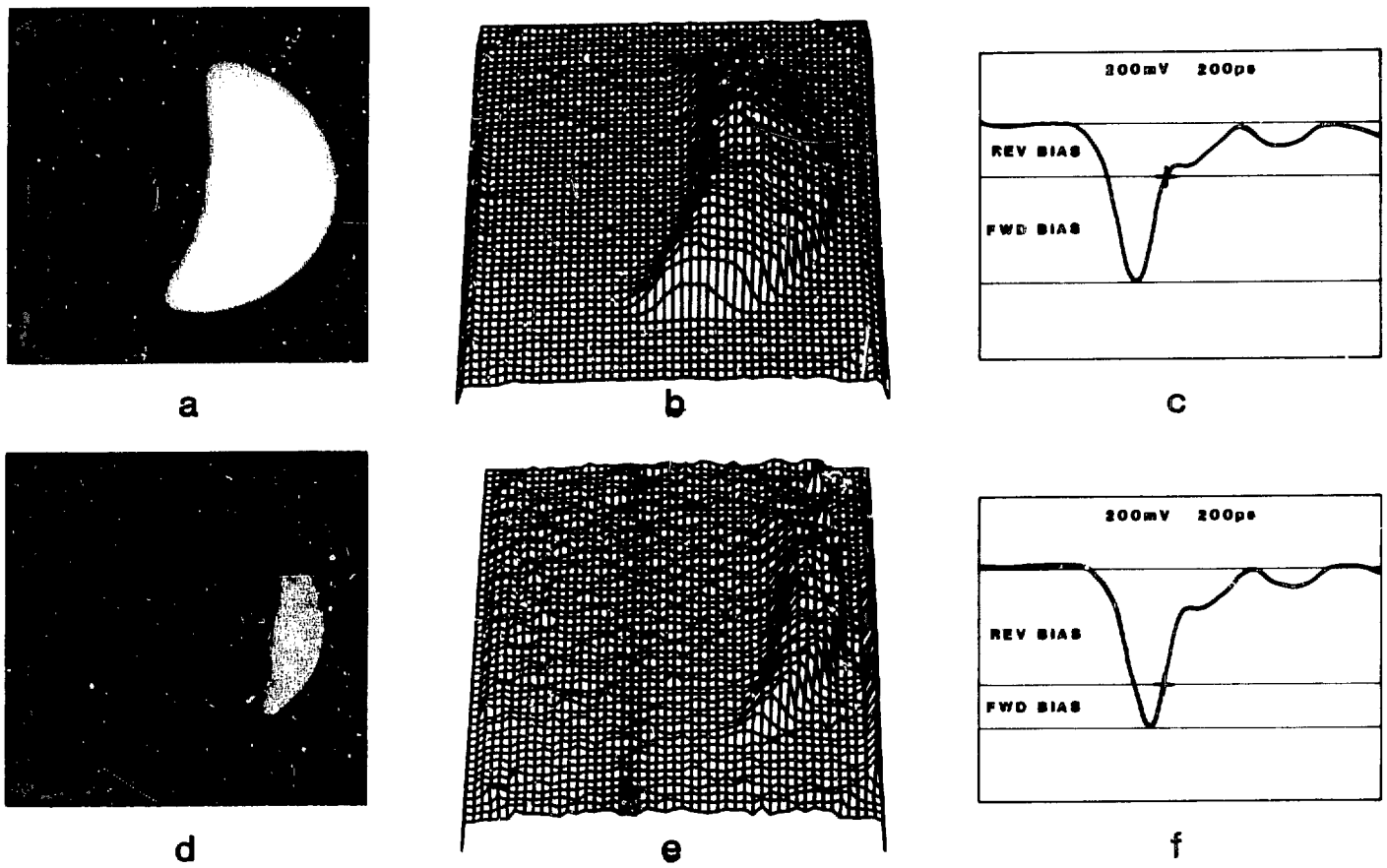

Fig. II-3. Gate performance for 2-tab MCPT at two reverse-bias voltages. The gate pulse, injected at the left, sequentially gates the photocathode as it propagates across the surface. Gating occurs at cross-hairs marked on c and f.

We demonstrated the system at Cape Kennedy to NASA and subcontractors. Earlier plans to use the prototype system on a shuttle launch were delayed by the Challenger disaster. We now plan to compare the UV system with an IR system developed by a private corporation (Xybion of San Diego) for use on military shuttles.

Forge: A Short-Pulse X-Ray Diagnostic Development Facility (P-14)

A new short-pulse x-ray calibration facility has been brought on line at Los Alamos to provide efficient and convenient dynamic characterizations of fast x-ray detectors. Static sources are generally inadequate for evaluating the dynamic performance of streak cameras, framing cameras, and other fast detectors. Important dynamic streak camera parameters to be determined include sweep linearity, spatial resolution, temporal resolution, range, distortion, and spectral sensitivity.

The Forge facility is used to characterize and improve x-ray streak camera designs, to develop and test fast framing camera concepts, and to provide first-order calibrations of the spectral sensitivity of x-ray detectors. Forge will also serve as a test bed for diagnostic systems consisting of x-ray optic elements coupled to x-ray detectors.

Optimum utility can be obtained from this x-ray source if the x-ray pulses are stable in amplitude, pulse width, and spectral shape and intense enough for low-sensitivity applications. Additional requirements include selectable pulse widths, a high level of system reliability, and a short cycle time (a few minutes) to provide rapid iteration. A real-time image recording and analysis capability enables us to perform iterative measurements efficiently and thus is highly desirable at this type of facility.

The Forge facility was designed to meet these requirements through the use of a high-power, short-pulse Nd:glass laser focused at 10^{13} to 10^{15} W/cm^2 to produce x-ray emitting plasmas. The laser system generates laser pulses of 1.064-μm light; pulse widths of 100 ps to 1 ns can be selected. We use a commercially supplied laser oscillator to generate a highly stable and reliable seed pulse. The laser amplifier chain is spatially filtered and optically relayed for optimum power and ability to focus at the target. The maximum amplifier aperture is 50 mm. The Forge laser now has four main amplifiers. These bring the range of operating energy levels and pulse widths to between 1.5 J in 100 ps and 15 J in 1 ns. Figure II-4 is a schematic drawing of the laser system (operating with only three amplifiers).

For x-ray generation, the oscillator output is passed through the main amplifier chain and then focused on a target. Focal spot diameters of 50 μm are easily achieved. Alternatively, the pulse at the output of the preamplifier may be harmonically converted to 532, 355, or 266 nm. This visible or UV signal may be diverted directly to shorter wavelength detectors. The UV pulse is particularly useful because some x-ray detectors have UV sensitivity.

Target materials are generally metals, such as gold, having high atomic numbers for maximum x-ray emission. Thin-slab geometries are adequate for x-ray pulse generation. Specific target materials may be used to obtain particular spectral emission characteristics.

X-ray detectors, primarily streak cameras, view the target through side ports at a 45° angle to the incident laser beam (Fig. II-4). The chamber vacuum is maintained at $\sim 10^{-6}$ torr, consistent with the high voltage and thin photocathode character of soft x-ray streak cameras. The distance from target to port is 30 cm, although re-entrant diagnostics may be positioned closer to the target.

This pulsed x-ray source facility has been operational since May 1986 and has been used extensively to test and evaluate a variety of x-ray streak cameras and detectors. Typical of the work done is the thorough characterization of the Hadland 540 and the Hamamatsu C1936 soft x-ray streak cameras, with dynamic spatial resolution measured at 5, 8, 10, 12.5, 16, and 20 lp/mm. Image broadening in the temporal direction, as well as a series of shots of increasing intensity to evaluate dynamic range (Fig. II-5), were also recorded.

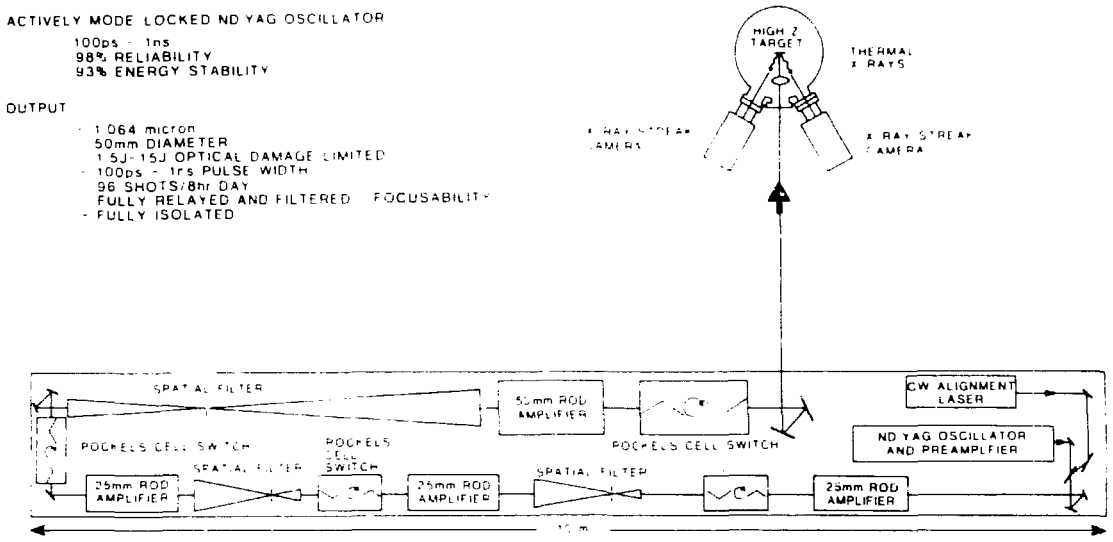

Fig. II-4. The Forge laser schematic layout showing the oscillator/preamp unit, which feeds an optical signal into an amplification chain. The chain of three glass rod amplifiers, Pockels cell switches, and spatial filters increases in aperture to a maximum diameter of 50 mm. The amplified laser pulse is focused on a target in the vacuum chamber to produce a pulse of x rays. X-ray detectors view the x-ray emitting plasma directly.

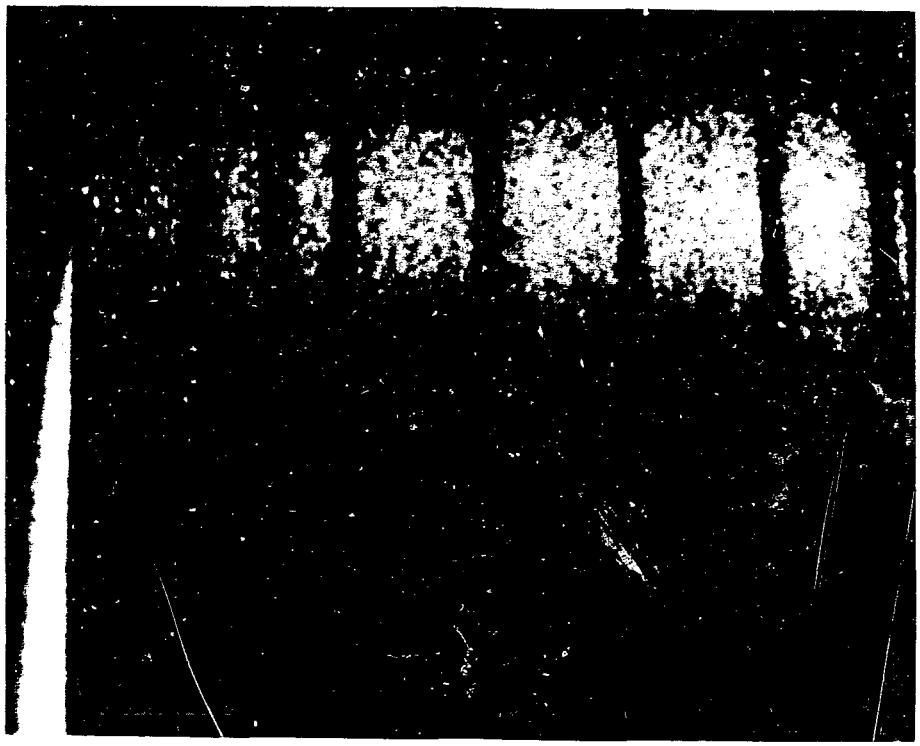

Fig. II-5. Dynamic resolution data from a Hadland x-chron 540 streak camera. In these data, resolution is observed in 15- and 10-lp/mm blocks. Resolution up to 20 lp/mm has been observed. Sweep speed is 100 ps/mm.

Transition Radiation (P-14)

Transition radiation refers to the electromagnetic radiation generated when a charged particle passes through an interface between two different dielectric media. One simple way to visualize this phenomenon is to picture the incident charged particle and its associated image charge as a collapsing/expanding electric dipole, which radiates because of the changing dipole moment. It is useful to remember that at relativistic velocities the radiation is forward-peaked, similar to Cerenkov radiation, and that the intensity peak per unit solid angle, unlike Cerenkov radiation, has γ_R^2 dependence (where γ_R is the usual relativistic factor). These particular properties are attractive for some diagnostic applications.

Within the weapons diagnostic program, the measurement of the γ-ray history and energy spectrum is considered to be of fundamental importance to our understanding of weapon physics and essential to the design and development of modern weapons. Over the last four years, a concerted effort has been made to develop new diagnostic techniques for determining the high-energy γ-ray spectrum, particularly the measurement of the 16.7-MeV D-T fusion gammas. This effort has centered primarily on analyses of electrons produced by gamma-to-electron conversion in thin metallic foils, either by conventional electron magnetic spectroscopy or by measurements of the Cerenkov light produced by these relativistic conversion electrons within a gas Cerenkov detector (GCD). Although we have demonstrated that a GCD can monitor D-T fusion burn and provide a certain degree of spatial imaging capability, transition radiation techniques show promise of providing diagnostic capabilities that could surpass, or at the very least complement, our current GCD capabilities.

In order to assess whether transition radiation could provide a useful diagnostic capability, we performed an experiment at the EG&G Santa Barbara Electron Linac. Our primary purpose was to determine the degree of difficulty of observing transition radiation under relatively ideal conditions and to look for the characteristic signatures of transition radiation. The signatures investigated included dependence of peak intensity on beam energy, dependence of angle of peak intensity production on beam energy, and polarization and variation with wavelength of the light produced. In our experiment, an electron beam of variable energy produced transition radiation upon passing through a 400-nm-thick aluminum foil deposited on a 5-μm layer of cellulose nitrate. The transition radiation was focused on the photocathode of a streak tube, whose response was observed on a video screen, digitized, and recorded for future data analyses.

To test the dependence of peak intensity and angle of peak intensity production on beam energy, we varied the electron energy and determined the peak intensity observed with the streak tube by taking a vertical intensity profile through the center of the annular digitized image. The measured variation of peak intensity with energy is given in Fig. II-6 along with the theoretically predicted variation normalized to the measured value at 15 MeV. Except for the observed value at 28 MeV, the peak intensity variation follows rather well the predicted γ_R^2-dependence on energy.

The measured variation in angle of peak intensity production with energy appears to be consistently a bit higher than the predicted values, although the overall shape is correct. The source of this discrepancy is not known. In addition, several initial measurements of the dependence of transition radiation production on wavelength tentatively, but not definitely, show agreement with the predicted variation.

In spite of the uncertainties mentioned above, the data, considered as a whole, are consistent with the predicted properties of transition radiation produced by an electron beam incident on a metallic foil. We have concluded that transition radiation can provide useful diagnostic capabilities within the weapon program. Experiments planned for the electron linac are aimed at developing a useful diagnostic package.

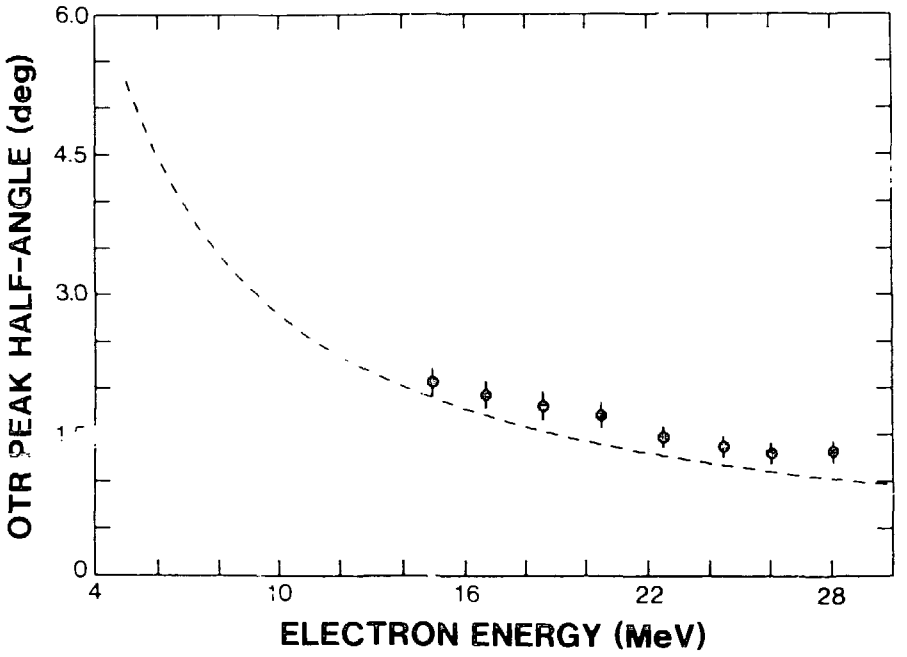

Fig. II-6. Measured and predicted variation of observed transition radiation (OTR) peak intensity with electron-beam energy.

HIGH-ENERGY-DENSITY PHYSICS (WEAPONS-RELATED)

Anomalous Plasma Emission (P-1)

Researchers have tried to understand processes that generate anomalous plasma emission at the plasma frequency ω_p in laboratory and astrophysical sources; for example, anomalous emission at the plasma frequency occurs in type III solar flares. We have devised an experiment to enhance our understanding of the processes that generate anomalous plasma emission. The experiment involved measuring the plasma electromagnetic emission in the infrared with good time resolution and measuring quantitatively the electron energy-distribution function. The nonthermal part of the distribution function creates an anomalous number of plasma waves that eventually convert to electromagnetic radiation. To select one of the possible processes that can convert plasma oscillations to electromagnetic waves, we must measure the nonthermal electron energy-distribution function as well as the anomalous plasma emission at ω_p. We have made a preliminary measurement of infrared emissions from a plasma over a wavelength range of 0.3 to 8 μm. The plasma wavelength in our plasma is $\sim$2 μm. We are also studying the nonthermal or runaway electron population.

The plasma source for this study is a collapsing gas shell Z-pinch, in which a hollow shell of argon, 2.5 cm in diameter and 0.25 cm thick, is injected through a supersonic nozzle across the 0.9-cm gap between the electrodes of a high-voltage power source. The source consists of a 72-kJ Marx capacitor bank that can pulse-charge a 1-Ω water transmission line to a peak voltage of 600 kV. Once peak voltage is reached, a switch between the water line and the gas load overvolts, applying nearly the full voltage across the load. The current flows through the hollow gas shell, causing the shell to ionize and implode. Once the shell collapses to the axis, it stagnates and converts the kinetic

energy acquired during the implosion to thermal energy and photon emissions. The implosion time is 200 ns, and the system reaches a 600-kA peak current at the time of stagnation. The velocity of the shell just before stagnation is 3×10^7 cm/s. The plasma is inertially confined on the z-axis for ~8 ns so that, in a sense, this device is a power amplifier. Kinetic energy, which is built up over a period of 200 ns, is converted to thermal energy and photons in 8 ns, producing a plasma with a temperature of 400 eV and an electron density of $2 \times 10^{20}/\text{cm}^3$.

Spectroscopic examination of the collapsed plasma revealed a nonthermal electron distribution at the time of stagnation. The He-like 2p-1s resonance line had six satellite lines on the low-energy wing, attributable to inner-shell excitation of lower ionization states. Because electrons require an energy exceeding 3 keV to excite these inner shells, and because the ions themselves are formed in a thermal bath of a few hundred electron volts, we concluded that an energetic electron beam was present. Estimates of the runaway electron-beam current made from the absolute intensity of the satellite line gave ~10 kA, which is not unrealistic considering that the plasma channel carries ~600 kA of current at the time of pinch.

We also measured the electron beam permeating the plasma at the time of pinch by mounting a Faraday cup on the symmetry axis of the Z-pinch to detect electrons passing along the axis and through the anode. The energy of the runaway electrons was measured by time-of-flight (TOF), attenuation in various filter materials, and change in TOF after the electrons passed through the filter materials. These measurements indicated that the runaway electron beam had an energy of ~25 keV with a current of ~10 kA.

X-ray streak measurements in the 1-keV range show that the x-ray emission from the pinched column has an unusual time dependence at any given spatial location: it turns on, turns off, and then turns on again. Each of these phases lasts only a few nanoseconds. We modeled this process by using a rate equation to calculate the number of runaway electrons present in the plasma column as a function of time. The fit of the model-predicted emission history is compared with the measured emission in Fig. II-7. This model assumes that the current density in the column, the collapse velocity, the field between the electrodes, and the number of particles per unit plasma length are all

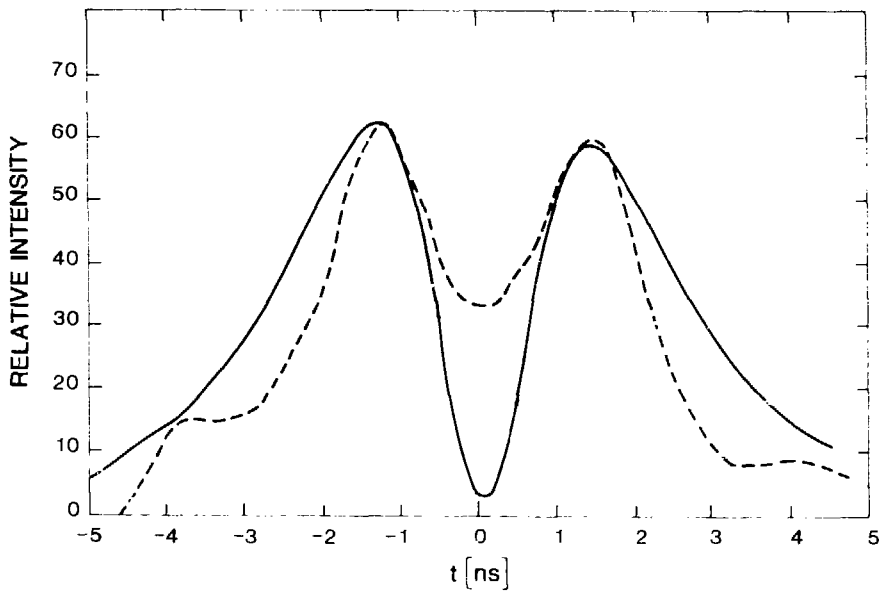

Fig. II-7. Relative intensity of the x-ray emission with energies about 1 keV as a function of time. The dashed curve is measured in the experiment, and the solid curve is predicted by our model.

constants in time. The runaway electrons can be formed only within one gyroradius of the axis, so the kiloelectron-volt x-ray emission region is smaller than the plasma size. A simple visualization of the model shows why two x-ray pulses are produced. As the column compresses, runaway electrons are produced, and there are enough ions so that these high-energy electrons excite some x-ray transitions. As the column pinches down farther, the electron density goes up and the mean-free path of the electrons goes down, thus stopping the runaway electrons and turning off the x-ray emissions. After the plasma reaches maximum compression, the column expands again, favoring the generation of runaway electrons and hard x-ray emission.

We are now making temporally and spatially resolved measurements of plasma emission from the visible through the infrared. Because the beam of nonthermal electrons that permeates the plasma at the time of pinch is so well characterized, a careful measurement of the absolute intensity of light emitted at the plasma frequency should enable us to select the mechanism responsible for the anomalous emission at the plasma frequency.

Experimental Study of Strongly Coupled Plasmas (P-1)

Capillary discharges in tubes with diameters greater than 100 μm have been used by others to produce x rays and to model wall-stabilized Z-pinches for fusion applications. By reducing the initial diameter of the capillary to 20 μm in polyurethane and discharging through it 340 kA of current in 300 ns, we have produced a low-temperature (10 eV), solid-density plasma. Such a plasma is particularly interesting and significant in that it is strongly coupled (nonclassical) and is governed by the same physics that applies to plasmas generated in stars and nuclear weapons. Hence, for the first time we can study directly in the laboratory the equation of state and transport processes of strongly coupled plasmas. In particular, we have been able to measure the electrical resistivity, η, of polyurethane in the low-temperature, solid-density plasma regime.

The capillaries are 2 cm long and 20 μm in diameter in polyurethane (Fig. II-8). The capillary is attached to a Marx bank and water line pulse generator that delivers 340 kA to the capillary in 300 ns. The cathode is pointed to assist in guiding the discharge down the capillary, which is evacuated from the anode side where the pressure is 10^{-5} torr. The evolution of the discharge is monitored by several diagnostic methods: current and voltage probes, axial and radial visible streak cameras, laser schlieren, and a four-channel, axial x-ray diode array.

A well-established ratio technique is used to determine an effective black-body temperature, which is found to vary between 7 and 10 eV for the first 100 ns of the discharge. If we neglect end losses and use particle conservation, we can estimate the density of the plasma. After approximately 10 ns the particle density equals solid density. An estimate of the average ionization of the plasma can be made using a Saha model. In our study, the calculated average ionization was 0.5 for the first 100 ns, yielding an electron and ion density of 5×10^{22} cm^{-3}. Using the experimental values, we noted that this material is near the strongly coupled plasma regime.

A simple model of the evolution of the discharge can be formulated if we assume that the plasma is 1) uniform in temperature and density, 2) ohmically heated, and 3) confined within a boundary defined by the measured radius. In addition, we assume that all of the energy dissipated in the plasma remains in the plasma. Under these restrictions we can determine the temperature at a given time by equating the enthalpy to the ohmic dissipation. The latter is a function of the driving current, the time-dependent volume of the plasma column, and the temperature-dependent electrical resistance, R(T), of the plasma. The classical way of modeling R(T) is through the Spitzer resistivity $\eta = bT^{-3/2}$, where b is a constant. Assuming this form for η probably represents the largest source of error in the model. Nevertheless, the model is a useful starting point for comparison with experimental results. It also serves as a guide for interpreting experimental results by yielding an estimate of the time-dependent temperature of the plasma: the experimentally determined radius-

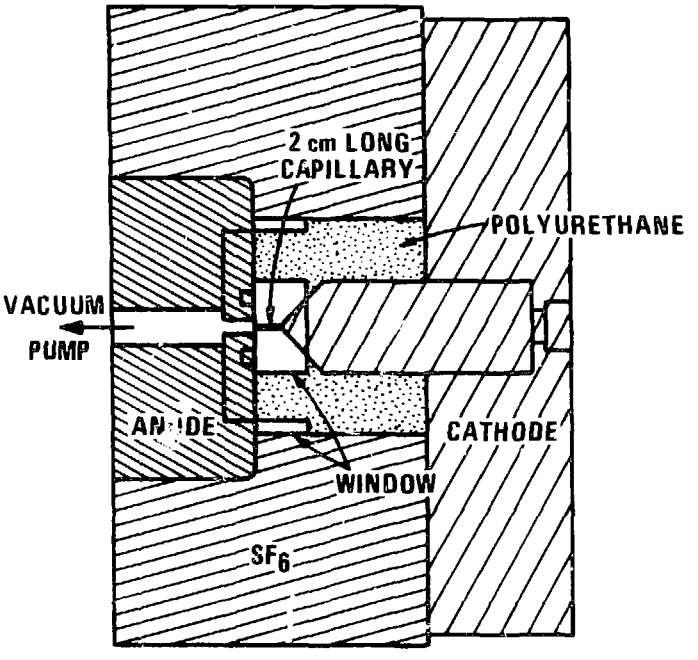

Fig. II-8. The polyurethane capillary and its position in the experiment. The cathode is pointed to guide the discharge down the capillary. The system is evacuated from the anode side to a pressure of 10^{-5} torr. The volume around the polyurethane is filled with SF_6 to improve the voltage holdoff characteristics. Flat windows are machined into the outside of the radial optical diagnostics.

versus-time information is combined with the Spitzer resistivity and a high-temperature plasma model for the enthalpy. In the present case, however, this process underestimated the experimentally determined temperature of the plasma. In an attempt to improve the agreement between the modeled and experimental temperatures, we raised the resistivity by a factor of 80 to force agreement with the data at 60 ns. With this *ad hoc* correction we see excellent agreement between the data and the calculation for late times.

The resistivity of the plasma as a function of time can be calculated from measurements of the voltage, the first derivative of the current, the current itself, the radius of the plasma, and the radius of the return conductor. This technique ignores the effects of velocity-dependent voltages. A plot of resistivity versus time is shown in Fig. II-9, where we note that the calculated resistivity is in qualitative agreement with the resistivity used in the modified model discussed in the preceding paragraph. It is not unreasonable to assume that the resistivity of the plasma under these conditions should exceed the values calculated from Spitzer.

We plan more detailed measurements and improved modeling, especially of the transport coefficients and average ionization of the plasma, to improve our understanding of the physics of near-solid-density, low-temperature, nonclassical plasmas generated in capillary discharges of small initial diameter.

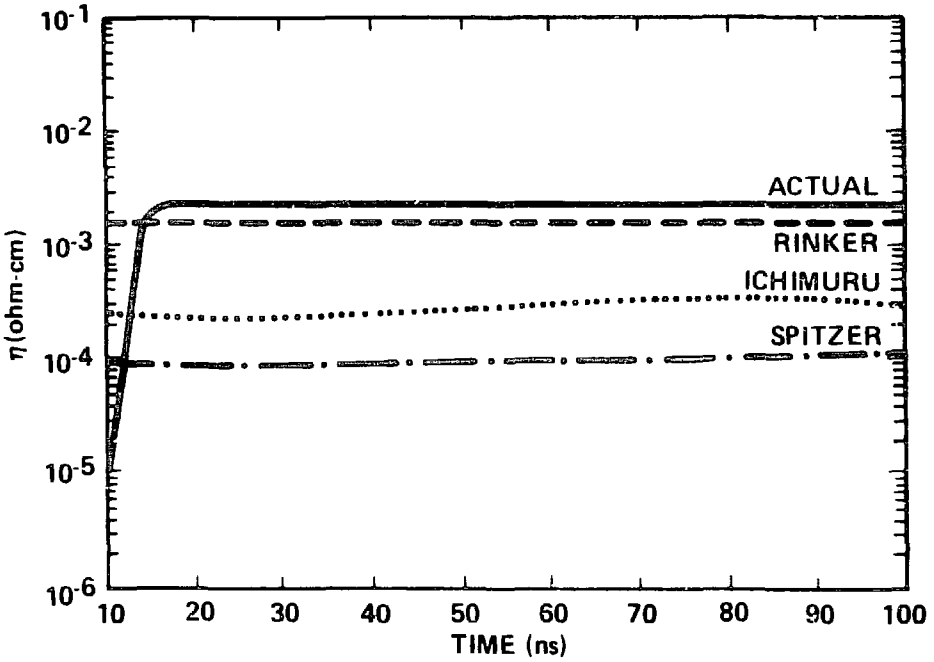

Fig. II-9. A plot of the measured resistivity (η) versus time. The resistivity was determined from the measured current, voltage, and radius. Also included in the plot are Spitzer resistivity (dash-dot line) for these conditions and the resistivity obtained from nonclassical plasma calculations (dashed and dotted lines).

Optical and UV/X-Ray Imaging Diagnostics for Imploding Plasma Experiments (P-1)

The Trailmaster/Pioneer I series of imploding plasma experiments is aimed at using an inductive storage driver to implode an ultrathin aluminum foil with a multimegampere, submicrosecond electrical pulse. The power pulse is produced by an explosive flux-compression generator and a fast plasma-compression opening switch. The goal is to obtain an intense source of soft x rays from the thermalization of the plasma kinetic energy when pinch occurs on axis.

An important diagnostic for these experiments is a fast camera that measures the dynamics of foil run-in and implosion symmetry. These measurements are made in the visible, UV, and x-ray portions of the electromagnetic spectrum by a framing camera. The camera is located 25 to 30 m away from the foil, in an instrumentation bunker, where it is shielded from the harsh environment of the experiment.

Figure II-10 shows how the framing camera is used for visible imaging of the imploding foil. The implosion image is transmitted to two large mirrors (150 to 200 mm in diameter) and to a large catadioptric telescope (275-mm aperture, f/11). A beam splitter assembly splits the beam coming out of the telescope into four parts and steers each onto one of four gated microchannel plates ("4-eyes"). A film pack attached to the 4-eyes camera records the data on hard film. The framing camera system has an overall spatial resolution, limited by the microchannel-plate, of 100 μm at the film. The temporal resolution is limited by the minimum gate open time of 5 ns; the interframe time can be adjusted to any desired value. Both the spatial and the temporal resolutions are sufficient for the present experiments.

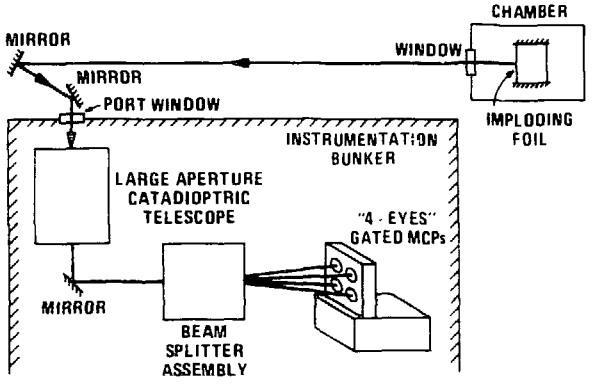

Fig. II-10. Schematic of framing camera used for visible imaging of imploding foil experiments.

To record UV/x-ray images, we first convert them to visible light and then transmit them by visible optics to the framing camera. Hence, there are three versions of the imaging system front-end, all of them disposable because the front end is blown away with each target chamber implosion. For visible imaging, a high-quality window is used on the target chamber. For UV/soft x-ray (3.5 to 100 eV) imaging, the window is replaced by a pinhole camera, appropriately filtered for the desired energy range. A fast fluor (e.g., a p-terphenyl-coated screen) converts the image into the visible and near UV. For harder x-ray imaging, we use the same pinhole camera in place of the window but add an MCP in front of the fast fluor to boost quantum detection efficiency and signal gain. In general, the response time of the fluor is selected to match the response time of the framing camera detectors.

The MCP gives this last arrangement several unique capabilities and advantages:

- Because the MCP is sensitive to x rays up to 10 MeV with a quantum efficiency of about 1%, we can take photographs of very high-energy x-ray emission. The photographs can then be transmitted in visible light, by mirrors, to a location shielded from the energetic x rays.

- MCPs have a fast response time. The temporal dispersion of the electrons is only about 100 ps. If a fast fluor is used, the radiation-to-light converter camera can have a time response of under 200 ps. In this case, a faster version of the 4-eyes camera would be needed to take advantage of the very fast front-end camera.

- Although the front-end camera has a very fast response time, it requires no fast electronics, only dc power supplies. Further, an MCP is relatively inexpensive ($1000 to $2000).

The framing camera is a versatile, efficient, rugged, and cost-effective instrument. The system has performed satisfactorily for every Pioneer I experiment. A unique and important feature of this camera is that the gain of each channel of the 4-eyes can be set independently, and each channel can also be attenuated separately. Thus, the dynamic range of the imaging system is very large and far superior to that of commercially available streak/framing cameras, where the attenuation is the same for all frames. The present framing camera is especially suitable for recording sequences of events in which the brightness changes by many orders of magnitude.

Plasma Heating Experiment at the P-1 Relativistic Electron-Beam Facility (P-1)

The object of this experimental effort is to attain a quantitative understanding of the interaction of a high-brightness electron beam with a dense plasma. Specifically, an experimental environment has been created to cause a nonlinear (two-stream) interaction between the electron beam and an independently produced dense plasma. In the absence of any nonlinear particle wave interactions, the energy coupling between the beam and the plasma is less than 0.1%. Calculations indicate that more than 15% of the beam power may be coupled to the plasma through a nonlinear beam-plasma interaction.

A high-brightness (low-divergence) relativistic beam is required for the production of a significant two-stream interaction. This requirement is a result of momentum and energy conservation in the interaction. At the P-1 Relativistic Electron-Beam Facility (REB), a magnetized foil-less diode can be used to produce a low-divergence electron beam. The experiments were performed with 60 kA of beam current, with an FWHM of 70 ns at a 3-MV Marx generator charge. The magnetic field must extend from the cathode region, where the electron beam is formed, to the interaction region, where the plasma is produced. Therefore, the plasma must be produced inside the magnetic field coil.

The plasma is produced by heating a 1-μm-thick, pure carbon foil with a high-energy (20-J), low-intensity (10^8 W/cm^2) CO_2 laser pulse. The heating produces a plasma in the magnetic field with a temperature of 1 eV and a density of $\sim 6 \times 10^{17}$/cm^3. One of the key aspects of our experiment is that the plasma is produced independently of the electron beam and inside the guiding magnetic field. Figure II-11 shows the experimental geometry.

To measure the amount of electron-beam power that is coupled into the plasma we used two methods: 1) a direct measurement of the temperature of the plasma and 2) a study of changes in the electron beam before and after the interaction. The temperature measurement was made spectroscopically in both the visible and the soft x-ray regions. A temperature measurement alone, however, is not a direct measure of the beam-plasma coupling. The coupling must be inferred

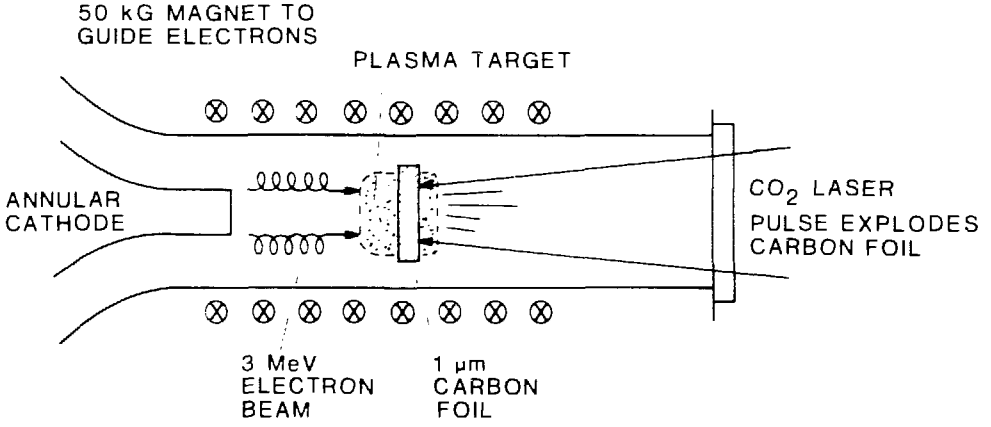

INTERACTION: 3 MeV, 50 kA ELECTRON BEAM WITH COOL, DENSE CARBON LASER-PLASMA

Fig. II-11. An outline of the plasma heating experiment at the P-1 REB machine. The plasma is produced inside the electron beam's guiding magnetic field by exploding a 1-μm-thick carbon foil with a CO_2 laser pulse. The electron beam is discharged into this plasma for all of the interaction experiments.

from an energy-balance model. Two such models are being developed, one a simple radiative balance model and the other a sophisticated magnetohydrodynamic (MHD) model that we are constructing in cooperation with Group T-4. Changes effected by the interaction on the electron beam are measured with beam-current and Faraday-cup monitors placed before the beam enters and after it exits the interaction region. With these diagnostics, we directly estimate the coupling by measurements of the current and electron-energy losses in the interaction. Using these methods, we estimated the peak coupling to be approximately 2% to 3%.

In some of our measurements of the interaction, we intentionally destroyed the nonlinear interaction. We did this either by eliminating the laser beam leaving a solid target for the interaction or by increasing the divergence of the electron beam. The strength of the interaction is dramatically reduced under these conditions.

Our experiments indicate that the interaction of a low-divergence, high-brightness, relativistic electron beam with a dense, cold plasma can result in significant energy coupling to the plasma. This coupling is nonlinear in nature, requiring that a plasma be formed and a low-divergence electron beam be used.

Physics of High-Power Microwave Generation (P-1)

We are using an intense relativistic electron beam to study the physics of microwave generation. In particular, we have investigated devices that exploit the formation of virtual cathodes to produce very high-power microwave radiation. These devices, which have received little attention until recently, have a number of attractive features. They operate at very high electron-beam current because beam propagation is not required, and they use a simple hardware configuration that does not rely on complex slow-wave structures. Before these devices can be used for practical applications, however, the underlying physics of their operation must be better understood.

Virtual cathode formation occurs when an electron beam carries so much current that it cannot fully propagate in the drift region downstream of the diode. The beam transport is inhibited by electric fields from beam space-charge, which allow only part of the current to flow. The remaining portion of the beam is reflected back into the diode region. The reflection point is the position of the virtual cathode. For an axisymmetric beam, the space-charge-limiting current, above which a virtual cathode forms, depends upon the relativistic factor γ, the ratio of wall radius to beam radius, and the shape of the beam.

Two processes have been found to lead to the production of high-power microwaves when the space-charge-limiting current is exceeded. In the first, called the oscillating virtual cathode, or VIRCATOR mechanism, both the amplitude and the position of the virtual cathode oscillate, causing a heavy modulation of the transmitted portion of the beam current (i.e., the virtual cathode acts as a gate, chopping the beam current). This process excites axisymmetric transverse-magnetic waveguide modes. In the second mode of operation, called the reflex mode, the electrons reflex between the real and the virtual cathodes, leading to the formation of coherent bunches of charge. This phase-bunching is similar to the bunching that occurs in a gyrotron and results from the energy-dependence of the electrons' relativistic mass. Again, axisymmetric transverse-magnetic waveguide modes are excited. Generally, both processes are present, but in a given device one may dominate over the other.

We have conducted experiments of two general types: with and without an imposed axial magnetic field. A schematic of the experimental region for the typical magnetized case is shown in Fig. II-12. The beam electrons are emitted from a 6-cm-diameter annular cathode (0.05-cm wall thickness) centered inside an 11.0-cm-diameter housing 1 to 4 cm from the anode. The anode is 1-cm-thick graphite with a 4.5-mm-wide slot. The beam is injected into an 18-cm-diameter waveguide and is guided by an axial magnetic field variable from 0 to 25 kG. For the unmagnetized experiment, we use the same hardware except that a thin foil (highly transparent to beam electrons) replaces

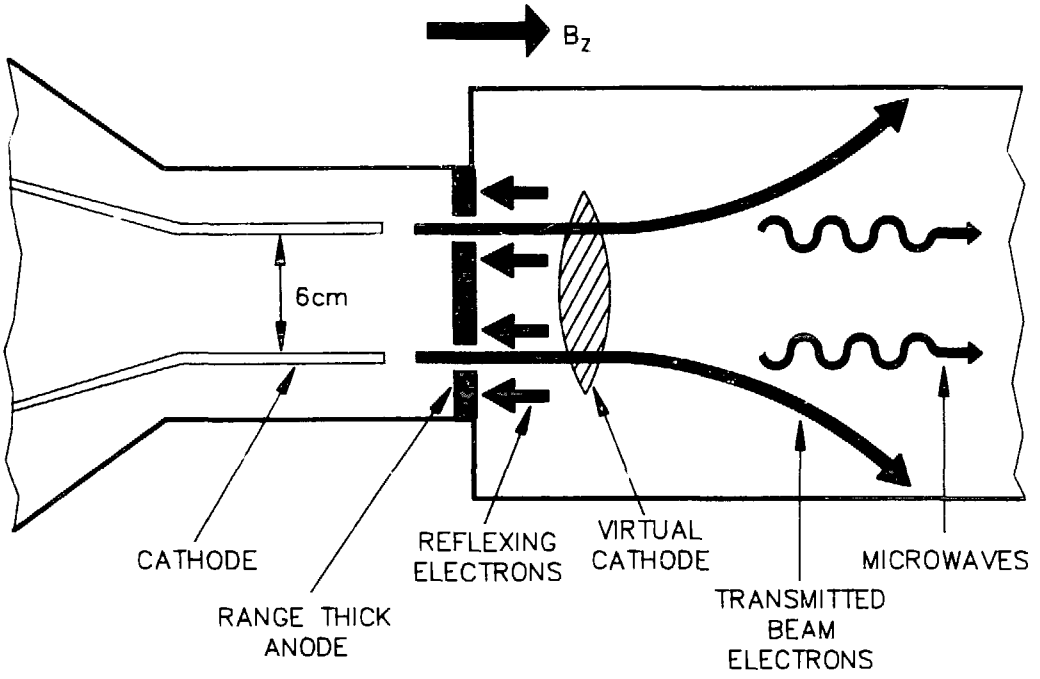

Fig. II-12. Microwave generation by virtual cathode formation; case of applied axial magnetic field (schematic).

the graphite anode. In addition to the annular, we use a variety of cathode shapes, with gap spacings varying from 1 to 2.5 cm. For the magnetized experiments the beam energy ranges from 1.4 to 2.2 MeV, depending on the gap spacing, with currents of 40 to 60 kA. For the unmagnetized experiments the energy varies from 1 to 3 MeV and the currents from 80 to 100 kA.

Microwave measurements are made either by allowing the microwaves to pass from the end of the system into the laboratory, where open-ended sections of rectangular waveguide are used to sample the radiation field, or by terminating the output waveguide with a microwave calorimeter that measures the energy. In the former case, waveguide electric field probes and microwave crystal detectors are used to measure the pulse envelope. Frequency measurements are made with bandpass filters and interferometric techniques.

We have developed a new microwave calorimeter design that overcomes some of the problems associated with other calorimeters. The calorimeter is fabricated from 0.075-mm-diameter stainless steel wires located on the surface of a 1-m-long cone. The wires are oriented to couple efficiently to symmetric transverse-magnetic waveguide modes having radial and axial electric field components. The wires are connected electrically in series so that the absorbed energy can be inferred from the change in resistance of the element after firing. This element has the following advantages: 1) it is highly transparent to debris and particle fluxes (because of its small cross-sectional area) while being a good absorber for microwaves; 2) it has the potential for determining the waveguide mode by imaging the element with an infrared camera; and 3) one need not wait for thermal equilibration to make a measurement because the change in resistance is independent of the absorbed energy distribution (to first order).

In a recently completed set of unmagnetized experiments, we produced 0.5 GW of microwave radiation at 17 GHz and 0.2 GW in the 30- to 40-GHz band. These power levels are as high or higher than the highest reported for these frequencies. We believe that the microwave power was limited by the formation of anode plasma that provided a source of ions to disrupt the virtual

cathode early in the beam pulse. To test this hypothesis, we carried out experiments in a geometry three times larger, which reduced the beam power density by a factor of 9 and significantly delayed the onset of plasma formation at the anode surface. We expected the output power to increase, because peak microwave emission should occur at near-maximum beam power instead of before it. We also expected the microwave frequency to be reduced by a factor of 3. Experiments with this new geometry confirmed most of these expectations. The peak microwave emission occurred at close to maximum beam power rather than before it as previously, and we measured a substantial increase in microwave power over that observed with the smaller geometry. Also, the frequency decreased by a factor of 3 as anticipated. Using a cathode consisting of several concentric rings, we produced power levels in the range from 3 to 5 GW at 5.8 GHz. The maximum energy per pulse was on the order of 180 J.

For the magnetized experiments, an axial magnetic field is used to guide the beam through the slot in the anode. Because the injected current is above the space-charge limit, a virtual cathode forms downstream of the anode. The oscillatory fields of the virtual cathode are expected to impart transverse momentum to the reflected electrons so that many of them are intercepted by the anode and prevented from reentering the diode region. The reflex radiation process is thereby eliminated, and the device operates exclusively in the VIRCATOR mode. Computer calculations made in Group X-10 indicate that this configuration has the potential for providing a more monochromatic, more efficient, single-waveguide-mode output.

In initial experiments with the magnetized device, in which the anode-to-cathode gap and the applied magnetic field were varied, the microwave power increased from zero to its peak value as the magnetic field increased from 0 to 5 kG. As the field strength was further increased to 22 kG, the microwave power decreased monotonically. Similar behavior is observed in computer calculations. We believe that for a weak magnetic field, very little beam current is transmitted through the slot, so the output power is low. For a strong magnetic field, the reflexing electrons are so tightly bound to the field lines that they reenter the diode; again, the power output is reduced. Thus, at an intermediate value of the magnetic field the power reaches a maximum. The frequency of the microwaves has been found to be independent of magnetic field as predicted by calculations. For conditions in which we obtain significant microwave power with the thick anode, we observe essentially no power when a thin anode is substituted for the thick anode. This finding indicates that the aperture is intercepting reflected electrons. Also, after many shots the anode shows a discoloration on the output waveguide side that is suggestive of electron impact.

One experimental configuration with a 9.3-kG magnetic field and a 3.7-cm anode-cathode gap was studied in detail. We observed a microwave burst about 30 ns long peaking at about maximum beam power. Measurements of the power density distribution were made, and the dominant waveguide mode was found to be TM_{02}. The inferred peak power level is about 1.4 GW at the dominant frequency of 3.9 GHz, with an additional several hundred megawatts radiated at harmonics.

In future experiments we hope to improve further the power output and efficiency of both the magnetized and the unmagnetized systems and to increase our understanding of the underlying physical processes.

Vacuum Pulse Conditioning and Risetime Sharpening on a Low nu/gamma Multi-MeV Electron-Beam Accelerator (P-1)

We are conducting a program to develop a fast-risetime (0.5 ns $< t_r <$ 10 ns), 100-GW electrical power pulse from a generator that normally supplies pulses of 3 MeV, 70 kA, 50 ns FWHM, with a current risetime (t_r) of about 20 ns at the load. The improvement achieved to date has resulted in a t_r as short as 4 ns (measured from 10% to 90% of the rise).

The work is motivated by two considerations. First, theoretical estimates of the efficiency of microwave production from our accelerator suggest that higher production efficiencies might be

obtained through improved electron coherence. Second, very fast-rising bremsstrahlung radiation experiments can be fielded using the fast-rising electron-beam pulse. In this way, we could simulate the radiation burst of a nuclear explosive in a laboratory environment.

During this project, we carried out design studies and experiments on power conditioning and pulse sharpening in the vacuum transmission line of the P-1 REB accelerator. Two approaches were undertaken: magnetically insulated transmission-line (MITL) pulse sharpening and vacuum-surface-flashover switch sharpening.

The first technique to be explored was the addition of a 3-m-long MITL to the output of the accelerator. Because of conductance losses during the propagation of the pulse to the output end of the MITL, this approach reduces the t_r of the final output pulse by discarding the slowly rising leading edge of the pulse until the arrival of the peak value. Risetimes as short as 4 ns have been achieved; the behavior is controllable by variations in generator voltage and diode impedance.

In another approach to t_r sharpening, we interposed a vacuum-surface-flashover switch in the cathode conductor of the vacuum transmission line (Fig. II-13). The switch is designed to prevent passage of the current and voltage until the voltage wave achieves a chosen value up to 4 MV. The switch then closes rapidly, and the t_r is limited by the inductance downstream and the circuit impedance. While the theoretical t_r limit of this approach is 5 ns, the limit behavior is independent of the load characteristics. It also is possible to use this method as a first stage of sharpening for input to the MITL sharpener, potentially resulting in final output risetimes of less than 1 ns.

Another element of the flashover switch system is a parallel diode upstream of the switch. This diode allows current to build up in the inductance of the vacuum transmission line upstream of the switch before it closes. Although the upstream diode has proven useful in controlling t_r for selected values from 5 to 20 ns, the sharpest t_r experiments with the flashover switch have been achieved without implementing the upstream diode hardware. In this case, the current in the vacuum line is limited to emission from the plasma propagating downstream along the length of the switch and from random sites along the center conductor upstream of the switch. Displacement current becomes important in this case, because the upstream transmission line charges electrostatically while the switch is open.

When the switch closes, the electrostatically stored energy is discharged forward across the switch. This current is superimposed on that of the forward-going wave emerging from the pulse-forming line of the pulse-power generator. The resultant wave has a sharpened t_r, with a current maximum that occurs earlier downstream of the switch than at upstream positions because of the current surge from the electrostatically stored energy.

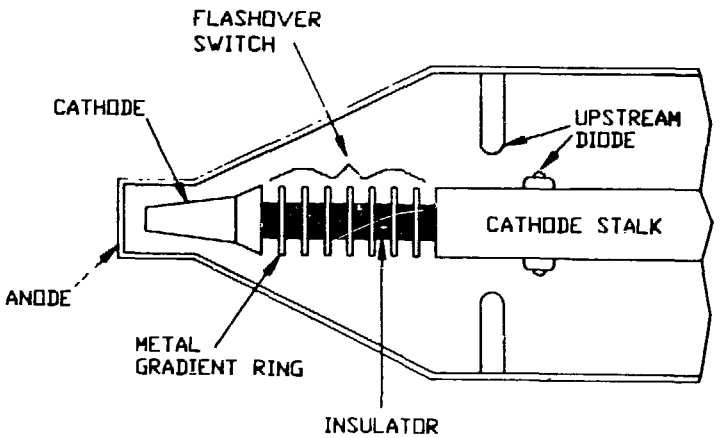

Fig. II-13. A flashover switch interrupts the cathode stalk in one method of t_r sharpening of power pulses

The success of this work has provided significant new opportunities for future research. For example, fast t_r systems allow us to achieve desirable experimental conditions much more quickly than before, eliminating the early part of the machine pulse that might disrupt the subsequent experimental conditions. As a result, more fragile, easily disrupted experiments, such as those having smaller geometries or more carefully controlled plasma conditions, can be performed. In addition, the shortened experiment time enables us to obtain improved particle and cell computer modeling of the experiments with shorter, less expensive run times.

DEFENSE PROGRAMS

Free-Electron Laser Program

Recent Results from the Los Alamos Free-Electron Laser Energy Recovery Experiment (P-15). The development of the Los Alamos Free-Electron Laser (FEL) has been an ongoing collaborative effort for several years, involving the Accelerator Technology (AT), Physics (P), Chemistry (CHM), and Applied Theoretical Physics (X) divisions of the Laboratory. This past year has been a particularly successful one in that we have attained a record-breaking extraction efficiency (2%) for an FEL oscillator operating at wavelengths below the microwave region and have demonstrated the energy-recovery experiments (ERX) with greater than 50% electron-beam decelerations. These results provide critical contributions to the program through time-resolved electron-beam diagnostics.

The Los Alamos FEL consists of a relativistic, 20-MeV electron beam produced by a radio frequency (RF) linear accelerator; a "wiggler" section composed of a series of permanent magnets with alternate north-south pole orientations; and an optical cavity in which one of the two end mirrors serves as the output coupler. Each second, the accelerator generates a 100-μs-long electron-beam macropulse consisting of about 2000 micropulses, 20 ps long, separated by 46 ns. The initial electron micropulse enters the wiggler region, experiences the alternating accelerations of the permanent magnets, and spontaneously radiates optically at about 10 μm. This optical pulse transits the optical cavity and 46 ns later arrives again at the middle of the wiggler, at the same time that the next micropulse arrives. The optical packets from successive micropulses thus add until the optical fields are strong enough for stimulated emission to occur from subsequent electron micropulses. The optical power builds up over 9 orders of magnitude in tens of microseconds and saturates at about a gigawatt peak power in the cavity. The output wavelength depends on the inverse square of the electron-beam energy and is proportional to the spacing of the wiggler magnet. Thus, the FEL is tunable and has high peak power.

To address the extreme range of time scales established by the electron-beam structure (ps to μs), several "streak" systems are employed. In these systems, a time-dependent deflection in one direction is used to convert one spatial axis into a time axis. We use both external deflectors of the accelerator beam and internal deflectors for the electron beam within a camera tube. The time resolution and coverage depend on the deflection rates, the physical space available, and the spot size of the electron beam. When the external deflector is used with an electron spectrometer, the nonenergy analysis direction is converted to a time axis so that the three-dimensional information (energy, intensity, and time) is produced at the spectrometer focal plane. Fused silica screens generate Cerenkov radiation during the electron-beam transit ($\beta = 0.99$), and the resulting visible image is recorded by intensified video cameras. By orienting the video camera appropriately, we can make each video raster line correspond to a different time or energy slice.

In the case of the "slow" external deflector, the streak system provides time-resolved energy spectra with 10-μs resolution. In the past year, we have taken advantage of this feature to analyze the FEL extraction efficiency in an on-line manner. We need only digitize a single raster line on the

video for both nonlasing and lasing conditions to compute the energy lost to lasing. Figure II-14 shows an example of the output giving the extraction efficiency (η) of 2%, an important milestone in the program. The figure shows that the lasing data have a lower energy distribution, tailing to the left.

When the "fast" RF-cavity deflector is used, a single micropulse can be selected by the shutter feature of the intensified camera, and a time resolution of about 20 ps can be attained. The location in time of lasing within the micropulse can actually be identified. We were able to determine that an energy broadening of the electron beam under nonlasing conditions at high peak currents was in fact a localized energy droop during the micropulse at the high charge locations. This effect is probably due to beamline wakefields (image currents in the beamline) that act as an energy drain on the micropulse and are most serious at beamline diameter discontinuities.

Using the "internal" streak system—i.e., a streak camera in which the electron beam within the streak tube is deflected—we can get time resolutions of 2 to 8 ps. The streak camera has been positioned both before and after the nonisochronous 60° bend to study the effects of the bend on the beam parameters. We have measured for the first time temporal widths of about 20 to 25 ps with accelerated charges up to 7 nC. These results indicate that the accelerator can produce peak currents that exceed 200 A (the design goal was only 100 A).

In the energy recovery experiment, the electron beam passes through the wiggler area and is then guided around a 180° bend to the decelerator structures. These RF structures extract energy from the electron beam. Bridge couplers are used to transfer the energy back into the accelerators, with the goal of increasing the overall efficiency of the system. A second electron spectrometer beyond the decelerators was used to demonstrate that the beam had lost more than 50% of its energy. The focal plane was again viewed by an intensified camera. Initially, the beam currents involved were below the detection threshold of the wall-current monitors, so the camera data were crucial. Subsequently, beam transport improved, and RF power flow was detectable in the bridge coupler.

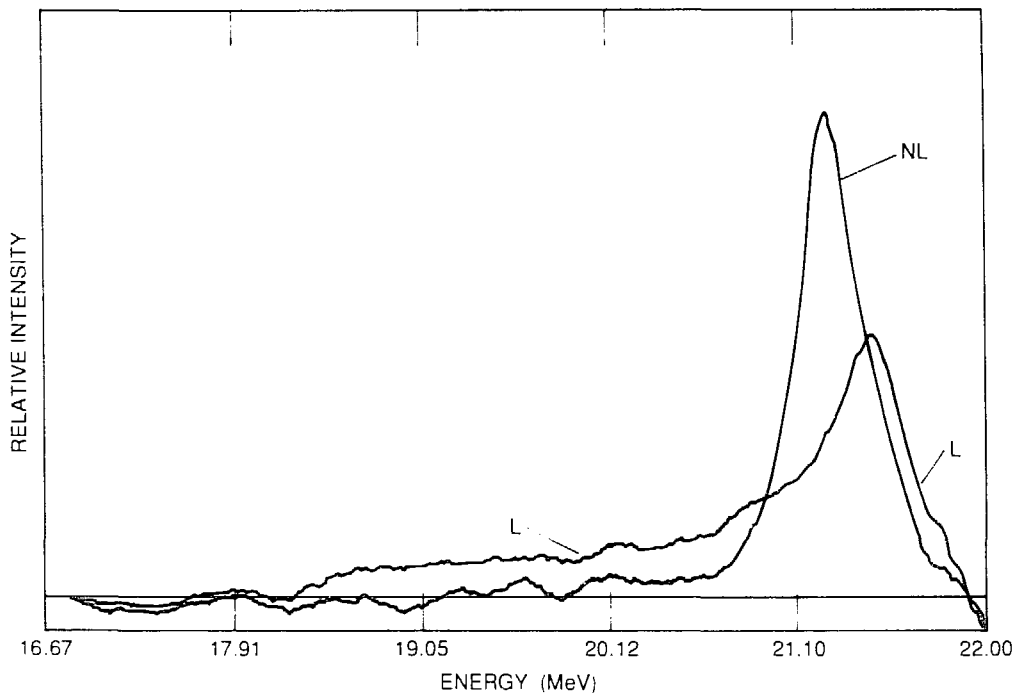

Fig. II-14. Graphics output from the on-line analysis for the 2% extraction efficiency case. The energy distribution for both the nonlasing (NL) and lasing (L) conditions are shown. The electrons that participate in lasing lose energy and are seen in the low-intensity tail toward the left of the intensity peak.

In summary, the time-resolved electron-beam diagnostic techniques based on streak (deflection) techniques have played an integral role in the FEL program in the past year. The extraction efficiency milestone, the energy-recovery milestone, the evidence for electron peak currents higher than the design goal, and the identification of wakefield effects were all determined with these diagnostics. Because lasing efficiency is strongly dependent on peak electron currents, the program will push towards higher efficiency guided by the diagnostics information. These successes have increased prospects for building an FEL operating at 1 μm.

Free-Electron Laser Resonator Development (P-5). Free-electron lasers require high-brightness resonators for maximum extraction efficiency. As a result, we need to develop special resonator/optics in order to obtain power levels appropriate for SDI applications. In the wiggler, the brightness (power/area/solid angle) of the optical beam must match that of the electron beam, and it must be as high as possible for high efficiency. The emerging optical beam must be allowed to expand by diffraction before it interacts with any optical surfaces in order to prevent coating damage and mirror heating. The coating development effort was managed in other divisions with some support from P-5. High-power resonator development in P-5 addressed four areas, primarily cooled-mirror development, resonator designs and experiments, grazing-incidence beam expanders, and optical propagation codes for resonators.

Cooled Mirror Development. To prevent optical damage and mirror distortion, we are working with two subcontractors to develop cooled mirrors on the basis of criteria generated in P-5. Bell Aerospace Corp. has begun fabricating subscale mirrors, and United Technologies is fabricating a proof-of-concept mirror. The mirrors will be tested at the Air Force Weapons Laboratory Thermal Distortion Test Facility.

Resonator Designs and Experiments. In addition to cooling the mirrors, we can cope with high optical intensities by inclining the optical surfaces to near-grazing incidence, thereby increasing the beam footprint area. The feasibility of using optics near grazing incidence was demonstrated in a long-base (64-m) laser resonator with an argon-ion gain medium simulating an FEL. We received the grazing-incidence beam expander earlier in the year from Perkin-Elmer Corp., where the expander had been designed and fabricated over a two-year period. One component of the cavity was a 60-cm-long, off-axis, hyperboloid grazing-incidence mirror placed at an 86° incidence angle. This optic provided two-dimensional beam expansion of approximately 7X for the next downstream optic and increased the footprint area by nearly 50X. The grazing-incidence beam-expanding optics permit us to use shorter optical systems with fluence loadings identical to near-normal-incidence configurations. This was the first use of grazing-incidence optics in a resonator.

We also pursued the design of coupled resonators and FEL master oscillator power amplifiers (MOPA). We demonstrated that by using MOPAs with FELs, we could obtain phased arrays and thereby get essentially unlimited power from RF-linac-driven FELs. In our conceptual design studies of high-power FEL oscillators, we found that several problems arise as the power increases. The main physics problem is gain-shaping of the optical mode as a result of the extremely high and narrow gain region. This effect leads to a mismatch of the optical mode with the cavity optics. When we attempt to compensate for one effect, oscillator start-up problems result. We are currently using computer simulations and experiments to address these problems.

Optical Propagation Codes. We have successfully modified the diffraction code GLAD (a code written by Applied Optics Research) to treat grazing-incidence-optics problems. This modification is a significant achievement because our approach, based on a combination of ray tracing and diffraction propagation techniques, is more accurate and powerful than any other technique currently in use. We have verified that the code correctly predicts the results obtained in the laboratory set-up of the grazing-incidence resonator in the optics evaluation laboratory.

In conjunction with Applied Optics Research, we have successfully coupled the code LOTFEL (a free-electron laser kinetics engineering code using the Weng Chow sideband approach) with GLAD (the diffraction optics and propagation code). The resulting code, GLADFEL, is the only one known to be capable of analyzing FEL kinetics and optics (including analysis of alignment tolerances and figure errors of elements) from end to end. The code is structured to be an engineering analysis code and runs in a reasonable time on the Los Alamos Cray Computer System. We hope to use it to generate and analyze various FEL systems of possible interest.

Neutral Particle Beam (NPB) Program (P-2, P-3, P-5, P-7, P-12, P-15)

In support of the SDI program, the Laboratory is undertaking a significant research and development effort to evaluate the importance of neutral atomic beams. Personnel from several P-Division groups are participating. The goals are to develop direct sensing techniques for evaluating the quality of such beams, to undertake advanced detector development, and to perform other important experiments.

We are investigating and plan to employ direct beam-sensing techniques. Here the beam, or part of it, penetrates through a physical sensor, and the resulting signal gives information about the beam. Such methods are at least partly interceptive. This technique differs from the laser resonance fluorescence (LRF) method, in which passage of a laser beam through a neutral hydrogen beam stimulates the emission of optical signals that provide information on beam direction. The LRF method, essentially noninterceptive, is being pursued by the Chemistry Division.

An attractive test machine developed at Argonne National Laboratory (ANL) is the 50-MeV, negative-hydrogen-ion (H^-) linear accelerator, which is the injector to the Intense Pulsed Neutron Source Facility. Although this machine will not be adequate for future neutral-particle-beam developments, it does provide interim opportunities for testing some of our fundamental concepts. In the following paragraphs, we discuss our efforts to develop new sources and to use the ANL source for beam-sensing experiments.

Ground Test Accelerator (GTA-1) Ion Injector. The development of a reliable H^- injector for the NPB experiment is one of the critical issues in the GTA project. The state of the art for building H^- injectors is barely adequate to meet the requirements of GTA in terms of output current, emittance control, and reliability. Moreover, the requirements of space qualifiability, power consumption, volume, and automatic startup and operation under computer control have barely been addressed until now. The task is even more difficult because we know too little about the physics of H^- injectors to make the fabrication of an injector a straightforward engineering task.

In January 1986, a small team from Group P-7 began to investigate the development of ion injectors for NPB accelerators and to address many of the issues relevant to the Integrated Space Experiment (ISE) project. The conceptual design of the injector was presented to the GTA project managers and to the program sponsor in an official design review held at AT-Division on June 18, 1986. The following relevant issues were addressed:

- Fabricating an ion injector to GTA-1 requirements;
- Establishing an interface and providing the hardware to allow Group AT-8 to solve the difficult problem of implementing fully automatic startup and control of an injector and an accelerator;
- Folding spaceflight constraints of weight, size, and power consumption into the design of injectors; and
- Planning experiments that will provide physics information for the GTA-2 injector design project.

Of several existing types of H^- sources, only the Penning or Dudnikov source is capable of producing the current and emittances required for high-current particle accelerators. The production of H^- in a Penning source is related to several factors, including the partial pressures of hydrogen and cesium in the discharge region and the temperature of the arc electrodes. By developing a pulse-modulated valve that will give us precise control of the flow of hydrogen through the discharge region, we expect to achieve a greater degree of control over the discharge conditions. A piezoelectrically controlled valve has been set up and is producing 25-μs pulses of H^- with a minimum of 10-μs dead time between pulses. Work is underway to develop a small Penning pressure gauge so we can resolve the details of the pressure pulses.

The output of the arc source is accelerated and transmitted to the input of a radio-frequency quadrupole accelerator by a low-energy beam transport (LEBT). The LEBT design, for which we are using the code TRACE, has been progressing well. TRACE is somewhat limited in that it does not include beam neutralization in the calculations except as a parameter that is included under operator judgment. The team has been exploring how the relevant plasma physics might be included in the code with the help of personnel from Groups AT-2 and X-1 and the Missouri Research Corporation.

The current plans call for having much of the injector in operation, under manual control, by late October or early November 1986.

NPB Magnetic Optics. The Beam Magnetic Optics group in P-12 has been given responsibility for the HEBT (high-energy beam transport), the 180° bend, and the expanding telescope for the GTA facility. The main objective of the GTA program is to provide an engineering test bed for a spaceflight accelerator. The program provides the key mechanism for transferring technology needed for the design, fabrication, and testing of a space-qualified NPB system. This information transfer should be a phased process, so the GTA program has been divided into GTA phases 1 and 2. Before GTA phase 1 can begin, several key components of the magnetic optics portion will be designed, built, and tested at ANL. Group P-12 has been chartered to provide mechanical design and procurement support for the Argonne experiments and for GTA phase 1. (See Fig. II-15.)

Current work is focused on designing and procuring hardware for an expanding telescope to be tested at ANL early in FY87. Several long-lead items—two permanent-magnet eyepieces and a permanent-magnet objective triplet—have been ordered. In one of the eyepieces neodymium iron, and in the other samarium cobalt, will serve as the permanent-magnet material; for the objective triplets, samarium cobalt will be used. All magnets are scheduled to arrive at the Laboratory in February 1987 for acceptance testing. Designs for the vacuum, support, and diagnostic systems are being refined.

Future work includes ordering magnets for the 180° bend; ordering a variable-field permanent magnet; and designing the vacuum, support, and diagnostic systems for the GTA phase-1 facility. Group P-12 will continue to work with consultants from Optomec to develop remote alignment methods for the magnets in the 180° bend.

NPB Beam Sensing. Personnel from Group P-12 are involved in the design and fabrication of much of the beam-sensing hardware for the ANL and GTA-1 experiments. Principal components in the beamlines are the noninterceptive LRF experiment and the interceptive pinhole, wire shadow, and optical-fluorescence direction-sensing techniques. Each of these systems requires extensive design development, now in a preliminary stage. The current plan is to design and build both beam-sensing systems with associated beamline piping for the ANL experiments and, after system testing at ANL, return all beam-sensing hardware to the Laboratory for installation in GTA-1. (See Fig. II-15.)

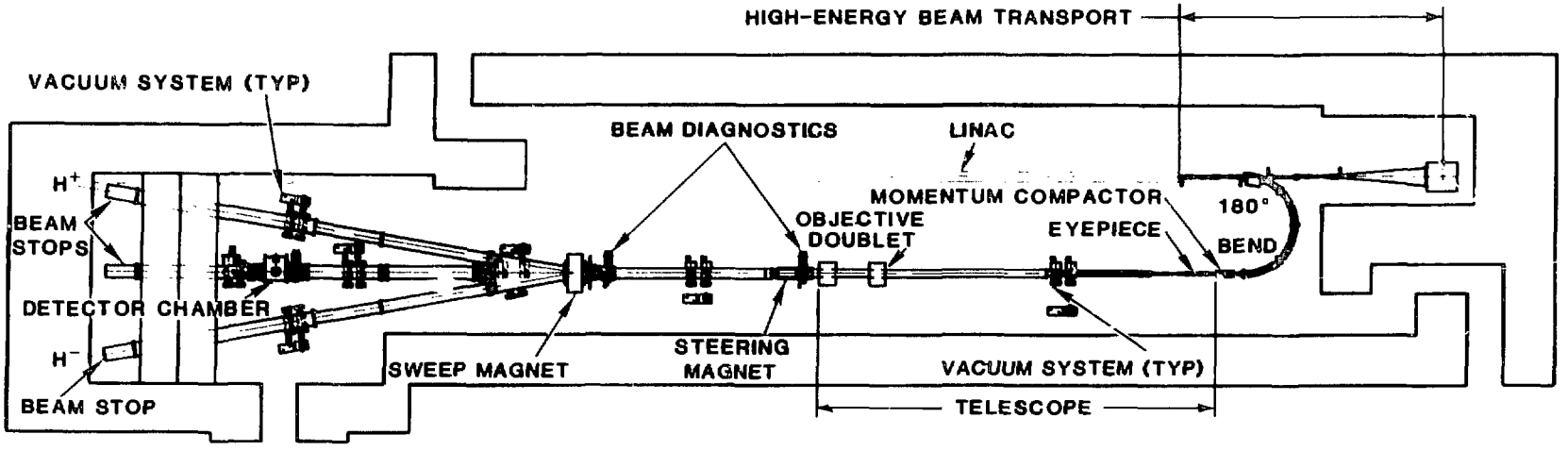

Fig. II-15. NPB GTA-1 magnetic optics/beam sensing systems.

Physicists, engineers, and technicians from Groups P-2, P-3, and P-15, primarily, are developing the interceptive techniques. The H^- beam passes through the objective triplet lens as an expanded beam with moderately low divergence (~25 μrad). It then passes through the steering magnet (M_1), three diagnostic boxes (not shown), and a charge-separation magnet (M_2) and then to the detection chamber.

To evaluate the quality of the expanded beam, we will employ the "pepper-pot" method. Into the middle diagnostic box we insert a thin metal membrane, ~15 microns thick, perforated by a rectilinear array of a few hundred small holes, each ~100 μm in diameter. Each hole is covered with a very thin carbon neutralizer foil. Because the incident H^- beam diameter is 10 cm (85% of intensity) and may be displaced 5 cm in any direction, the diameter of the pinhole membrane was chosen to be 20 cm. On passing through the membrane, the H^- beam is converted to mostly protons. However, immediately downstream of each pinhole is a small-diameter beam of neutral hydrogen atoms. Magnet M_2 separates the charged from the neutral particles, and the array of neutral pinhole-formed beams propagates downstream to the detector chamber.

In the detector chamber, the particle beam strikes a 22-cm-diameter thin fluorescent screen and creates a light image that is reflected from a 45° mirror through a window in the chamber. Outside the window, a lens focuses the beam from the mirror on a charge-coupled imaging device (CCD) with 640,000 pixels. The beam from the accelerator comes in macro pulses, 100 μs long, with a peak H^- current of about 1 mA. Each of the derivative pinhole-formed neutral beams will contain about 10^5 atoms per macro pulse. The intersection of each such beam with the screen creates a low-level pulse of light. The optical system converts these many light pulses into electrical signals in the surface of the CCD. The information content of the signals is read into a computer, which extracts data about the positions and shapes of the intersections on the screen. Together with the spacing of the holes in the pinhole membrane, this information tells us about the quality or emittance of the expanded beam.

The object of this work is to understand the aberrations of the magnetic-optical system. When we compare our data with the predictions of the particle-transport codes, we will know more about the validity of the magnetic design procedures.

An Organic Scintillator Neutron Detector for Use as a Mass Sensor. A crucial aspect of the proposed SDI is the ability to discriminate between enemy warheads and decoys during the midcourse segment of the trajectory of an intercontinental ballistic missile (ICBM). One promising discrimination method is to interrogate an object with an NPB and detect neutrons scattered from that object. From the number of scattered neutrons one can deduce the mass of the object and, hence, differentiate between massive warheads and light decoys (in order to be useful, decoys must be plentiful and therefore light). An integral part of such a system is a device that can efficiently detect scattered neutrons in a potentially hostile environment. As an outgrowth of our experience in building large-scale neutron counters for intermediate-energy physics research, Group P-2 is developing a unique concept for such a detector.

Figure II-16 is a diagram of the detector and its operation. A high-energy neutron, produced by a nuclear interaction of the NPB with the target, enters the detector, which consists of a number of planes of organic scintillator (three are illustrated in the diagram). Because neutrons are electrically neutral and therefore are highly penetrating, the incident neutron will pass through a number of detector planes before undergoing any interaction. Eventually, the neutron will undergo a nuclear reaction with a hydrogen or carbon nucleus in one of the scintillator planes, which we choose to call the "generator." Because the incident neutron energy is large, in a substantial fraction of these interactions an energetic proton will be ejected within a few degrees of the direction of the neutron. The proton, however, will loose energy in the scintillator through electromagnetic interactions with the scintillator molecules. This energy will be re-emitted in the form of light that can be detected by photomultiplier tubes located at the ends of the scintillator. The proton will continue to lose

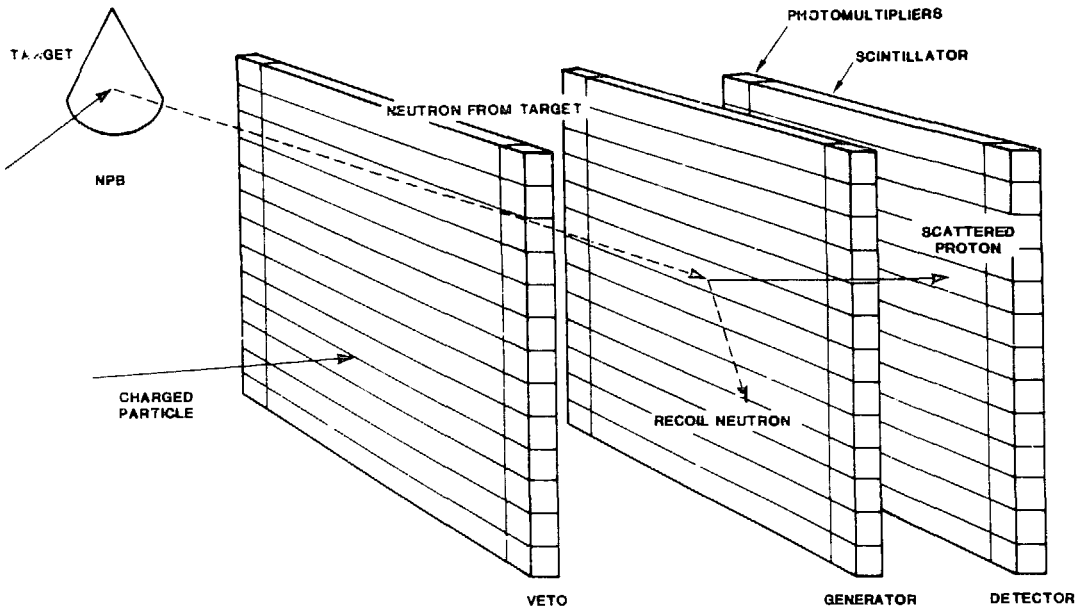

Fig. II-16. Organic scintillator mass sensor.

its energy in additional planes of the scintillator until it finally comes to rest. By segmenting each plane into a large number of cells, with photomultipliers at both ends of each cell as shown in the figure, we can determine the position of the proton as it passes through the plane. (The vertical position is determined simply by the position of the cell producing the signal and the horizontal position by comparing the difference in time required for light to propagate to either end of the cell.) Thus, the path of the proton can be traced and the general direction of the incident neutron deduced. If several neutrons scattered from the target are detected, the direction of the target can be calculated within a few degrees.

The detector design is also well suited to operation in a background that may include large numbers of gamma rays, low-energy neutrons, and charged particles. Charged particles will begin to deposit energy as soon as they enter the detector, so the signal in the first plane can serve to veto all such events. Gamma rays and low-energy neutrons will deposit energy more or less uniformly throughout the volume of the detector. By segmenting the detector sufficiently, we can set thresholds on the photomultiplier signals above the level of this background but still below the much higher level of the signals produced by the high-energy scattered protons. Furthermore, gamma rays and low-energy neutrons do not produce coincident signals in at least three adjacent planes, a requirement for tracing the path of the scattered protons.

Thus, our detector should be able to detect high-energy neutrons efficiently and to suppress signals from background sources. In addition, it should be capable of providing information on the direction of the target, which would be useful in verifying the results of the NPB interrogation.

In order to test these concepts, we are constructing a prototype device consisting of a charged-particle veto detector and three planes of neutron detectors, each having six to ten cells. The prototype will be tested for operation in high gamma-ray fluxes at the SDI Test Facility, soon to be completed at the WNR at LAMPF, and for operation in neutron fluxes at the GODIVA critical mass facility. Results will be compared with other mass sensor concepts that are being developed concurrently at Los Alamos and elsewhere.

Electromagnetic Launcher Program Rail Guns (P-7)

Our efforts in the Los Alamos Railgun Project have been devoted primarily to the study of the plasma armature and how it affects railgun performance. Among the many experimental and theoretical activities carried out this year, three are particularly noteworthy: completion of the HYVAX experiments, measurements of the plasma voltage gradient, and ablation measurements on the MIDI-2 railgun.

The HYVAX railgun has been the principal experimental tool of the Los Alamos Railgun Project for the past two years. In March 1986 the last experiments were performed on the HYVAX apparatus. In these experiments, we investigated the distributed operating mode and the effect of distributed current feed on plasma armature dynamics. The experimental results demonstrated that distributed operation is feasible even when the length of the plasma armature is so great that it extends on both sides of the current feed point.

An experiment was designed and carried out to measure accurately the voltage gradient in a typical railgun plasma. The measured value of 130 V/cm is independent of discharge height over the range investigated (6 to 25 mm). Subsequent measurements on the 100-mm-diameter HIMASS railgun test confirmed that this voltage gradient is nearly independent of discharge height. This result is an important input for various systems studies in which an attempt is made to predict the operating characteristics of large railguns. It is now clear that power losses in the plasma armature of large railguns will be significant and that improvements in system efficiency will only come with a better understanding of the plasma armature.

The MIDI-2, a new experimental railgun, has been commissioned. This is a relatively low-current device designed for quantitative studies of the plasma armature and its interaction with railgun bore materials. Using a "free-arc" technique, in which there is no projectile to limit the arc velocity, we were able to measure the effect of bore insulator ablation on maximum plasma velocity. The measured velocity varies inversely with the square root of the average atomic weight of the insulator material, in agreement with the model of ablation drag developed at Los Alamos last year.

Satellites for Laser Diagnostics (P-5)

The P-5 program for detecting ground-based laser tests from reconnaissance satellites was motivated by the recently perceived vulnerability of U.S. space-based assets to degradation and destruction by ground-based laser weapons. Even the current capabilities of high-power lasers, with only slight modifications to their decade-old technology, could represent a threat to space-based assets.

Our first task was to establish a preliminary mission definition for a reconnaissance satellite. The system objectives were

- Detection of a high-power laser;
- Verification of a high-power laser test;
- Determination of the laser wavelength;
- Determination of the test location;
- Estimation of the laser power; and
- Estimation of the pulse width and repetition rate.

The mission of a laser-detection satellite was defined by 1) estimating the atmospherically scattered light and, therefore, the detection S/N that could be detected by a satellite; 2) estimating

what information was obtainable, both at medium-earth orbit and at a geosynchronous orbit, with optics of a reasonable size; and 3) grouping laser sources according to both atmospheric windows and possible detector technology.

As a result of our work we recommended a preliminary mission definition for a near-term effort, with an existing space platform located in mid-earth orbit, and for a long-term effort, with a new satellite in geosynchronous orbit. In addition, we began a conceptual system design for the near-term effort, including a design for a telescope with crossed diffraction gratings, which will allow simultaneous spatial and spectral viewing over a wide field of view. Further, we concluded that

- Only a limited amount of information is obtainable from a single, isolated laser event;
- Laser experiments could be scheduled to avoid detection by anything other than a satellite in geosynchronous orbit;
- The first four system objectives could be achieved, and the last two partially achieved, with a mid-earth-orbit satellite having optics of a reasonable size, during the satellite's look time;
- Continuous viewing and detailed probing of the ground experiment would probably require large optics located in geosynchronous orbit; and
- An advanced Department of Energy satellite program could benefit greatly from technology currently under development for the SDI effort.

Ground-Based Laser-to-High-Altitude-Target Analysis (P-5)

Our work on this program was directed primarily toward conducting an analysis to define the requirements for the optical components of a ground-based laser-to-high-altitude-target system and to demonstrate that the optics would be feasible and economical. The approach taken was first to analyze, in brief and approximate fashion, a number of possibly critical problems including laser gain and laser optics, mirror damage thresholds, mirror heating and distortion during the total mission, and transmission losses from the laser to the target. A program for analyzing the entire system, from the laser to the target, was then developed and used for studies of various system configurations.

Laser Analysis. We were provided with data for the deuterium fluoride (DF) pulsed laser showing the output of kinetics codes in the form of total extracted energy as a function of output coupling for a simple stable resonator. In order to calculate the output for the cases of interest, a two-pass amplifier or an unstable oscillator in which the intensity is slightly nonuniform throughout the cavity, it was necessary to determine an equivalent gain, saturated intensity, and absorption and to integrate the gain equation through the cavity. Although the gain and saturation values accurately matched the extraction-versus-output coupling curve for the stable resonator, this procedure led to unexpectedly low total gains for the system of interest. More analysis will be required to determine whether the basic approach of using equivalent values for gain and saturation can be effective for the transient, multiline, pulsed DF system, or whether another approach must be found.

Optical Damage. The systems being considered require mirrors that will withstand 100 to 300 J/cm^2 in pulses 100 μs long. Although there are no data for such long pulses, results for 0.1 to 20 μs show that time-scaling for bare copper or aluminum by the square root or cube root of time is appropriate and that thresholds of 300 J/cm^2 can be reached.

Laser-to-Target System Analysis. A simple computer model was written to calculate the energy on a target after propagation from the ground laser to a mirror in geosynchronous orbit, to a mirror in low orbit, and then to the target. The input parameters include the laser dimension, the extracted energy, the assumed atmospheric transmittance, and an assumed value for the wave front and mirror quality. Beam spreading and diffraction effects are included. A summary of results is shown in Fig. II-17, where we show the fraction of laser energy collected within a given diameter on target as a function of laser diameter and space-mirror diameter. The peak and average fluences on each of the mirrors have also been calculated to show that for the nearly diffraction-limited cases, the geosynchronous mirror would see a peak of at least twice the allowed level of 300 J/cm^2. Inasmuch as the average fluence is much lower, it is likely that the beam can be slightly spread with a great reduction in the peak fluences.

Assuming the practicality of the large lasers needed for this program, it appears that delivering the energy to target is feasible with space mirrors that are slightly larger than those required for other systems but that have significantly more relaxed requirements on their figure accuracy (0.1 μm rather than 0.05 μm). A need for additional modeling of lasers has been identified, and specific optical design is needed to maximize the energy collected on target while meeting a maximum fluence on the space optics.

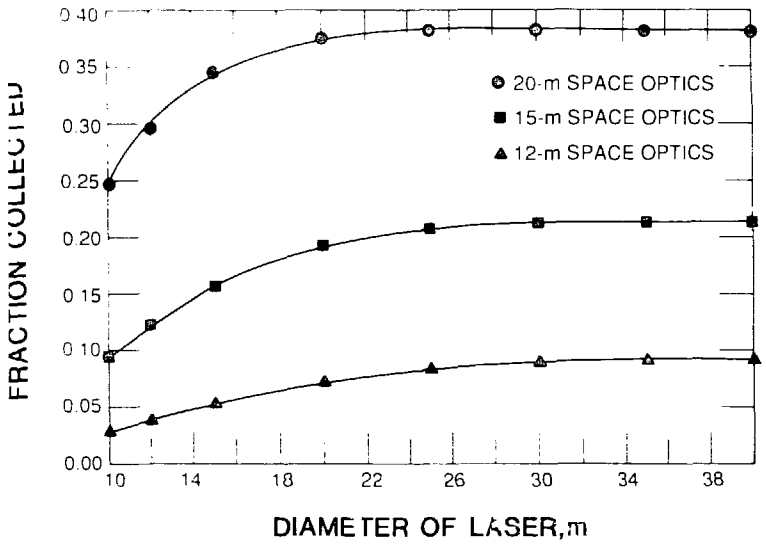

Fig. II-17. Beam transmission onto 3-m-diameter target.

Development and Current Status of an "Intelligent" Autonomous Computer Program (P-5, S-1, S-DO)

Most of the work to date in the area of artificial intelligence applications has used the "expert" systems approach in conjunction with the "if-then" production rules to solve problems. We feel, however, that the peculiar strengths of computers—i.e., large, flawless memory and speed of manipulation—can best be used if we formulate the design problem in precise mathematical terms along with clearly defined concepts and precise language. Consequently, what we have defined as an "intelligent" program relies on the introduction of metrizable performance and configuration spaces, a mapping from the performance into the configuration space represents the design process, and

the inverse of the mapping represents design evaluation. We consider programs to be "intelligent" when they can perform tasks currently requiring human effort and when they are able to improve their performance with practice and experience. The scheme we employ for information storage approximates the concept of the content memory because it makes possible the retrieval of general information (e.g., range of values in which the derived characteristics lie) pertaining to a specified set of devices.

We rely on two principal elements: we codify the problem with a particular mathematical structure, and we use probabilistic processes where they are useful and appropriate.

The performance and configuration spaces are spanned by all the variables we need to specify the performance and configuration data for the technical device being designed. The recognition that these spaces must be defined compatibly with the performance objective function is an essential element of our approach. Every design process contains, explicitly or implicitly, an optimization procedure. In our case, we have generalized the simulated annealing method for optimization.

We chose optical lens design for the first application because this area is so well developed that designs and performance evaluations can be carried out computationally without expensive and time-consuming experimental verifications. Consequently, several designs can be completed and evaluated in one day, and the "learning" ability of the program can be assessed in a relatively short time. We have demonstrated that generalized simulated annealing can be used with commercially available codes to optimize lens designs and that the mapping from the performance into the configuration space is a useful representation of the design process.

The first result has been demonstrated with designs of a one-element ("landscape") lens. We used the wave-front variance averaged over a representative set of rays as the objective function to be minimized; it has two widely separated minima that are almost equally deep. Variation of system parameters in random-walk analysis demonstrated that for some sets of parameter values the algorithm tends to locate the nearest minimum and that for other values the algorithm is able to climb out of one basin and locate a lower minimum. In some design calculations, the generalized simulated annealing located optima that a standard optical design code was unable to find without "coaching" from the human designer. We also encountered cases in which generalized simulated annealing located optima faster than did a gradient method. This occurs often in multidimensional problems where each determination of the gradient requires a number of function evaluations equal to the dimensionality of the problem.

The second result has been demonstrated by the design of 44 two-element lens systems to the following specifications: effective focal length of 2.5 cm (1 in), back focal length greater than 1.88 cm (0.75 in), f-numbers ranging between 5 and 10, and fields of view ranging between 10° and 30°. To make the graphical presentation of the results possible, we condensed performance and configuration spaces to two dimensions each; in actual design calculations, these spaces were appropriately multidimensional. The condensed performance space, shown in Fig. II-18, is spanned by the f-number and the field of view; the condensed configuration space, shown in Fig. II-19, is spanned by the optical power of the first (P_1) and second (P_2) elements. The design of the two-element lens system, as formulated here, is equivalent to determination of the image of the region R (in the performance space) in the configuration space. The image under the design mapping is to be determined with the optimization of "optical quality" of the lens system. We determined the image with the commercially available Code V, which has its own objective function and optimization routine.

The result, presented in Fig. II-19, shows that the image of region R consists of two disjoint rectangles with fuzzy boundaries in the performance space, depending on the order of positive and negative power elements. Our program knows that initial configurations in these two regions lead to designs that meet the specifications with acceptable image quality; conversely, attempts to design to specifications in region R, beginning outside either region C_1 or C_2, end up with configurations in the interiors of C_1 or C_2 after guided optimization. This result is indicated by the designs labeled 1, 2, 3, and 4 in Fig. II-19.

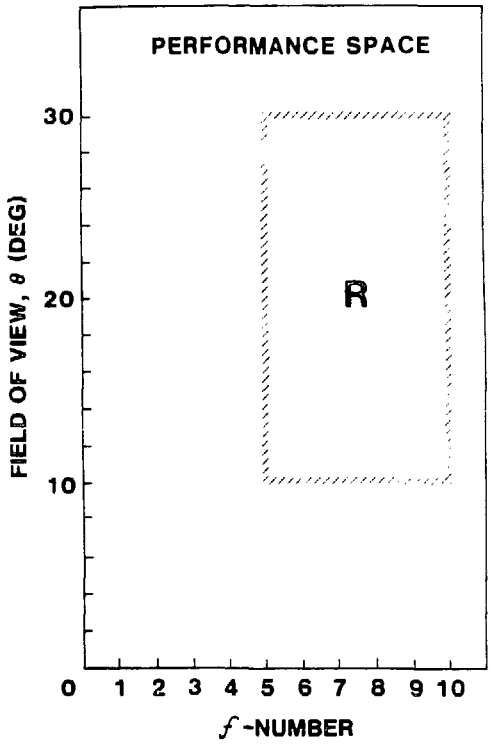

Fig. II-18. Condensed performance space: two-element lens system designs.

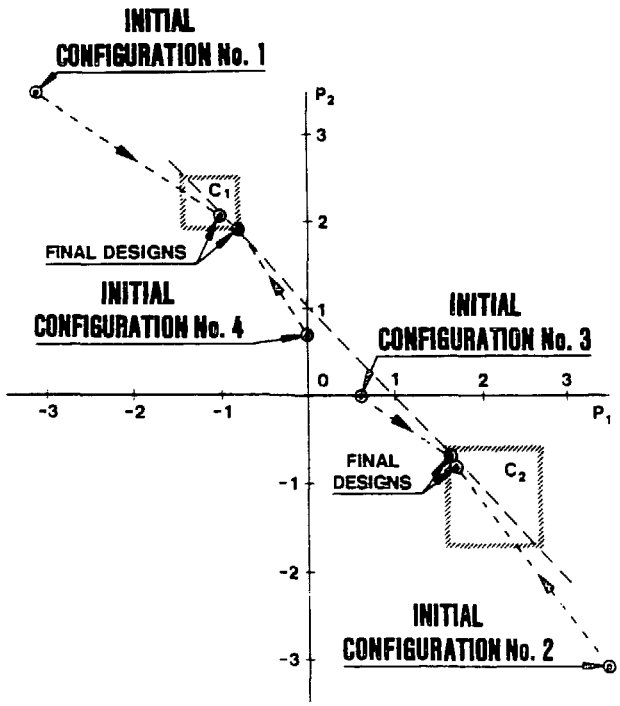

Fig. II-19. Condensed configuration space: two-element lens system designs.

It is worthwhile to note that the only analytically derivable description of image region C_1 or C_2 is the condition $P_1 + P_2 = 1$ (focal length of 1 in.); the additional limitations are consequences of the optimization of image quality.

We have two near-term objectives in this work. One is to integrate the generalized simulated annealing algorithm with some generally available optical design and analysis code like Code V or ACCOSV. This will enable us to verify the ability of the algorithm to optimize complex multi-element designs and to establish the feasibility of our approach to the development of intelligent design programs. The other objective is to investigate and to enhance the performance of the optimization algorithm. That includes improvement of computational efficiency and derivation of satisfactory termination criteria. An example of this activity is our recent notice of the connection between simulated annealing and the classical "Gambler's Ruin" problem and attempts to exploit that connection.

The long-range goal is to produce an intelligent and efficient lens design program that can be left in a computer long enough to design several thousand lens systems and to verify that the designers have not overlooked some good designs.

C-Lamp Project (P-5)

The Antares Laser Facility at Los Alamos National Laboratory was chosen as the site of a series of related experiments for the C-Lamp project. The principal participants in these experiments were from Groups P-5 and IT-3, from Sandia National Laboratories in Albuquerque, and from the Department of Defense, the sponsor. Other organizations participating in the experiments included Martin Marietta, Perkin-Elmer, EG&G, Patrick Air Force Base, Air Force Avionics Laboratory, Atmospheric Science Laboratory, SRI International, Lockheed Missiles & Space, and Scitec.

The project objectives were to detect the scatter of laser radiation over unique paths and under a variety of specified atmospheric conditions in order to verify the irradiance received by different measurement instruments. These experiments, conducted in the Antares Laser Building, required modification of the front-end CO_2 drivers to bring them to a peak pulse energy of 1.2 kJ per 1.5-ns pulse, 10 minutes apart. New mirrors, salt windows, and gas mixes were incorporated in the system, and an opening was made at the west-end access cargo door to divert the beam from the basement to the rooftop. Seventeen hundred square feet of all-weather grating was installed for catwalks on the roof, along with experiment pads, safety rails, and stairways from the second level to the rooftop. A carousel mirror mount (an in-house Laboratory design) was put in place as were secondary mirror mounts with protective housing. Some of the rooftop gear is shown in Fig. II-20.

In operation, a CO_2 laser beam was directed from the basement of the Antares Laser Building up the west wall and across the rooftop operation area to a gold-coated target board, which had been bead-blasted for a 600-grid equivalency. We measured the back reflections of the target at normal incidence. After striking the target board, the beam was widely dispersed to different detector sites located one mile or more away. The detectors were calibrated and proof-tested for obtaining data at the wavelengths of interest and under a variety of operating conditions.

During the test period, 882 shots were run. Of these, 86% provided useful data for further experiments conducted elsewhere in the C-Lamp Program. The P-5 team received a letter of commendation from the Defense Intelligence Agency.

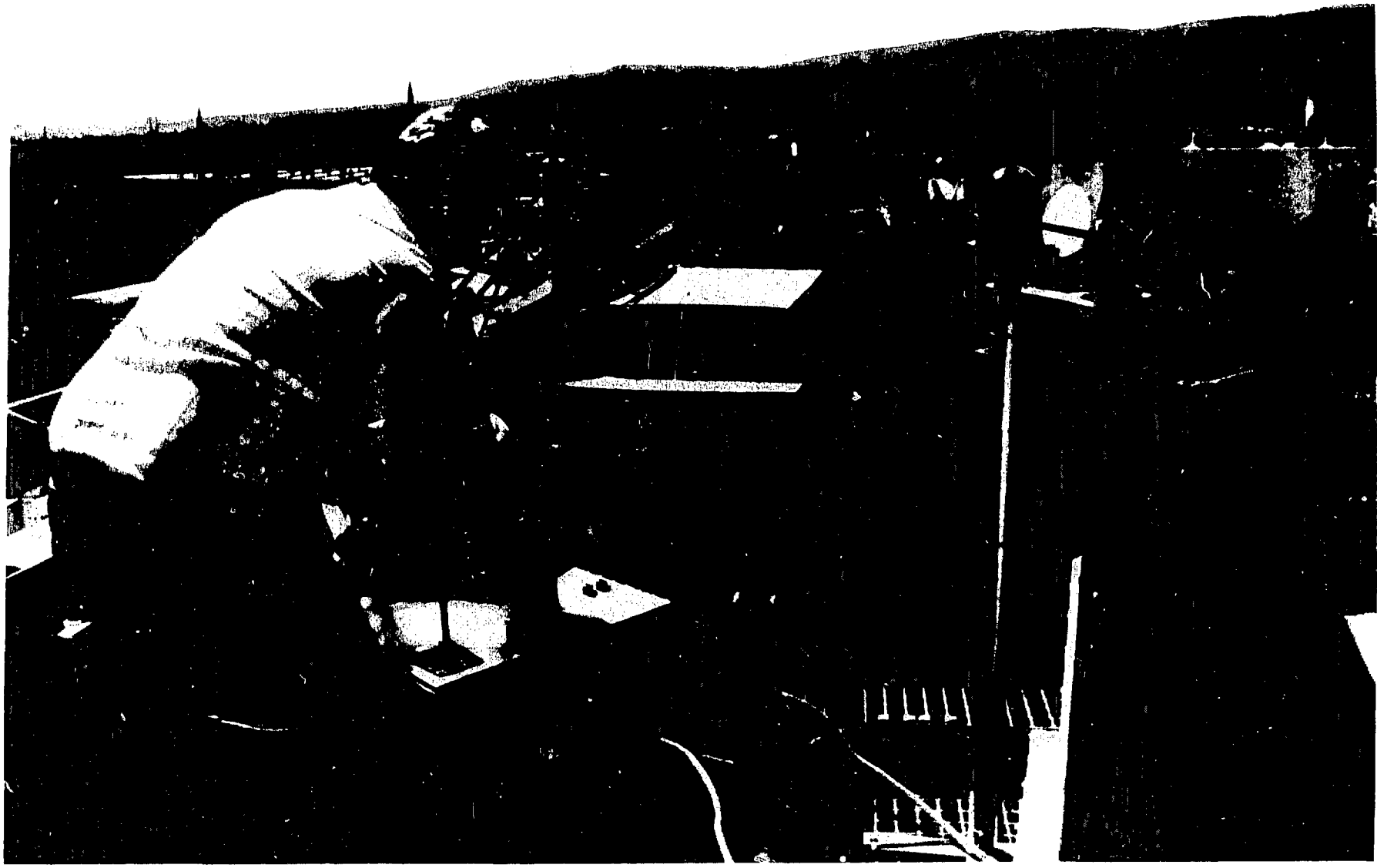

Fig. II-20. Grating, mirror mounts, and target alignment.

FACILITIES DEVELOPMENT

Synchrotron Beam Lines (P-12, P-14)

Our goal has been to design and construct a general-purpose, state-of-the-art x-ray facility that exploits the capacities of the vacuum ultraviolet (VUV) and x-ray rings at the National Synchrotron Light Source (NSLS). We are planning to span the energy range from about 20 eV to 25 keV with high resolution, high intensity, and good higher order and stray-light suppression. The beam lines we develop will be well characterized and easy to use and will have flexible experimental stations. At least two Los Alamos and two EG&G personnel will be assigned at the NSLS to operate the beam lines, help users, and pursue research.

In order to accomplish these objectives, we are building four beam lines, two at port U3 on the VUV ring and two at port X8 of the x-ray ring. The overall schedule calls for construction of the beam line to be completed by mid-1987.

Of the two beam lines at port U3, one will be equipped as a spectroscopy line (U3C) covering the energy range 20 to 1250 eV and the other as a nonmonochromatic radiometric line (U3A) for the energy range 100 to 2000 eV. Similarly, at port X8 we plan a soft x-ray, 800- to 6000-eV, ultrahigh-vacuum (UHV) line (X8A) and a hard x-ray, 5,000 to 25,000-eV line (X8C). These lines will be used for radiometry, spectroscopy, and x-ray scattering experiments.

The first Los Alamos synchrotron radiation beamline, U3C, is in its final stages of characterization. The first experiments on this line, the calibration of 12 metal multilayer crystals in support of a Nevada Test Site (NTS) experiment, were successfully performed in January 1986. (A typical multilayer response curve is shown in Fig. II-21.) The results are being used to interpret data from the NTS test. The full experimental program on this line is scheduled to commence in summer 1986, beginning with a study of several heavy electron systems in which we will use photoelectron

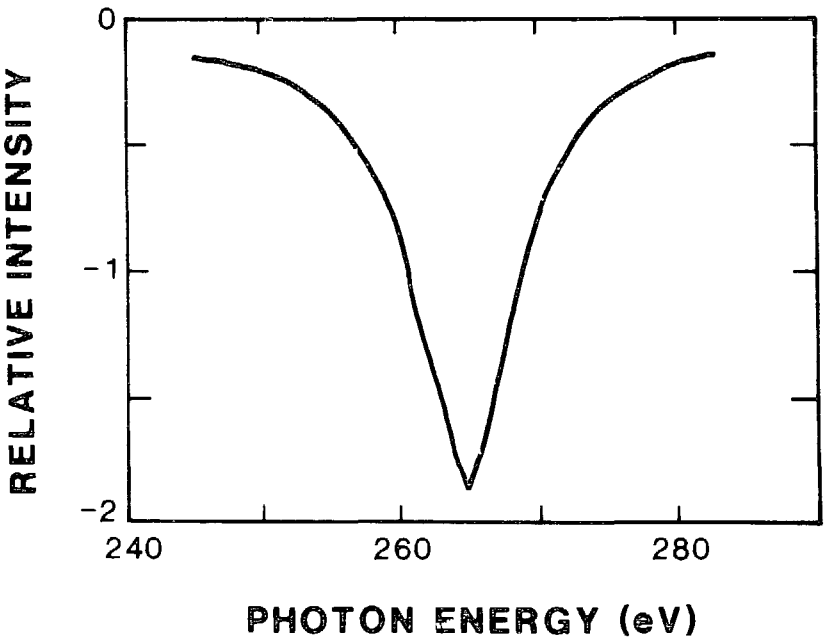

Fig. II-21. Typical diffraction profile of a metal multilayer crystal as measured on U3C.

spectroscopy (PES). Preliminary PES measurements on gold and carbon have been compared with earlier such data as calibrations of the system. In these studies we use primary photon energies between 200 and 800 eV, whereas past PES studies on heavy-fermion systems have concentrated on the resonance structure near 100 eV. We hope that by going to the higher excitation energies, we can minimize resonant structure and final-state effects to allow a better comparison with theory. For meaningful comparisons with the theoretical calculations, high-resolution data will be required. Resolving powers of approximately 1000 are necessary. This requirement will test the limits of the beamline. The experiments will be performed in collaboration with Neal Shin of Sandia National Laboratories, who is providing the PES sample chamber and associated equipment.

The characterization of U3C thus far shows that the line is functioning very near design specifications. Spectra showing the output of the Extended Range Grasshopper (ERG, named "grasshopper" for its physical appearance) monochromator for the 2.0-m, 3.7-m, and 5.0-m gratings are shown in Fig. II-22 (the original grasshopper has only a 2.0-m grating). The remaining characterization studies involve measuring and reducing harmonic and stray light content in the primary

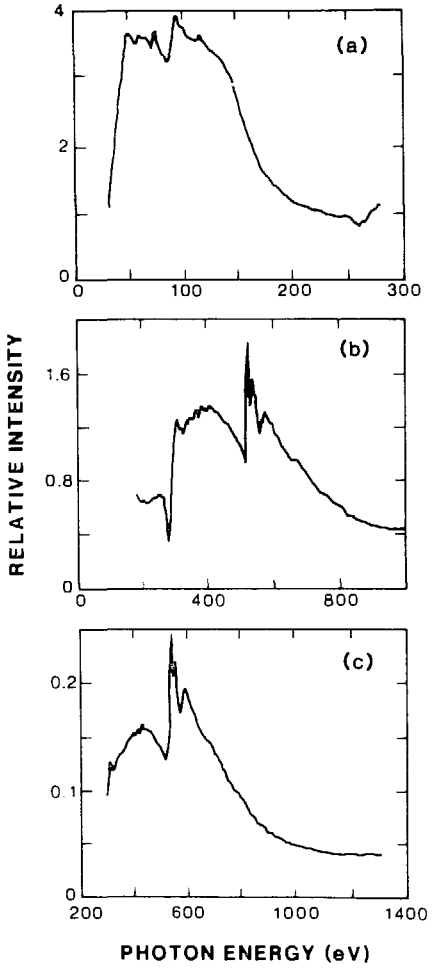

Fig. II-22. Spectra showing the output of the ERG monochromator for three gratings. (a) 2.0 m, (b) 3.7 m, (c) 5.0 m. An aluminum photodiode detector and 35-μm slits were used with all gratings.

monochromatic beam and measuring and improving the resolving power of the monochromator. The refocusing mirror and diagnostic chamber will be used in part of this effort.

Work has begun on the construction of U3A, the second VUV line. This is a focused "white light" beamline that will be used primarily for detector calibration and other specialized experiments.

The design for the hard x-ray beamline has been completed, and hardware procurement is underway. This proposed 5- to 25-keV beamline consists of a vacuum access line incorporating a four-crystal, fixed-exit-beam monochromator with a resolving power of 10^5. The harmonic and stray light will be reduced to less than 1% of the first-order light. From the monochromator, the beam will pass to an end-station apparatus, contained in a hutch, consisting of a beryllium window, an EXAFS system, an x-ray diffraction system featuring a 4-circle goniometer, and detector systems for radiometry. Some experiments may require windowless ionization chambers together with special pressure-monitoring equipment and perhaps a differential pumping system.

The design for the soft x-ray beamline is about 80% complete. This proposed 0.8- to 6-keV beamline consists of a vacuum access line incorporating a UHV double-crystal monochromator with a resolving power of 10^3 to 10^4. The line will be developed so that harmonic and stray light is reduced to less than 1% of the first-order light. From the monochromator the beam will pass to an end-station apparatus consisting of a UHV sample chamber and/or an ionization chamber EXAFS system and detector systems for radiometry.

Pegasus, a Megajoule Pulsed-Power Facility for High-Energy-Density Physics Research (P-1)

We are constructing a multi-use pulsed power facility called Pegasus, whose driving source will be a capacitor bank with 1.5 MJ of stored energy when charged to 120 kV. When fully charged, the bank will discharge a current of up to 13 MA in less than 3 μs into a low-inductance radial transmission line with provisions for a coaxial load in the center (total inductance ~10 nH). The center section of the radial feed will be of a tri-plate design, which will allow us to use two separate load chambers and will enable us to switch the current from one load to the other during a shot. This arrangement will provide complete physical isolation of, say, an exploding opening switch from a very fragile foil load for fast implosion studies. Experiments planned for the facility vary widely and encompass many areas, such as x-ray production, foil implosion physics, and opening switch performance, that are needed for programs in fusion, SDI, and weapons physics.

The bank will consist of four modules, each with a stored energy capacity of 360 kJ, based on technology developed by Maxwell Laboratories for the Air Force Weapons Laboratory capacitor bank, Shiva. Figure II-23 is a schematic drawing of the system. Detonator switches will be used to switch the bank because of their lower capital cost, greater current-carrying capacity, much lower probability of prefire, and greater inherent reliability as compared to spark-gap switches such as those used at Shiva. The switches are modular in construction and could allow us to schedule four shots per day if switch turn-around were the limiting shot-rate factor. Practically, however, the shot rate will be determined by the load turn-around time, for the current densities and magnetic field pressures normally used destroy the load section in the experiments. The detonator switches were developed and designed by P-1 in collaboration with Los Alamos Group M-7.

P-1 designed the tri-plate radial feed transmission line and matching coaxial load section. The center tri-plate section is ~3 m in diameter and is made of 5-cm-thick aluminum plates. The center section can accommodate most bank upgrades that will fit into the building housing Pegasus. The diameter of the bank is 6.8 m. The dielectric between the plates will be Mylar, and the tri-plate region is designed to withstand a 500-kV pulse for 1 μs. The plates were fabricated by an outside contractor.

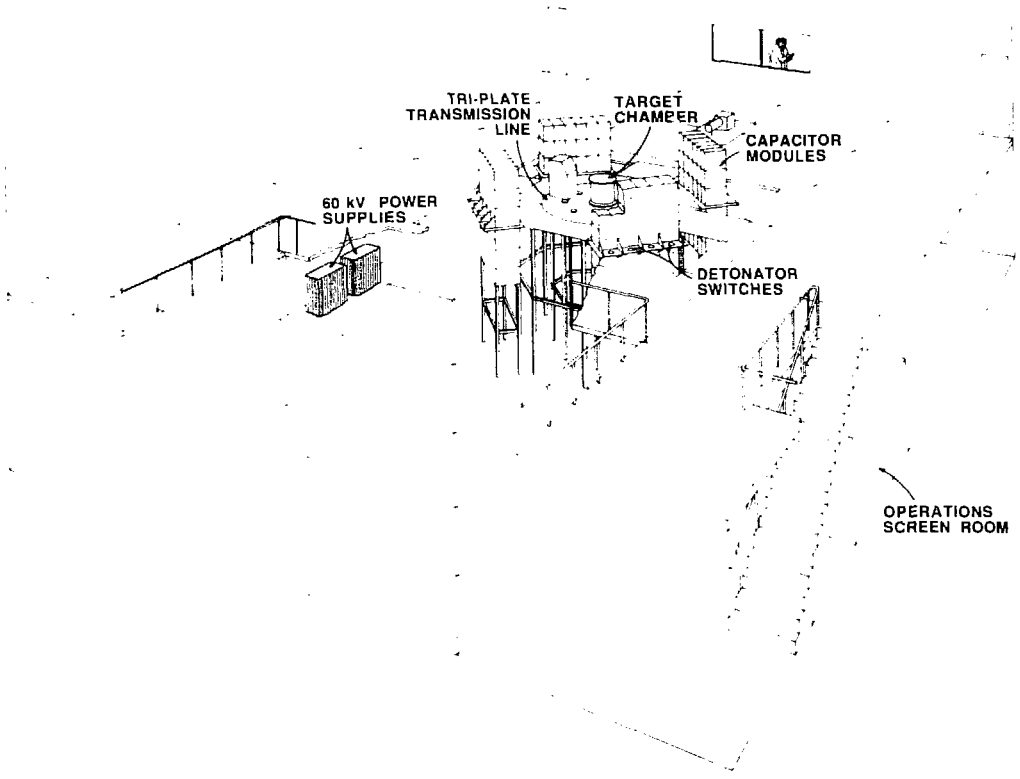

Fig. II-23. Pegasus four-module. 1.5-MJ fast capacitor bank.

An integrated computer system will perform all bank operations, data acquisition, and analysis. All peripheral equipment including computers will be operated on battery power through uninterruptable power supplies (UPS) during shots. All connections to all screen rooms will be fiber-optic cable or pneumatic lines. With this arrangement and the UPS system, ground loops and subsequent instrumentation problems are greatly reduced.

Ion-Beam Facility (P-9)

A new and complementary capability was added to the Ion-Beam Facility (IBF) this year. The two large electrostatic accelerators have served well in supplying particle beam with energies from 1 to 25 MeV (singly charged). The low end, below 1 MeV, has always been difficult: in order to obtain reasonable optical properties for the particle beam, we have had to electrically short most of the machine to keep up the electrical gradient over a short section. The new machine, a small tandem, fills this gap by providing beams in the energy range 0.2 to 3.4 MeV.

As delivered, the ion source produces only protons or deuterons, but an alpha source is planned for next year. The machine was purchased by ESS Division to perform calibrations for particle-detector systems mounted in satellites and space probes. It is available for general use under the auspices of P-9. The machine was installed in a room built for the large magnetic spectrometer (Q_3D). The original circular track built for Q_3D angular distributions will be used for neutron TOF angular distributions with the new accelerator.

III. LASER RESEARCH, DEVELOPMENT, AND APPLICATIONS

INTRODUCTION

Since their invention, lasers have been important tools for physics research. Because they can concentrate energy into high-power (terawatt), ultrashort (from nanosecond to less than picosecond) light pulses, and focus that power into small volumes, lasers are capable of producing very high energy densities comparable to those produced in nuclear weapons. As a result, physicists now have the opportunity to study the basic properties of atoms and plasmas under such extreme conditions and to determine how (or whether) laser-heated plasmas can be used to produce inertially confined fusion (ICF) burn in the laboratory.

Studies of laser-matter interactions aimed at addressing the uncertainties of ICF also challenge our basic understanding of matter at high energy densities. Thus, we are attempting to learn more about laser-plasma instabilities; energy transport and radiation emission in high-density, high-temperature plasmas; the physics of highly ionized atoms out of local thermodynamic equilibrium; and fusion capsule implosions and the associated hydrodynamic instability behavior. The laser-target research efforts described here also offer the possibility of spinoffs to other areas of research.

In addition, the Physics Division has been developing facilities that will provide new opportunities for research. Aurora is a prototype KrF laser (248 nm) that will test the feasibility of "angular multiplexing" architectures for such UV lasers and their applicability to ICF. While our initial goal is to test the laser technology, we hope to exploit the multikilojoule Aurora for both ICF research and weapons-related, high-energy-density physics research into such areas as hydrodynamics and instability growth, nonequilibrium radiation transport in highly ionized plasmas, and radiation flow.

A unique and exciting tool just coming into use as a research facility is the Los Alamos Bright Source, a picosecond KrF laser. Subjecting atoms and solid targets to the extreme, coherent, electromagnetic fields of this laser, at power densities of 10^{15} to 10^{20} W/cm^2, research at the Bright Source promises to open new regimes in the study of laser-atom excitation mechanisms; the structure and properties of multiply excited, highly ionized atoms; relativistic electron-photon interactions; and other frontiers of atomic and plasma physics research.

The Division has engaged in a variety of studies in laser physics and technology in order to develop the possibilities offered by these new tools. Some of the continuing research activities are discussed here. In addition, we describe the Division's work toward the development of a heavy-ion source that would ultimately be coupled to a large accelerator; if successful, such a source could supplant lasers as drivers for ICF and high-energy-density research.

HIGH-ENERGY-DENSITY PHYSICS RELATED TO INERTIAL-CONFINEMENT FUSION

X-Ray Production and Dynamics of Short-Wavelength Laser-Produced High-Z Plasmas (P-4, P-14, X-1, University of Rochester/LLE)

In high-atomic-number plasmas (e.g., gold) heated by high-intensity (10^{13} to 10^{15} W/cm^2), short-wavelength lasers ($\lambda < 500$ nm), a significant portion of the absorbed laser energy can be reradiated as soft x rays (mostly below ~1 keV). This fact can be important for "indirect-drive" approaches

to ICF. When this technique is used, the laser energy is converted to x rays, which are then used to ablate and compress a pellet containing deuterium-tritium (D-T) fuel. Experiments and radiation-hydrodynamic simulation codes such as LASNEX, which is used to design ICF targets, indicate that x-ray emission increases at shorter wavelengths because light is absorbed at higher plasma densities, leading to cooler plasmas with lower hydrodynamic energy losses. An increase in x-ray conversion efficiency is also expected as the laser irradiation intensity is reduced. Several years ago, however, experiments with planar gold targets at the Argus laser at Lawrence Livermore National Laboratory (LLNL) showed a decrease of x-ray emission below $\sim 10^{14}$ W/cm^2. In order to understand which aspects of the laser-target physics were responsible for this effect, we have for the past two years undertaken a series of experiments at the University of Rochester OMEGA laser (λ = 351 nm), in collaboration with the Rochester experimental team.

In these experiments, we attempted to perform uniform irradiations of spherical targets consisting of CH substrates with gold coatings of various thicknesses. The spherical geometry simplifies theoretical analysis as well as the integration of measured x-ray emission over solid angle. We investigated LASNEX model predictions of several observables including the depth of energy penetration during the laser pulse, the time-dependence of x-ray emission, the radial extent of the x-ray emitting region, and the x-ray emission spectra. We have done this over a range of incident intensities from 4×10^{12} to 4×10^{15} W/cm^2 by varying the target size at a fixed laser energy. We expect significant changes in these observables over this intensity range, with particularly important changes in the spatial localization of the x-ray emitting region occurring near 10^{14} W/cm^2. We also compared nominally identical experiments using two different laser-energy/target-size combinations to achieve the same on-target intensity.

To study these issues comprehensively, we measured time-resolved absolute x-ray flux below 2 keV using an x-ray-diode spectrometer, detailed spectra (both time-integrated and time-resolved using x-ray streak cameras) from 0.3 to 3.5 keV, and x-ray emission spatial distributions with microscopes and pinhole cameras. In addition we monitored the laser energy absorption and the signatures of plasma instabilities occurring in the laser-plasma interaction.

The x-ray conversion efficiency $E_{(h\nu<2\ keV)}/E_{absorbed}$ showed a puzzling behavior (Fig. III-1). Our first experiments using only six beams of OMEGA and about 250 J (in a 600-ps laser pulse)

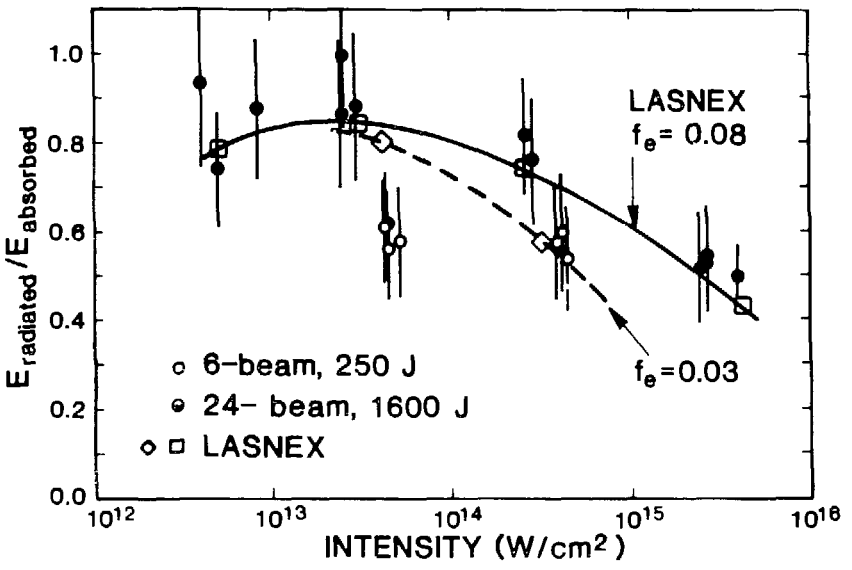

Fig. III-1. X-ray conversion efficiencies from spherical gold-coated targets irradiated by 600-ps pulses of 351-nm laser light (f_e is a measure of thermal flux transport inhibition; f_e = 0.08 is near-classical heat transport, and f_e = 0.03 is inhibited transport that was required to match plane-target data).

produced results very similar to the LLNL flat-target data and disagreed with theoretical predictions. However, our later 24-beam, 1600-J experiments showed a very different intensity dependence, in agreement with the LASNEX simulations. These simulations predict essentially no dependence on the laser-energy/target-size combination for a given intensity.

By varying the thickness of the gold layer so that the laser "burns through" (ablates all of the gold) during the laser pulse, we determined the depth of laser energy penetration and the radial extent of the x-ray emitting region. High-Z materials like gold are much more efficient radiators of soft x rays than are low-Z materials like CH; thus, as the layer thickness is reduced so that CH replaces gold in the plasma during the laser pulse, the x-ray emission is reduced. Because the radial extent of the emitting regions should become narrower (reduced from $\sim$50 μm to $<$10 μm) as the intensity is increased above 10^{14} W/cm^2, we expect a more abrupt reduction at the time of burnthrough for high-intensity than for low-intensity shots. In our experiment, burnthrough depths are of the order 100 to 1000 Å.

The time-integrated measurements of x-ray emission as a function of gold thickness (for both 6- and 24-beam experiments) indicate that the energy penetration depth and the radial extent of the emitting region are apparently well modeled over our intensity range. Corroborating data exist on the energy penetration depth (from plasma instability threshold measurements and the onset of carbon emission lines in the x-ray spectra) and on the extent of x-ray emission (from x-ray microscope images of the target limb). Time-resolved measurements show most of the expected gross features: sub-keV x-ray emission is abruptly reduced at burnthrough time for high-intensity shots, although the post-burnthrough emission is greater than the calculations predict (Fig. III-2); it persists after burnthrough for lower intensities. More subtle details of the emission histories are less well calculated. On the basis of all of these measurements, it appears that the LASNEX simulations are correctly predicting the gross hydrodynamics and energy flow in these laser-produced plasmas.

However, time-integrated sub-keV spectra (obtained for the 24-beam data only) show details that differ significantly from the calculations. The emission near 250 eV (attributed primarily to transitions into the gold O-shell) is considerably stronger than calculated relative to the 400- to 900-eV emission (attributed primarily to transitions into the gold N-shell). A dependence of the N-line emission strength on gold layer thickness also appears in the data but not in the calculations, suggesting that even though the calculated radiated energy agrees with experiment in the 24-beam case, the emission processes are not correctly modeled in detail. This possibility is also suggested by the detailed differences between the calculated and the measured late-time emission histories (Fig. III-2). On the other hand, the centroid of the N-line emission shifts from 400 eV at 4×10^{12} W/cm^2 to 800 eV at 4×10^{15} W/cm^2 as the mean charge state of the emitting gold increases, in good agreement with the predictions.

Thus we have learned that the spatial and temporal dynamics of these high-Z plasmas — in particular, the hydrodynamics, energy penetration, and localization of x-ray emission in the plasma — appear to be generally well modeled. We have also identified a number of aspects of the experiment that suggest problems in the atomic or radiation physics modeling that goes into the LASNEX simulations. These plasmas are not in local thermodynamic equilibrium (LTE), and current models assume an "average-atom" model of the plasma to make non-LTE calculations tractable. Theoretical work needs to be done to address these issues and to assess the impact of megajoule-scale experiments on predictions.

Furthermore, while the 24-beam kilojoule experiments produce high x-ray conversion efficiencies comparable to the theoretical predictions, the 6-beam, 100-J experiments agree with the previous low-energy planar experiments and diverge from the predictions at low intensity. No such scaling of the target radiation energetics is predicted by the modeling. More experimental and theoretical work addressing this issue is required.

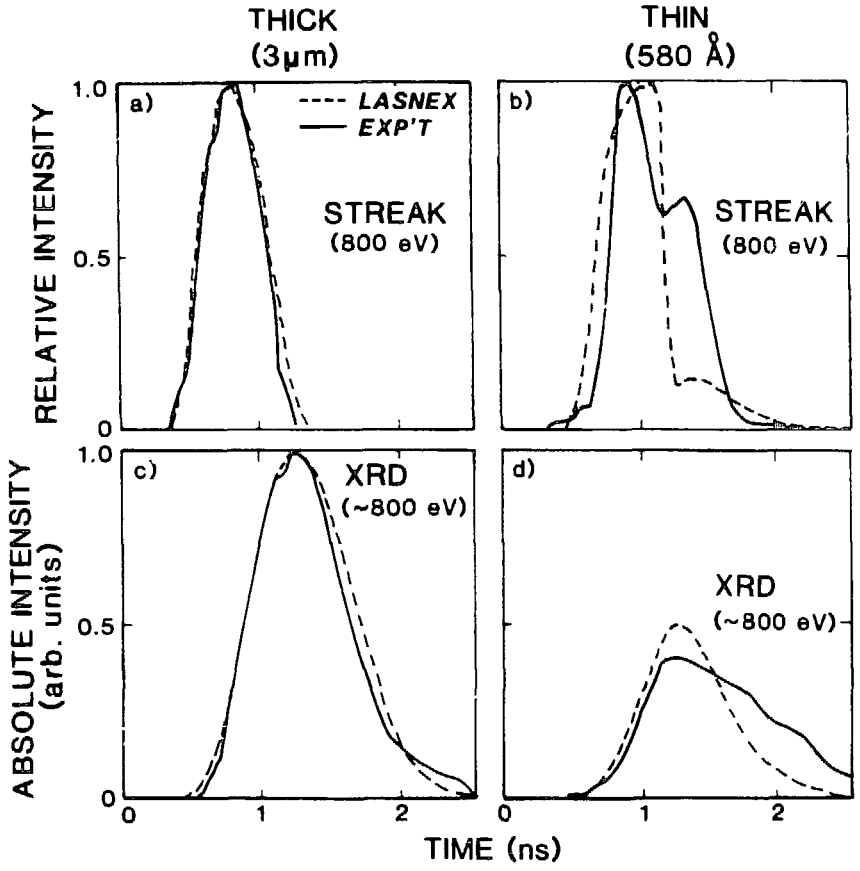

Fig. III-2. X-ray emission histories for thick and thin gold-layered spherical targets in the spectral region of the gold N-lines (800 eV). All data are at 4 × 10^{14} W/cm^2 irradiance. Time resolution was ~300 ps for x-ray-diode (XRD) data and ~15 ps for streak data.

Transient X-Ray Diffraction; Application to X-Ray Switching and Study of Transient Materials Properties (P-4, University of Rochester/LLE)

We are studying experimentally the changes in the x-ray diffraction properties of crystals under intense subnanosecond laser heating. Historically, the basic motivation for this work has been the need for investigations of fast x-ray switching and shuttering techniques; more recently, we have also become interested in the study of basic transient materials properties (such as phase changes) and of shock propagation and elastic-plastic response in opaque materials.

Although several techniques for switching x-rays have been known for over a decade, these techniques have been experimentally demonstrated only to the limit of the tens-of-nanoseconds time scale. Our work on transient x-ray diffraction has led to a method of switching x-rays on a time scale of hundreds of picoseconds. The basic idea is shown in Fig. III-3. We produce an intense source of line radiation for a period of 1 ns by focusing a high-power laser beam on a target containing an appropriate element. The x-ray lines of interest are then Bragg-reflected from the diffracting crystal. During the x-ray pulse, a second laser beam, delayed with respect to the first, illuminates the crystal. The large temperature gradient (and shock) subsequently induced in the crystal gives rise to a thermal strain, which significantly broadens the rocking curve of the crystal and reduces the peak

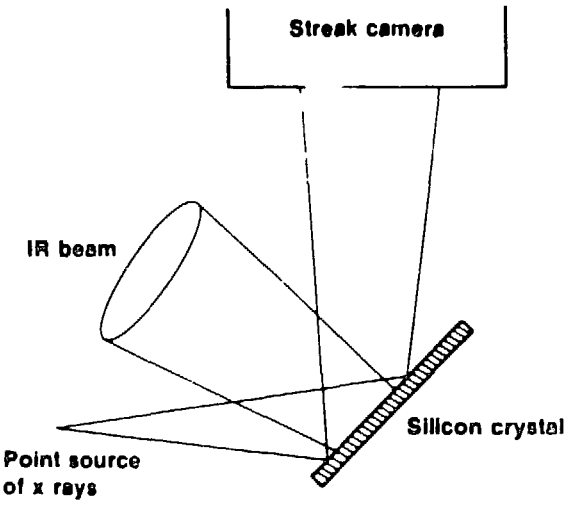

Fig. III-3. Experimental setup for study of transient x ray diffraction

reflectivity. The angular distribution of the diffracted radiation is thus altered, and with appropriate placement of beam blocks, both on-off and off-on switching of x-ray line radiation should be obtained on the time scale of the thermal strain induction, as described in the paragraphs following.

One beam of the LLNL Phoenix laser, containing 25 J of 0.53-μm light in a pulse of FWHM 1 ns, was focused down to a 30-μm-diameter spot on a polyvinylchloride (PVC) target, producing an intense source of the resonance line of helium-like chlorine at 4.44 Å. This radiation was diffracted from a silicon (111) crystal into an x-ray streak camera with a CsI photocathode. During the diffraction process, the crystal was illuminated with an irradiance of about 1 J/cm ^{2} of 1.05-μm light covering approximately 10 cm^2 of the crystal surface.

Typical experimental results are shown in Fig. III-4. Figure III-4a shows the temporally resolved spectrum of the radiation diffracted from an unirradiated crystal. The two lines are the resonance and intercombination lines of helium-like chlorine. The dielectronic satellite lines, which appear as a broad band on the higher wavelength side of the other two figures, are not present here because of a slight misalignment of the crystal that caused the satellite to miss the photocathode. Figure III-4b shows the diffracted radiation from an illuminated crystal, the peak of the heating beam delayed with respect to the peak of the x-ray-producing beam by 500 ps. The lines broaden and merge together toward the end of the pulse. In Fig. III-4c, no delay occurs between the heating and the x-ray-producing pulse, so broadening is evident early in the pulse. The broadening is sufficient to completely smear out the three original peaks discernible at the start of the pulse. From the angular separation of the peaks (~1000 arc seconds), we gain an approximation of the width of the rocking curve of at least 500 arc seconds. This value compares with an original width (in the unperturbed crystal) of ~50 arc seconds.

A theoretical model of the alteration of diffraction has been constructed and applied to the analysis of these data. The model indicates that the measured rocking curve is highly sensitive to the details of the thermal strain profile in the material. New applications thus suggest themselves: in addition to practical subnanosecond switching of x-ray line intensities by laser illumination of a crystal, the technique of temporally resolved diffraction offers significant potential for investigations of transient properties of materials under extreme conditions. Areas of interest include the observation and study of the transition from elastic, uniaxial compression to plastic flow behind shock waves and of shock-induced or other transient phase transformations. All of these applications are being pursued in near-term experiments.

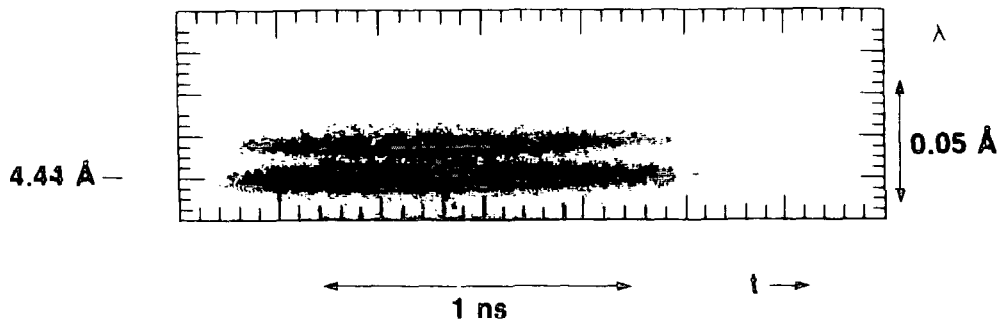

(a) **Streak from an unirradiated crystal**

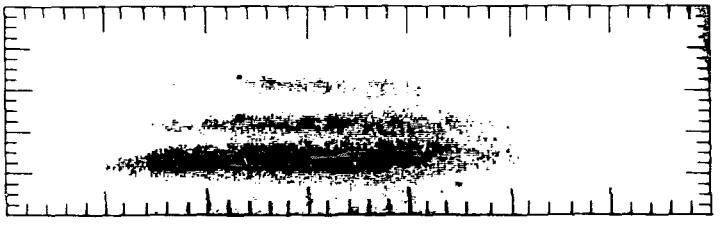

(b) **Heating pulse 500 ps after x-ray-producing pulse**

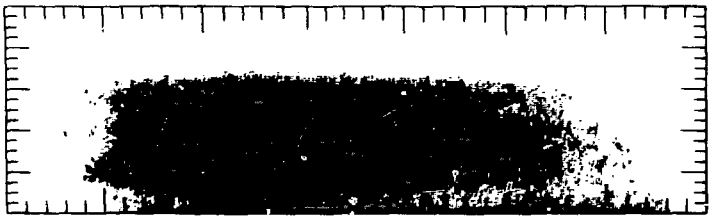

(c) **Heating pulse coincident with x-ray-producing pulse**

Fig. III-4. Experimental data for transient x-ray diffraction.

High-Density Implosion Research (P-4, University of Rochester/LLE)

Impressive progress has been made recently toward attaining the extremely high densities ($>10^{24}$ e^-/cm^3) known to be required for success in inertial confinement fusion. To further this progress, we have performed experiments on the Omega laser at the University of Rochester and have developed calculational and analytical techniques for measuring and characterizing very dense plasmas.

As compressed (electron) densities rise well above 10^{24} cm^{-3} in laser implosion experiments, we encounter some formidable problems in using the traditional radiation (spectroscopic) diagnostic

techniques: for example, the compressed core may be too cool for useful self-emission, or it may be surrounded by a high-areal-density pusher that does not allow emission to escape.

Nuclear diagnostics will continue to receive considerable emphasis, but spectroscopic measurements must be pushed as far as possible because of the wealth of information, both temporally and spatially resolved, that they provide. Perhaps most important, radiation/spectroscopic diagnostics may be of considerable value to basic hydrodynamic and instability studies of laser implosions. One way to extend the range of usefulness of radiation diagnostics is to develop absorption spectroscopic techniques, such as those we have been exploring for several years.

Last year, we developed new calculational techniques and applied them to older data from the Los Alamos HELIOS laser (λ = 10 μm). In addition, we have performed tests of new absorption spectroscopic techniques on the Omega laser (λ = 351 nm).

The absorption spectroscopic studies performed on HELIOS were in the so-called self-backlit mode, illustrated in Fig. III-5. Under the conditions that were prevalent in HELIOS implosions, high temperatures are obtained in the core. The continuous x-ray emission from the core passes out through the pusher and undergoes absorption at wavelengths characteristic of atomic species in the tamper. The resulting absorption lines can yield information on the temperature (T_e), the density (ρ), and the ρR product (density times thickness) of the tamper. A typical example of absorption spectra resulting from such experiments is shown in Fig. III-6.

We have successfully modeled these results by developing and using several calculational codes. For example, we used the OPLIB opacity tables (Group T-4) to generate detailed absorption data as a function of material temperatures and densities. This information was in turn incorporated in LASNEX hydrodynamic models of particular laser implosion shots. (We also developed a small stand-alone code to begin to assess non-LTE effects.) With this direct prediction of diagnostic measurements, experiment and modeling can be readily compared. Detailed characterization of pusher conditions, temperature, density, etc., is now possible. The natural extensions of this work are 1) time-resolved measurement of the absorption lines in order to give pusher parameters as a function of time during the implosion; and 2) use of an external source of radiation to perform the absorption probing, which would allow for the absorption measurements to be made even when self-emission cannot be used.

We performed a series of tests using an external radiation source on the Omega laser system. The problem is to arrange for adequate spectral coverage while probing the physically small compressed core. Because crystals are used as the dispersing device, the spectral coverage translates to angular dispersion from the backlighting source. In our tests on Omega, we used a variety of source materials to produce strong bands of radiation. Surrogate targets (unheated) that were of the same size as typical compressed cores and had absorption edges in the spectral regions of interest were backlit in these tests. Our results demonstrated that our system had the following characteristics: adequate spectral coverage, adequate spectral resolution (largely determined by the effective source size of the backlighter), and adequate spatial discrimination in the simulated compressed core. Tests of this sort, on actual laser-compressed targets, are planned for the near future.

The development of these new techniques opens up many new possibilities for implosion research. One particularly interesting area is basic hydrodynamic and instability experiments. Specific instability experiments are being designed in both spherical and cylindrical geometries for the Omega and the Nova (LLNL) lasers. Absorption spectroscopic backlighting will be used as a key element of these experiments, together with the kind of calculational analysis techniques discussed.

Long- Versus Short-Pulse CO_2 Laser Irradiation of Solid Spherical Targets: Evidence for Different Turbulent Regimes (P-4, X-1)

In the 1970s, CO_2 lasers looked promising as drivers for imploding deuterium-tritium fuel to the temperatures and compressions required for practical thermonuclear energy yield. They had been proven to have characteristics that could be scaled to large sizes, good energy efficiency, good

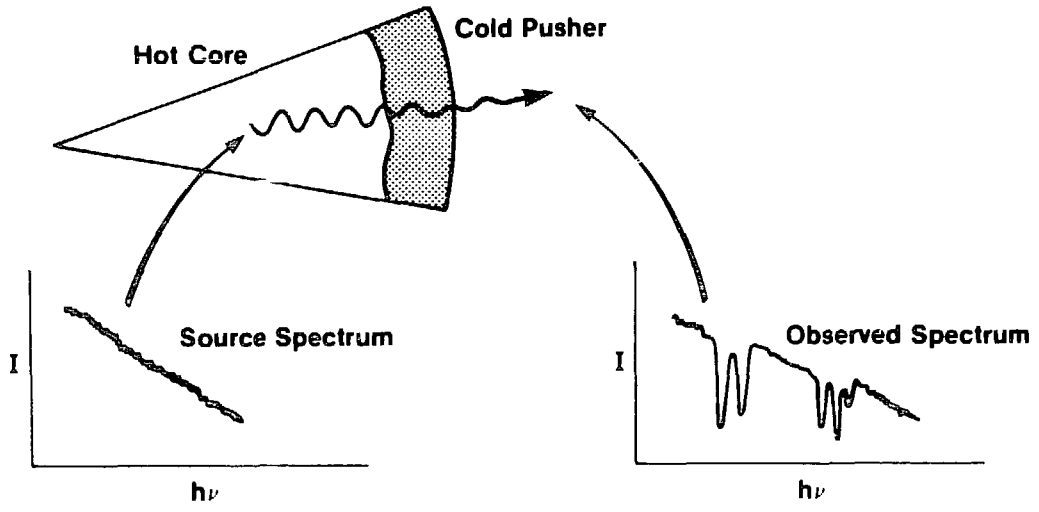

Fig. III-5. Diagnosis of pusher conditions with absorption spectroscopy.

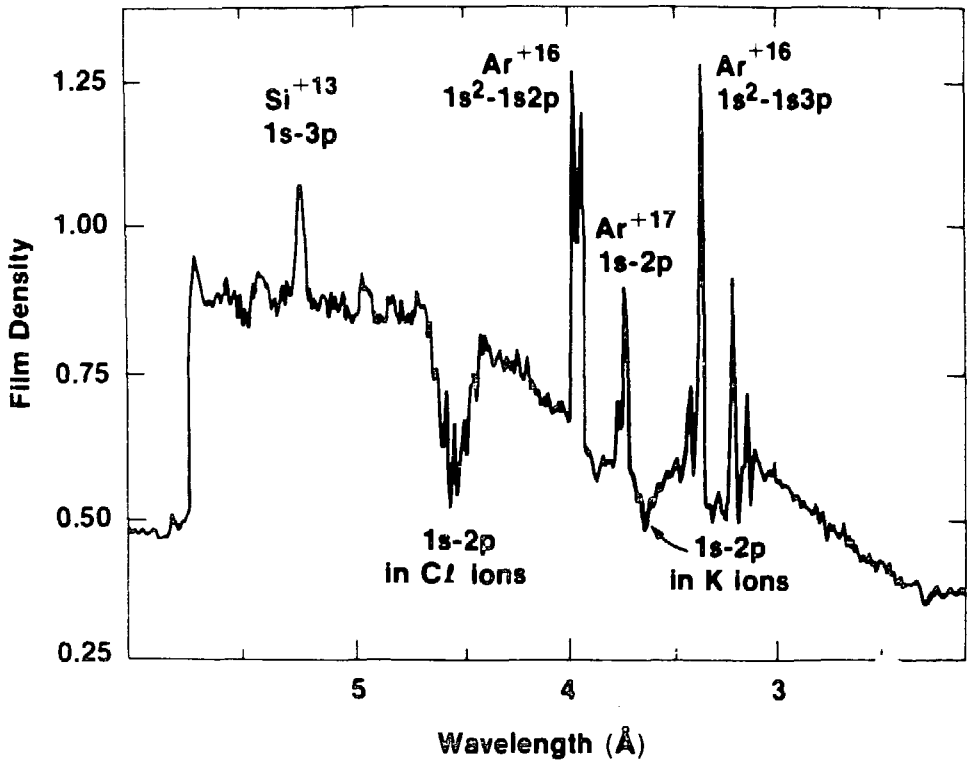

Fig. III-6. Absorption lines from CO_2-laser-imploded targets: glass shells, KCl + CH coating layers, DT + Ar fill.

focusability, and apparent drive uniformity arising from lateral hot-electron transport. They showed promise of offering a high shot-repetition rate, and they were expected to be relatively economical in terms of both construction and maintenance costs.

A decade of research with CO_2 lasers (using 1-ns laser pulses) has disclosed a formidable problem: the laser energy absorbed by the target is converted directly to high-energy suprathermal ("hot") electrons. These electrons penetrate the outer (ablator) layers of the target and raise the temperature of the central D-T fuel before it can be compressed by the implosion. Perhaps more important, the hot electrons reduce the effective energy coupling because of the gentle ablation pressure profile arising from hot-electron penetration and because of energy losses to the acceleration of high-energy ions. The temperature T_h of these electrons can be hundreds of keV and scales roughly as the square root of laser intensity. Hot-electron distributions are generally inferred from the high-energy x-ray bremsstrahlung spectra they produce when stopped by the target material. Many ways of reducing (or using) the production of hot electrons have been tried without success.

The motivation for investigating the long-pulse (>5-ns) regime stemmed primarily from its relevance to driving reactor-size targets, which require drive pulses considerably longer than the 1 ns at which most of the CO_2 database had been obtained. In particular, because of the complexity of competing processes for the generation of hot electrons in the extended low-density plasma produced by long pulses, it was not clear whether T_h would rise, fall, or stay the same in the long-pulse regime. Hence, we needed to resolve this important question empirically.

We have partially answered the question for directly driven targets by an extensive series of experiments at the Antares CO_2-laser facility. In these experiments we used short (1.4-ns FWHM) and long (5-ns) pulses incident on solid spherical copper targets coated with a 50-μm-thick layer of gold. (Figure III-7 shows the shape of the long pulse.) The short-pulse intensity scaling law for T_h was obeyed for long pulses on large targets, but an additional reduction factor of 1.7 was found for small targets. Encouraging as these time-integrated results are, the time-resolved results from hard-x-ray spectrometry are even more significant because they indicate that pulse shapes different from those employed could achieve a much greater reduction of T_h.

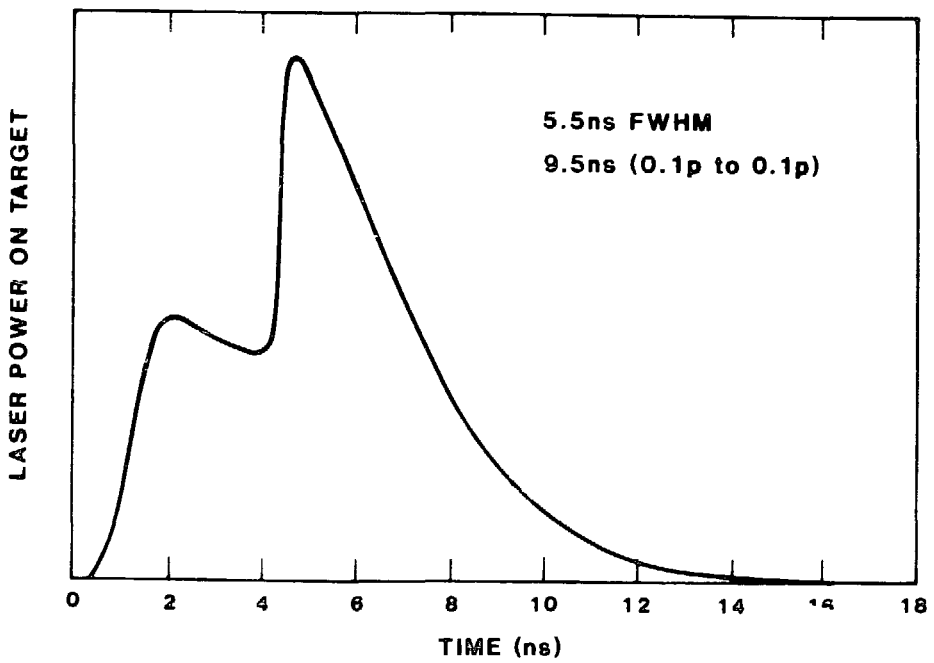

Fig. III-7. Typical long-pulse laser-power profile obtained from the addition of two CO_2 lines

The temporally deconvolved results from a hard-x-ray spectrometer show a decline in T_h from the initial 300 keV to 35 keV at 5 ns, when the laser pulse is just past the main peak and considerable laser energy still remains to be delivered (Fig. III-8). (In some other cases, the reduction at 5 ns is a factor of 4 instead of 9, but the pattern is basically the same.) The correlation of T_h is apparently stronger with the derivative of the laser power than with the power itself.

The dependence of T_h on the rate of rise of the laser intensity had been suggested several years ago as a consequence of the predicted strong dependence of the local plasma turbulence on the local rate of power rise. The turbulence-induced T_h was expected to be very high when the power was rising steeply and low when the power was constant or declining. Also anticipated was a strong but rapidly declining initial spike in T_h. In these model calculations, the dependence of the turbulent state on the risetime of the laser pulse is invoked by changing the boundary conditions of the plasma calculation from an equilibrium to a nonequilibrium regime when the laser risetime is faster than a turbulence-induced collision time, assumed to be approximately the ion-acoustic collision time. The nonequilibrium calculation produces an enhanced population of very energetic electrons. What is new here is the dependence of the turbulent state on the laser risetime, which was not invoked in previous work. The expectations of this model are consistent with the time-resolved hard-x-ray data from long-pulse shots. (Short-pulse shots cannot be adequately deconvolved by our procedure because of the limited bandwidth of the detection system.)

The implication of this model of plasma turbulence is that the pulse shapes employed in the long-pulse experiments were only marginally suited for producing low turbulence and low T_h. A somewhat longer pulse with a slow, monotonic rise to a level value should result in a dramatic

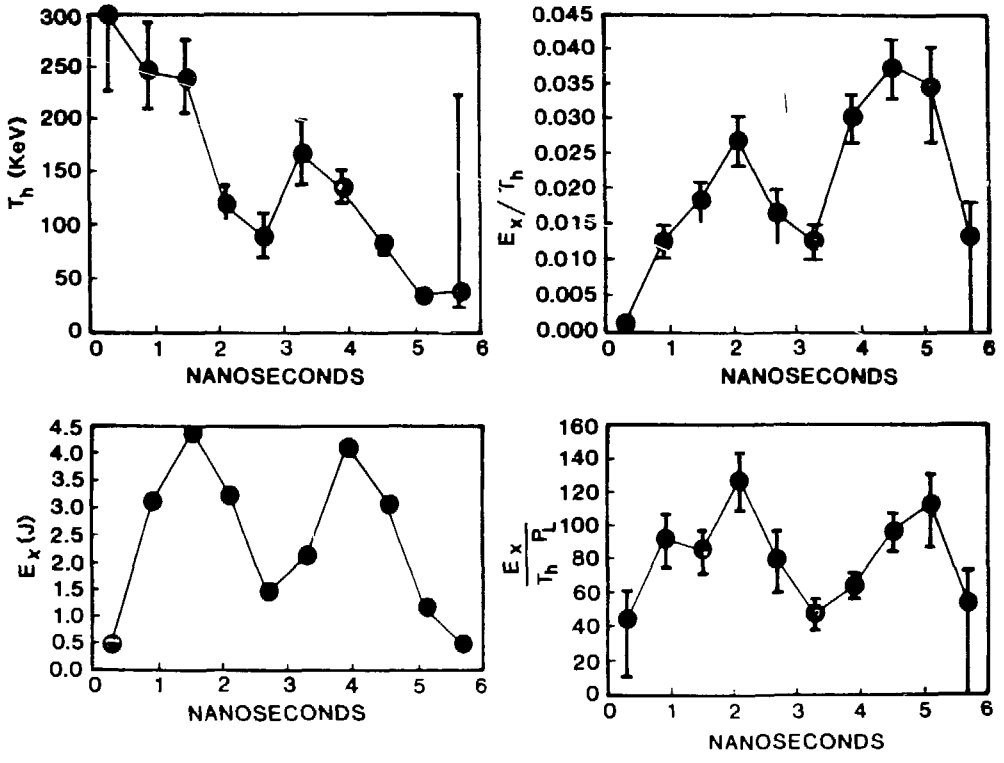

Fig. III-8. Temporally unfolded results from hard-x-ray spectrometry for a 2.1-mm-diameter target irradiated with 20-kJ long pulse. Upper left, hot electron temperature T_h; lower left, radiated x-ray energy E_x in each time bin; upper right, E_x/T_h (proportional to electron energy deposited in target); lower right, E_x/T_h divided by laser power, P_L (proportional to fraction of laser power deposited in target).

further reduction in T_h beyond what has been observed. Achieving much better uniformity of laser irradiation than we obtained in the long-pulse experiment is also predicted to be important.

A central question regarding the efficacy of long pulses for driving implosions concerns the fraction of the incident laser energy absorbed by the target and the fraction actually deposited in the ablator (the effective absorption fraction). The laser absorption fraction as a function of target diameter is about the same for long pulses as for short.

The issue of effective absorbed energy (absorbed energy minus that lost to driving coronal-plasma expansion of fast ions) is more complex and not completely understood. However, the hard-x-ray yield due to hot electrons, inferred from bremsstrahlung emission above ~30 keV, implies greatly reduced preheating; but these data are not immediately interpretable in terms of ablative drive, which depends on the distribution of thermal energy in the ablator. As an indicator of thermal energy, soft-x-ray power as a function of time (obtained from spectrometry in the <3-keV region) for short- and long-pulse shots on 620-μm-diameter gold targets shows a factor-of-2.4 enhancement of total soft-x-ray energy in the long-pulse mode relative to the short; x-ray conversion is enhanced from <2% of incident energy to ~5%. Also of interest, the ratio of soft-x-ray energy (3 eV to 3 keV) to hard (>30 keV) is nine times larger for long pulses than for short (independent of target diameter). Finally, calculations show agreement with data obtained in the intermediate region of photon energy, 3 to 15 keV, indicating that the total x-ray energy above ~3 keV is somewhat larger in the long-pulse mode than in the short.

These experimental results, showing greatly reduced T_h along with a marked downshift to softer x-ray energy, by themselves augur well for an improvement in implosion drive over our initial estimates for Antares, which were based on short-pulse data from HELIOS. Coupled with the implications of a [illegible]na turbulence model, which predicts that we could obtain a much greater reduction in T_h, as well as spectral downshifting, by employing an improved pulse shape and better irradiation uniformity, these results can lead to the conclusion that long-wavelength lasers might drive implosions more effectively than we previously believed. However, whether CO_2 lasers could compete effectively with lasers of shorter wavelength remains doubtful.

LASER PHYSICS

EAGLE Laboratory (P-16)

The EAGLE (Excimer and Gas Laser Experimental) laboratory was established at the beginning of FY86. The purpose was to examine key kinetic processes that take place in KrF (248-nm) lasers and to find ways of increasing laser output and efficiency. Collaboration with theoreticians revealed the importance of determining accurate cross sections and rate constants for the updating of computer codes. An emphasis was therefore placed on conducting basic research on the KrF system using commercial excimer lasers as tools for probing a controlled volume of gas.

Several key experiments were identified. Earlier experiments on XeCl (308-nm) had demonstrated an increase of up to 50% in the energy output of a discharge-pumped XeCl laser seeded by as little as 10 mJ (less than 10% of the unperturbed energy output) of 308-nm radiation. This experiment was repeated in the EAGLE laboratory on KrF. We obtained an energy enhancement of up to 50% when a KrF laser was seeded with a small amount of 248-nm radiation. This result has been identified as an optical (not a photochemical) effect.

In addition, because Kr_2F^* is suspected to be an important nonsaturable absorber in KrF lasers for the ICF Program, both absorption and emission studies of this molecule were undertaken. The experimental results over the past year have been encouraging. In the tabletop experiments, Kr_2F^* is strongly produced through photoassociation of the KrF B state, followed by three-body formation. This allows studies of Kr_2F^* to be performed in an environment free of other molecular species. Preliminary investigations indicate that the KrF D state is the product of Kr_2F^* absorption of

248-nm photons. We have also determined that the Kr_2F^* absorption cross section at 248 nm is much smaller than expected, which suggests the presence of another strong absorber in electron-beam-pumped devices.

We are currently conducting optical absorption studies to determine whether the upper laser level (B state) of KrF is itself absorbing 248-nm photons. At present, this process is not included in the computer codes used to model KrF lasers. Also, we are planning experiments that will determine the effect of temperature on absorption cross sections and formation rate constants. This work is crucial to our obtaining a better understanding of the KrF laser and will continue to provide insights into the future direction of the Laboratory's commitment to KrF.

Effect of Radiation on Optics (P-16)

Laser optics — mirrors and windows — may be subject to ionizing radiation, e.g., to x rays from e beams. Radiation is known to darken fused silica and ionic crystals (F-center formation), and some of the darkening is known to be transient. Our study is directed toward determining the effect of radiation on the operation of a laser.

The approach is to pass light through a sample of window material or reflect it from a mirror and, at the same time, irradiate it with an electron beam from a Febetron 705 accelerator. The wavelengths of interest are the UV (KrF, XeF), the 4-μm (DF), and the 10.6-μm (CO_2).

Preliminary results obtained at 248 nm show radiation-induced darkening of fused silica windows, with at least three different recovery times, in agreement with previous measurements.

This work will not only help us to determine the effect of ionizing radiation on lasers but will also contribute to our knowledge of the mechanism of radiation darkening.

FACILITIES DEVELOPMENT

Aurora: A KrF Laser System for Inertial Confinement Studies (P-DO, P-4, P-5, P-7, P-12, P-16)

Aurora is a multikilojoule KrF laser system used to address many issues in the ICF endeavor. It will demonstrate the critical technologies involved in scaling KrF drivers to high energy and will serve as an engineering test bed for megajoule-class laser-fusion systems. In particular, Aurora will be used to examine the following:

- Uniform e-beam pumping of large laser volumes
- Efficient energy extraction from the KrF medium
- Optical angular-multiplexing systems that can be scaled to large system designs
- Control of amplified spontaneous emission (ASE) and parasitics
- Alignment of multibeam systems
- UV pulse propagation over long paths
- Staging of large KrF amplifiers
- Novel approaches to optical hardware that can lead to cost reductions for larger systems
- Target physics

The basic approach is to replicate the 5-ns front-end output pulse using aperture slicers, beam splitters, and mirrors to produce a 480-ns-long pulse train consisting of 96 beams, each of 5-ns duration. These angularly separated encoded pulses are adjusted individually at the entrance pupil of an optical relay system. The beam train is then relayed through two single-pass laser amplifiers (the preamplifier, or PA, and the intermediate amplifier, or IA) and through a double-pass laser amplifier (the large-aperture module, or LAM). The beam train is aligned to this point by two automated alignment systems. One system points each of the 96 beams through the entrance pupil of the PA at the correct angle. The second keeps the primary mirror of the LAM aligned in real time.

To deliver short-pulse KrF laser energy to fusion targets, the complete system will include a target facility and decoder (demultiplexer) optics to remove the time delays from the multiplexed beam train.

If we are to apply KrF lasers to ICF economically, the laser aperture must be scaled to large sizes because the energy output increases rapidly with increases in the size of the components. The LAM is the final amplifier of Aurora and is representative of the size of the KrF laser amplifier module believed to be needed for a fusion-prototype system. The laser aperture is 1 m by 1 m, and the active gain length is 2 m. It has produced more than 10 kJ of 248-nm laser radiation when configured as a nonoptimized unstable resonator. The LAM is the largest and most energetic existing UV laser of its type so far reported.

The Aurora laser system will serve as a straightforward scaling test to a size that is at the state of the art. System integration is underway, and the goal is to finish the baseline Aurora system by FY88 so that target experiments can begin at this versatile new source. Here, we discuss some of the progress that has occurred this year in the Aurora development effort.

Aurora Front End. An interim front-end system has been operational for several months. This system is required to produce a 5-ns pulse at energies of 250 mJ and a contrast ratio of 100/1 for the first demonstration of angular multiplexing (improved contrast is required for target experiments). A Pockels cell switch-out approach has been implemented and is producing a single 5-ns, 18-mJ pulse at a contrast ratio of 12,000/1. This pulse is then split and amplified in parallel in two discharge-pumped amplifiers, yielding a combined pulse energy of better than 450 mJ and a contrast ratio of 100/1. The low contrast ratio of the final output is the result of amplification without temporal multiplexing and can be improved at the expense of system complexity. The ultimate output contrast ratio, however, is limited to approximately 10,000/1 by the switch-out leakage and subsequent amplification in a nonenergy-storage amplifier. The total timing jitter of the 5-ns output pulse relative to a fire command signal is 2 to 3 ns, and long-term timing drifts over several hours are less than 10 ns. This interim system has been used to demonstrate a full 96-beam pattern at the input to the PA without interstage amplification by the small-aperture module (SAM).

Gain Characterization of Aurora Amplifiers. Small-signal measurements have been conducted on the large electron-beam-pumped amplifiers in Aurora. To date, these measurements are most extensive for the PA. The first large-volume amplifier, the PA has a gain length of 3 m and a 20-cm-by-20-cm aperture. The purpose of the measurements was to determine whether the pumping reliability and the spatial and temporal gain uniformity of the device met design goals. The measurements were made using a small Lasertechnics KrF probe laser, with the beam split into three separate beams to sample the gain at three points during each shot. A beam splitter and reference diode monitored the intensity of the probe laser pulses entering the amplifier chamber. Three additional photodiodes monitored the intensity of the amplified signals. Because the probe-laser pulse was less than 20-ns FWHM, it measured the gain effectively at a single point in the 600-ns amplifier pulse. Varying the time delay of the probe pulse allowed us to perform temporal measurements.

Preliminary results indicate that the PA meets the design criteria. Overall average peak small-signal gains of better than 100 have been recorded, far exceeding the design goal of 50. The time-

dependent measurements indicate a gain curve that, although not flat, is greater than 50 for about 500 ns; thus, sufficient amplification is provided for all pulses in the angular multiplexed pulse train. Spatial measurements indicate a 10% top-to-bottom decrease in the small-signal gain coefficient. The source of this asymmetry is a small tilt of the cathode structure relative to the anode, which causes a higher current density at the top than at the bottom of the amplifier chamber. This problem is easily corrected mechanically. The machine's reliability has steadily increased with repeated operation, to satisfy another major goal of these measurements. Small-signal gain measurements are now beginning on the next large electron-beam-pumped amplifier, the IA. The goals of these measurements are identical to those specified for the PA.

The Aurora Laser Optical and Beam Alignment System. The Aurora laser system is being built in two phases to test detailed design concepts for optically multiplexing large KrF laser-fusion systems. The goal of Phase I is to build and test large KrF amplifiers and to extract energy in a train of 96 short optical pulses. The goal of Phase II is to demonstrate an end-to-end optically multiplexed laser-fusion system useful for target experiments. Figure III-9 is a conceptual drawing of the entire Aurora system. Initially, 48 of the available 96 pulses encoded and amplified in Phase I will be decoded and brought to target in Phase II. The Aurora optical system is of the proper scale to enable us to develop a meaningful engineering data base of cost-effective optical designs, component-fabrication approaches, glass-mounting techniques, coatings, and alignment systems for larger KrF optically multiplexed laser-fusion system designs.

The following is a summary of the current status of the Aurora Optical System:

- The front end and encoder have been aligned and colinearized in the UV. Two 5-ns pulses were generated by the front-end system, multiplexed into a 96-element train of 5-ns pulses by the 12-fold and 8-fold encoders, and then routed to the input pupil of the main amplifier chain.

- Amplification of the pulse train from the 12-channel slicer through the SAM (the small amplifier before the PA) has been achieved. In our experiments, we have succeeded in obtaining optical angular multiplexing through this first amplifier, thereby establishing the general feasibility of the concept. The beams are now being routed to subsequent amplifiers.

- All of the interamplifier optical system hardware is on hand and has been checked out off-line in preparation for its installation and integration into the system.

- We have completed 96-beam alignment tests with the encoder in conjunction with the alignment system benchmark software. These tests have proven that the alignment system will meet Aurora's requirements.

- The Aurora decoder building is now finished and is being prepared for the installation of decoder hardware.

- The system design for Phase II is complete. Detailed design of the decoder hardware is well underway. Contracts for all long-lead items such as glass blanks, polishing, and coating are in place. Mechanical and alignment system hardware is being designed and built.

Aurora Target Research. The long-range goal in laser fusion is to produce a net thermonuclear energy yield in the laboratory by imploding a small D-T fuel mass. Because laser efficiencies are generally <20%, high-gain target capsules are required. To achieve high gain, a small central volume of the fuel is ignited by compression and a converging shock, and propagating burn proceeds through the remaining fuel. The implosion and shock are created by rapid, intense energy deposition in the outer layers of the target (the ablator). This energy comes either directly, from illumination by the laser beam, or indirectly, through x-ray conversion. In either case, the key questions

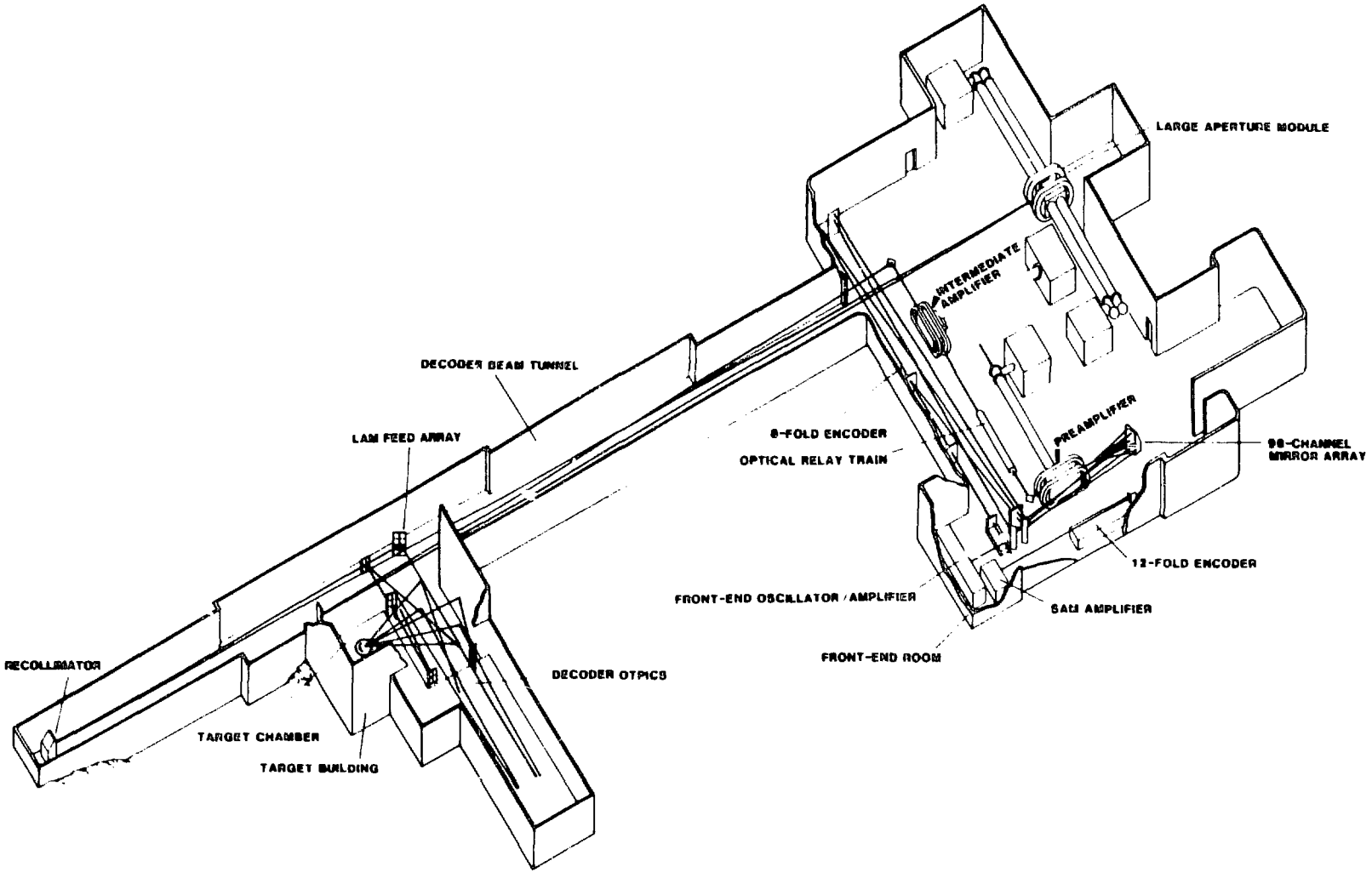

Fig. III-9. Aurora: The Los Alamos short pulse, multikilojoule, angular multiplexed KrF ICF laser system

are 1) What are the minimum laser energies required for ignition and for high gain (~100), and 2) Is there a laser (or other driver) technology that can meet the energy and other requirements practically and at sufficiently low cost.

In our approach to answering these questions, we use the KrF excimer laser Aurora and combine our previous favorable experience with the electron-beam excited-gas lasers at Los Alamos with the favorable target coupling exhibited at short wavelengths by glass lasers at other laboratories. Once we have demonstrated the feasibility of the KrF technology, we intend to use Aurora to test important target-physics issues.

Two principal areas of experimental target research on Aurora will be 1) laser-target coupling, including the control of laser-plasma instabilities and the physics of "indirect-drive" (radiation-driven) targets; and 2) planar hydrodynamics and growth of fluid instabilities. We hope to establish a data base and physics understanding that will enable us to extrapolate from low-energy experiments on Aurora to ignition experiments of the future. The data base will provide information on absorption of laser light, deposition of this energy and efficiency of conversion to x rays, achievable symmetry and uniformity of target drive, preheat, and the like. Especially relevant to these issues is the extent to which plasma instabilities and beam refraction are supported by plasma motion during the 5-ns Aurora pulse. The impact on these processes of the unique beam profile and bandwidth capabilities of Aurora will also be investigated.

An essential element of these studies is the demonstration that multiplexed KrF lasers are indeed viable laser-fusion drivers. Thus, numerous beam-related issues, such as focusability, contrast ratio, cross talk, and long path propagation, will be addressed. Finally, Aurora provides an opportunity for a more general study of the physics of high-energy-density matter in areas other than those related to the immediate ICF application.

To provide for these studies, we are constructing a target irradiation chamber and related instrumentation for use with the Aurora system. Conceptional design of the target chamber system began in early 1985, and detailed hardware design started in midyear. The design for the target system appears in Fig. III-10. The system is designed primarily to use 48 of the 96 Aurora beams for one-sided irradiation of targets, with the possibility of subsequently adding the remaining 48 beams in a two-sided configuration.

The system consists of a spherical target chamber, a beam cone, and a lens plate. The chamber is a split sphere, 1.56 m in diameter, made of 7.56-cm-thick stainless steel. It is connected to the beam cone by a bellows, and the lens plate is hard-mounted to the large end of the cone. The lens plate contains 48 lens cells that focus the 48 beamlets on a target near the center of the chamber. Beam pointing is done by the final aiming mirrors in the decoder room. The entire envelope is under high vacuum, and the lenses act as vacuum windows. To permit focusing, the beam cone rides on a precision rail system parallel to the major axis.

The individual beamlets should reach an average best-focus intensity of $\sim 5 \times 10^{14}$ W/cm^2. The ensemble of 48 beams, with an f/2 envelope, should reach $\sim 8 \times 10^{15}$ W/cm^2, with 50% of the energy in a circle $<120\mu$m in diameter.

The following is a summary of the status of the target system as of September 30, 1986:

- Designs for the target chamber, beam cone, and lens plate have been completed.
- The target chamber hemispheres have been forged, machined, and delivered.
- Lens plate spinning, welding, and machining have been completed.
- The target transport system has been modified, assembled, and bench-tested.
- Preliminary designs for the target-viewing and data-acquisition systems have been completed.
- The vacuum-system design is complete.

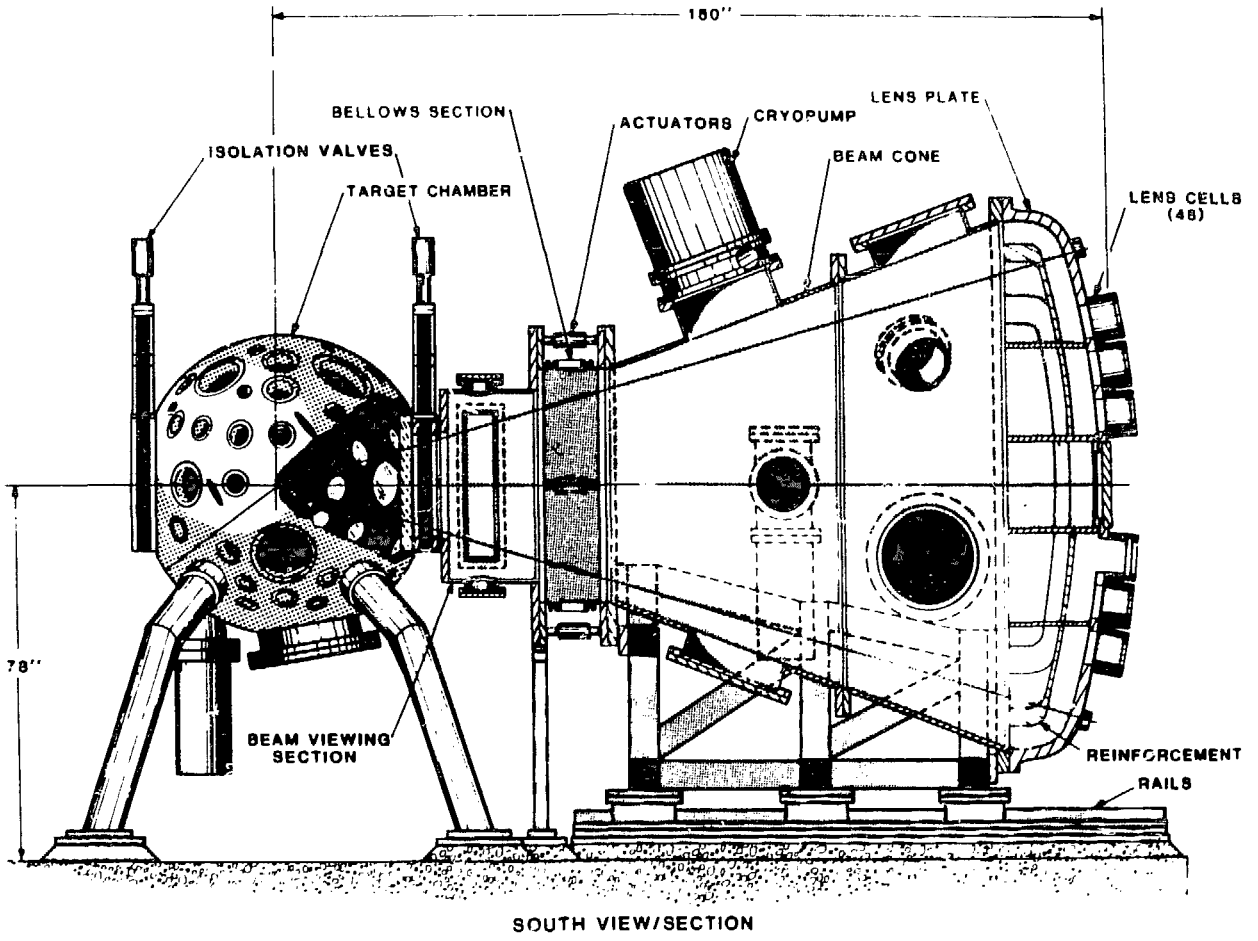

Fig. III-10. Aurora target-irradiation system, side view.

- X-ray and absorption systems for target diagnosis are being designed. Other diagnostics planned for this system are in various stages of development or acquisition.

Many of the subsystems for this project, including vacuum, diagnostic, target-transport, and data-acquisition instrumentation, have been adapted from the HELIOS CO_2 laser system at Los Alamos.

With this target facility, we should be able to do extensive and useful experiments that will not only determine the feasibility of multiplexed KrF laser architectures but also establish a laser-target interaction data base for scaling to ignition-size experiments.

Design of a 100-kJ KrF Power Amplifier. In 1983, as part of the Laboratory's effort in ICF, the task of scaling KrF laser systems to sizes that would have meaning for fusion power plants was undertaken. The original approach was to design a 100-kJ KrF driver that would make use of the Antares buildings for the front end, intermediate amplifiers, and target system. Studies of possible architectures were completed by TRW and AVCO Everett under the Laboratory's direction. In 1984 the scope of the 100-kJ effort changed, and we began to concentrate on the design, construction, and testing of a large, 100-kJ power amplifier module (the PAM).

The PAM program was divided into two efforts: the Laboratory was responsible for the design of the full 100-kJ amplifier, while industry undertook the design and construction of a PAM prototype. AVCO Everett won the contract to design and construct a single expanding-flow diode and to integrate it with a pulsed-power system that was to be supplied by Maxwell Laboratories, Inc.

A modular approach to the design of the 100-kJ PAM was adopted. The purpose was to simplify maintenance and repair and to reduce the costs associated with such large laser amplifiers. The device is pumped by ten identical expanding-flow diodes, five on each side, which permits a significant reduction in the required magnetic field guide. The complete PAM had been carried to the preliminary design stage by February 1986.

The program has been discontinued at this point, pending further results from extensive KrF scaling investigations and scoping studies for optimized reactor-scale architectures.

The Los Alamos Bright Source (P-1, P-4, P-16)

The development of high-brightness lasers has opened the possibility of studying laser-atom interactions where the laser electric field equals or exceeds the atomic electric field. For example, at a laser intensity of 10^{17} W/cm^2, the electric field is about 9 GV/cm, whereas the field in a hydrogen atom is about 6 GV/cm. Clearly, at such laser intensities and higher, one would expect to observe new physics in laser-atom interaction studies.

At present, several laboratories working in this area are reporting novel experimental results at high laser intensities, which, however, are still below the equal-electric-field case. Most of the results pertain to multiphoton and above-threshold-ionization (ATI) phenomena observed in electron spectra and ion charge-state distribution measurements. There is considerable disagreement about the physical processes responsible for the observations. One school of thought is that everything can be explained as a conventional step-wise multiphoton process made more probable by the higher intensities available. The other is that the laser electric field induces coherent collective motion in the electron shells of an atom, leading to a new atomic physics phenomenon. The most likely explanation is that laser intensities now available are in an intermediate regime, where the anticipated collective atomic effects are not yet fully realized. More complicated experiments, particularly some novel efforts in solid targets, are under discussion. However, the major direction of this program must be toward higher intensities. At present, our focused intensity is approximately 10^{15} W/cm^2. Near-term improvements in focusability should enable us to raise the intensity to $\sim 10^{17}$ W/cm^2. Another stage of amplification available by mid-FY87 should get us into the 10^{18}- to 10^{19}-W/cm^2 range. Several other laboratories should have equivalent facilities by that time, but by then we should be the first to take the next step toward a 10^{20+}-W/cm^2 facility and the first to study the physics in this high-intensity regime. After we understand the physics at these high intensities we could pursue practical applications in this area, such as x-ray sources, new lasers, and particle-acceleration schemes.

Laser Development. From the standpoint of laser development, the Los Alamos Bright Source (LABS) program has two objectives: 1) to understand the physics and improve the technology of ultrafast (picosecond) generation and amplification, and 2) to produce the brightest light source possible.

Construction of the Bright Source Laboratory and laser system began in March 1985. By June 1986, a working laboratory had been established, and the "front-end" was routinely and reliably producing 1-ps, 248-nm pulses amplified to the 10- to 20-mJ level.

Picosecond UV pulse generation starts in the front end with a Nd:YAG-pumped mode-locked visible dye oscillator at 648 nm. A single 1-ps pulse from the output train of the oscillator is amplified in a XeCl-pumped three-stage flowing-dye amplifier. Output from this amplifier is heterodyned to 248 nm in two nonlinear crystals. The output is 5 to 10 μJ at any repetition rate up to 50 Hz.

Amplification to the 10- to 20-mJ level has been accomplished in a pair of commercial discharge-pumped KrF amplifiers at repetition rates up to 25 Hz, although typical operation is at <5 Hz.

Studies of detailed pulse-amplification physics are just beginning and are largely dependent on the parallel development of ultrafast UV optical diagnostic techniques and equipment. Straightforward spatial filtering techniques are expected to improve the beam quality to near the diffraction limit in the near term, allowing focal spot intensities to reach 10^{17} W/cm^2. This source would be one of the two or three brightest laboratory light sources in existence. Further intensity increases of 1 to 2 orders of magnitude are possible in the amplifier stage that is now being designed.

Experimental Plan. In our first series of experiments we will use gas targets to study the interaction of high intensity laser radiation with atoms. We intend to look at multiphoton ionization phenomena by addressing three topics:

- Measurement of the charge-state distribution resulting from multiphoton ionization in several gases under varying laser intensities.

- Measurement of the extent of ionization as a function of gas pressure: by producing a high-pressure gas jet from a capillary, we can enter a region where the isolated-atom view of ionization does not apply, so that electrons liberated from one atom will be able to interact with another atom, causing secondary ionization; at this threshold, a drastic change should occur in the degree of ionization attained.

- Characterization of the system at sufficiently low pressure that — on the average — there is only one atom in the focal volume: for each laser pulse, we can detect which ionization state is produced and, by using a low-resolution detector, what photon energy spectrum is produced with that ion, thereby building up a spectrum associated with the production of each ionization state and developing a model to explain the intermediate states of the atom as it becomes ionized.

After this initial series of experiments we plan to measure electron and photon spectra resulting from laser-atom interactions. The diagnostics required for these experiments are in various stages of completion. A few of them are described in detail in the following paragraphs.

Gas-Jet Target Characterization. A gas-jet target in a vacuum is required for high particle density at the focal spot but low density elsewhere. Because the focal volume is small, a small jet (<100 μm) is required. The flow field and density distribution in the jet must be characterized. In preliminary work in this area, we have obtained schlieren images of small jets (~150 μm in diameter) using different gases (Ar, Xe, CCl_2F_2) at various pressure ratios. We will continue to operate the schlieren system in order to measure gas jets in a vacuum system and to explore the use of smaller jets.

Ion Time-of-Flight Diagnostic. Ions generated in the laser focus will be accelerated to 2.5 keV per charge on the ion, passed through a 50-μm-diameter aperture, and allowed to drift in a 50-cm-long field-free region. The ions will be detected and their signal amplified and collected as a function of time. The ion time-of-flight system is capable of resolving different ionization stages from the target and different isotopes of the heavily stripped ions. The system will have its own pumping station, including a 50-l/s turbopump, and will be able to detect single ions.

Electron Spectrometer for Multiphoton Ionization Studies. A time-of-flight electron spectrometer is being designed for the multiphoton ionization studies. The instrument depends upon a magnetic field parallelyzer, or inverse magnetic mirror concept, in which electrons emitted into nearly 2π Sr from the interaction region are accepted into the collection entrance of a microchannel plate detector at the end of a 100-cm drift tube. Preliminary calculations show that typical energy resolutions of $\Delta E/E \sim 0.03$ at 10 eV are attainable, without the use of retarding potentials, and that significantly better resolution can be attained with static retarding fields. We have completed detailed calculations, which follow the helical trajectories of the electrons in the magnetic field.

X-Ray Detection and Correlation. We have installed gas proportional counter x-ray detectors having a resolution of about 50 eV from 100 to 1000 eV. They have been mounted to subtend as much of the solid angle as possible without interrupting any portion of the laser beam. A search is now on to find the electronic elements we need to do the correlation of the photons with the ionization stage produced. Our first experiment will be to focus the laser into a gas and observe whether any photons with energies above 100 eV are produced.

Measurement of Laser Parameters. Before progress can be made in attacking the advanced atomic physics experiments we have planned, the laser beam parameters must be accurately measured. The following are descriptions of and results from experiments designed to measure the pulse width, focal spot size, and beam quality of the laser.

Laser Pulse Width. The measurement of picosecond laser pulses is a question often successfully addressed by using nonlinear crystals in an autocorrelation technique. The method does not work well with the new class of high-intensity lasers based on KrF laser amplifiers because of the 248-nm wavelength. Still, knowledge of the pulse duration is important for experiments conducted at these facilities. Workers at the University of Illinois have tried difference-frequency autocorrelation measurements and a two-photon fluorescence in xenon. Others report having taken measurements with interferometric methods and virtual gratings. We report here the results of a double-slit diffraction experiment that determines the pulse coherence time and thus the minimum possible pulse width and the maximum possible power.

The idea is based on simple double-slit diffraction. If a retarder is placed over one slit, as in Fig. III-11, the transmitted beamlet will be delayed with respect to its companion at the other slit.

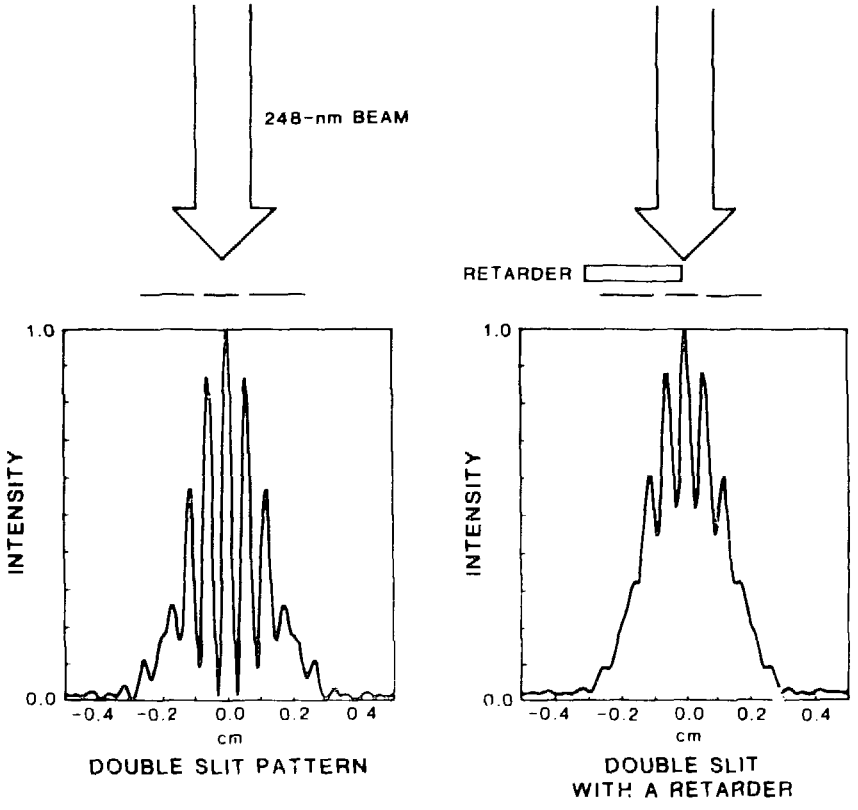

Fig. III-11. Pulse-width measurement with a double slit

If the delay is long enough, the two beamlets will not arrive at the detector simultaneously and cannot interfere to produce the double-slit pattern. Depending on the thickness of the retarder, the resulting diffraction pattern will vary between the classical double-slit pattern and the superposition of two single-slit patterns.

It was discovered that for a reasonable slit separation, a near-field formalism was required to describe the double-slit patterns. He-Ne laser tests showed excellent agreement with predictions. As the delay δt increases from zero, the contrast of the fringes from the double slit decreases. A gaussian shape has been assumed for the coherence function, and the contrast ratios, valley-to-peak intensity ratios of the central fringe, have been tabulated for different delays. The experiment then consists of measuring the contrast ratios for retarders of various thickness x to derive the coherence time τ. The delay actually consists of two parts, δt_x due to the retarder and δt_0 due to inherent properties of the wave front. The consequence of this division is that even when no retarder is used, the contrast is worse than expected and the fringes are somewhat washed out.

Photographs of the fringe patterns help us recognize disturbances in the wave front. Along the length of the slits, the intensity is not constant and the fringes tend to wave back and forth. Differences in intensity through the two slits (whether integrated or instantaneous) appear as a loss of contrast. Integrated differences show asymmetric patterns in addition to poor contrast. A phase difference shows itself as a displacement of the pattern to or from line center. This can explain the waviness of the pattern; and if the phase difference is not constant during the pulse, the fringes will shift during the pulse, blurring the pattern and spoiling the contrast.

Experiments have been conducted both at Los Alamos and at the University of Illinois at Chicago. Pulse reproducibility was assumed, and averaged data were plotted for several retarder thicknesses (Fig. III-12). As predicted, the fringes wash out and the contrast ratio increases with delay. In the Chicago experiment, τ was found to be 0.6 ± 0.1 ps, which is consistent with other measurements. At Los Alamos, where measurements were made without a spatial filter, τ was measured to be 1.1 ± 0.2 ps. A measurement with a streak camera having a resolution of 2 ps yielded $\tau = 2.1$ ps. An autocorrelator on the 648-nm dye laser employed to produce the 248-nm beam gave $\tau = 1.8$ ps for the red beam. The pulse width is thus bracketed between 1.1 and 2.1 ps by these measurements. With focal spot size measurements and energy measurements, the focused intensity inferred was 5×10^{14} W/cm^2.

Spot Size Measurements. To determine correctly both the laser intensity and the intensity distribution, we must measure the shape and size of the focal spot. The difficulties in obtaining these measurements are due to the short wavelength (0.248 μm) and high intensity ($>10^{16}$ W/cm^2) of the laser and the expected small size of the focal spot ($\sim$1 μm diameter).

An equivalent-plane measurement was made on the Bright Source by measuring the focal spot of a 50-mm-diameter, f = 279-mm parabolic mirror. We used a reflecting microscope objective (with a numerical aperture of 0.65) together with a high-quality UV splitter, attenuator, and mirrors to make the measurement.

Preliminary data indicate that the laser beam can be focused to near the diffraction limit but that it is not spatially uniform. Spatial filtering is required to clean up the beam exiting from the amplifier. Work on the construction of a spatial filter is in progress.

Laser Beam Properties Using A Shear Plate. Because of the short pulse length of the laser, new difficulties arise when we attempt to measure the beam properties at the focal plane. We are pursuing a shear-plate-interferometry approach. By this method, a small fraction of the beam is split off for monitoring. The reflection from the rear is used to monitor the energy. The reflection from the front is directed at the shear interferometer. The beam reflected from the two sides of the interferometer cavity interfere to make what is called a shear interferogram. The interference pattern is a measure of the derivative of the wave front, while the intensity of the interferogram measures the beam's spatial energy distribution. Thus, the spatial distribution of the phase and the amplitude of the laser beam is measured, allowing us to use wave optics to predict the intensity and phase distribution in any plane.

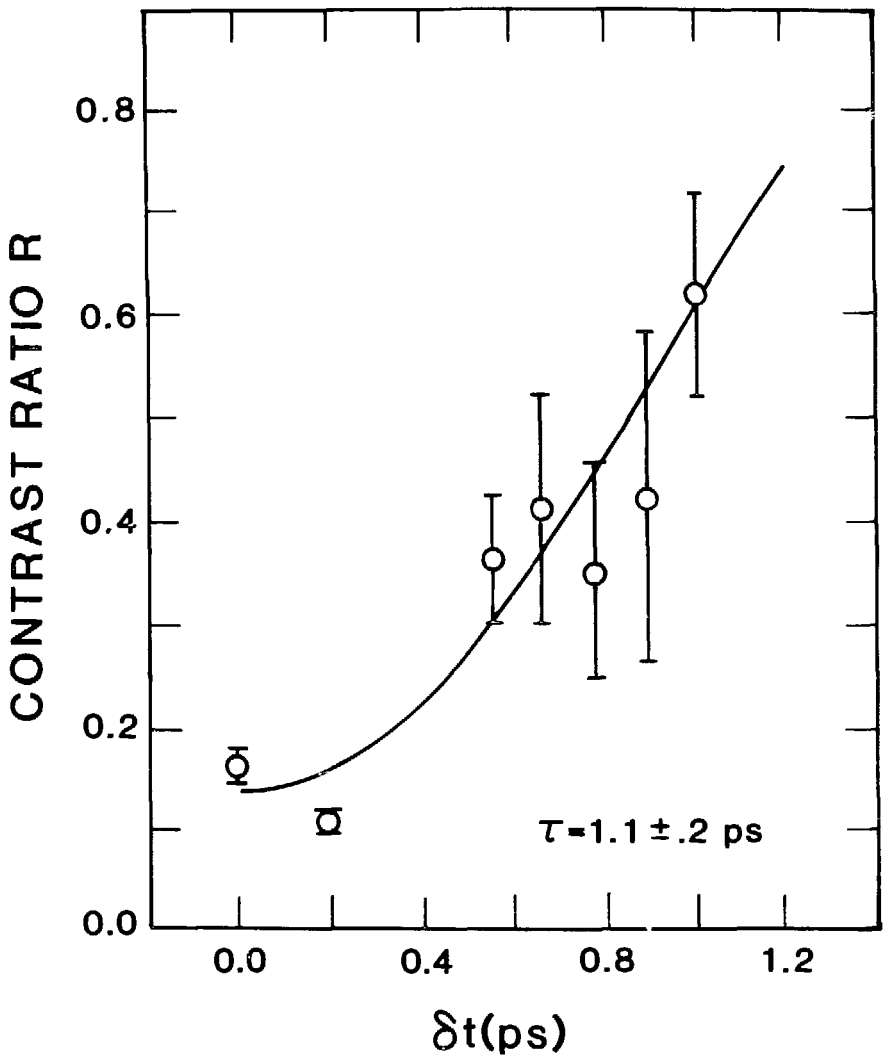

Fig. III-12. Fringe contrast ratio versus retarder delay in picoseconds, together with a fit from an analytic model used to deduce the coherence time, τ.

Progress on the Los Alamos Heavy-Ion Injector (P-7, P-12)

As part of the U.S. Department of Energy's Heavy Ion Fusion Accelerator Research program, Los Alamos is designing and building an accelerator to produce multiple high-voltage, high-current ion beams needed for injection into linear-induction accelerators that are being developed by LBL. Heavy ions hold great promise for application to inertial confinement fusion. Among their advantages are the following: 1) theoretical target coupling is good, 2) charged-particle accelerators generally have high electrical efficiency, 3) many charged-particle accelerators operate at high pulse-repetition rates, and 4) large charged-particle accelerators have a well-developed technology. LBL has been charged with the development of linear-induction accelerators appropriate to this application.

Because the transportable current increases considerably with ion energy, it is desirable to inject multiple beams for a pulsed electrostatic accelerator at as high a voltage as is practicable.

The design criteria for this accelerator include the following:

- Number of beams, 16
- Particle energy, 2 MeV
- Current per beam, 150 mA
- Ion mass, 27 (Al^+)
- Pulse length, 6 μs
- Beam-normalized emittance, 4×10^{-7} π-m-rad
- Energy and current flatness, 0.1%

The injector design is shown in Fig. III-13. The high-voltage pulse will be generated by a 2-MV Marx generator with a special circuit to control voltage pulse flatness. The Marx generator and the accelerating column will be cantilevered from opposite ends of the containment vessel, which will be pressurized to 65 psig with a 30/70 mixture of SF_6/N_2.

The ion source for this injector is being developed at the University of New Mexico. We have concentrated our efforts on metal-vapor vacuum-arc ion sources with biased grids to control plasma prefill in the extraction gap. These sources have the following advantages:

- Rapid turn-on
- Simplicity of fabrication and operation
- Generation of clean plasma with little species contamination
- Production of a wide variety of ions
- High ion flux

Recent experiments have given current densities of 15 mA/cm^2 for both Al^+ and In^+. The beams were predominantly in the +1 ionization state with no observable species contamination. Emittance less than 3×10^{-7} π-m-rad was measured.

The accelerating column is made up of a stack of high-purity alumina cylinders brazed to niobium electrodes, which feed the voltage through from the grading rings on the outside of the column to the accelerating electrodes inside. Brazing with TiCuSil alloy produces a fillet at the niobium-ceramic bond that will affect the voltage flashover at the ceramic-vacuum interface. We have succeeded in removing the fillet with a carefully controlled electrostripping process. Experiments on a 20-cm-i.d. by 7.3-cm-long test sample showed flashover at 103 kV in 1 μs before the fillet was removed and holdoff in excess of 250 kV for 50 μs after electrostripping. In operation, the 7.3-cm-long column sections must hold off 175 kV.

Beam transport considerations require that the beam energy flatness out of the injector be extremely good—the goal is $\pm 0.05\%$. The largest perturbation on the beam voltage is voltage droop of the Marx generator, arising from the charge flow (current $\times$ time). The beam current is not large, but when the current in the Marx charge resistors and trigger resistors is taken into account, the total charge flow is so large that we cannot compensate for it by making the Marx capacitance larger. We have tried several circuit designs to achieve this compensation and have found that a design incorporating an LC inversion generator provides better compensation than did the RC decay circuit we used in our initial attempt.

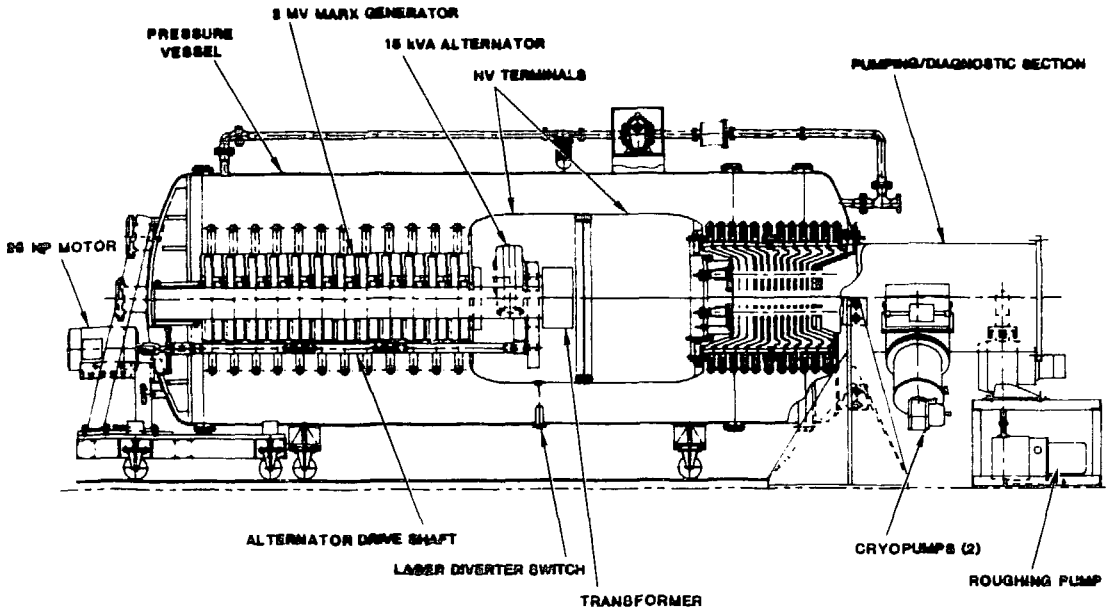

Fig. III-13. Heavy-ion injector.

The size of the Marx interstage trigger-coupling resistors is determined by a trade-off between better triggering and the Marx voltage droop rate. The minimum value of trigger-coupling resistor required to keep the droop small is in the neighborhood of 20 kΩ. Testing of the Marx with this magnitude of trigger coupling gives extremely large delays and jitter. Our past experience with this type of Marx generator indicates that trigger-coupling resistors are required to be no larger than 1 kΩ. We have tried a new trigger coupling scheme, using a small resistance in series with a small (order of 1 nF) coupling capacitor in place of the large resistor. The results were very satisfactory in a small model Marx generator. We will be trying this soon in the full injector Marx.

During the remainder of FY86, we expect to complete the design of the ceramic column and operate the prototype Marx generator up to the 800-kV level. Next year, budgets permitting, we expect to add stages to the Marx to take it to the 1-MV level. One column model (1-MV capability) will be completed with electrodes and a single vacuum arc ion source, and one beam of Al^+ will be accelerated to 1 MeV. The following year, the system will be extended to a 2-MeV capability.

At present all system components have been designed, and fabrication has been completed on everything except the ion sources and the field shaping hardware for the accelerator column. The pressure vessel is being installed, and we expect to complete the installation by the end of FY86. Assembly and high-voltage testing of the Marx generator and accelerating column will continue in FY87.

IV. NUCLEAR AND PARTICLE PHYSICS

INTRODUCTION

Nuclear physics activity in the Physics Division has evolved from a base in low-energy nuclear physics to include efforts in medium-energy nuclear physics and in particle physics. The first two deal primarily with strong-interaction dynamics and the third with weak interactions. A major new program is the study of the gravitational interaction of the antiproton.

In the low-energy nuclear physics efforts described here, we are developing new techniques and capabilities and applying them to innovative measurements that are directly relevant to laboratory programs. In medium-energy physics, the activities include classical studies of hadronic probes of nuclear targets as well as the extension of those ideas to collisions involving heavy ions. These studies are being extended to threshold production of eta mesons at LAMPF and to the use of the Drell-Yan process to investigate the antiquark content of nuclei. Weak interactions are examined in nonaccelerator studies, as exemplified by the use of tritium beta decay to measure the antineutrino mass, and through searches for rare K decays at Brookhaven. Our developing program to measure the gravitational interaction of the antiproton requires very low-energy antiprotons, but the work must be done at the high-energy laboratory at CERN, a facility that is capable of producing antiprotons copiously and providing them at appropriate energies.

LOW-ENERGY NUCLEAR PHYSICS

Low-Energy Nuclear Reactions for Fusion Energy (P-3)

In our evaluations of basic fusion-energy reactions, we have indicated that large systematic errors may have been made in some of the earlier measurements and have stressed the need for accurate remeasurements of the cross sections for most of these reactions. In particular, beam-energy uncertainties caused by the use of foil-contained gas targets could have been a source of significant error at energies below the Coulomb barrier, where the reaction cross sections change very rapidly with incident energy.

In view of this situation, we constructed a low-energy fusion cross section (LEFCS) apparatus for determining the cross sections for nuclear reactions among the hydrogen isotopes at low energy. These cross sections are important to the design of the first magnetic- and inertial-confinement fusion reactors that may eventually provide sufficient energy for commercial use. These reactors are expected to operate in the temperature range kT = 1 to 30 keV, which corresponds to laboratory bombarding energies having a large overlap with our experimental range of 10 to 120 keV.

We have completed our study of the D(t,α)n reaction and are in the final data-analysis phase of our study of the D(d,p)T, D(d,^{3}He)n, and T(t,α)nn reactions.

The experiments are performed by accelerating negatively charged D or T ions through a windowless, cryogenically pumped, flowing gas target of D_2 or T_2 and into a beam calorimeter. The target density is measured and the calorimeter is checked by using particle beams with energies of several

MeV from the tandem Van de Graaff accelerator at the Los Alamos Ion-Beam Facility. A calibrated resistor stack is used to determine the beam energy to high precision. The charged-particle reaction products are detected in silicon surface-barrier detectors.

D(t,α)n Reaction. We measured the cross section for the D(t,α)n reaction at 17 triton bombarding energies from 12.5 to 117 keV (equivalent deuteron bombarding energies from 8.3 to 78.1 keV). Over this energy range, the cross section spans 4 orders of magnitude, and the reaction is dominated by s-wave capture (isotropic angular distribution) into a $3/2^+$ state in ^{5}He. When comparing measurements of charged-particle cross sections below the Coulomb barrier with other experiments or calculations, it is more informative to use the so-called astrophysical S function rather than the rapidly varying cross section itself. S is obtained from the cross-section σ by factoring out the energy dependence of the de Broglie wavelength and the Coulomb penetrability in the incident channel. For d + T we have

$$S = 0.59962\ E_d\ \sigma \exp[1.40411\ E_d^{-1/2}] \quad . \tag{1}$$

where E_d is the deuteron bombarding energy in MeV, σ is the cross section in barns (b), and S is expressed in units of MeV-b.

In Fig. IV-1, we compare our data with some of the other data in the literature. The LEFCS data are accurate to 1.4% absolute over most of the energy range, the error rising to 4.8% at the lowest energy. These errors are at least a factor of 3 smaller than those of previous work. Note

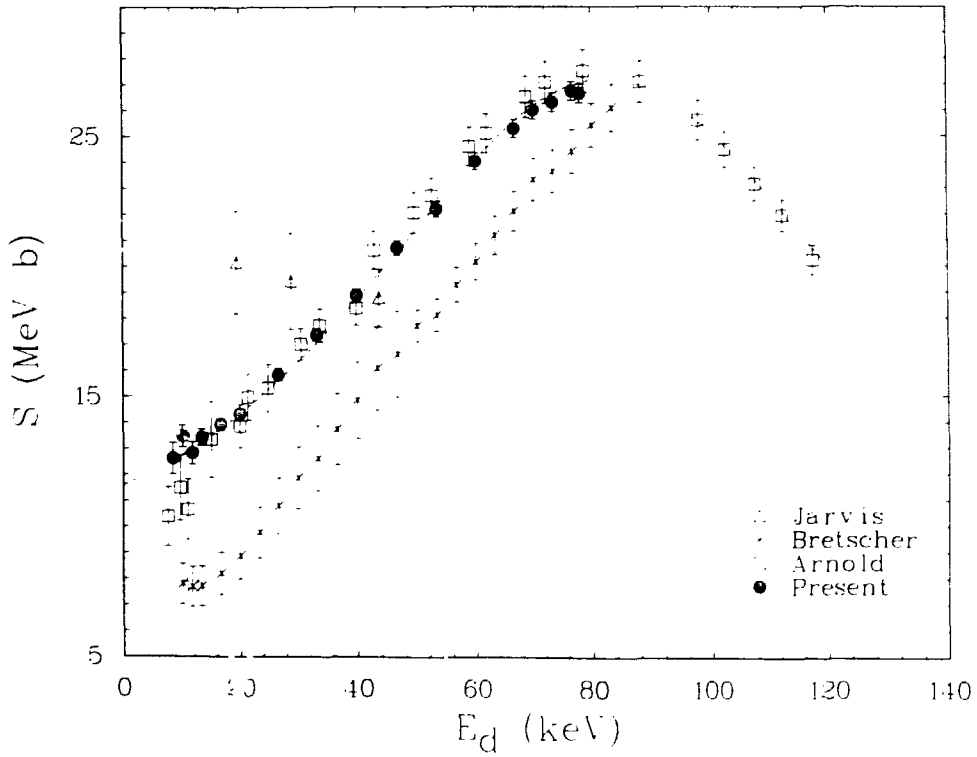

Fig. IV-1. The S function, Eq. (1), versus equivalent deuteron bombarding energy for the D(t,α)n reaction. Present data are compared with some previous work. Note the suppressed zero. Total errors are indicated. The curve is the result of a single-level R-matrix fit.

that S displays the typical bell shape appropriate to a reaction that proceeds through an isolated resonance state. The dashed curve shows the result of a single-level R-matrix fit to a data base up to 250 keV that included selected data from the literature as well as the LEFCS results.

D(d,p)T and D(d,^{3}He)n Reactions. By simultaneously detecting p,t and ^{3}He, we measured the differential cross sections for the D(d,p)T and D(d,^{3}He)n reactions. The preliminary extraction of the cross sections from the raw data has been performed, with a few small corrections yet to be made. In this report we indicate absolute errors of 3%, although when the final error analysis is completed, we expect most of the data to be more accurate.

A remarkable difference between these reactions and the d + t reaction is the large angular anisotropy present in the d + d differential cross sections $\sigma(\theta)$, even at these low energies. We have therefore fitted our preliminary values for $\sigma(\theta)$ to the form $a + b\cos^2\theta$, assuming that s- and p-waves predominate. Earlier work has shown that d waves begin to manifest themselves at the higher energies in our range. Therefore, in our final analysis we will add a $\cos^4\theta$ term to the fitting function. From our fits to $\sigma(\theta)$ we can derive the integrated cross section and convert those to an S function:

$$S = 0.5\ E_d\ \sigma \exp[44.4021\ E_d^{-1/2}] \quad . \tag{2}$$

where E_d is in keV, σ in b, and S in keV-b. These results are shown in Fig. IV-2. Over most of our energy range, the cross section for the n^{3}He branch is larger, but decreases more rapidly with decreasing energy, than that for the pt branch. Although we find that the present data agree reasonably well with earlier results, our data are several times more accurate and will allow us to obtain the most reliable low-temperature reactivities to date.

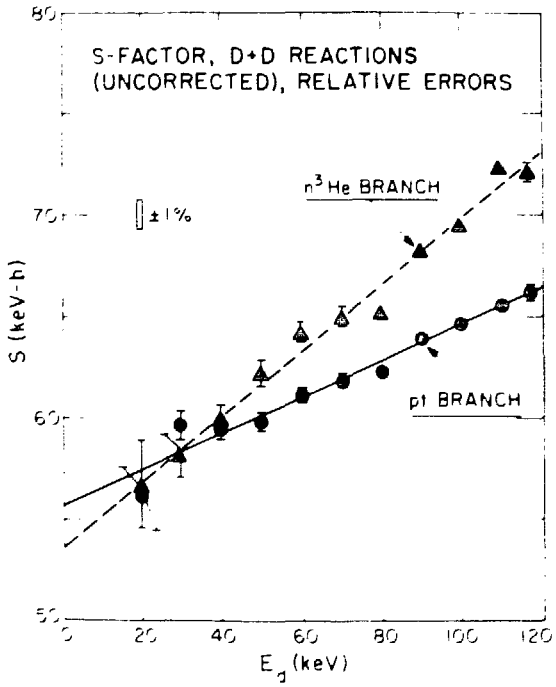

Fig. IV-2. The S function from Eq. (2) for both branches of the d + d reaction versus deuteron bombarding energy. Note the suppressed zero. Only statistical errors are shown. The straight lines are from least-squares fits to the data.

T(t,α)nn Reaction. We have completed our measurements of the cross section for the T(t,α)nn reaction, having obtained data at triton bombarding energies of 115, 105, 90, 75, 60, 45, and 30 keV. Two major complications presented by this reaction are the flowing of tritium in our windowless gas target and the emergence of the detected α particles from the reaction with a continuum of energies. This latter effect makes background determination more of a problem than it is for reactions where the yield is contained in a narrow peak. The background is caused mainly by neutron interactions in the detectors. Therefore, to aid in the determination we have covered one of the two 45° detectors with a tantalum absorber that is thick enough to stop the charged particles but thin enough that it has no appreciable effect on the neutron spectrum.

We have derived preliminary cross sections from the measured spectra by the following procedure: 1) We calibrate the tritium target density by accelerating deuterons, measuring the T(d,α)n yield, and using our previously measured cross sections for that reaction. 2) We interpolate across the D(t,α)n peak. 3) We extrapolate the T(t,α)nn spectrum to zero energy. 4) We subtract the neutron-produced background. 5) We integrate the yield over lab solid angle. In the future we will develop a reaction model to aid in the cross-section extraction. With such a model we may be able to predict reliably the associated neutron spectrum from t + t. Even without the model, we estimate that we can extract cross sections to better than 5% at most energies. In Fig. IV-3 we show the results of the preliminary σ extraction, converted to the S function

$$S = 0.5\ E_t\ \sigma \exp[54.3378\ E_t^{-1/2}] \quad , \tag{3}$$

where E_t is in keV, σ in b, and S in keV-b. At present, we assign errors of 5% to the LEFCS data. Our data seem to agree best with the data of Serov et al. and to confirm Hale's analysis quite well

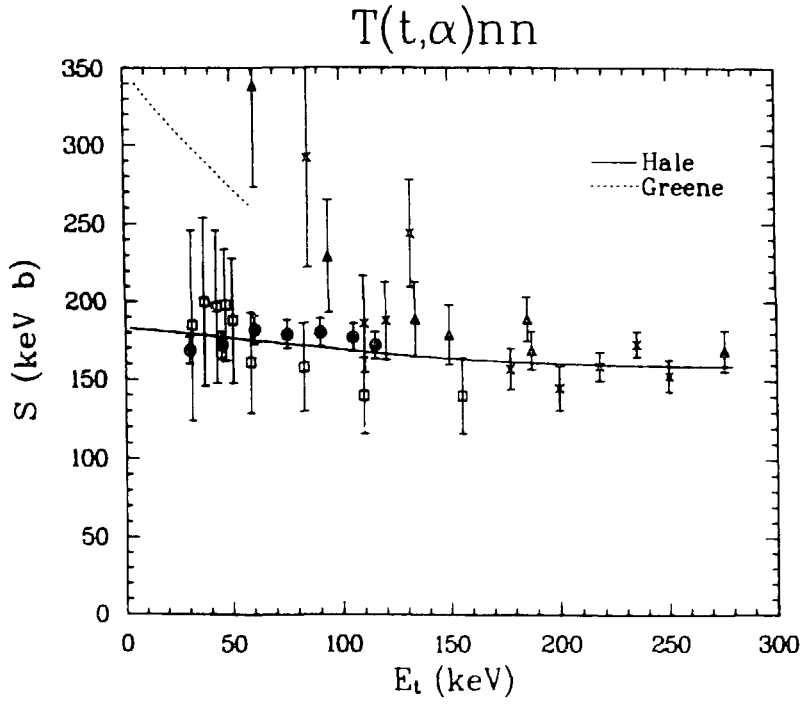

Fig. IV-3. The S function of Eq. (3) versus triton bombarding energy from the T(t, α)nn reaction. The solid circles are the preliminary LEFCS data shown with 5% errors. The squares are data of Serov et al. [*Sov. J. At. Energy* **42**, 66 (1977)]; the triangles are data of Goverov et al. [*Sov. Phys. JETP* **15**, 266 (1962)]; and the crosses are data of Agnew et al. [*Phys. Rev.* **84**, 862 (1951)]. The solid curve is from an R-matrix analysis, and the dashed curve is from Greene's evaluation.

(Fig. IV-3). We disagree with Greene's analysis, which was evidently influenced by the Govorov data. Further analysis of these data is in progress.

Measurement of the ^{7}Be(n,p)^{7}Li Cross Section from 0.03 eV to Approximately 300 eV (P-3)

The ^{7}Be(n,p)^{7}Li cross section is of great interest for radiochemical diagnostics of tests of nuclear devices. The interpretation of the diagnostic is complicated by the high ^{7}Be burnup cross section. The loss of ^{7}Be through this process has never been fully understood because the cross section, until now, has never been measured.

We have completed a measurement of the ^{7}Be(n,p)^{7}Li and ^{7}Be(n,p)^{7}Li*(0.48 MeV) cross sections from 0.03 eV to ~300 eV. The measurements were made using a 95-ng (~30 mCi) $^{7}BeF_2$ sample and a single 5-cm-diameter solid-state detector placed approximately 3 cm from the sample. Simultaneous measurement of the outgoing proton energy and the incident neutron energy was made possible by using the "white" neutron source, driven by the newly commissioned proton storage ring (PSR) at the WNR facility at LAMPF. All of the data were collected in about 10 hours, with the PSR running at about 25% of the design intensity (~25 μA). The ^{7}Be measurements were made relative to the ^{6}Li(n,α)t cross section. To convert these relative measurements to absolute cross section, the absolute ^{7}Be(n,p)^{7}Li thermal cross section was measured at the Omega West Reactor. The data from these two experiments have now been fully analyzed, and the combined results are shown in Fig. IV-4.

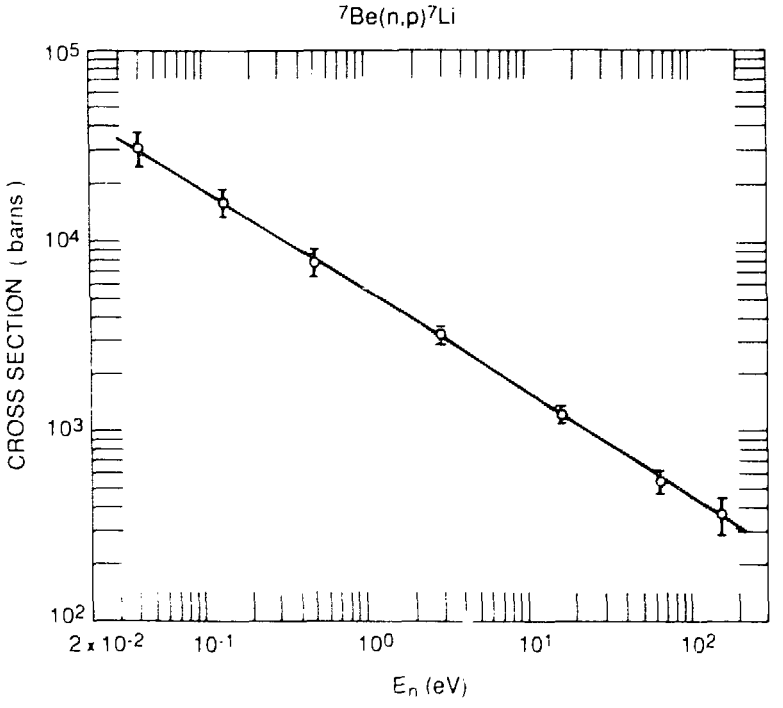

Fig. IV-4. Cross section versus neutron energy for the ^{7}Be(n,p)^{7}Li reaction (only a few of the data points are shown here).

During the latest break in the LAMPF run cycle, we made substantial improvements in our apparatus. This, together with increased running time for users at the PSR during the next run cycle, will enable us to extend these measurements to neutron energies of a few keV.

This is expected to be the first in a series of measurements on radioactive targets. We are planning similar measurements on the unstable nuclei ^{22}Na, ^{54}Mn, ^{55}Fe, and ^{57}Co during this LAMPF run cycle. The high intensity and low duty cycle of the PSR, together with the experimental techniques we have developed, enable us to take measurements that cannot be made anywhere else in the world on these and many other unstable targets.

Gamma-Ray Laser (Graser) Research (P-3)

The laser has revolutionized optics. Many other fields of science and technology, previously unrelated, have benefited from the use of coherent radiation in the infrared, visible, and ultraviolet regions of the spectrum. The development of lasers that would generate radiation at still shorter wavelengths, comparable with atomic dimensions, can likewise be expected to lead to a vast array of new scientific and technological developments. The unique characteristics of x- and gamma-radiation (i.e., penetration, ionizing ability, short wavelength, interaction with electrons in inner shells of atoms and with nuclei) would be greatly enhanced by the properties (coherence, intensity, monochromaticity, directionality, time- and frequency-dependence, and the like) that distinguish radiations generated by stimulated emission.

The basic requirement for a gamma-ray laser (graser) – a pulsed, directable source of coherent gamma radiation in the near- or sub-angstrom region of wavelengths, resulting from nuclear transitions – is that the gain by stimulated emission can overcome the photon losses. Obviously, the nuclear resonance cannot be Doppler-broadened; the transitions emitting gamma-rays must be recoilless (e.g., through the Mössbauer effect). Only then can nuclear resonances be sharp enough. The active nuclei must therefore be incorporated in a cool, solid host, preferably a single crystal that also supports the Borrmann effect (anomalous transmission of photons channeled between Bragg-reflecting planes in crystals) to minimize photon losses. The concentration of active nuclei must be sufficient for gain but not so high that the nuclei introduce excessive nonresonant absorption.

Pumping and the initiation of lasing, however, must not inhibit the Mössbauer and Borrmann effects. This requirement poses a dilemma: narrow-line Mössbauer emission is observed only in: short-lived (<10-μs) transitions that are not highly converted; the power required to pump them directly would dissipate the solid host. Long-lived transitions are unduly broadened and so have inadequate gain.

To resolve the dilemma, we propose to divide the pumping into a slow operation that supplies most of the excitation and a fast (but gentle) step that initiates lasing. The concept involves the successful completion of the following steps:

1. Slow pump – Most of the excitation energy would be imparted slowly by a nuclear reaction, probably with an accompanying chemical concentration, to yield a sample of excited nuclei having a lifetime long enough to accommodate its production and other subsequent operations that precede the lasing event.

2. Separation from other reaction and decay products – Isomeric states of a single nuclide would be separated in quantities sufficient for the completion of the succeeding steps.

3. Incorporation of the isomer within a host crystal – Because recoilless emission is essential, the judicious selection and preparation of the host would be no less important than the selection and preparation of the active nuclide.

4. Transfer from storage to lasing state – This would be the crucial step; it must not destroy the host. Interlevel transfer by narrow-band resonant radiation is a demonstrated fact – an essential feature of the well-developed techniques of Mössbauer spectroscopy. Moreover, in recent experiments

at DESY and at Novosibirsk, intense, narrow-bandwidth, tunable x-radiation generated by electron undulators in storage rings has excited the 14.4-keV Mössbauer level of ^{57}Fe from the ground state. Such radiation might be capable of inducing transfer if the intensity requirements prove low enough that we can avoid unduly damaging the host or broadening the nuclear resonance. One way to reduce these effects would be to prepare the host as a superlattice, the active dopant being disposed periodically with a lattice spacing that gives the same Bragg angle as that of the radiation to be stimulated. That would exploit the Borrmann and anomalous nuclear interaction effects and match the velocities of the transfer and gamma radiations.

5. Superradiant emission. Collective spontaneous emission from nuclei, predicted in 1959 by Dicke, was observed in 1973 by Feld and collaborators. Its relevance to the graser field was recognized as early as 1964 by Terhune and Baldwin.

The following are examples of the Division's progress toward accomplishing these five steps.

Nuclear Isomer Separation (P-3, MIT). The first step in making a graser is to provide a nuclear population inversion. However, when nuclear excited states are produced by a nuclear reaction, many more ground-state nuclei are usually formed. A separation step is generally required. The work reported here demonstrates the possibility of isomer separation; a particular nucleus for making a graser has not been finally identified.

Atoms containing nuclear isomers ^{197m}Hg (nuclear half-life 24 hours) have been selectively photoionized by a three-step laser procedure, demonstrating the feasibility of separating nuclear isomers for a gamma-ray laser. The isomers were made at the Laboratory's IBF tandem Van de Graaff accelerator and flown to the MIT Laser Center in Cambridge, Massachusetts. There the mercury vapor was bombarded by three pulsed laser beams of wavelengths 254, 286, and 696 nm. Mercury atoms containing isomeric nuclei were ionized by exciting two atomic discrete states sequentially and then ionizing with a third photon. In the first two steps, the laser frequency was chosen to excite only atoms with isomeric nuclei and not those with ground-state nuclei. Hyperfine structure was mapped out by varying the frequencies of the first two lasers to prove selective ionization.

In efforts to develop alternate methods of separation, we are conducting an "optical piston" experiment. Here, a capillary cell containing sodium vapor in an argon buffer gas is bombarded by the beam from the P-3 CW ring dye laser. The laser is tuned just below the sodium atomic absorption line, so that only sodium atoms moving toward the laser beam are excited. The cross sections for velocity-changing collisions are greater for excited sodium atoms than for ground-state sodium atoms, so there is a drift of sodium atoms along the direction of the laser beam. We have thus far observed a movement of 2 cm.

This work and simultaneous independent Russian work are the first demonstrations of selective ionization of nuclear isomers, but a physical separation of the isomers has not yet been performed. We hope to extend the optical piston work to mercury (requiring a difficult frequency-doubling step) and to demonstrate the first laser isomer separation. Once a graser candidate has been identified, we should be in a position to rapidly develop a separation technique for that particular element and to provide a sample for demonstrating superradiance.

Graser Kinetics (P-3, MIT). The general concept is summarized in Fig. IV-5. The upper half of the figure shows macroscopic aspects and the lower half, microscopic; the left half shows host-dependent phenomena and the right half, the radiative aspects. A host crystal is doped with the active nuclides in the form of a doubly periodic superlattice, into which transfer radiation can excite several Bragg-reflected waves simultaneously. The induced gamma radiation, similarly, is emitted into multiwave modes. The geometrical construction in the lower left quarter of the figure shows the wave propagation and reciprocal lattice vectors involved in the formation of a four-wave Borrmann mode, which can interact preferentially with magnetic dipole and electric quadrupole transitions while the photoelectric absorption by atoms (an electric dipole interaction) is suppressed. Higher-

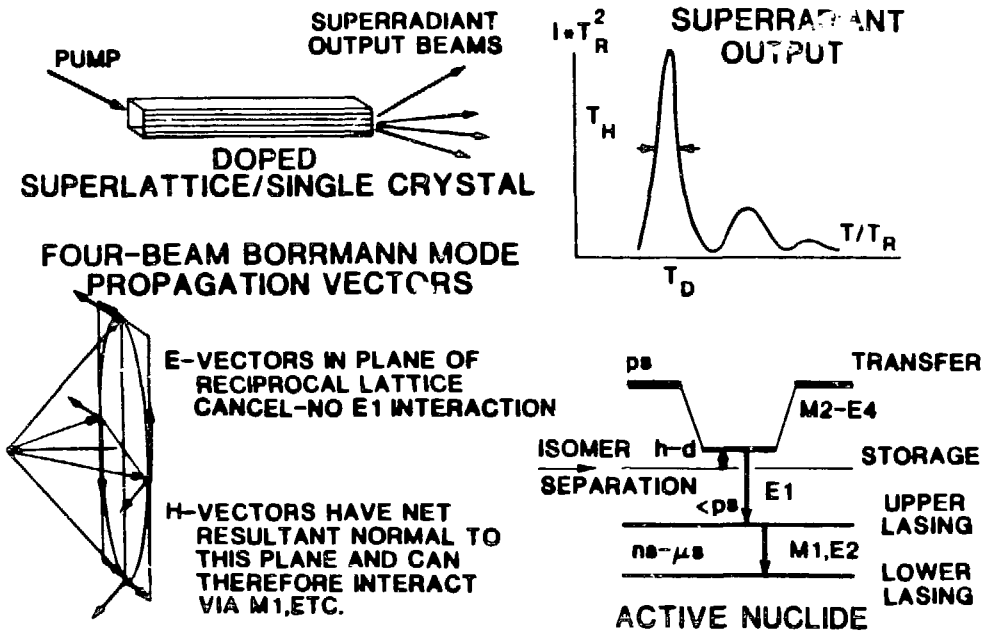

Fig. IV-5. Schematic diagram of steps in a conceptual graser system

order modes are also possible. A separated isomer with the level scheme shown at the lower right is the dopant for the superlattice; if the transfer radiation can rapidly populate the upper lasing state, then the system should behave as a Dicke superradiator, with the time-dependence shown in the upper right diagram.

Our kinetics studies of this concept show that if an appropriate nuclide with this level scheme does exist, multiply beamed superradiant outputs of nanosecond duration and at multimegawatt levels of intensity should be expected. We have learned of work at Rochester, on the kinetics of pulse-induced melting, that shows time-lags after the delivery of the fusing fluence before the crystal integrity is lost; we are now trying to ascertain the conditions under which those time-lags would suffice to ensure the evolution of superradiance after the transfer step. Most important, we are trying to develop a single, unified theory of the emission of radiation by a system of highly excited nuclei in a crystal lattice. This theory would be an alternative to the piecemeal approach used at present, which combines results from the theories of the Mössbauer and Borrmann effects with formulas derived in the semiclassical propagation theory of superradiance. Such a theory would be of value to the study of proposed systems, as a guide in the selection of candidate nuclides, and for the evaluation of proposed transfer mechanisms.

Interlevel Transfer (P-3, T-DO). The crucial step in pumping a graser is the transfer from a previously prepared storage level to the upper state of the lasing transition. To investigate the transfer with separated isomers would be a complicated and difficult task. Instead, we have initiated an experimental program to investigate proposed mechanisms (under study in T Division) for achieving interlevel transfer by using the nuclide ^{235}U as the target material. The lowest excited state lies only about 70 eV above the ground state in this nuclide, the angular momentum change required is comparable with that expected for the graser nuclides (when and if one or more are found), and the ground state is only mildly radioactive. The experiments to be performed would feature intense

subpicosecond pulses of extreme ultraviolet radiation generated by the "Bright Source" laser under construction. Nonlinear effects recently observed with this radiation encourage the expectation that the nucleus will be excited when the electronic structure is highly excited.

Radiative Lifetimes of Am I Atomic Levels (P-3, INC-4, INC-11, University of Mainz)

We have completed a program of measuring the unknown lifetimes of j = 5/2, 7/2, and 9/2 atomic levels of Am I (neutral americium) in the wavelength region between 426 and 640 nm. These levels are, in principle, candidates for optical pumping experiments on americium fission isomers to determine their spins, hyperfine splitting, and isomer shifts. In such experiments, the signal will be the fission fragment anisotropy measured after pumping (with polarized laser light) the very limited number of fission isomers [~0.1/s produced via (p,2n) or (d,2n) reactions] stopped in an inert gas atmosphere. In addition to the nuclear and atomic spins, the anisotropy depends on the laser light polarization (σ, π), the laser intensity, the lifetime of the excited level, and the relaxation time of the polarization due to collisions with the buffer gas atoms.

We have measured the lifetimes of levels in Am I by a single photon-counting technique. A mixture consisting of 300 μg of AmO_2, 6.4 mg of Dy_2O_3, and 6.0 mg of lanthanum was pressed into a pill and placed in a tantalum crucible, which was electrically heated to about 1500°C. At this temperature the oxide reduction proceeded quite rapidly. The Am/Dy metal vapors were deposited on a tantalum foil positioned ~4 mm from the nozzle of the crucible. After the evaporation, the catcher foil was heated to a temperature of 700°C. The resonance light from the interaction zone of the vapor and the laser beam was focused on a cooled photomultiplier tube. Suitable interference filters were used to suppress the intense thermal radiation from the catcher foil.

We used an optoacoustic modulator to chop the beam from the P-3 Coherent Inc. 699-29 ring dye laser system. We determined the radiative lifetimes by a decay curve analysis of the photon yield during the beam-off period.

The measurements at 14 wavelengths between 3426 and 640 nm gave lifetimes ranging between 50 and 7800 ns. With these values, it is now possible to choose an atomic transition for optimizing optical pumping in the fission isomer experiments.

Improvements in the Performance of Bismuth Germanate Detectors (P-2, P-3)

Scintillators made of bismuth germanate (BGO) have played an important part in the measurement of neutron-induced gamma-ray cross sections at the WNR facility. However, two problems with BGO limit its usefulness for this application. The first is the relatively poor energy resolution of BGO. This property can lead to problems in unfolding the spectra measured with these detectors into cross sections. The other problem with BGO is its relatively long fluorescence decay time, which can lead to unacceptable amounts of pulse pileup distortion under conditions of moderate to high counting rates during a typical experiment.

During the past 18 months, we have investigated several methods for improving the energy resolution of BGO. Some of these were very successful. In particular, cooling the scintillator from room temperature to about −20°C improved the energy resolution by 20%. A further improvement of about 10% can be made by roughening the surfaces of the scintillator rather than polishing them, as is usually done.

We have also attempted to upgrade the performance of BGO at high counting rates. Gating the output from the BGO scintillator to a short time can lessen count-rate effects by reducing the time over which the system is sensitive to pileup distortion. Unfortunately, this method degrades the energy resolution. We then investigated the trade offs between the need for good resolution and the need to reduce pileup distortion at high count rates. As a result of these studies, we developed a

new system of electronics for the BGO detector that significantly reduces pileup distortion and also gives us the flexibility to choose the proper balance between energy resolution and pileup distortion.

The new BGO detectors and the electronics system were tested during two experiments at LAMPF during the last run cycle, and they performed well. A more stringent test of the new system will be made when experiments commence at the new target-4 facility at WNR later this year.

WEAK-INTERACTION NUCLEAR PHYSICS

The Los Alamos Experiment on the Beta Decay of Free Molecular Tritium (P-3, P-10)

Modern interest in the masses of the neutrinos stems both from a widely held theoretical conviction that zero is an unlikely value for the mass of any fermion and from observational evidence that the universe is filled with nonluminous, nonbaryonic gravitating matter. On the one hand, a finite neutrino mass would be the first conclusive sign that the Standard Model of Glashow, Weinberg, and Salam is incomplete, as is generally believed (the Standard Model has no mechanism for generating neutrino mass); on the other hand, a mass in the experimentally accessible range would neatly close the universe. There has been much discussion about whether massive neutrinos would inhibit the formation of galaxies, and it is now thought that two different forms of dark matter may exist, one (neutrinos) that accounts for both the total density and the large-scale structure of the universe, and another (cold dark matter) that leads to the formation of galaxies and their halos.

The question of whether the electron antineutrino has finite mass has received considerable attention since 1980, when a Soviet group, Lyubimov et al., presented evidence for a 35-eV mass, almost exactly that required to close the universe. Their method was a careful study of the shape of the beta spectrum in tritium decay. The presence of neutrino mass is revealed by a distortion of the phase space available to the electron near the maximum energy available in the decay. The experiment has been scrutinized by many people; and although some problems with the analysis have been pointed out and since corrected, this group still claims evidence for a 30-eV mass. Concern remains, however, about several systematic problems in the experiment. Perhaps the most fundamental concern relates to the source properties. The source used is tritium substituted for hydrogen in an amino acid, valine. After beta decay of one of the tritium atoms has occurred, various electronic and molecular excitations occur in the source molecule. The energy loss due to these final-state effects must be accurately accounted for to ensure that a spurious neutrino mass is not generated. In addition, the specific activity of tritium in the source is low, and the betas lose a great deal of energy in exiting the source. Again, an improper treatment of this energy loss can result in a spurious neutrino mass.

The experiment at Los Alamos is designed to overcome these systematic problems by using free atomic and molecular tritium as the source. The final-state effects can be calculated exactly for free atomic tritium and to sufficiently high accuracy in molecular tritium that they have a negligible effect on the determination of the neutrino mass. In addition, the specific activity is unity, there is no backscattering in the source, and the energy loss is small and can be calculated and measured accurately. These properties allow us to search for a finite neutrino mass in a model-independent manner.

While the interpretation of our data is systematically very clean, the experimental apparatus used to measure the beta decay of free tritium is quite complex. The source consists of a highly polished 3.7-m-long, 3.8-cm-ID aluminum tube inside a 4-m-long superconducting solenoid. Tritium is introduced at the center of the tube, pumped away at both ends by mercury diffusion pumps, and recirculated. The source tube is held at 160 K to increase the source activity and to minimize

recombination of atomic tritium. The entire tube is biased at typically −8 kV. The beta spectrum is scanned by changing the source bias, which provides constant-energy electrons for analysis by the spectrometer. This minimizes systematic problems and raises the energy of betas from the source above that of the background betas originating from tritium decays elsewhere in the system. Betas from tritium in the tube spiral along the field lines. At one end of the source tube they are reflected by a magnetic pinch; at the other end they are accelerated to ground potential. This provides a source intensity of about 10^{16} atoms/cm^2 with a usable total intensity of 500 μCi. The betas are transmitted through a 2 m long section of differential pumping and are focused to provide an image on a 1 cm-diameter collimator at the entrance to the spectrometer. The source strength for each data point is determined by counting a small fraction of the extracted betas in a solid-state detector which is close to the collimator but out of the field of view of the spectrometer. This detector is biased at the source potential so that its acceptance efficiency varies with the source potential in the same manner as the spectrometer injection efficiency varies with the source potential. The spectrometer is a 5 m long toroidal beta spectrometer with a position- and energy-sensitive gas-proportional counter at the focal plane.

The system has been fully operational for one year, and we have taken several data runs with tritium. Using a gaseous ^{83m}Kr conversion line source, we have measured the system resolution at 38 eV. The first four data sets have been analyzed, enabling us to set an essentially model-independent limit on the electron antineutrino mass of 27 eV at the 95% confidence level, with a best-fit value near 0 eV.

This limit rules out the central value (30 ± 2 eV) of the Soviet claim, but does not yet rule out the full range (17 to 40 eV) they claim is possible. However, our limit does dispose of the possibility that the electron antineutrino has enough mass to close the universe by itself.

We expect to improve the spectrometer resolution to better than 30 eV by careful realignment of all components and to increase the count rate and reduce the background with a new silicon microstrip focal plane detector. These modifications should enable us to reach the 10-eV level of sensitivity.

A High-Statistics Normal Muon Decay Experiment (P-3, University of Chicago, SIN)

The LAMPF High-Statistics Normal Muon Decay experiment (also known as the LAMPF TPC experiment) is designed to measure the momentum distribution of positrons from normal muon decay, $\mu^+ \to e^+ \nu_e \bar{\nu}_\mu$. In its more general form, that spectrum (integrated over the positron polarization and to first order in m_e/m_μ) is

$$\frac{dN}{x^2 dx} \propto 3(1-x) + \frac{2}{3}\rho(4x-3) + 12\frac{m_e}{m_\mu}\left(\frac{1}{x}-1\right)\eta$$

where m_e and m_μ are the positron and muon masses, respectively, x is the reduced energy of the positron ($x = 2E/m_\mu$, where E is the positron energy), and ρ and η are two Michel parameters. The constants ρ and η predominately determine the shapes of the high- and low-energy parts of the decay spectrum, respectively. Their currently measured values are $\rho = 0.7518 \pm 0.0026$ and $\eta = 0.007 \pm 0.013$. The accepted model of the electroweak interaction is the Weinberg-Salam-Glashow theory, which, for the conditions of interest here, leads to the results $\rho = 3/4$ and $\eta = 0$, in good agreement with experiment. The TPC experiment is designed to improve upon the limits of the error in ρ by a factor of 5. Such an improvement has strong implications for possible extensions of the electroweak interaction beyond the Standard Model.

During the last year, the TPC experiment has made strides toward its goal of obtaining a physics result by the end of FY86. During the spring and summer of 1985, an electrostatic separator was-

installed in the muon beam-line. That separator allowed the spins of the experiment's longitudinally polarized, subsurface muons to be rotated by 90°. In this experiment, such a rotation is equivalent to having an unpolarized beam (an unpolarized beam gave an improved acceptance and better control over potential systematic errors in the experiment). Also, a new 2-mm-thick stopping scintillator target and target veto counter were installed at the entrance of the TPC to make triggering of the apparatus more reliable. The TPC electronics system was improved, as well. The upgrade of the computer system, which was started the year before, was completed with the installation of an array processor. As a result, the data-acquisition program enabled us to obtain better diagnostics of the apparatus in real time. Finally, a polarimeter was installed in the beam-line so the muon spin rotation after the separator could be measured. These upgrades of the TPC apparatus were completed before the first run of the experiment in 1985.

Three beam runs were made with the apparatus during LAMPF's 1985 running cycles. The first two were to test the separator and polarimeter apparatus. In the third run, which was approximately 60 shifts long, about 4×10^7 muon decays were written to some 600 magnetic tapes. A typical muon-decay event and the results from the on-line track fitter are shown in Fig. IV-6. After the last run had been completed, approximately 50 more magnetic tapes of cosmic ray and calibration data were written.

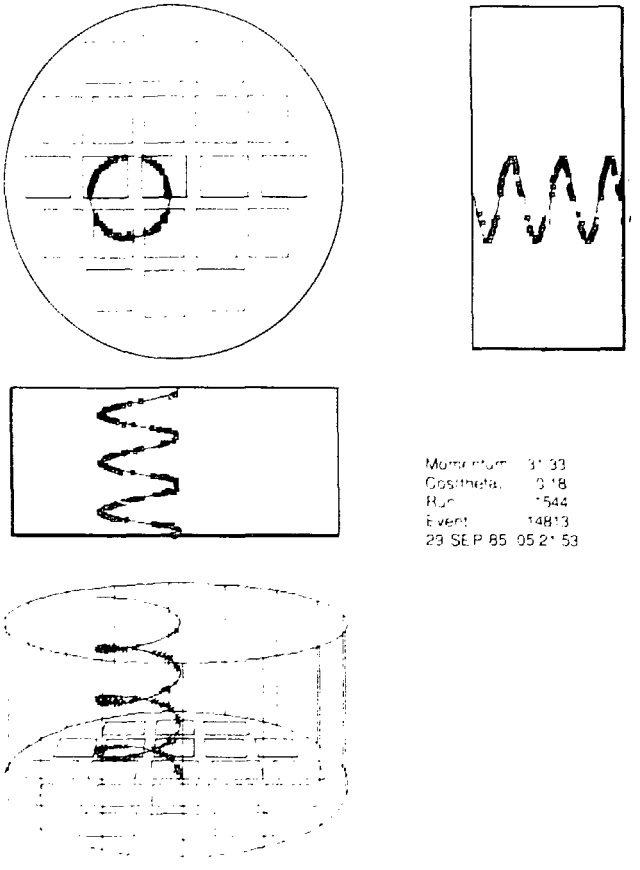

Fig. IV-6. A typical muon decay event as seen in the TPC. At top left is a view as seen by the incoming muon, below that is a side view, and at top right is a top view. The bottom figure is a three-dimensional projection. Also shown are the results of the on-line track fitter.

Since January 1986, the group has been working on data analysis. More accurate algorithms for coordinate reconstruction from the raw TPC data and better algorithms for helical track fitting have been developed. Currently the resolution of individual coordinates along a sense wire is about 1 mm and the resolution in the drift direction is about 2 mm. The new track fitting algorithms, which more accurately than normal take into account the stochastic processes (e.g. multiple scattering, dE/dx energy losses, etc.), are generally useful. In a partial analysis of data from the physics run which ended in December 1985, we have obtained an rms $\Delta p/p$ of 0.5% averaged over the positron decay spectrum from its maximum of 52.8 MeV/c down to about 12 MeV/c, where the experimental acceptance begins to run out. We plan to complete the muon decay analysis by the late summer of 1986.

Calorimetric Measurement of Thermal Neutron Flux (P-3)

For many experiments, such as the determination of the neutron half life and the measurement of absolute neutron cross sections, precise knowledge of a neutron flux is essential. Many techniques have been employed: gold foil activation, $^{10}B(n,\alpha)^7Li$ with accurately weighed boron foils, and $^3He(n,p)^3H$ in proportional counters. With any technique it is difficult in practice to measure the absolute neutron flux to better than 0.5%. Recent advances in the measurement of charged particle beams and in low temperature engineering suggest a way to improve the precision substantially. The method is essentially independent of any neutron cross section.

We are constructing a device that totally absorbs a neutron beam in ^6LiF crystal with the generation of a precisely known amount of heat per neutron. This forms the basis for a highly accurate calorimetric determination of neutron flux. The general design considerations, expected performance, and anticipated systematic errors lead us to conclude that a practical calorimeter will be capable of measuring the flux of a high-quality thermal or subthermal neutron beam to a precision of approximately 0.05%. We expect that a calorimeter of this type will have important applications to measurements of standard cross sections and of the basic properties, such as half life, of the neutron.

HIGH-ENERGY, HEAVY-ION PHYSICS: ULTRARELATIVISTIC NUCLEAR COLLISIONS (P-2)

Experiments with ultrarelativistic heavy ion beams are now being conducted at the Super Proton Synchrotron (SPS) at CERN and at the Alternating Gradient Synchrotron (AGS) at Brookhaven National Laboratory (BNL). The purpose of these experiments is to study nuclear matter at energy densities comparable to those prevailing in the first few microseconds after the "big bang." In situations of high density or temperature a new state of matter, quark-gluon plasma, could be formed. The process would involve deconfinement of the constituent quarks in individual nucleons and formation of a "soup" of quarks and gluons that could traverse nuclear matter freely. At this time we have no accurate predictions of the exact conditions required for the formation of quark-gluon plasma. Experimentalists will have to examine various combinations of projectile-target and nucleon-energy in order to infer the existence of the plasma. Further, neither the changes induced by plasma formation in the spectra nor the composition of emitted particles is well understood. This places an additional burden on experimentalists who must measure reaction products with exceedingly elaborate detail.

The Los Alamos group is involved in two experiments: the high energy lepton and ion spectrometer HELIOS experiment at the SPS, CERN, where 200 GeV/nucleon ^{16}O and ^{32}S beams impinge upon heavy targets, and experiment 814 at the AGS, BNL, where 15 GeV/nucleon ^{28}Si and ^{16}O beams are studied. In both experiments large solid angle calorimetric coverage will track

the energy flow in coincidence with particles detected by magnetic spectrometers. In the HELIOS experiment, the spectrometer views the central "fireball" in order to diagnose the highest energy density region. In experiment 814, a very forward spectrometer examines the momentum loss of incident particles to provide a better understanding of the "stopping power" of heavy nuclei.

The HELIOS Experiment at the CERN SPS*

The outstanding performance of the CERN SPS-PS-LINAC complex in the latter part of 1986 allowed a number of pioneering ultrarelativistic nuclear (URN) experiments at CERN, including HELIOS, to successfully complete a full 17-day period of 200-GeV/nucleon and 60-GeV/nucleon oxygen running. Earlier, 45 days of 200-GeV and 450-GeV protons and variable energy secondary hadron beams were available to debug both the nuclear-beam physics and the lepton physics parts of HELIOS and to take proton-nucleus data as an invaluable physics reference base for the oxygen-nucleus measurements. In addition, a few days of 450-GeV proton beam were dedicated to running with compact, high-pressure D_2 and H_2 targets developed by P-2 and MST-7 at Los Alamos. Proton-proton transverse energy measurements were made with this target in HELIOS, giving us proton-proton, proton-nucleus, and oxygen-nucleus measurements, all taken with the same apparatus. We note also that a hybrid emulsion experiment was performed in HELIOS with a fast-moving emulsion stack as a target. The target "movement" was time-correlated to the normal HELIOS data-acquisition system, allowing one to identify (and thus quickly scan) events in the emulsion for any given HELIOS trigger (e.g., high transverse energy). This powerful technique was made possible by our collaboration with groups from Rome, Bari, and Torino.

In general, the performance of the HELIOS detector was excellent for both the proton and the oxygen runs. On-line triggers employed in the nuclear-beam physics runs in 1986 included a silicon-pad-based interaction trigger, a number of transverse energy thresholds for each of three pseudorapidity intervals (including full coverage), single muons and muon pairs, single and multiparticles in the external spectrometer, photons (i.e., conversion electron pairs) in the converter-external spectrometer, and multiplicity in the 800-element silicon-pad ring detectors.

Both very thin passive targets (Al, Ag, and W) and a sophisticated active target with the same elements were used in the 1986 measurements. The performance of the active target is encouraging, although much work remains to be done to obtain unambiguous localization of the interactions with a given wire in very high transverse-energy, oxygen-heavy nucleus collisions. The combination of energy loss in the beam-counting scintillator and total energy measurement by the calorimeters in HELIOS provides a powerful means of rejecting large background transverse-energy events generated by upstream interactions and double-beam particles. As a result, we are assured of excellent signal-to-noise ratios even at very high transverse energies. The VME-based data-acquisition system performed reliably, writing 100 events per burst (20,000 bytes per event) to tape. Los Alamos contributions to the data-acquisition system include the acquisition and support of the main computers (VAX 750 and microVAX II) and the design and implementation of the on-line run control system.

* With collaborators from Bari University, Italy; Brookhaven National Laboratory; Brussels IIHE, Belgium; CERN, Switzerland; Heidelberg University, Germany; Lund University, Sweden; McGill University, Canada; Montreal University, Canada; Moscow Lebedev Phys. Inst., USSR; Moscow Phys. Eng. Inst., USSR; Novosibirsk Inst. Nucl. Phys., USSR; Oxford University, U.K.; Pisa University/INFN, Italy; Pittsburgh University; Rutherford Laboratories, U.K.; Rehovot Weizmann Institute, Israel; Rome University/INFN, Italy; Saclay CEN DPhPE, France; Stockholm University, Sweden; Tel Aviv University, Israel; Torino University/INFN, Italy; and University College, London, U.K.

The primary Los Alamos responsibility, the external magnetic spectrometer, was ready and performing to design specifications before the proton-nucleus physics runs started in September 1986. The central elements—the large drift chambers upstream and downstream of the magnet—were stable throughout the running. We used a CERN developed temperature- and pressure-controlled CO_2-ethane gas system to obtain an average position resolution of 200 μm (over a 40-mm drift distance) in the drift direction and of approximately 8 mm in the charge division direction (vertical). The 11-element time-of-flight (TOF) system, the 5-element aerogel array, the external calorimeter stacks, and the single- and multiparticle trigger system all operated reliably, as did the various on-line monitoring and calibration systems and software drivers that were constructed for the spectrometer. The Heidelberg photon converter-proportional chamber was successfully integrated into the external spectrometer and was used both in trigger and readout mode to identify photon candidates by conversion electron pairs.

Although delays in the installation of the uranium-liquid argon calorimeter limited the program, significant tests of the electron correlation logic (relevant to the lepton physics part of HELIOS) were performed in 1986. The Moscow transition-radiation detector, the BNL silicon-pad detector, the CERN drift chambers, and the Los Alamos-Torino scintillator-pad array were operated together for the first time.

The Rutherford-CERN off-line analysis framework (SANDRA) and data base, the CERN-based calorimeter analysis programs, the Saclay muon spectrometer analysis programs, and the Los Alamos-Heidelberg external-spectrometer analysis programs have all been developing in parallel during the setup and running. Concerning the latter, we note that the segment-finding and track-fitting programs have been written and tested, as have the particle-identification and event-information correlation programs. The overall integration of the external spectrometer programs into the HELIOS framework is in progress.

An example of the quality and quantity of the 1986 HELIOS data is given in Fig. IV-7. The transverse energy distributions in the pseudorapidity range -0.1 to 2.9 are shown for 200-GeV proton- and pion-lead and 200-GeV/nucleon oxygen-lead interactions. The data sample used here for the oxygen beam is from the September 1986 SPS-PS tests and corresponds to only a few tapes of the hundreds taken later in 1986. The pseudorapidity region shown covers the target and a good fraction of the central region in oxygen-lead collisions. The significance of these data is twofold: 1. Analyses indicate that a 16-fold convolution of the proton-lead spectrum is required to reproduce the oxygen-lead measurements. This implies that each projectile nucleon interacts fully in the target and that no "induced" transparency is observed. 2. At the largest observed transverse energies in the oxygen-lead interactions, well over one-half the kinematically possible energy is seen to be deposited in the oxygen-lead center of mass. This is determined by calculating the available center-of-mass energy for 16 projectile and 50 target nucleons and comparing the result with the center-of-mass energy required for a transverse energy of 225 GeV in the stated pseudorapidity range, assuming isotropic emission of particles from a 66-nucleon "fireball" in its rest frame.

This result is only the first step, for we will now look at the pseudorapidity and azimuthal structure of the energy flow, its composition and transverse momentum distribution (by way of the external spectrometer and photon converter), and its multiplicity structure (silicon rings). We will compare these to the incident energy (200 and 60 GeV/nucleon) as well as the target (aluminum through tungsten) and projectile (pion, proton, and oxygen) mass.

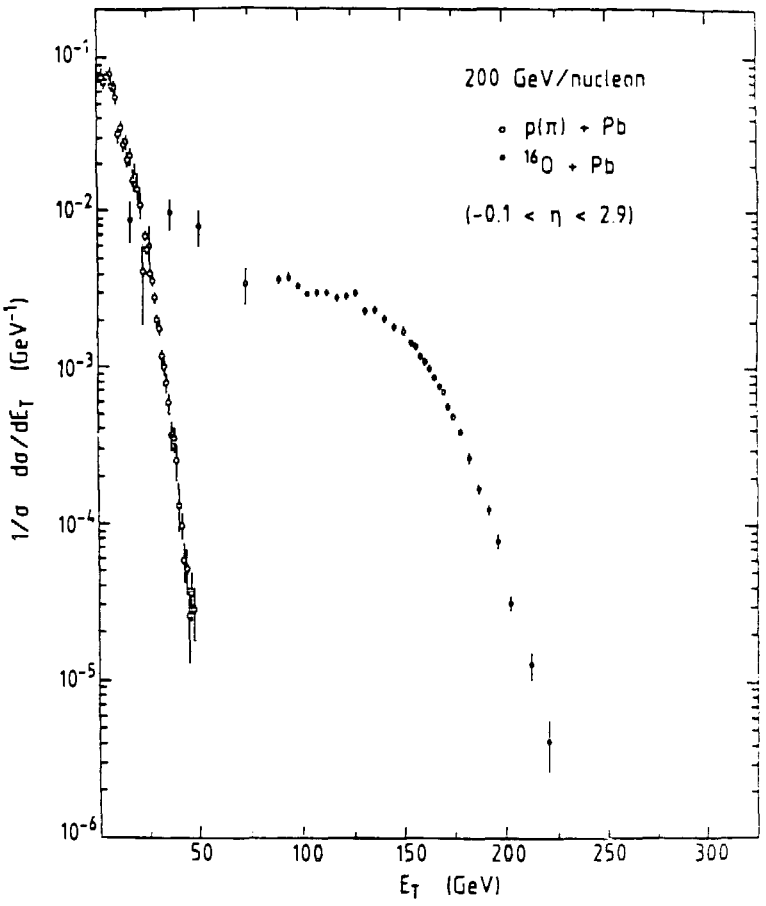

Fig. IV-7. The transverse energy distributions for 200-GeV proton- and pion-lead and 200-GeV/nucleon oxygen-lead collisions measured in the pseudorapidity range −0.1 to 2.9 in the HELIOS experiment in 1986.

Experiment 814 at the BNL AGS*

During 1986 the E814 collaboration made important decisions about the time scale to which it wished to adhere and the type and complexity of charged particle tracking detectors it needed to address the physics goals. The desire to have a working participant calorimeter by middle to late 1988 and the choice of a hybrid tracking system quite different from the HELIOS-type drift chambers, which the Los Alamos group could have rather easily duplicated, led to a decision that we should focus our efforts on the calorimeter and leave the tracking to other E814 groups. Accordingly, we have proceeded to design the device and are engaged in tests of scintillator-fiber light coupling, radiation damage, assembly quality control, and component testing as well as simulations of calorimeter response to charged and neutral particles. A prototype is to be assembled by late 1987 and tested in hadron beams at LAMPF.

* With collaborators from Brookhaven National Laboratory, CERN, Hahn-Meitner Institute Pittsburgh University, State University of New York at Stony Brook, Tel Aviv University, and Texas A & M University.

Figure IV-8 is a design drawing of the calorimeter. The device consists of four identical quarters (the prototype being, in principle, one of the quarters). The quarters are mounted in such a way that the forward-spectrometer aperture can be changed by sliding or lifting. A careful finite-element analysis of the mechanical design performed at Los Alamos resulted in a robust construction held together by hollow steel rods (Fig. IV-8). The hollow rods can also be used as passages for radioactive calibration sources.

The segmentation of the calorimeter is the result of careful simulation and extensive modeling of the calorimeter's response by the GHEISHA cascade code. The electromagnetic part is two segments deep along the beam direction, each segment consisting of 3-mm uranium and 3-mm scintillator plates. The hadronic part is also two segments deep, but here 6-mm uranium, 15-mm iron, and 2.5-mm scintillator plates are used. The total depth is 4.3 interaction lengths. The fourfold segmentation in depth along the beam direction will enable us to correct the device for the varying responses of low-energy particles. The device is segmented radially into 8 and azimuthally into 16 sections. There is no compelling reason to segment further either radially or azimuthally, as the particle shower size is the limiting factor.

The stringent limitations on longitudinal depth placed on the device by other elements in E814 speak for use of the densest absorber available (i.e., uranium). The most compelling argument for uranium, however, is the self-calibrating feature it brings to the calorimeter. Calorimeters using other absorbers require expensive, elaborate, and often unreliable calibration systems.

The aforementioned depth constraint also allows little room for readout and leads us to choose a wave-shifting fiber-optic scheme. Such a readout does enable us to use a compact assembly, but it also introduces problems in the scintillator-readout coupling. We have investigated this coupling

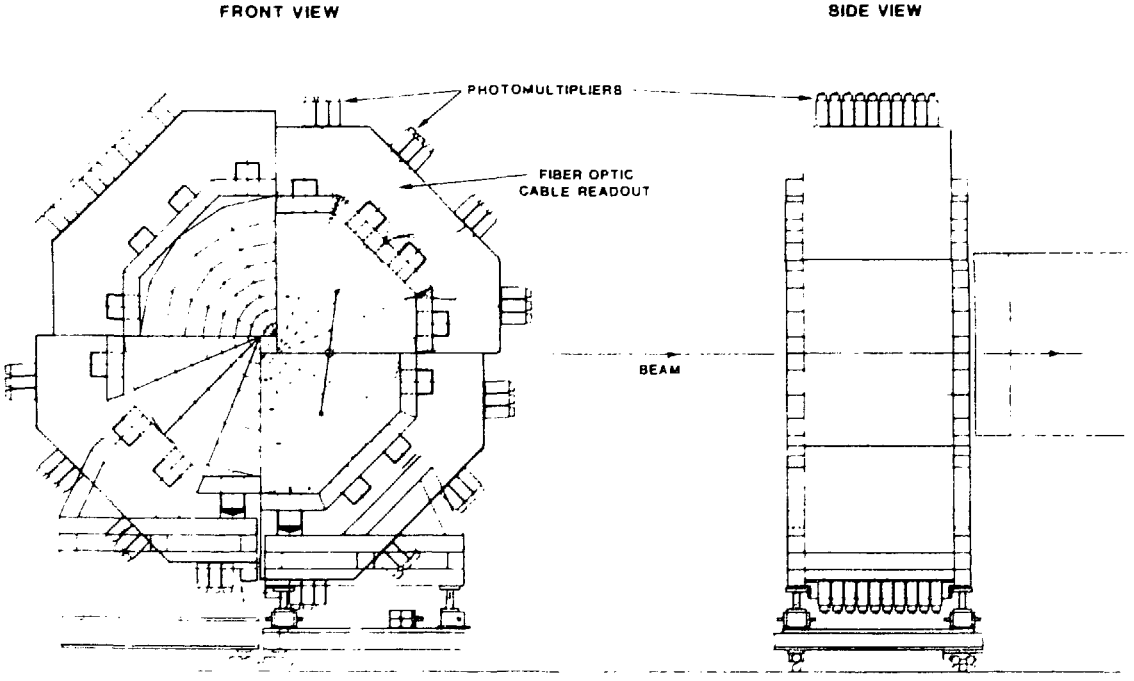

Fig. IV-8. A [illegible] of the BNL E814 participant calorimeter. The uranium-scintillator calorimeter with [illegible] readout consists of four identical quadrants mounted so as to allow a variable forward [illegible] is segmented into two electromagnetic and two hadronic parts.

and its plate-to-plate reproducibility. A good solution has been found, and we are now testing the plate-to-plate variation. The question of deteriorating light output due to radiation damage to the scintillators, fibers, and glue is now under study, and we hope soon to have results that will allow us to proceed with the assembly of the prototype. This problem cannot be underestimated, for it has led to serious resolution loss in HELIOS calorimeters. We consider it necessary to do our own tests because various published results on the effects of long-term, low-dose radiation on scintillators and fibers are inconsistent and sometimes even contradictory. We are also studying phototube and base assembly choices.

ANTIPROTON PHYSICS: A MEASUREMENT OF THE GRAVITATIONAL ACCELERATION OF THE ANTIPROTON (P-3, P-15, AT-1, S-4, S-DO, T-2, T-11, T-8*)

A fundamental measurement in experimental gravity that has not yet been done is the measurement of the gravitational force on antimatter. A difference in the acceleration of protons and antiprotons in the Earth's gravitational field is one of the dramatic predictions of modern theories of gravity. Our gravity experiment (PS200) at the Low-Energy Antiproton Ring (LEAR) at CERN will test directly the equality of particle and antiparticle gravitational masses in the baryon sector with protons (p) and antiprotons ($\bar{p}$).

We plan to use the TOF technique pioneered by Witteborn and Fairbank in their measurement of the gravitational force on the electron. With this approach the particles are launched vertically up a drift tube. The TOF of the particle up the tube, together with the initial velocity, gives a measure of the gravitational force acting on the particle. For a vertical launch and a given drift length, there is a critical initial velocity that will cause the particle to leave the drift region at close to zero velocity. For all initial velocities lower than the critical one, the particle simply does not have enough initial kinetic energy to make it to the detector. Thus, there will be a cutoff time, t_c, in the TOF spectrum.

In our experiment we will be dealing with a one-dimensional Maxwell-Boltzmann distribution of velocities. To measure the gravitational effect on $\bar{p}$, the initial velocity — and hence the kinetic energy distribution — must be low enough in average value so that the resulting TOF spectrum has sufficient particles near t_c for a significant measurement. The energy required is more conveniently measured in kelvins (K) than in the more familiar MeV or keV. The realm of high-energy physics is somewhat arbitrarily indicated to start at 10^{14} K (10^{10} eV) and to extend upward without limit through 10^{16} K (10^{12} eV). Normal LEAR operations span the temperatures between 5.8×10^{10} K to 1.5×10^{13} K (1.3 GeV to 5 MeV). Antiproton temperatures in the range of 1 to 10 K are required for the gravity experiment. In order to achieve this antiproton temperature, we are designing a radio-frequency quadrupole (RFQ) decelerator and ion-trap system. This system will extend the normal LEAR operating temperatures by 10 orders of magnitude, opening very exciting possibilities for antiproton research in the areas of chemistry and of atomic and condensed-matter physics.

The overall system we are planning is displayed schematically in Fig. IV-9. The experimental sequence starts with the extraction of a 2-MeV bunched beam from LEAR (which is being upgraded to provide a 2-MeV fast-extracted beam with the good emittance required by our experiment). The bunched beam in LEAR has a macrotime structure set by the eighth harmonic buncher already in the LEAR ring. A single-phase packet of this bunched beam is fast-extracted from LEAR and delivered to the entrance of our experimental beam line. A microtime structure matched to the operating frequency of the RFQ decelerator will also be imposed on the macroburst. In the figure,

* With collaborators from Rice University, Texas A & M University, Kent State University, Case Western Reserve University, University of Pisa, University of Genoa, NASA/Ames Research Center, and CERN.

an external bunching section is shown although bunching in LEAR would make the most efficient use of antiprotons. The bunched beam at 2 MeV is decelerated to 20 keV in an RFQ currently under design at Los Alamos. With a suitable bending magnet in the beam line the 20 keV beam can be made available to our experiment or to others.

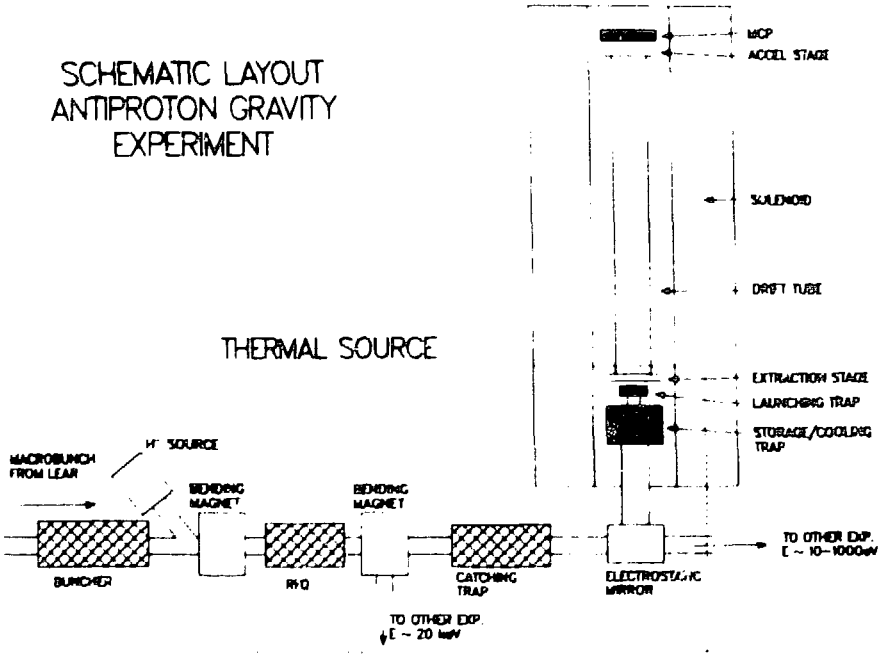

Fig. IV-9. Overall system for the low energy beam line required by the antiproton gravity experiment. The horizontal beam line can deliver beam in the energy range 10 to 1000 eV; the vertical beam line delivers beam at 0.001 eV or less for the gravity experiment.

Immediately following the RFQ is the first stage of pulsed ion traps that will be used to capture, store, and cool the antiprotons. The first stage catching trap is shown in schematic cross section in Fig. IV-10. This device is cylindrically symmetric about the horizontal axis and is designed along the lines of a Penning trap. The multiring configuration provides a harmonic potential along the horizontal axis, centered at the electrode with the circular cross section, when the electrodes symmetric about this one are at specially matched potentials. Small apertures (~0.6 cm in diameter) in the endcap electrodes at the far ends of the multiring array allow the beam burst to enter or exit. A magnetic field along the horizontal axis, generated by the solenoid shown in the figure, radially confines the burst. The beam burst emerging from the RFQ, initially 50 cm long, enters the catching trap (from the left in the figure), decelerates to 5 kV as it enters the elongated electrode, and is reduced to a 25 cm burst length. When the entire burst is inside, the potential on the elongated electrode is quickly (in ~ 15 ns) brought to ground before the burst starts to propagate inside the multiring array. The down-stream endcap electrode is maintained at −8 kV so that the burst decelerates inside the trap and eventually turns around. Before the burst can propagate more than halfway back, the potential on the entrance endcap electrode is brought up to −8 kV, trapping the burst. While trapped, the antiprotons are resistively cooled to 10 to 100 eV by well-established ion trap techniques. The particles then transfer through a 90° electrostatic mirror into a harmonic trap (located in the vertical beam line) for further resistive cooling. In this intermediate trap, the particles are cooled to ~ 5 to ~ 10 K and are stored in preparation for transfer, 100 at a time, into the final launching trap.

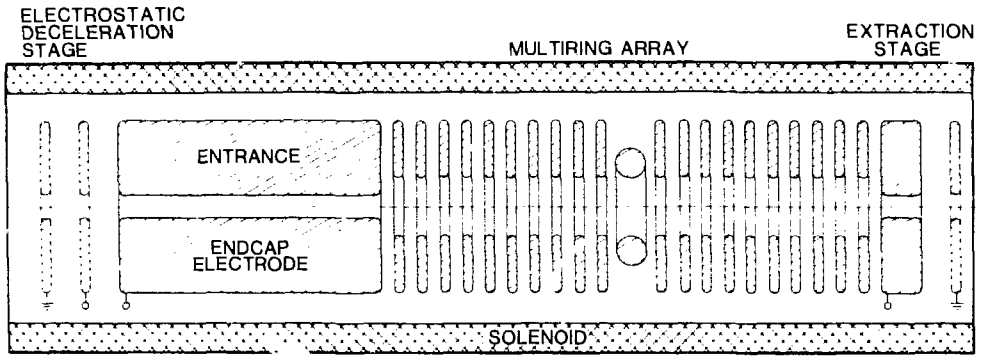

Fig. IV-10. Schematic cross section of the first-stage catching trap. The device is azimuthally symmetric about the horizontal axis. The entrance electrode is elongated to accommodate the beam burst length after the electrostatic deceleration stage.

Once the launching trap is loaded, the potential is suddenly dropped and particles are released upward into the drift tube. A microchannel plate at the top of the drift tube is used to measure the TOF. The vertical ion-trap drift-tube system must operate at extremely low pressures ($\sim 10^{-14}$ torr) to avoid loss of antiprotons through annihilation with any residual gases. Consequently, this system will be cooled to ~4 K to freeze out potential residual gases.

The calibration standard for our measurement of the gravitational acceleration of the antiproton will be the H^- ion, which has the same electromagnetic properties as the antiproton. An ion source upstream of the RFQ (Fig. IV-9) will inject H^- ions into our beam line at 20 keV. We will not energize the RFQ during the injection period so that we can exercise the system independently of the operation of the LEAR beam. For a 1% measurement of the gravitational acceleration of the antiproton, 10^6 to 10^7 particles must be launched. Each eighth harmonic macrobunch from LEAR will provide $\sim 10^8$ particles, sufficient for one TOF spectrum with some safety margin. Many TOF spectra will be required in order to ensure reproducibility. Each antiproton run will be followed by a run with H^- ions.

Equipment that will be used to study and demonstrate the proposed method of measurement is under development at the Los Alamos IBF and at Texas A & M University, Rice University, the University of Pisa, and the University of Genoa.

At the IBF we have constructed two major research tools: 1) a small ion source and vacuum apparatus to study the operating characteristics of microchannel plates (the type of particle detector we envisage using in the gravity measurement) and 2) a low-energy beam line (~5 to ~100 keV negative or positive ions) feeding a small Penning trap (trapping volume of a few cm^3) mounted in a vertical, 6-T superconducting solenoid magnet. Above the Penning trap and in the fringe field of the magnet, we have mounted a microchannel plate to detect ions released from the trap. The first device is ready for use. The second is being used to study the trapping of external ions (mainly H^- ions) and is also yielding information on the ultimate vacuum attainable in such a room-temperature system, the features needed in future trap designs, and the type of H^- ion source to be taken to LEAR. To date, we have attained pressures as low as 5×10^{-11} torr in the system and have reached a major milestone by trapping 10-keV H^- ions with a mean life in the trap of a little over 1 s.

The Texas A & M group is developing a small launching trap embedded in a cryogenic environment and is studying cooling techniques for trapped particles. The Rice University group is assembling a computer system and will construct and help test a prototype catching trap. The groups at the Universities of Pisa and Genoa are studying stochastic cooling traps and particle-detection methods and are carrying out background studies at LEAR.

The gravitational mass of the antiproton is a fundamental measurement that has not yet been made, nor has any theoretical argument convincingly anticipated the result of such a measurement. Our attempt to determine the gravitational mass of the antiproton will test the weak equivalence principle for antimatter and will provide a powerful constraint on modern attempts to unify gravity with the other forces of nature.

PARTICLE PHYSICS

Study of the Nuclear Antiquark Distribution through High-Mass Pair Production (E-2, P-3, MP-4*)

The premier problem in nuclear physics today is to understand the relevance of quarks and quantum chromodynamics (QCD) to the structure of nuclei. At one extreme, if quarks are absolutely confined, an understanding of nucleons and their free-space interactions may be sufficient for an understanding of nuclear systems. At the other extreme, if quarks can "leak out" and communicate directly with quarks in other nucleons, understanding quark degrees of freedom in nuclei will be of the utmost importance.

The one existing piece of experimental evidence that bears directly on these issues is the famous EMC effect, named after the European Muon Collaboration, which made the discovery. The group observed that very high-energy muons exhibit different scattering probabilities depending on whether the target consists of free nucleons or nucleons bound in nuclei. Because muons of this energy range directly probe the nucleon quark distribution, the obvious interpretation of this observation is that nuclear matter exerts an effect on the confinement of quarks. This, however, is not a unique interpretation. In fact, models of nuclei that involve only classical nuclear physics are also able to account for the EMC data.

Our interest in possible high-energy experiments relating to these issues arose from an examination of the impact on nuclear physics of an advanced hadron facility (AHF). On the basis of this study we were convinced that a purely electromagnetic reaction, known as the Drell-Yan process, not only was the source of an exciting program at an AHF but also could be employed in an experiment at an existing accelerator facility to understand the real origin of the EMC effect. As is shown in Fig. IV-11, the Drell-Yan process occurs when a quark and an antiquark from either the incident beam or the target annihilate to form a massive virtual photon, which then decays to a muon pair. The power of the Drell-Yan process is realized by an experiment in which ultrahigh-energy protons are allowed to interact with targets of either free nucleons or nucleons bound in nuclei. A precise comparison of the muon-pair production probability for the two targets reflects the change in the antiquark distribution in the target nucleon. The experimental conditions are chosen so that beam-quark target-antiquark annihilation dominates over the beam-antiquark target-quark process. This situation is clearly complementary to muon scattering, which cannot distinguish between quarks and antiquarks.

Figure IV-12 compares theoretical estimates of the quantity R,

$$R = \frac{(\mu^+\mu^- \text{ cross section})^{Free}}{(\mu^+\mu^- \text{ cross section})^{Bound}} \cong \frac{(\text{anti-up-quark distribution})^{Free}}{(\text{anti-up-quark distribution})^{Bound}} ,$$

with the expectations from the experiment described in the following paragraphs. The predictions are from two very different models of the EMC effect, which give nearly identical results for those

* With collaborators from Fermilab, State University of New York at Stony Brook, University of Illinois at Chicago, University of Washington, University of Texas, and Rutgers University.

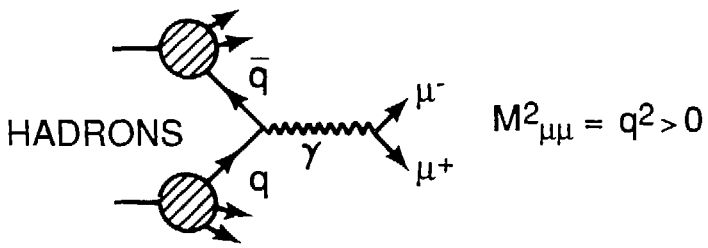

Fig. IV-11. Feynman diagram for the Drell-Yan process

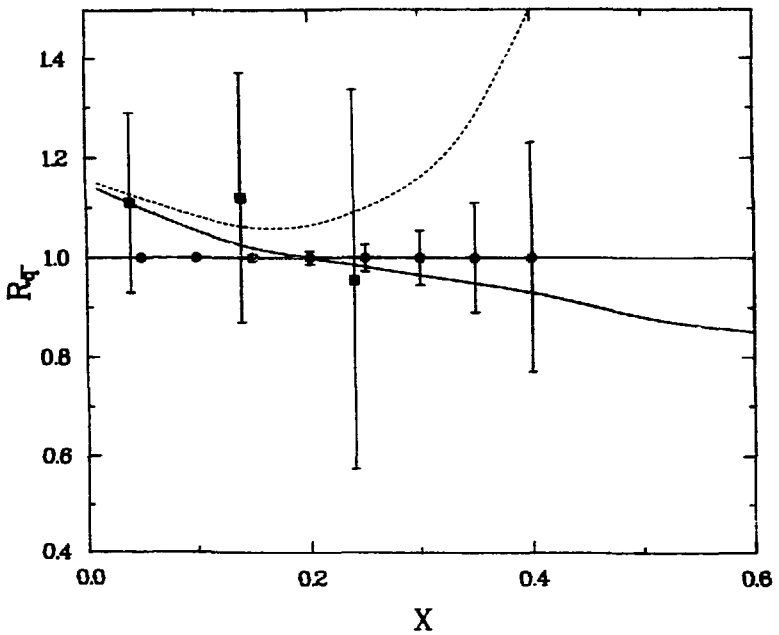

Fig. IV-12. Comparison of the pionic enhancement model (dashed line) and the rescaling model (solid line) with charged-current neutrino scattering data for the A-dependence of the antiquark distribution $R = q^{Fe}(x)/q^{N}_{(x)}$. Also shown are estimates at the error bars obtainable in Fermilab experiment E772 (points along the line R=1).

data. Clearly the Drell-Yan process would be able to choose between these models, which, roughly speaking, ascribe the EMC effect to a fundamental QCD effect in nuclei (rescaling) or to classical nuclear physics (pion enhancement).

The experiment we have proposed is the measurement of dimuon pairs from the bombardment of ^{2}H and ^{40}Ca targets with 900-GeV protons at Fermilab. The experiment was considered by the program committee at Fermilab in April 1986 and was approved in June 1986. It is scheduled to run from March 15 to August 15, 1987. Although the plan is to use an existing spectrometer (E605), many technical problems must be solved before we can measure the nuclear antiquark distribution at the required level of precision. Many of the problems center around the challenge of distinguishing

the approximately three good $\mu^+\mu^-$ events per minute from the instantaneous event rate, which is 8 orders of magnitude higher. A very sophisticated multilevel triggering device based on specialized event-analysis computation is the key to the solution.

This experiment is spearheaded by the Los Alamos contingent and will involve a large number of personnel from P Division during the coming year. Not only are the physics goals very exciting, but the technological problems and their solutions show promise for further application to other areas of research at the Laboratory.

Eta-Meson Production Experiments at LAMPF (P-2, MP-4, Q-1, University of Virginia)

The roles of heavy mesons (η, ω, ρ, σ, and the like) in nuclear physics are essentially unexplored. Little information exists about the interactions between heavy mesons and nucleons, and almost nothing is known about their interaction with nuclei. We lack knowledge largely because the existing meson factories do not have enough energy to produce these heavy mesons. Accelerators of higher energies, such as the AGS and the proposed LAMPF II, are required for such studies. We noted about two years ago, however, that the pion beam at LAMPF is sufficiently energetic to produce η mesons though the $\pi + N \rightarrow \eta + N$ reaction. In a series of experiments performed at LAMPF, we have used a variety of experimental techniques to successfully measure the (π, η) reaction on several nuclear targets. The experiments are described in the following paragraphs.

$P(\pi^-, \eta)n$ Reaction. This reaction is identified by using scintillation counters to measure the neutrons and BGO counters to measure the $\eta \rightarrow 2\gamma$ decay. This was the first time that the meson had been detected at LAMPF.

$^3He(\pi^-,t)\eta$ Reaction. Using the large-aperture spectrometer (LAS) at LAMPF, we can clearly identify the tritons from this reaction. Figure IV-13 shows the triton spectrum measured at 680-MeV/c π^- beam momentum. This was the first time that a discrete nuclear final state had been resolved in the (π, η) reaction.

Subthreshold $^3He(\pi^-, \eta)t$ Reaction. The LAMPF π^0-spectrometer was used to measure η through the detection of $\eta + 2\gamma$ decay. The η mesons are clearly identified in the invariant mass spectrum (Fig. IV-14). The $^3He(\pi^-, \eta)t$ reaction was measured at several beam momenta between 680 MeV/c and 590 MeV/c. These are called subthreshold η production because the beam momenta are below the threshold of the $\pi^- + p \rightarrow \eta + n$ reaction. The observed cross sections of the $^3He(\pi^-, \eta)t$ reaction are significantly larger than those predicted by theorists.

Inclusive (π^+, η) Reaction on Several Nuclei. Figure IV-15 shows the inclusive (π^+, η) cross section as a function of the target mass. The solid curves show that the mass dependence of the inclusive cross sections allows us to deduce the η-N total cross section.

These experiments represent the first efforts to study the (π, η) reaction with sufficient energy resolution that discrete nuclear states can be identified and at beam energies near or below the free threshold. From the comparison between the $(\pi^\pm, \eta)$ and the $(\pi^\pm, \pi^0)$ reactions, new information on the mechanisms of charge-exchange reactions are revealed. The energy and mass dependence of the (π, η) cross sections also provides unique information on the η-nucleon and η-nucleus interactions. In a similar fashion, one could study other heavy mesons at a facility such as the proposed LAMPF II accelerator.

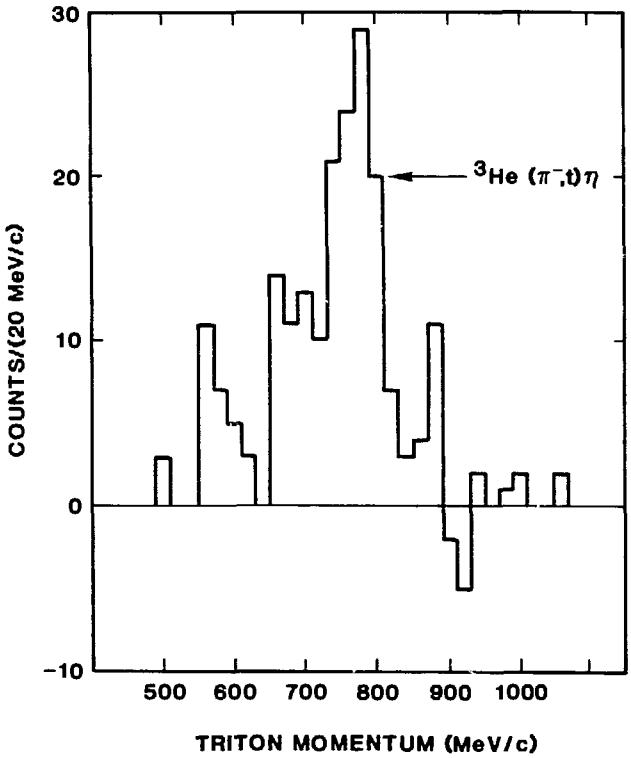

Fig. IV-13. Energy spectrum of the ^{3}He(π^-,t) reaction at 680 MeV/c.

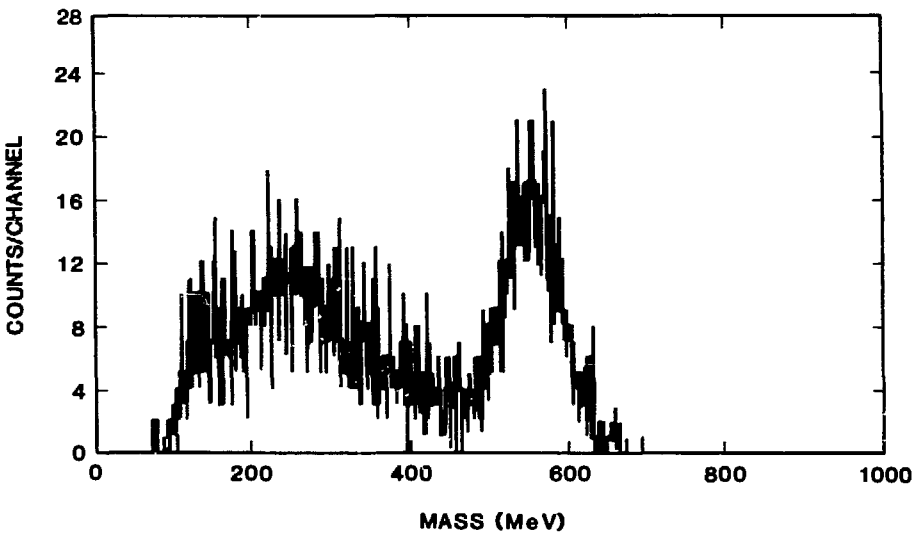

Fig. IV-14. Invariant mass plot for the two photons detected in the π^- + ^{3}He reaction at 680 MeV/c with the LAMPF π^0-spectrometer.

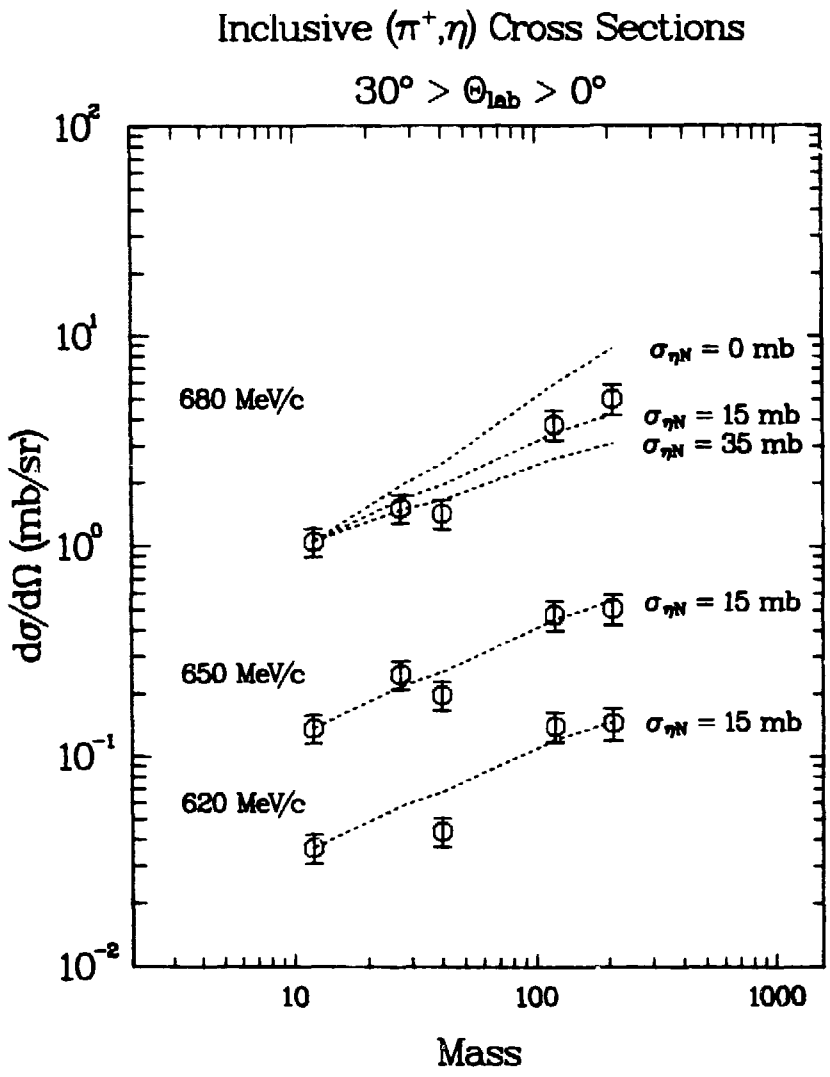

Fig. IV-15. Inclusive (π^+,η) cross sections on several target nuclei. The dashed curves are Glauber calculations using various η-N total cross sections.

We are also constructing an eta-spectrometer, shown schematically in Fig. IV-16, to be used in future η-production experiments. The design principles of the eta-spectrometer are similar to those of the LAMPF π^0-spectrometer. However, we have chosen NaI and BGO crystals, rather than lead glass, as the material for the shower detectors and the converters in order to improve on the energy resolution. The eta-spectrometer will also be a model apparatus for detecting π^0, high-energy gamma rays, and charged particles. The eta-spectrometer is near completion and is scheduled for use in a LAMPF experiment late in 1986.

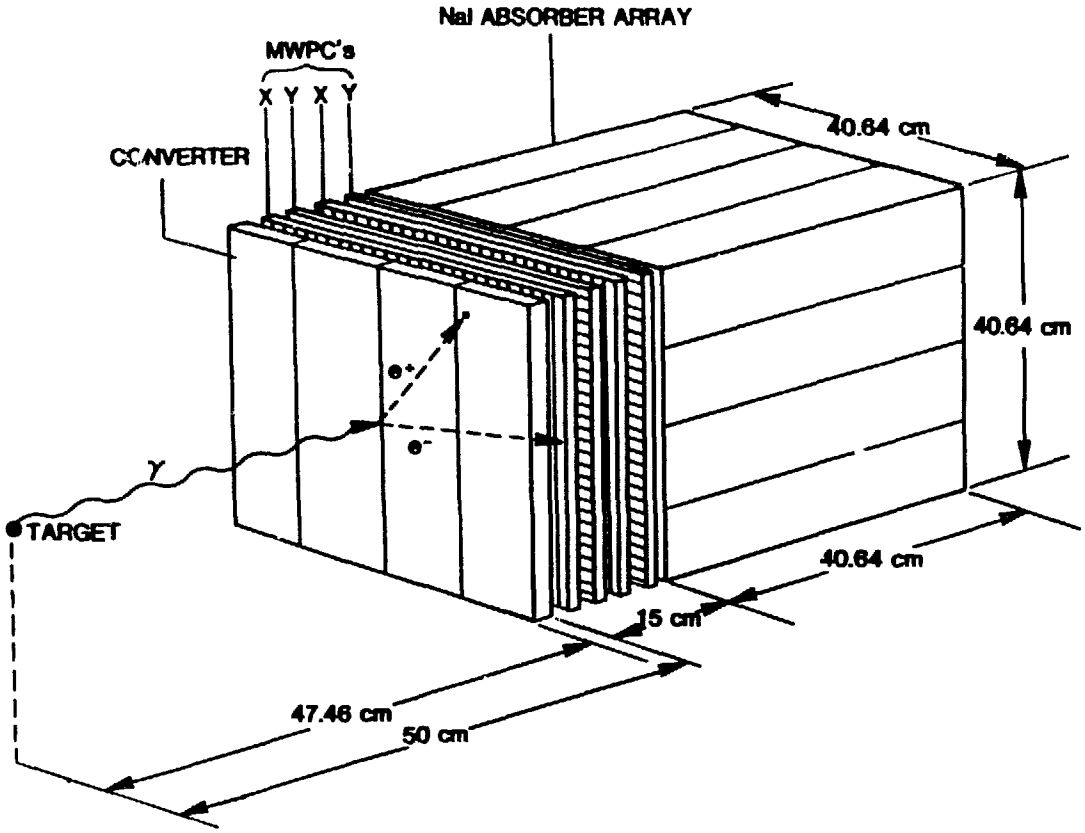

Fig. IV-16. Schematic diagram of one of the two identical arms of the eta-spectrometer. The converter is made of BGO slabs.

A Search for Very Rare K_L Decays (P-3, MP-4, MP-13*)

In 1984 a group from Los Alamos, along with groups from other institutions, formed a collaboration to search for previously unseen decay modes of the long-lived neutral kaon (K_L). The primary goal of the experiment, conducted at BNL, is to search for the decay $K_L \rightarrow \mu e$ at a branching ratio sensitivity of 10^{-12}, representing some 2 orders of magnitude greater sensitivity than has previously been achieved. If the decay is observed, it will indicate a violation of separate muon and electron number conservation and, therefore, new physics. The apparatus will simultaneously detect 10^2 to 10^4 decays of the form $K_L \rightarrow \mu\mu$. Until now, the total world sample of those decays is only 27 events from three different experiments. The large number of events in our experiment will provide data for a search for a nonzero polarization of the μ's. If found, such a polarization would be an indication of a new CP-violating process. The experiment will also be able to detect the decay $K_L \rightarrow ee$ at a sensitivity of 10^{-12}. Because the Standard Model of the electroweak interaction predicts that process to be at a much lower branching ratio than our sensitivity, the detection of this decay would be an indication of new physics beyond the Standard Model. We will also search, with less sensitivity, for other decays such as $K_L \rightarrow \mu\mu\gamma$, $K_L \rightarrow ee\gamma$, $K_L \rightarrow \mu\mu ee$, and the like.

* With collaborators from Stanford University, University of California at Los Angeles, University of Pennsylvania, College of William and Mary, and Temple University.

The apparatus begins with a K_L production target, which is part of a new BNL beam line. The experiment will ultimately run with 10^{13} protons on target per beam pulse. After passing through the target, the beam traverses sweeping magnets, collimators, and an evacuated decay volume. The charged-particle tracks resulting from K_L decays in the decay volume will be detected by drift chambers located in front of, between, and behind two momentum-analyzing magnets. The magnetic fields will be adjusted so that particles exiting the final magnet will produce tracks parallel to their entrance trajectories in the first magnet. That feature is used to provide high-speed, on-line determination of the momentum of charged particles in the second-level trigger of the apparatus. The chambers are of very low mass in order to minimize the distortion of the charged-particle trajectories. Output from the drift chambers enters in succession scintillator hodoscopes, a Cerenkov counter (from which data are used in the first- and second-level triggers), and a lead glass array. The latter provides for π-e separation at a level of 10^{-3}, for a quick electron energy measurement in the on-line trigger, and for photon energy and position measurements. Behind the lead glass is a 2.7-m-thick steel muon filter and, behind that, another trigger hodoscope and the rangefinder/polarimeter. The latter provides an on-line measure of the muon momentum by means of range analysis and is used to determine muon polarization in the $K_L \rightarrow \mu\mu$ part of the experiment.

During the last year, the Los Alamos group has been involved in several aspects of the collaborative experiment. We have worked on the beam line, the shielding calculations, computer procurement, trigger electronics, and various aspects of the rangefinder/polarimeter design and development. We also provided some of the equipment used in the beam tests. The equipment was sent to BNL on May 1, 1986, for a beam-development run, which showed that more work must be done on the K_L beam line. This work should be completed in time for a data-taking run that will begin in early FY87. A second data-taking run will begin later in the year. The goals of the experiment are to achieve a branching ratio sensitivity of about 10^{-10} on $K_L \rightarrow \mu e$ by the winter of 1987. We expect that it will take at least one additional run in 1987 to achieve the ultimate precision of 10^{-12}. We plan to submit another proposal to BNL, requesting more running time in a mode that will enhance the polarization measurement of the experiment.

CHARGE-EXCHANGE AND POLARIZATION PHYSICS: STUDIES OF SPIN TRANSFER IN MEDIUM-ENERGY CHARGE-EXCHANGE REACTIONS (P-2, MP-10*)

Since 1980 the investigation of nuclear dynamics through inelastic scattering reactions with nucleons has undergone an exciting revolution in experimental technique and theoretical framework. These studies had long been cursed by the enormous complexity of the underlying elementary nucleon-nucleon (N-N) interaction, one involving a complex summation over virtually every spin and isospin dependence allowed by basic symmetries. In 1980, the invention of experimental techniques for measuring complete sets of polarization transfer (PT) observables in medium-energy $(\vec{p},\vec{p}')$ reactions spurred the development of theoretical models showing that such measurements can provide the means for sensitively studying the individual spin and isospin components of N-nucleus scattering probabilities. Furthermore, because at medium energies each such component can be interpreted as the product of an effective N-N interaction amplitude and a nuclear structure form factor, 1) PT measurements on chosen transitions with known nuclear structure can be used as filters to select or exclude components of the effective N-N interactions and to map their separate momentum dependences; and 2) once the effective N-N amplitude is thus precisely calibrated, N-nucleus PT measurements can provide uniquely selective information on the nuclear response in

* With collaborators from Indiana University Cyclotron Facility, Ohio State University, Ohio University, and Oak Ridge National Laboratory.

regimes where its structure and underlying dynamics are less well determined. Our pioneering $(\vec{p},\vec{p}')$ studies have been used for both of these purposes as well as for establishing the basic validity of the experimental and theoretical approaches.

Studies of continuous isovector spin-dependent excitations are especially interesting because for free N-N interactions involving both isospin and spin transfer, the associated scattering amplitudes can be directly related to specific elementary meson exchange processes. Deviations in the spectrum of such modes from expectations based on embedding the free N-N interaction in the nuclear medium may thus provide important new insight into impacts of the nuclear many-body environment on long-wavelength subnucleon dynamics and their feedback into nuclear structure.

Investigation of a particular spin-isospin N-nucleus scattering component requires a beam that is "polarized" in both spin and isospin and the measurement of both the spin and the isospin of the outgoing nucleon. Although proton polarizations are easy to produce and measure, the $(\vec{p},\vec{p}')$ reaction is not optimal for studying isovector spin modes because it is generally dominated by isoscalar spin-independent processes. We have therefore undertaken the development of techniques for PT measurements in the $(\vec{p},\vec{n})$ charge-exchange reaction. Here the isospin polarization comes automatically, numerous interesting reactions involve "background-free" ground state-to-ground state transitions, and the energy dependence of the underlying N-N interaction permits us to alter dramatically our sensitivity to spin merely by changing the incident beam energy. However, the efficient measurement of intermediate-energy neutron polarizations is a significant new challenge.

To exploit the maximum power of the $(\vec{p},\vec{n})$ reaction in general, we must measure complete sets of PT observables for a variety of excitations. This is our long-term goal. At present, however, only the Indiana University Cyclotron Facility (IUCF) has a high-duty-factor, high-resolution neutron-TOF system for $(\vec{p},\vec{n})$, and this only for polarizations normal to the reaction plane. We have therefore concentrated our initial efforts on measurements of the normal polarization transfer coefficient $D_{NN}(\theta)$ [or equivalently the normal spin-flip probability $S_{NN}(\theta) = (1 - D_{NN})/2$].

At laboratory scattering angle $\theta = 0°$, this observable is especially simple. From an experimental standpoint, $D_{NN}(0°)$ reduces to the ratio P_n^f/P_p^i of the final-state neutron polarization to the incident-proton polarization. Theoretically, it should be different from unity only to the extent that spin transfer is important to the transition in question. And $D_{NN}(0°)$ should be distinctly sensitive to the parity of spin-dominated excitations; as a general rule we expect natural-parity transitions to have $D_{NN}(0°) \geq 0$ (spin-flip probability $\leq 1/2$) while unnatural-parity transitions should yield $D_{NN}(0°) < -1/3$ (spin-flip probability $> 2/3$). First measurements for $D_{NN}(0°)$ at 160-MeV beam energy were discussed in earlier reports. The measurements were designed to test the predictions by investigating $D_{NN}(0°)$ for excitations with independently known spin dependences, and they convincingly demonstrated the anticipated behaviors and sensitivities.

During the current review period additional data have been obtained at IUCF for beam energies of 80, 120, and 200 MeV. We have particularly concentrated on exploiting the selectivity offered by $D_{NN}(0°)$ measurements as a new means for characterizing the structure of the giant resonance region of the nuclear continuum. Figure IV-17 compares results for $^{90}Zr(\vec{p},\vec{n})$ at 120 MeV to those previously reported at 160 MeV. The spin-flip data in these figures have been sorted into 1-MeV bins to reduce statistical scatter.

Several interesting features emerge from these data. In particular, the 160-MeV D_{NN} spectrum implies regions where natural and unnatural parity excitations are alternately most important. The $0^+ \rightarrow 0^+$ isobaric analogue state, for which $D_{NN} \equiv 1$, is notably absent in the spin-flip cross section σS_{NN} but stands up prominently in the non-spin-flip spectrum. Because it lies in a region dominated by Gamow-Teller (GT) strength ($\Delta J^\pi = 1^+$), it is particularly evident as a marked positive fluctuation in the excitation spectrum of D_{NN}. Also, the observed values of $D_{NN}(0°)$ for the region of the giant GT resonance are close to the nominal value of $-1/3$ expected for isovector 1^+ transitions and are consistent with theoretical predictions that most of the cross section in this region corresponds to GT excitations. The essentially zero value found for $D_{NN}(0°)$ near $E_x = 20$ MeV is particularly noteworthy. There is also an obvious bump in the non-spin-flip spectrum but nothing

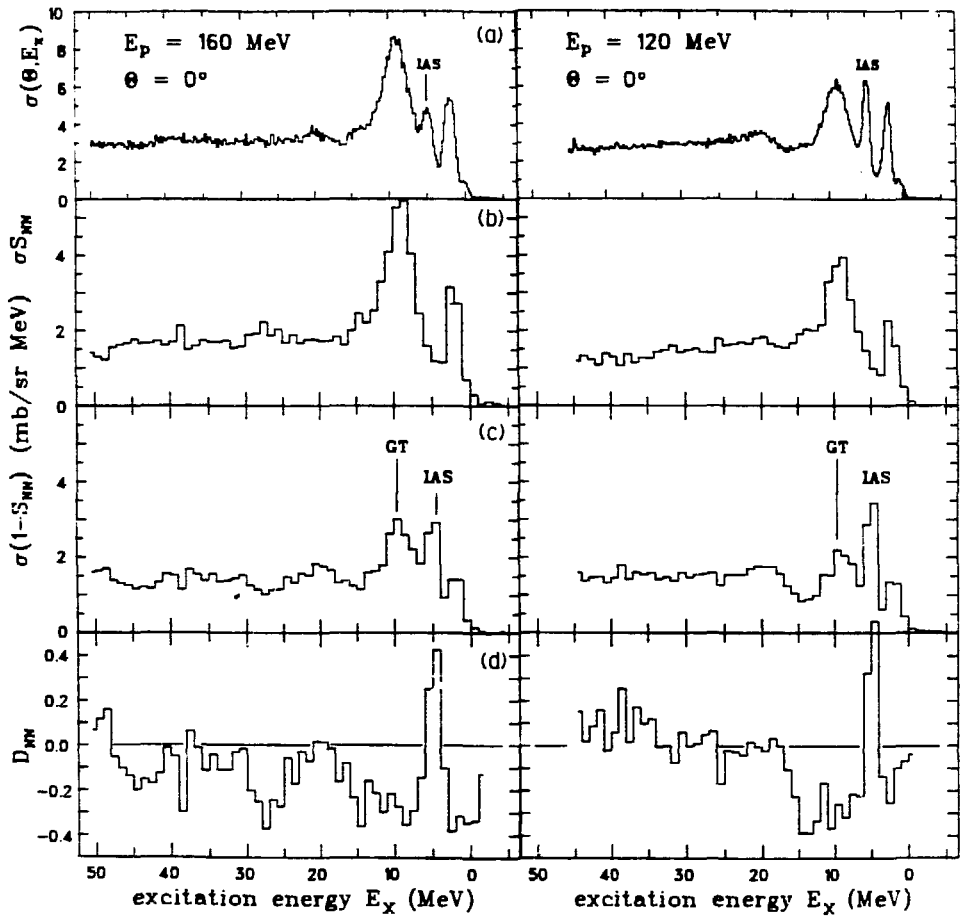

Fig. IV-17. ^{90}Zr($\vec{p}$,$\vec{n}$) 0° excitation spectra at 160 and 120 MeV for (a) the overall, (b) the spin-flip, and (c) the non-spin-flip differential cross sections and for (d) the normal polarization transfer coefficient.

particularly noticeable in the spin-flip cross section near this excitation energy. The measurements thus indicate that a large fraction of the 0° strength in this region has natural parity. This result is at odds with recent calculations by Osterfeld, Cha, and Speth, who predict very little 0° natural-parity ^{90}Zr(p,n) strength for E_p = 200 MeV. The location of natural-parity strength indicated by our 160-MeV measurements is in good agreement with low-energy measurements, which are most sensitive to the non-spin-flip component of the 1^- resonance.

For excitation energies larger than 25 MeV, the apparently alternating regions of natural and unnatural parity strength apparent at 160 MeV are no longer evident at 120 MeV. It is possible that these differences can be attributed to changes in the effective N-N interaction as a function of energy and momentum transfer. Alternatively, this change may indicate that reaction mechanisms more complicated than nearly free N-N scattering in the nuclear medium are becoming important at the lower beam energy. We are currently investigating both possibilities.

We have also obtained similar ($\vec{p}$,$\vec{n}$) spin-transfer data for ^{6,7}Li and ^{13,14}C at 80 MeV; for ^{6,7}Li, ^{12,13,14}C, and ^{15}N at 120 MeV; for ^{6,7}Li, ^{12,13,14}C, ^{11}B, ^{15}N, and ^{19}F at 160 MeV; and for ^{6,7}Li, ^{12,13,14}C, ^{15}N, ^{27}Al, ^{40,42}Ca, and ^{90}Zr at 200 MeV. Reduction of all but the 200-MeV data is

complete, and systematic analysis is in progress. Such an extensive basis for study in an energy range where the relative strengths for exciting spin-flip versus non-spin-flip modes vary over a wide range will provide valuable new tests of nuclear structure models and will constrain their predictions in a much more basic and stringent fashion than mere comparison of cross sections.

We will soon concentrate on exploiting the new capabilities becoming available for medium-energy polarization studies. To measure complete sets of polarization transfer observables in $(\vec{p},\vec{n})$ as well as $(\vec{p},\vec{p}')$ reactions, we are devoting major effort to the development of a large-acceptance, highly efficient broadband polarimetry system for neutrons in the 100- to 800-MeV energy range.

In the more distant future, we hope to implement a limited neutron spin-precision capability at IUCF so that we can at least progress to measurements of N-type spin-transfer angular distributions there. Although $D_{NN}(0°)$ is sensitive primarily to the natural- versus unnatural-parity aspects of a transition, its angular distribution is expected to reflect the specific underlying angular momentum multipoles. The interplay between these various multipoles will also generally affect $D_{NN}(\theta)$ differently than for the cross section. Consequently, given our already rather extensive 80- to 200-MeV 0° data, even such a moderate advance in experimental capability should provide important new information on the nuclear spin-isospin response in this energy range.

V. WNR/PSR/LANSCE FACILITY FOR NUCLEAR AND CONDENSED-MATTER PHYSICS

LANSCE DEVELOPMENT (P-8, P-9, AT-3)

The Weapons Neutron Research (WNR) facility was built in 1978 as a pulsed-neutron source. The neutrons are produced by spallation reactions that occur when 800-MeV protons from the Los Alamos Meson Physics Facility (LAMPF) strike a heavy metal target. Each proton striking the target produces approximately 20 neutrons: at a proton current of 5 μA, an average of $\sim 6 \times 10^{14}$ neutrons/cm^2/s is produced.

The tungsten target (called target 1) is at the center of the intersection of the three arms of a "T," each arm consisting of a can containing water. The energy of the neutrons is moderated (lowered) as the neutrons collide with the hydrogen atoms in the water. Neutrons emitted from the moderator surfaces traverse an evacuated flight path to interact with the samples under study. Because the proton beam is pulsed, time-of-flight (TOF) methods are used to determine the neutron energy.

When the WNR was conceived in the early 1970s, the facility was to include a Proton Storage Ring (PSR). Funding for the PSR was finally authorized in 1980, and construction was completed in the spring of 1985. The PSR is designed to accept 800-MeV protons from LAMPF over a period of 750 μs and, by storage techniques, to time-compress the pulse to 270 ns. The stored proton beam has an average current of 100 μA at 12 Hz. At this low repetition rate, the very narrow, intense proton pulses maximize the intensity and energy resolution of the resultant neutron beam.

During the construction of the PSR, the WNR target-1 system was upgraded so that it could handle the more intense proton beam expected and also to optimize the moderators for specific neutron-scattering instruments. This upgrade made it necessary to construct a new target facility at which unmoderated or fast neutrons can be used to perform experiments for basic and weapons physics applications. Construction of this new target area began during FY86. The new target, together with another target called target 2, now make up the WNR facility. With the commissioning of the PSR and the upgrading of the target system, the target-1 facility was renamed the Los Alamos Neutron Scattering Center, or LANSCE.

Within approximately two years, LANSCE is expected to be the world's most intense pulsed-neutron source, with a peak thermal neutron flux of more than 1×10^{16} neutrons/cm^2/s. This number is given with the assumption that the PSR will be operated as described and that a target of depleted uranium will be used for neutron production.

Several important developments within the past year have brought LANSCE closer to becoming one of the world's premier facilities for neutron-scattering studies of condensed matter. The most important of these by far was the start of the commissioning of the PSR in April 1985 and the subsequent achievement of 30% of the design average current (30 μA at 12 Hz) and of nearly 50% of the design peak current in the ring. The peak neutron flux was approximately 100 times more intense than the flux obtained with previous WNR operations and was applied to condensed-matter and nuclear-physics research. Funds were made available for designing the much-needed new experimental hall and support building, and construction of the experimental hall will begin in FY87. The low-Q diffractometer (LQD), a new spectrometer for small-angle neutron scattering, has been completed, and test runs have begun. The LANSCE facilities group has provided a new split-target, moderator-reflector assembly; has operated, for the first time, a liquid hydrogen moderator for spectrometers that require cold neutrons; and has furthered the development of an advanced

data-acquisition system. In addition, substantial progress has been made toward the establishment at the WNR of a new white source of neutrons for nuclear physics research in the 1- to 500-MeV range.

TARGET/MODERATOR/REFLECTOR SYSTEM (P-9)

The new target system a target/moderator/reflector (TMR) has a tungsten target split into two halves with a void between and with four moderators surrounding the void space. The split target is a unique arrangement, with a "flux-trap" region (the void) feeding the moderators and providing a reduced fast-neutron background that would otherwise pass through the flight paths to the experiments. The TMR geometry will eventually permit up to 17 neutron flight paths to operate simultaneously with 6 optimized moderators.

Of the four moderators in place, three are cans through which refrigerated water is circulated at a stable temperature of 7.2 ± 0.3°C. The fourth is a liquid-hydrogen-filled can held at 20 K by a 400-W helium refrigerator system. For the ambient-temperature water moderators, the neutron spectrum is Maxwell-Boltzmann at thermal energies, but proportional to 1/E at epithermal energies, with an intensity of 3×10^{11}/E(eV)-neutrons/(eV-sr-pulse) at 100 μA. In addition, the neutron pulse width is inversely proportional to velocity at epithermal energies so that TOF experiments have constant energy resolution in that energy regime.

The physical setting for the TMR assembly is shown in Fig. V-1. The target/moderator region is surrounded by a cylinder, 1 m in diameter by 1 m high, composed of a layer of beryllium inside a layer of nickel. The cylinder is embedded in an iron biological shield. The distance from the target to the outside surface of the iron shield is about 4 m. The beryllium, nickel, and iron nearest the

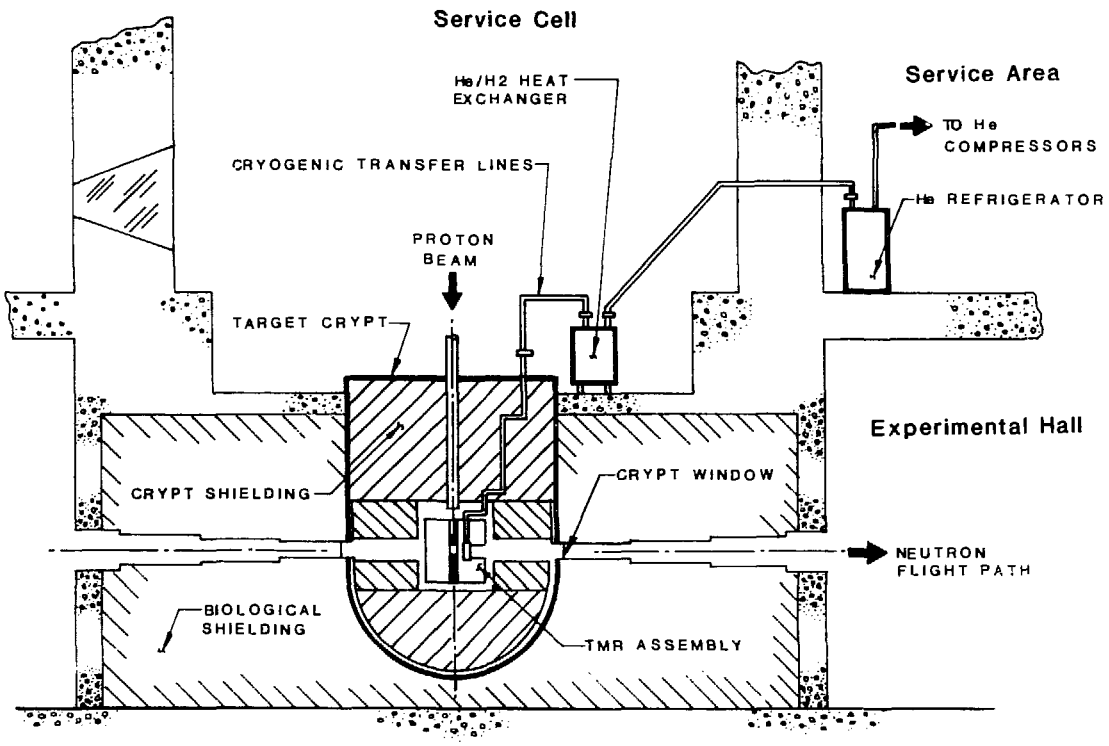

Fig. V-1. Physical arrangement of the LANSCE TMR system, showing shielding layout and refrigerator for H_2 moderator.

target act as a reflector, feeding neutrons back into the moderators. This arrangement enhances the thermal neutron performance by 10% to 20% over that obtained in a traditional pure beryllium reflector. Farther away from the target, the nickel and iron serve only as shielding.

DATA-ACQUISITION SYSTEM FOR LANSCE (P-9)

Over the past year the FASTBUS data-acquisition system has advanced from its beginning as a Laboratory project through its first use as a prototype system to its current stage: four fully integrated systems in use within the LANSCE facility. User response to the new systems has been enthusiastic, for the hardware and software have proven to be functional, reliable, and easy to use. Like the hardware foundation on which the system is built, the software nucleus is complete. However, many extensions and enhancements, particularly an increased graphics capability, are planned for implementation over the next year.

In the new data-acquisition system, FASTBUS (an IEEE bus standard developed by the DOE for high-performance data acquisition) is used in conjunction with application-specific modules designed and built to capture the data without intervention from the front-end microVAX computer. The system is configured so that each neutron-scattering instrument has its own autonomous microVAX and FASTBUS electronics. These front-end systems are, in turn, linked to a central host system, or cluster, which provides access to expensive shared peripheral devices, such as printers and data archival media. This architecture ensures maximum decoupling of separate experiments and, at the same time, provides a highly redundant system. An Ethernet system running DECNET provides systems nodes with a common communication path.

The FASTBUS subsystem comprises four custom module types and a commercial QBUS processor interface (QPI). Two of the modules are directly involved with the time-interval measurement typical of pulsed-neutron-scattering experiments with a white source; of these, one acts as a master clock defining time bins and the other as a TOF input buffer module. The third module type provides a limited, but fast, processing capability for events. The last type provides histogramming memory. Once set up, the FASTBUS system can acquire data without the attention of the microVAX front end, thereby providing another level of decoupling in the system. In addition, this feature leaves the processing power of the microVAX available for analysis in near time, enabling the experimenter to evaluate how future beam time may best be used. The current design allows average count rates of more than 2 MHz and peak rates of 50 MHz. The FASTBUS data-acquisition command language (DACL) has progressed through the requirements specification and formal design phases into the implementation phase of development. Materials scientists are currently using the kernel system in their experimental programs, to define the experiment configurations and to provide an advanced, high-performance data-storage subsystem and an integrated system for executing and synchronizing data-acquisition jobs in a background mode.

NEUTRON-SCATTERING INSTRUMENTS AT LANSCE (P-8, LS-7)

Five neutron-scattering instruments were in operation at the start of LANSCE production in 1986: the single-crystal diffractometer, the filter difference spectrometer, the constant-Q spectrometer, the high-intensity powder diffractometer, and the neutron powder diffractometer. The last, completely rebuilt, has been relocated at 32 m from the source in a small building outside experimental room 1 and is now a high-resolution instrument with $\Delta\lambda/\lambda$ of approximately 0.15%. Commissioning of a sixth spectrometer, the LQD, will also begin during this run cycle. A prototype of the LQD was successfully operated in December 1985 and was used to characterize the spectral properties of the new liquid hydrogen moderator.

The LQD is particularly useful for structural experiments. Many studies in the fields of biophysics, metallurgy, polymer science, and the like require a knowledge of geometrical relationships in solids

and liquids where distance scales are in the range of 10 to 1000 Å. For example, structural biologists wish to be able to study objects ranging in size from that of single proteins in solution, through that of DNA/protein assemblies, up to that of large virus particles. Metallurgists may wish to examine nucleation and growth of voids in radiation-damaged bulk samples, or phase separation in alloys. Neutron scattering at low values of momentum transfer Q is of great value for these studies because of the reciprocal relationship between Q and distances in the scattering object. If we use long-wavelength radiation together with very small scattering angles, we can obtain data at low Q and measure properties of long correlation distances in the scattering medium.

The LQD at LANSCE is being installed on flight path 10 (the northeast corner) in the existing experimental hall and will be at least partially operational by October 1986. The proposed total flight path of 12.65 m allows us to use neutron wavelengths out to 13 Å before frame overlap, without choppers or filters. An elevation view of the instrument is shown in Fig. V-2. This flight path views a liquid hydrogen moderator that will produce a neutron spectrum peaked at a wavelength of 2.4 Å but with usable flux from 0.3 to 15 Å.

A significant feature of the LQD is that a broad range of Q is measured in a single experiment without any collimation or detector changes. This will allow high-precision model fits in the range of sizes from 10- to 300-Å radius. We have used a Monte-Carlo simulation to compare data that might be obtained in a given length of time at the LQD and at the D-11 diffractometer at the Institut Laue-Langevin. The latter spectrometer is currently the best small-angle instrument in the world. The calculations show that the quality of the data obtained from the LQD and the D-11 will be comparable: our precision will not be quite as good, but our extended Q-range will allow fitting to more complex shapes.

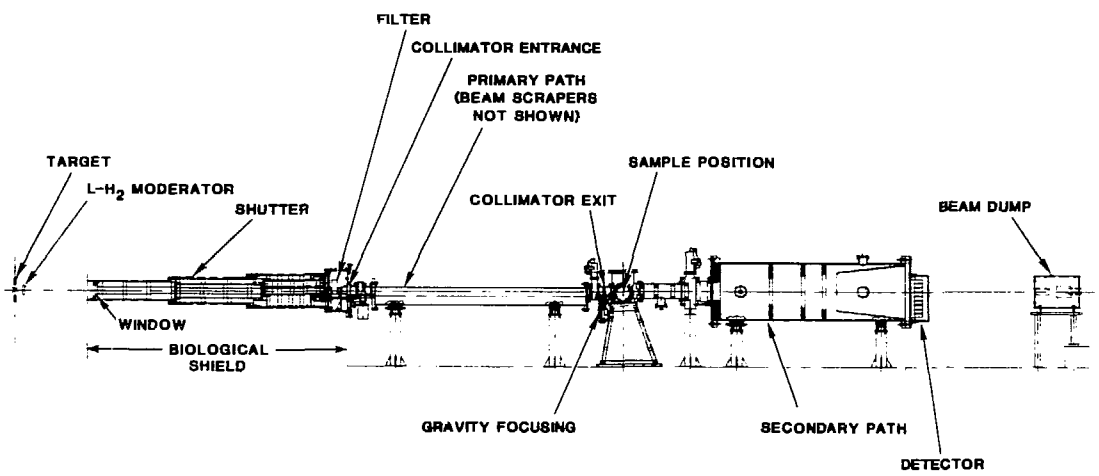

Fig. V-2. Elevation view of the LQD. The length of the incident flight path is 8.50 m; the secondary path is 4.00 m long. Provision is made to select one of three collimators; the actual collimation section is 3.65 m long. The gravity focusing device moves the collimator exit to select neutron trajectories (as a function of velocity) so that all wavelengths converge at the detector. The sample chamber is 300 mm in diameter and 450 mm high, so a variety of special environments can be installed. If the chamber and pipe spool are removed, a clear area 1 m long is available for apparatus.

WNR FACILITY (P-3, P-9)

To recover our capability for doing basic and applied research with fast neutrons, which was lost when the target-1 source was optimized for LANSCE, we have designed a new target facility that is now under construction. The new area, target 4, will be shielded to permit as much as 20 μA of proton beam on target. An 8° bending magnet allows us to elevate the new white source and its flight paths above those of the existing low-current target-2 area; a high-resolution, small-angle (p,n) experiment can be operated simultaneously with the white source; and the neutron flight paths for the new target-4 area view the production target at forward angles, providing a source extending to nearly 500 MeV with a neutron intensity much greater than that previously available above ~10 MeV. Seven penetrations through the target-4 biological shield view the production target at angles ranging from 15° to 90°.

The target-2 target-4 combination, now designated the WNR facility (Fig. V-3), will be operated by P-3 during the next LAMPF cycle. When completed, the WNR will be the premier fast-neutron TOF facility in the United States.

Construction began in late May of 1985, and the first phase of the facility was commissioned on schedule with five flight paths ready in time for experiments during the 1986 LAMPF cycle: a 250-m flight path for high-resolution, medium-energy (p,n) reaction studies; a 15-m flight path at 30° for fast-neutron capture and gamma-production experiments; a 40-m flight path at 15° for (n,p) experiments; a second 40-m flight path at 30° for SDI mass sensor testing; and a 20-m flight path at 60° for fission and total cross-section measurements.

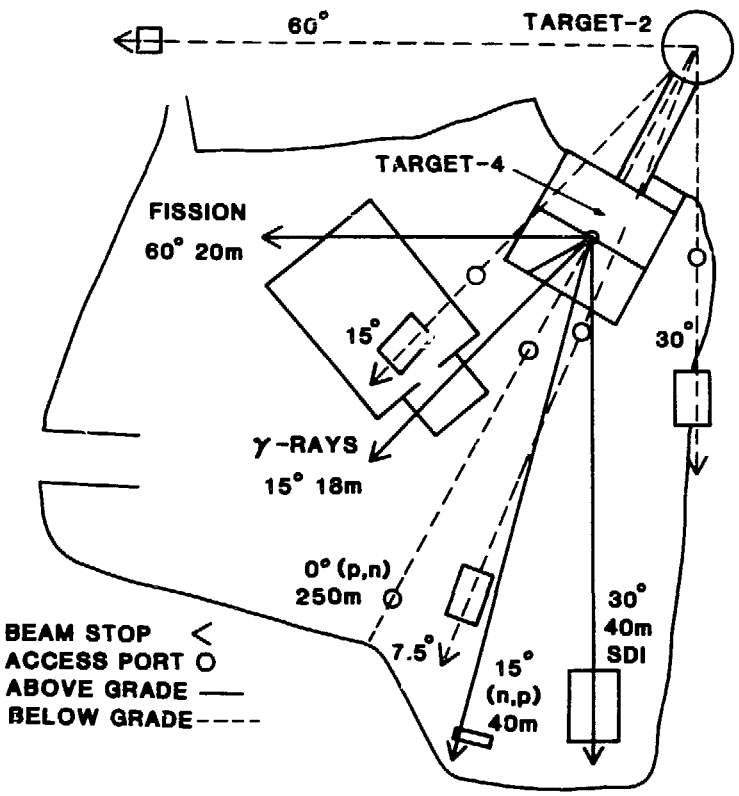

Fig. V-3. Plan view of the WNR facility. The proton beam enters through target 2 and can be used in either the target-2 or the target-4 complex.

VI. CONDENSED-MATTER PHYSICS

INTRODUCTION

The term condensed-matter physics (CMP) encompasses a wide range of topics dealing with the solid and liquid states of matter. In the Physics Division, the emphasis is on experimental rather than theoretical CMP, and our work is directed toward several areas that serve to provide the fundamental underpinnings of the Laboratory's materials science and technology requirements for both defense and energy programs. Research is performed to examine the behavior of materials ranging from the simplest to the most complex—some may be considered unusual—and often under extreme conditions of temperature, pressure, or magnetic field. Much of this work evolved from past efforts by Group P-10 in "low-temperature" physics, and we continue to use a number of the tools of that discipline. But an important recent thrust has been the development of the LANSCE facility, devoted primarily to CMP, which gives P-Division a large stake in this field.* In addition, the Center for Nonlinear Studies (CNLS) and the Center for Materials Science (CMS), established several years ago, have provided and nurtured significant opportunities for intergroup and interdivisional collaborations in CMP research areas having a strong impact on Laboratory programs. The role of P-Division physicists in these collaborations continues to grow.

Groups P-8 and P-10 are heavily committed to studies in structural physics, where the objective is to determine the static and dynamic structural properties of molecules, crystals, and phase transitions. Our primary emphasis is on the use of various spectroscopies to probe sample materials held at ultrahigh pressures (to the megabar range) in diamond anvil cells (DACs) and on using neutron scattering as a probe especially well suited to examinations of magnetic structures and hydrogenic materials. We are also attempting to adapt high-pressure cells for neutron-scattering experiments.

The study of electronic processes in condensed matter is a topic central to solid-state physics and especially to the elucidation and description of the ground states of systems, manifested by superfluidity, superconductivity of several possible types, a large variety of magnetic configurations, spin-density waves, charge-density waves, and the like. Of considerable interest are the interplay and competition among these processes in a group of materials that have come to be known as "heavy fermions" inasmuch as the Fermi-liquid formalism developed to describe normal (but degenerate) and superfluid ^{3}He also describes the electronic manifestations of these materials because of the unusually large effective masses assigned to the electrons responsible for the effects.

The Division's growing interdisciplinary endeavors in nonlinear physics feature collaborations between theorists and experimentalists. Of particular interest is the use of quantum fluids—^{4}He and mixtures of ^{4}He and ^{3}He liquids—as model systems for exhibiting and studying many classes of general classical phenomena, such as hydrodynamic turbulence.

Part of the mission of Group P-10 has been fundamental studies and, where appropriate, development of novel heat engines and refrigerators offering the promise of high-efficiency operation in practical applications. The novelty of these engines arises from two sources: first, we look at well-established principles in new ways (e.g., thermoacoustic theory has been expanded to new

* Until a reorganization in October 1986, Group P-9 was involved in the development and operation of the neutron source, while Group P-8 was responsible for developing spectrometers and using them primarily for CMP research projects. After the reorganization, these functions were consolidated and are now the responsibility of the group called LANSCE.

engine configurations, and the magnetocaloric effect has been adapted to cyclic processes over large temperature spans); and second, we have incorporated unusual working materials, such as liquid sodium and para- and ferromagnets, into the designs. The results of some of these efforts are likely to have considerable impact on future heat engine/refrigerator systems.

Finally, the Division has made progress toward establishing, in conjunction with CMS, an ion-beam facility devoted to surface science.

STRUCTURAL PHYSICS

Dynamics of Molecular Hydrogen Complexes (P-8, INC-4)

The H-H bond is the most fundamental chemical bond. Transient molecular hydrogen bonding has been proposed in catalytic systems such as the hydrogenation of alkyl-cobalt carbonyls. The isolation of a metal complex with a dihydrogen molecule bonded to the metal, therefore, presents an unprecedented opportunity to study the H-H bond in an unusual state of activation, i.e., a presumably intermediate species in a catalytic reaction. Such complexes have recently been isolated and extensively characterized by G. J. Kubas and coworkers. Single-crystal neutron and x-ray diffraction studies of $W(CO)_3(PRr_3^i)_2(H_2)$ and an analogous compound, $Mo(CO)_3(PCy_3)_2(H_2)$, show a unique side-bonding of H_2 to the metal. In addition, the H-H bond is found to be considerably weakened: i.e., the crystallographic results show a bond length of 0.82 Å, and spectroscopic work shows an H-H stretching frequency of 2690 cm^{-1}, as compared with 0.74 Å and 4160 cm^{-1}, respectively, for the free molecule.

We have now performed extensive spectroscopic studies with the aim of gaining a more fundamental understanding of the dynamics of the molecular hydrogen complex. Thereby, we have not only confirmed the molecular nature of the bound hydrogen molecule but have also shown the substantial weakening of the H-H bond. The frequencies of the six normal modes represent a stringent test for *ab initio* theories that aim to explain the nature of the molecular hydrogen-metal bond.

In addition, we have considered what further details about the dynamics of the bound hydrogen molecule can be learned from the rotational energy levels. The inelastic neutron-scattering spectra for both the (PPr_3^i) and (PCy_3) analogs show a split torsional mode for the hydrogen molecule at about 335 and 370 cm^{-1}. This observation can be interpreted by assuming that the rotations of the hydrogen molecule are constrained to a plane perpendicular to the W_H^H axis (i.e., one-dimensional rotation) and that there are just two equivalent orientations of the molecule along the P-W-P axis as the crystallographic data suggest (i.e., a potential with twofold symmetry). The energy levels for such a system can be computed in a straightforward way. With the further assumption of the elongated H-H bond (which reduces the rotational constant of the molecule), excellent agreement can be obtained for the observed transitions with a barrier height of about 780 cm^{-1}. Because calculations of the intramolecular barrier by P. J. Hay give a value of 105 cm^{-1}, we may conclude that a large portion of its height is the result of intermolecular interactions.

The studies clearly demonstrate the possible sensitivity of inelastic neutron scattering on a high-intensity spectrometer, such as the Filter Difference Spectrometer (FDS) at LANSCE, where, even in the presence of 66 other hydrogen atoms in the ligands, the vibrational spectrum of the H_2 molecule could be isolated by isotopic substitution and subtraction techniques. This work also illustrates the essential complementarity of optical and neutron techniques, all of which were necessary to the completion of the vibrational data for this unique system.

Hydrogen Site Occupancy in the Rare-Earth Dihydrides: Yttrium, Lanthanum, and Cerium (P-8, Sandia National Laboratories)

Determination of the preferential hydrogen-site occupancy in the rare-earth dihydrides is a problem of considerable interest in the physics of metal hydrides. These systems generally form a cubic

CaF_2 structure, containing two tetrahedral (t) sites and one octahedral (o) site per metal atom, near the dihydride composition. Under normal conditions of pressure and temperature, hydrogen shows a preference for t-sites. However, several rare-earth hydrogen systems (e.g., yttrium, lanthanum, and cerium) show some occupancy of o-sites before all the available t-sites near the dihydride composition are filled. This fraction of o-sites occupied at the dihydride composition has been called the intrinsic disorder. Results of our initial studies of the temperature and concentration dependence of o-site occupation and of the optic mode vibrational frequencies on YH_x for $x \sim 2$ proved sufficiently intriguing that we continued our work on rare-earth dihydrides with studies of CeH_x and LaH_x, both of which exhibit o-site occupancy for $x \sim 2$.

Inelastic, incoherent neutron-scattering data for lanthanum hydrides (Fig. VI-1) show typical optic mode spectra for t-site occupation (a) and low- and high-temperature spectra for t-site and o-site occupation (b and c). The large structured peak appearing at ~100 meV and above is the vibrational spectrum of t-site hydrogen. The width and structure of this peak are believed to result from dispersion in the optic mode. The much weaker peak evident at 70 to 80 meV is characteristic of the o-site hydrogen vibrations, which have been shown to be dispersionless. Because inelastic neutron-scattering intensities are (among other factors) directly proportional to the number of scatterers, the ratio of the integrals over the o-site and t-site peaks is directly proportional to the ratio of site occupancy. We also analyzed powder-diffraction data for yttrium and lanthanum hydrides, using the CaF_2 structure, to determine the occupation at the o-sites and t-sites. Figure VI-2 shows the fraction of hydrogen atoms on o-sites (one-half the intrinsic disorder) for all samples determined by one or both of these methods.

We found no evidence of o-site occupation in the $LaH_{1.9}$, $CeH_{1.9}$, and $CeH_{2.0}$ samples. Furthermore, the o-site peak appears to be split near 78 K in the lanthanum and cerium hydrides, which may be the result of a lowering of site symmetry of the o-site hydrogen. It has been suggested that these hydrogen shifts along the [111] direction point to a new site with distinctly different La-H distances, leading to nondegeneracy of the optic mode frequencies. This shift also increases the number of available hydrogen sites by a factor of 8 and may account for the relative constancy in the occupation of o-sites at lower temperatures.

In the simple lattice gas model, the intrinsic disorder is expected to *increase* with temperature, so it is remarkable that the disorder is found to be *lower* at 900 K than at 300 K (Fig. VI-2). An attempt to reconcile this inconsistency led to a model that invokes proton-proton repulsion in the excited vibrational states to prevent the occupation of the nearest neighbor o-site and t-site. This model, however, also requires a decrease in the o-site occupations at lower temperatures (<400 K), which is not observed in the data. Modifications to this basic model, including the introduction of vibrations of the metal lattice and proton-proton interactions, showed that a decrease in entropy occurs when hydrogen moves from t-sites to o-sites, so that the total entropy increases with increasing temperature even though site disorder decreases.

For rare-earth hydrides, the appreciable difference in metal lattice free energy depending on whether a proton is at an o-site or at a t-site allows the intrinsic disorder to decrease with increasing temperature. The lattice expands when hydrogen is added to t-sites but contracts when hydrogen goes into o-sites. Thus, the entropy of the metal lattice increases when protons go into t-sites but decreases when they go into o-sites.

The equation describing the o-site occupation for small intrinsic disorder and low temperatures has two solutions. The solid-line solution, shown in Fig. VI-2, is favored if attractive o-o interactions dominate, which is suggested by the linear decrease in the lattice constant for $x > 2.0$, where o-site occupation increases.

A curious feature of the data is that o-site occupation is not apparent in $LaH_{1.9}$, although considerable disorder exists at higher concentrations in this metal. Simple theory predicts that the intrinsic disorder should be reduced only to about 0.05 at $x = 1.9$ if it is 0.1 at $x = 2.0$, because, typically, for values of $\delta(=2\text{-}x)$ near 0.02, the second solution to the equation describing o-site occupation (dashed curve in Fig. VI-2) gives the lower free energy. In this case the intrinsic disorder given by the model is about 0.001. Thus, the model that describes the temperature dependence also correctly predicts the negligible o-site occupancy for $x < 2.0$.

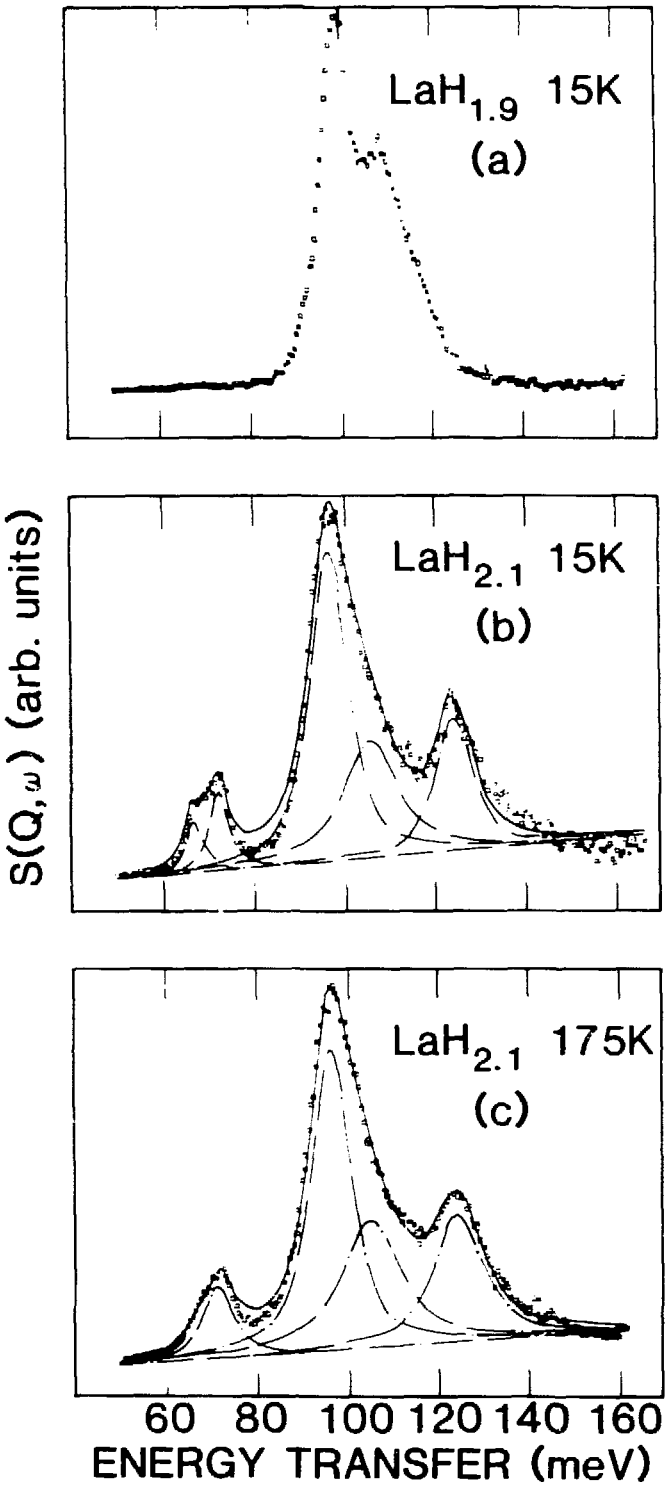

Fig. VI-1. (a) Inelastic, incoherent neutron-scattering spectrum of $LaH_{1.9}$ at 15 K. The broad peak at 98 meV is due to t-site hydrogen, and no o-site occupation is evident. (b) Inelastic, incoherent neutron-scattering spectrum of $LaH_{2.1}$ at 15 K and (c) at 175 K. The broad peak at 98 meV is due to t-site hydrogen and the peak at 72 meV to o-site hydrogen.

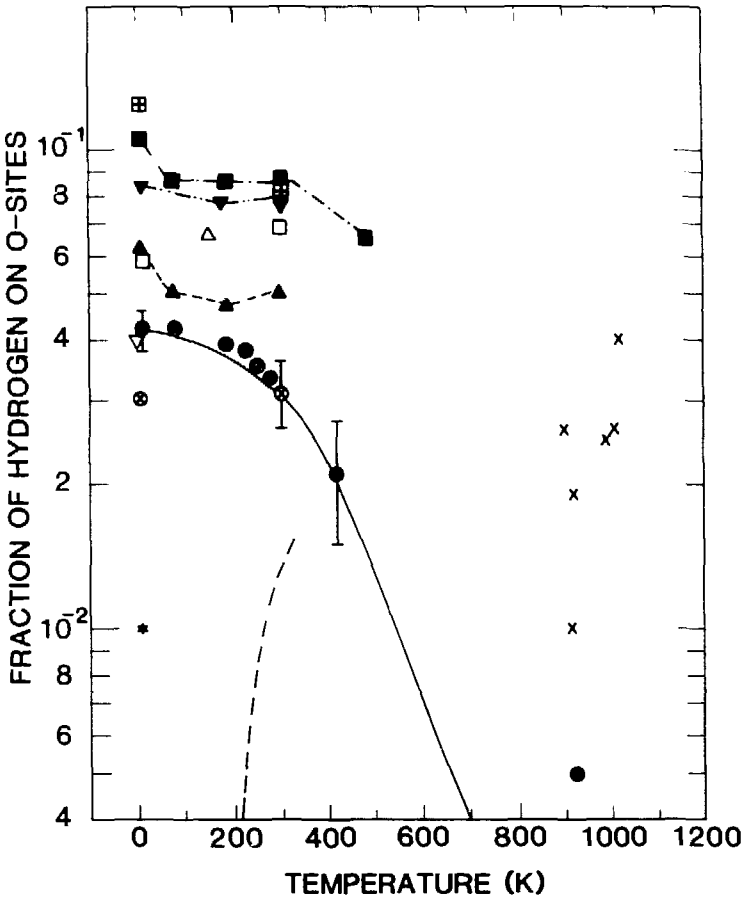

Fig. VI-2. The fraction of hydrogen atoms on o-sites as a function of temperature and concentration. The solid curve is the model fit to the $YH_{2.0}$ data, and the dashed line is the second solution at low temperatures. Solid and crossed circles and squares are our data; other symbols represent various other authors' data.

In summary, the intrinsic disorder (o-site occupation) has been shown to decrease monotonically with increasing temperature for three rare-earth hydrogen systems (cerium, lanthanum, and yttrium) and also to decrease to zero for x = 1.9. Both observations have been qualitatively explained by the same model on the basis of detailed entropy calculations. We have furthermore shown that inelastic neutron scattering is an effective technique for determining relative site occupancy and is also very sensitive to small distortions of the surroundings of a hydrogen interstitial site.

Nitrogen at Pressures up to 130 GPa (P-10, M-6, Lawrence Livermore National Laboratory)

A topic that is currently of high interest to materials science is the behavior of molecular crystals at very high pressures, in particular those crystals composed of diatomic molecules. The search for molecular dissociation and the formation of "man-made" monatomic crystals having unusual metallic properties have been the subjects of numerous theoretical and experimental studies. Important

to the latter is the development of DAC's that provide static pressures exceeding 100 GPa (1 Mbar) and enable us to probe the sample using many conventional experimental techniques.

Recently nitrogen has been predicted to become metallic over the pressure range 70 to 100 GPa. To test this prediction, we subjected nitrogen to pressures up to 130 GPa at 300 K in DACs. From Raman scattering and direct visual observations, we found that nitrogen remains an insulating diatomic molecular solid under these conditions. It does not become metallic, although it does turn brown above 110 GPa.

Raman scattering reveals three new phases at 20, 66, and 100 GPa, which are distinguished by branching of the vibronic modes of δ-N_2. In addition, one mode increases in frequency to a broad maximum at 66 GPa and then decreases, in a manner similar to that of H_2. In H_2, such behavior was attributed to a weakening of the H-H band. In N_2, three other vibronic frequencies continue to increase, showing the situation to be more complicated than just a weakening of the N-N bond.

Melting Curve of N_2 (P-10, M-6, University of California at Los Angeles)

Recent theoretical work by D. A. Young (LLNL) indicates that the nature of the molecular disorder is crucial to the determination of melting curves, and, possibly, solid-solid transitions involving varying types of molecular disorder.

We have extended the melting curve of N_2 to pressures and temperatures as high as 12.5 GPa and 670 K, using newly developed high-temperature DACs. Although the cells can achieve pressures as high as 20 GPa at 1000 K, chemical reactions between the N_2 sample and components of the DAC limit the pressures that can be held for the hour or so required to make measurements. We are assembling a new spectroscopy system capable of measuring Raman spectra in a few minutes. With this system we expect to be able to use the full temperature range of stability of the DAC.

High-Pressure Mössbauer Spectroscopy of Molecular Crystals (P-10, Tel Aviv University)

The Mössbauer Effect (ME) the recoil-free emission and absorption of γ rays has heretofore been little used with the DAC because of low counting rates from small samples. In the case of ^{129}I, however, we have been able to apply this powerful technique to the DAC for a microscopic inspection of the metallization process in elemental iodine, because ^{129}I is a long-lived fission product and has superb ME spectroscopic properties for studying the behavior of solid molecular iodine. I_2 has become archetypical for high-pressure studies of dissociation. It becomes metallic at P = 16 GPa, a pressure easily achieved with DACs, and several conductivity, x-ray diffraction, optical-gap, and Raman studies have been made under those conditions. The x-ray results suggested a first-order crystallographic phase transition at 21 GPa to a body-centered orthorhombic *monatomic* crystal. If so, the ME could provide unambiguous confirmation of this transition as well as additional information about the system.

The ME transition in ^{129}I is from the ground state I = 5/2 to the first excited state I* = 7/2 levels. The electric quadrupole spin Hamiltonian governing the hyperfine interaction splits both levels, and the spectra obtained yield the quadrupole splitting (eqQ), the asymmetry parameter (η) of the electric field gradient (efg), the isomer shift (IS), and the relative abundance if there are inequivalent sites. The efg tensor arises primarily from the p-hole in the closed shell configuration $5s^25p^6$. Owing to the formation of a molecule, this hole is in the z-direction of the I-I bond, and eqQ should have a negative sign. The deviation of the pure molecular axial symmetry is reflected in the magnitude of the asymmetry parameter. The IS is proportional to the s-electron density; because the valence electrons are the p-electrons, however, we in practice measure the concentration of p-holes as a function of pressure.

The results obtained can be summarized as follows. The "molecular nature" of iodine is preserved up to 16 GPa. At this pressure, where iodine becomes metallic, a new spectral component,

characterized by a positive eqQ and a very large asymmetry parameter, appears. This component reflects the formation of a new structure, not detected by previous elaborate x-ray studies. We interpret this new structure as a quasi-one-dimensional system composed of an I_2-I_2 chain that provides the path for the metallic conductivity. The new structure coexists with the "molecular crystal." The abundance of this component increases with pressure, and at 24 GPa a new component appears, apparently because of a strong intrachain interaction at the basal plane of iodine. This two-dimensional structure was seen in the x-ray studies and was interpreted as a monatomic crystal. However, our results show a strong interacting molecular nature of iodine up to 30 GPa, although trends of the data support molecular dissociation with increasing pressure. The proposed model of low-dimensionality phases present in high-pressure iodine is supported by the published electrical conductivity results; however, more data are needed. This work elucidates new and intricate mechanisms in the evolution of the dissociation of molecular crystals. It definitely points to a continuous, nondrastic series of crystallographic changes.

Development of Sapphire-Anvil High-Pressure Cells for Single-Crystal Neutron Diffraction in Deuterium (P-10, M-6)

To calculate the properties of hydrogen or deuterium at very high pressures, we must know the crystal structures and compressibilities of these two isotopes. Because several laboratories have failed in their attempts to obtain this information above 3 GPa from high-pressure x-ray diffraction in DAC's, we are developing high-pressure sapphire-anvil cells suitable for single-crystal neutron diffraction with the Laue camera developed at LANSCE. Although the cell was designed to reach 8 GPa with a sample volume near 0.5 mm^3, we have achieved over 8 GPa on samples as large as 0.11 mm^3. We expect to be able to use thicker samples with the new rhenium-alloy gaskets that we are developing for high-temperature, high-pressure DAC studies.

ELECTRON PROCESSES IN CONDENSED MATTER: GROUND-STATE PHYSICS

Spin-Polarized Hydrogen, H↓ (P-10)

Atomic hydrogen recombines to form molecular hydrogen with an energy release of 4.5 eV per molecule. However, this can only occur in the spin-singlet state of the two electrons. Polarizing the electronic magnetic moments by applying large magnetic fields, 8 to 10 T, at low temperatures, 0.1 to 0.6 K, results in a metastable gas, spin-polarized hydrogen H↓. Because the interatomic potentials in H↓ are repulsive, there are no bound states and no phase changes to the liquid or solid state down to T = 0 K. Realization of this idea came in 1979, when Silvera discovered that coating the walls of a container with superfluid helium would inhibit the adsorption of H↓ on the walls and allow appreciable densities of H↓, $\sim 10^{17}/cm^3$, to be stabilized.

We take considerable interest in this unique gas because it is the only system that remains a gas of reasonable density at T < 0.5 K, where the thermal de Broglie wavelength of the particles becomes longer than the range of interatomic potentials, causing strong quantum effects to come into play. The most dramatic expectation for H↓ is that it will undergo a Bose-Einstein condensation (BEC) to a superfluid state at sufficiently high densities and low temperatures: $n_c \propto T_c^{3/2}$ describes the relationship between the critical density and critical temperature for the onset of BEC.

Attempts made elsewhere to achieve BEC by compressing H↓ to $n_c \sim 10^{20}/cm^3$ at T ~ 0.5 K have failed owing to the presence of a three-body recombination channel that destroys the sample rapidly at $n > 10^{18}/cm^3$. Our efforts at Los Alamos are focused on lower temperatures T ~ 1.0 mK where BEC may be achieved at lower densities $n \sim 10^{17}/cm^3$, at which the three-body rate is negligible. At these low temperatures, the presence of a bound state for H↓ on the He surface ($E_B \sim 1.0$ K) leads to adsorption and rapid recombination; therefore, present schemes rely on

neutral-atom magnetic traps. These traps are very shallow and are only filled by ultracold gas atoms. H↓ created at higher temperatures must be thermalized by a transfer of energy to the He-covered walls, a process referred to as accommodation. At T < 0.1 K, this process is predicted to become very inefficient, approaching zero with an asymptotic temperature dependence of $\sqrt{T}$, reflecting the increasing mismatch of the thermal de Broglie wavelength of the H↓ with the width of the He surface potential profile. Aside from its practical importance, the measurement of energy accommodation of H↓ by helium surfaces is an interesting problem in its own right and has attracted much recent theoretical effort.

We began our work in spin-polarized hydrogen with the development of a high-flux, low-temperature dissociation source of H↓. The conventional technique is to dissociate H_2 in a room-temperature or liquid-nitrogen-cooled rf discharge tube; the atomic hydrogen must then diffuse down tubes into the low-temperature region. The region of tubing at T > 2.0 K cannot be protected by superfluid helium and catalyzes recombination of most of the atoms. In addition, the use of an open tube containing helium to connect the low-temperature region with a room-temperature source presents a large heat load and mandates that we employ a very high-power $^3He/^4He$ dilution refrigerator (DR) to remove heat below 1 K.

Our dissociator operates at ~0.5 K within the vacuum can of the DR. Molecular hydrogen gas introduced through a heated capillary is sprayed on the cold interior wall of the dissociator and forms a solid frozen layer. This layer is covered by the superfluid helium film. An rf pulse 10 to 100 μs long, induced by an external coil, strikes a discharge and accelerates charged particles into the frozen hydrogen, producing atomic hydrogen that is trapped in the gas phase when the helium film quickly reforms after the rf pulse is terminated. H↓ fluxes $>10^{14}$/s have been achieved, making this dissociator an attractive source of H↓ for loading low-temperature traps.

During the past year we completed a study of factors affecting the performance of our low-temperature dissociator: rf power, pulse repetition rate, and dissociator temperature. We discovered that the primary factor determining H↓ flux is the dissociator temperature. To start the low-temperature discharge, the helium vapor density has to surpass a minimum value in order to support a glow discharge, because only through the He discharge can rf energy be coupled into the tube. At dissociator temperatures of <0.5 K, we found that we can initiate a discharge by evaporating a cloud of He gas with a fast heater pulse timed just before the rf pulse. At T ≥ 0.7 K, the number of dissociative collisions decreases, H-recombination in the gas phase increases, and the migration time of the dissociated H atoms from the discharge tube is extended. Understanding the dissociation process was important for optimizing the performance of the low-temperature dissociator.

We have completed our first measurements of the thermal accommodation coefficient α(T) over the temperature range 0.18 to 0.40 K. We employed a straightforward stationary-state measuring technique to determine the heat flux conducted by H↓ from a superfluid-^{4}He-film-covered bolometer biased above ambient temperature. Calculations show that energy accommodation between H↓ and a liquid helium surface occurs predominantly by sticking-evaporation collisions. The incoming H↓ loses ~1 K in the creation of a ripplon (quantized surface capillary wave) and is bound to the surface; after a time depending exponentially on 1/T, the atom evaporates with a kinetic energy representative of the surface temperature. Inelastic collisions with the surface are believed to make a negligible contribution to energy transfer. The limiting $\sqrt{T}$ dependence for α is not expected until low millikelvin temperatures are reached, and thermal accommodation at the temperature range of our measurements is expected to be a sensitive function of the H atom-He surface potential.

Our measurements show α(T) ∝ T over the range 0.18 < T < 0.40 and reaching a value of $\alpha(0.18) = 0.10 \pm 0.01$, implying that at this temperature ~10 collisions with the helium surface are required to produce one sticking-evaporation event and consequent energy accommodation. The numerical values are in agreement with a recent calculation based on a Morse-type potential for the H atom-He surface interaction, with a well depth adjusted to yield a bound state energy of 1 K. These are the first measurements to show α(T) decreasing with decreasing temperature and to corroborate the sticking-evaporation mechanism for energy transfer. Extension of these measurements to lower temperatures with a pulsed evaporation technique is expected to reveal further details of the H↓-He surface interaction.

Pressure-Induced Electronic Changes in Europium (P-10)

High pressure provides an added dimension in studies of the interplay of various electronic interactions in materials. We have used Mössbauer spectroscopy to measure two properties that give unique information about such interactions: the isomer shift (related to the f-shell occupation and valence in rare-earth solids) and the hyperfine field (related to the magnetization in solids) for ^{151}Eu nuclei in europium metal contained in a DAC. We interpret the results as evidence of an unusual coexistence of intermediate valence and antiferromagnetic states at low temperatures.

Intermediate valence and magnetic ordering in the rare earths are examples of states that can come about as a result of the interactions or "correlations" of localized f-electrons among themselves and with the remaining electrons. In europium metal the intermediate valence state is brought about by pressure, admixing the $4f^6(6s5d)^3$ (trivalent, Eu^{3+}) state with the ambient-pressure $4f^76s^2$ (divalent, Eu^{2+}) state. The Eu^{2+} state has a net 4f-shell magnetic moment; the Eu^{3+} state does not. Below 90 K, divalent europium metal is antiferromagnetically ordered at ambient pressure.

We have investigated the magnetic properties of the intermediate valence state in europium metal. Empirical evidence in europium alloys and compounds shows a seeming incompatibility between magnetic ordering and intermediate valence. Similar evidence has been noted in samarium compounds, whose intermediate valence state also involves a mixture of magnetic and nonmagnetic 4f-shells. In thulium-based solids, the two phenomena are compatible inasmuch as a mixture of two magnetic states is present.

Recent theoretical calculations have, nonetheless, shown the possibility of a coexistence of intermediate valence and magnetic ordering in europium-based materials. Because each of the phenomena is known to exist separately either at low temperature or at high pressure, we have investigated this possibility for europium metal in both regimes simultaneously.

We find that the isomer shift changes considerably with pressures up to 11 GPa, indicating a shift from the Eu^{2+} toward a Eu^{3+} state. At the same time, the low-temperature magnetic hyperfine field decreases from 200 to 90 kG, implying a reduced europium magnetic moment with pressure as expected for a transition toward Eu^{3+}. Near 12 GPa, europium undergoes a phase transition; preliminary data in this new phase also suggest a coexistence of magnetic order and intermediate valence. We have begun to look for a similar coexistence in EuO, which is intermediate-valent at high pressure and room temperature and is ferromagnetically ordered at ambient pressures below 70 K.

Although the electromagnetic interaction is well understood, its consequences in the solid state are manifold and complex. We expect the measurements we have been making to contribute to a better understanding of electronic interactions in the technologically important f-electron solids.

Neutron Powder Diffraction on f-Electron Materials (P-8, MST-5, MST-13, Virginia Commonwealth University)

The rapidly developing technique of time-of-flight (TOF) neutron powder diffraction used in conjunction with the powerful powder-profile-analysis (Rietveld) technique is making possible a whole class of new experiments that would have been impossible a few years ago. The technical features that contribute to these advances include 1) the high resolution at high d-spacings, which is intrinsic to the TOF technique; 2) the presence of high-energy neutrons in the spectrum, which is intrinsic to a pulsed neutron source; and 3) the general availability of computer hardware and software, which enables us to extract the maximum amount of information from each experiment. It is now routine to obtain information on strain and thermal vibrations (Debye-Waller factors), together with crystallographic data, for both single and multiphase samples.

At LANSCE we are conducting a series of experiments on f-electron materials in order to gain a better understanding of f-electron magnetism, which is receiving renewed attention in connection with heavy-fermion superconductivity, and to investigate various crystallographic transformation

phenomena of interest in the context of plutonium metallurgy. As an example of each of these efforts, our experiments on UPt and Ce-Th are described in this section.

The intermetallic compound UPt is a rare example of ferromagnetism occurring in the transition metal-actinide alloy. The Curie temperature is 30 K, and the ordered moment had been determined by magnetization measurements to be 0.3 μ_B per uranium atom. In an attempt to understand why the ordered moment is so small, we undertook neutron diffraction measurements to determine the distribution of magnetic moments in the ordered state. We found that the magnetic structure of UPt was much more complicated than had been previously known: it is, in fact, ferrimagnetic, i.e., simultaneously ferro- and antiferromagnetic. The value of the ordered moment is actually 1.0 μ_B, and the partial structural cancellation leads to the smaller value as determined by magnetization measurements. The complex magnetic structure also explains several puzzling features of the pressure and composition dependencies of the magnetic properties.

Cerium metal exists in several crystallographic forms, two of which are (amazingly!) face-centered cubic, the alpha and gamma forms. The transformation between the alpha and gamma forms involves a 15% decrease in volume, and the metallurgical aspects of the transformation are not well understood. The alpha-gamma transformation of a $Ce_{0.9}Th_{0.1}$ has been characterized completely (the thorium is added to suppress the occurrence of yet a third phase). One feature of this transformation is that both phases are present simultaneously over a wide temperature range. We have made direct measurements of the strain in both phases simultaneously during the course of the transformation and have shown that the thermal vibrations of both phases are approximately equal. Similar experiments are planned for plutonium alloys, which present a more complicated phase diagram.

Muon Knight Shift and Zero-Field Relaxation in the Heavy-Fermion System (U,Th)Be_{13} (P-10, MP-3, MST-5, University of California at Riverside, Texas Technical University, University of Wyoming, Illinois Institute of Technology)

It has become increasingly evident that the so-called f-band heavy-fermion (HF) materials exhibit a new and unique ground state of condensed matter. The unusual properties of HF materials include 1) a large low-temperature susceptibility (χ) and a large linear coefficient of specific heat, indicating an electron effective mass of ~200 m_e or greater, where m_e is the free-electron mass; 2) a high-temperature Curie-law χ with a nonintegral number of Bohr magnetons, suggesting itinerant magnetism; 3) a large total entropy per atom, suggesting highly localized electronic excitations; and 4) a small resistivity near T = 0, which decreases with decreasing temperature, indicating the formation of a coherent electronic state involving f- and conduction-band electrons.

In addition, four HF systems ($CeCu_2Si_2$, UPt_3, UBe_{13}, and URu_2Si_2) undergo unique superconducting transitions. It is believed that the heavy f-electrons themselves become superconducting. Furthermore, in conventional Bardeen-Cooper-Schrieffer (BCS) superconductors the energy gap is only weakly anisotropic; therefore, transport, specific heat, and spin-relaxation measurements are exponentially activated below T_c. By contrast, HF superconductors exhibit power-law (T^n) behaviors, indicating that the gap vanishes in certain regions of the Fermi surface. In analogy with ^3He, one suspects that HF superconductors have unconventional pairing and, further, that the superconducting interaction is purely electronic rather than electron-phonon in nature. Key questions to be answered regarding HF materials are 1) how does the HF state form in condensed matter, and 2) what is the nature of the superconductivity.

The muon Knight shift K_μ, the change in measured precession frequency compared with the muon's Larmor frequency in the applied field, probes the local spin susceptibility χ, which is sensitive to the superconducting (χ_s) and normal-state (χ_n) properties. For example, in an even-parity BCS state, one has spin-singlet pairing, and thus χ_s (T = 0) vanishes in the absence of spin-orbit coupling. (One expects strong spin-orbit coupling in uranium-derived wave functions.) For simple models of odd-parity, spin-triplet superconductivity $\chi_s(0) = \chi_n$. In addition to probing the nature of spin pairing in superconductors, muon spin relaxation (μSR) is a sensitive tool for measuring local magnetic field distributions and can therefore be used to detect the onset of magnetic order.

We report here μSR studies in $U_{1-x}Th_xBe_{13}$ at between T = 0.3 K and T = 300 K. The x = 0 material (UBe_{13}) becomes superconducting at T = 0.86 K, whereas for x = 0.033, the superconducting transition occurs at T $\simeq$ 0.6 K. In addition, a second large peak in the specific heat has been observed for x = 0.033 at T_{c2} = 0.4 K. This second transition has been interpreted from ultrasound measurements as being due to itinerant antiferromagnetism (AFM).

In the normal state, K_μ is directly proportional to our measured bulk susceptibility for T < 100 K, indicating that the Knight shift samples the same electrons (mostly 5f) as the susceptibility. The hyperfine magnetic field H_{hf} is found to be $-(1.84 \pm 0.13)$ kOe/μ_B. The total K_μ is assumed to be comprised of a temperature-independent part, from an orbital susceptibility χ_{orb}, and a temperature-dependent part, from the f-electron-dominated susceptibility χ_f(T). From the intercept of a χ versus 1/T plot, χ_{orb} is found to be $\chi_{orb} \simeq 1 \times 10^{-3}$ emu/mole. The low-temperature linear $K_\mu(\chi)$ relation, extrapolated to $\chi = \chi_{orb}$, then yields $K_\mu(\chi_f = 0) = (0.18 \pm 0.03)\%$, as shown in Fig. VI-3.

The temperature dependence of K_μ in the superconducting states of the x = 0 and 0.033 alloy systems is quite different. For x = 0, K_μ falls monotonically so that $\chi_s/\chi_n \simeq 0.55$ at $T/T_c \simeq 0.35$. For x = 0.033, however, K_μ is essentially independent of temperature below T_c (Fig. VI-3). The decreased spin susceptibility in the superconducting state of UBe_{13} is consistent with two possible anisotropic states with either even or odd parity. (An even or odd parity *isotropic* state is inconsistent with the considerable body of other experimental evidence for strong-gap anisotropy mentioned

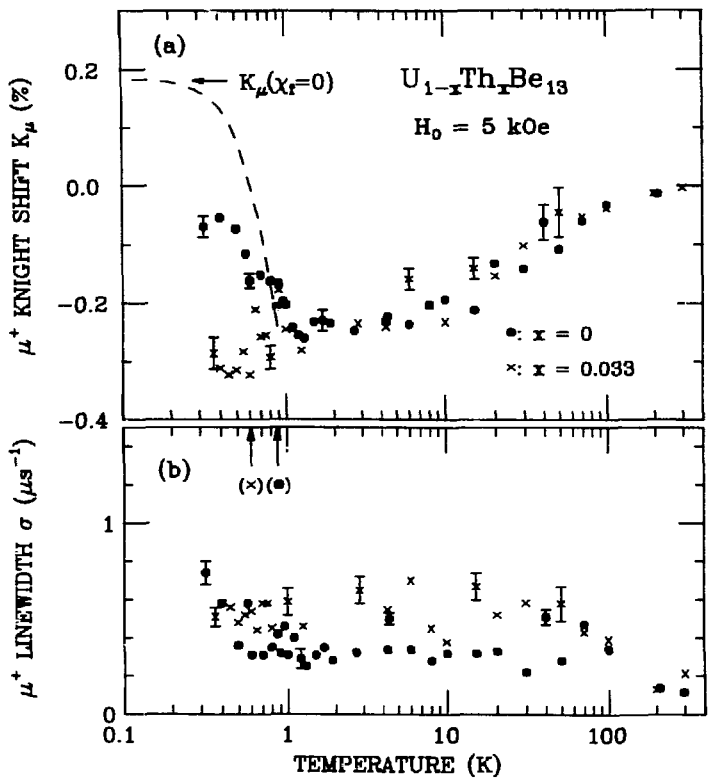

Fig. VI-3. (a) Temperature dependence of μ^+ Knight shift K_μ between 0.3 and 300 K in $U_{1-x}Th_xBe_{13}$, x = 0 and 0.033; applied field H_0 = 5 kOe. The superconducting transition temperatures are indicated by arrows, labeled by the symbols in parentheses. The dashed curve gives the estimated Knight shift in a conventional superconductor with no spin-orbit scattering. (b) Temperature dependence of μ^+ gaussian linewidth σ; conditions as in (a).

above.) Anisotropic, odd-parity Cooper pairing yields $\chi_s(0) = \chi_n$, which is contrary to our Knight shift data if the order parameter is free to rotate in the field. A reduction of $\chi_s(0)$, together with an increased μ^+ linewidth, would occur if the order parameter were pinned to the lattice. Indeed, an increased linewidth is evident (Fig. VI-3b). Anisotropic, even-parity pairing gives $\chi_s(0) = 0$ in a ^{3}He-like theory; however, spin-orbit scattering is expected to increase $\chi_s(0)$ and is expected to be strong for uranium-derived wave functions. The different behavior for the x = 0 and x = 0.033 samples seems to imply that the addition of Th impurities increases the spin-orbit scattering strength or that there exist two distinctly different superconducting states, with different spin susceptibilities, in the (U,Th)Be_{13} system. We plan to sort this out by taking further measurements with varying Th concentrations.

We have also measured the temperature dependence of the μSR linewidth in zero-field for $U_{1-x}Th_xBe_{13}$ for x = 0 and 0.033 in the temperature region $0.20 \leq T \leq 2$ K. The (Kubo-Toyabe) linewidth in pure UBe_{13} is consistent with inhomogeneous dipolar broadening due to ^{9}Be nuclear dipoles and shows no change in magnitude below the superconducting transition at $T_c = 0.86$ K. The linewidth observed in the normal state of the x = 0.033 material is about 15% larger than that in UBe_{13}, presumably because of a change in the equilibrium site of the muon induced by the addition of the Th impurities. Also, no change in the linewidth is observed just below the superconducting transition at $T_{c1} \simeq 0.6$ K in (U,Th)Be_{13}. However, a 15% increase in the linewidth is observed at $T_{c2} \simeq 0.4$ K. Such a change is too large to have been produced by the known change in lattice constant at T_{c2} and is thus most certainly due to the onset of magnetism instead. Assuming dipolar coupling to the muon, the increase in linewidth is consistent with an increased magnetic moment of about 10^{-3} μ_B/U-atom. This small change would have been unobservable in either the neutron-scattering or the nuclear magnetic resonance (NMR) studies reported previously by others. Our measurement thus constitutes the first unambiguous determination of the magnetic character of this state. Whether the state occurring at and below T_{c2} in (U,Th)Be_{13} is due to itinerant magnetism, weak local magnetic moments, or an exotic magnetic superconducting state is still uncertain.

Muon Spin Relaxation in the Heavy-Electron Superconductor UPt_3 (P-10, MP-3, MST-5, University of California at Riverside)

After the discovery of heavy-fermion superconductivity (HFS) in $CeCu_2Si_2$ and UBe_{13}, Stewart and others at Los Alamos reported a third HFS system, UPt_3. In addition to the usual properties associated with these materials, UPt_3 exhibits spin-fluctuation behavior similar to that previously reported for $TiBe_2$ and UAl_2. Thus it was suggested that UPt_3 may represent the first known system to exhibit coexistent bulk superconductivity and spin fluctuations. As a further indication of this coexistence, the substitution of thorium for uranium in UPt_3 has been shown to induce a spin-density-wave-like state at around T = 6.5 K, suggesting that the UPt_3 ground-state is nearly unstable with respect to magnetic excitations.

Because μSR is such a sensitive probe of magnetism, we have investigated some magnetic properties of UPt_3 over the temperature interval 0.165 to 20 K in both zero and applied magnetic fields. For the zero-field data, the external magnetic field at the sample was nulled to within $\pm$10 mOe. Susceptibility data indicated a superconducting transition at 0.41 K $\pm$ 0.01 K for our sample, which was prepared as an arc-melted polycrystalline ingot. Metallurgical analyses indicated light interstitial impurity concentrations of ~100 to ~150 ppm at.% and a second-phase upper limit of 1% to 2%.

For the temperature range $T \leq 15$ K (Fig. VI-4), both the zero-field and the low transverse-field (100-Oe) data show relaxation rates larger than expected from nuclear dipolar fields alone. (The calculated nuclear dipolar relaxation rates σ_{VV} shown in Fig. VI-4 have a range of values depending upon which interstitial site is assumed for the μ^+ occupation.) Higher-field (5-kOe) transverse μSR

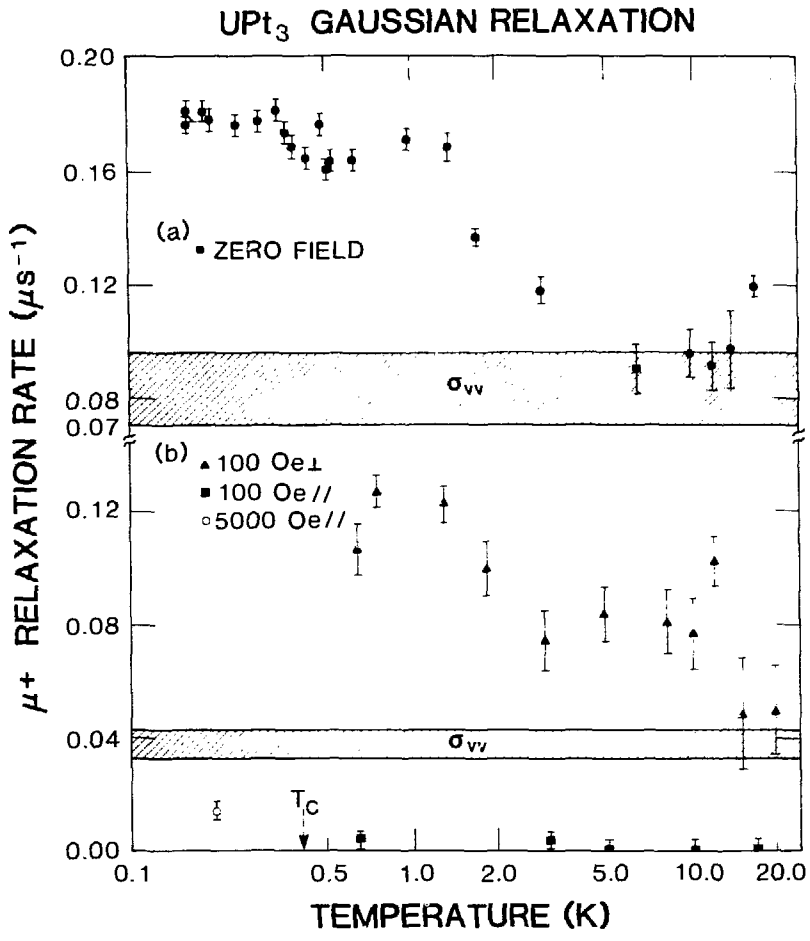

Fig. VI-4. (a) μ^+ gaussian relaxation rates in polycrystalline UPt_3 taken in zero-applied field as a function of temperature. (b) μ^+ relaxation rates obtained in low transverse fields (100 Oe $\perp$), low longitudinal fields (100 Oe $\parallel$), and a high longitudinal field (5 kOe $\parallel$) as a function of temperature. The vertical arrow at 0.41 K denotes the superconducting transition temperature, T_c, as determined by ac susceptibility measurements. The cross-hatched areas correspond to the calculated Van Vleck linewidths, σ_{VV}, the limits being μ^+ site dependent.

rates are shown in Fig. VI-5. Over comparable temperature intervals, the higher-field rates are three to four times as large as the 100-Oe data, indicating field-dependent relaxation. By contrast, all of the μ^+ relaxation rates in longitudinally applied fields are essentially zero below about 17 K (Fig. VI-4b). These longitudinal-field results are consistent with a quasi-static relaxation mechanism in transverse and zero fields. This means that the observed temperature dependence is due neither to μ^+ hopping nor to motional narrowing of the μ^+ local field by relaxation of ^{195}Pt nuclei.

The principal experimental result presented here is that one observes a larger-than-expected, field-dependent, quasi-static, μ^+ relaxation rate for $T \leq 15$ K in UPt_3. To explain this finding we consider three hypothetical mechanisms: 1) precipitations of a spurious magnetic second phase, e.g., UPt, might have contaminated our sample; 2) strong indirect coupling between μ^+ and ^{195}Pt moments, mediated by band electrons, might be present; or 3) the band (heavy) electrons themselves might possess a weak form of magnetic order. We have investigated these possibilities and conclude

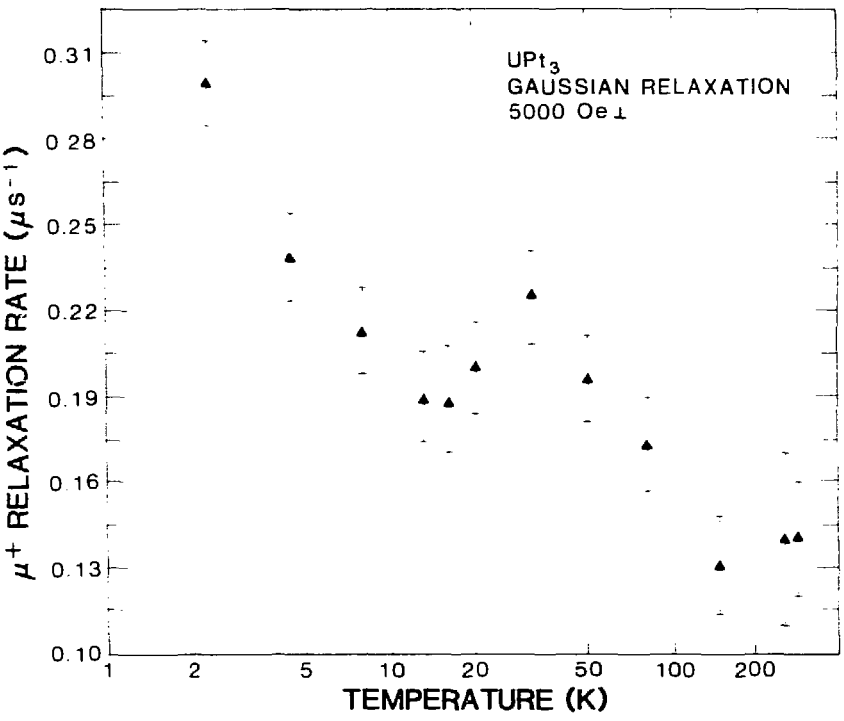

Fig. VI-5. μ^+ gaussian relaxation rates in polycrystalline UPt_3 taken in a 5-kOe transverse field as a function of temperature.

that the third is most feasible. The small rise in linewidth observed in zero field at T_c (Fig. VI-4) occurs because the local-field distribution produced by the weak magnetism is changed slightly upon entering the Meissner state. This, therefore, may be considered as further evidence for the extremely weak magnetism observable only through μSR measurements.

High-Pressure Studies of Heavy-Fermion Compounds (P-10)

The discovery of HF behavior in cerium and uranium-based intermetallic compounds has generated an intensive experimental and theoretical study of this phenomenon in which the effective mass of electrons is enhanced by 2 to 3 orders of magnitude relative to the free-electron mass. Hydrostatic pressure has proven to be a very important variable in studies of these compounds. Because of pressure-dependent interactions between nearly localized f-electrons and the spd conduction band, a large, very narrow, resonant density-of-electronic-states appears at the Fermi energy, a condition often attributed to the Kondo effect. At very low temperatures, quasi-particles within this resonance interact to form a coherent Fermi-liquid ground state, which in the case of HF compounds may take any of three forms: 1) paramagnetic, 2) magnetically ordered, or 3) superconductive. The width of the resonance sets one characteristic energy scale of these systems to be of order 100 K or less. The coherent ground state is characterized by another energy scale that is typically 1% to 10% of the higher energy scale. Hydrostatic pressure has been found to have a pronounced effect on these scales.

From a rather extensive study of the electrical resistivity measurements as a function of temperature and pressure in a large number of HF cerium- and uranium-based compounds, we have observed several general effects of pressure on these materials. The first is that interactions responsible for the heavy, mass-coherent state are extremely sensitive to pressure. In the case of Ce- and U-based compounds, the effective mass of the heavy electrons is depressed by pressure, corresponding to

an increase of the low-temperature energy scale. Second, pressure experiments reveal that several competing mechanisms must be present to reduce both the small energy scales and the ultimate ground-state configuration. At high temperatures, the dominate mechanism is Kondo interactions, independent of the lattice site. At low temperatures, interactions between f-atom sites, due possibly to RKKY or quadrupolar couplings, appear to be responsible for producing a coherent state. It may be only the ratio of these two energy scales that determines the ground state configuration. Finally, experiments indicate that, at least for U-based HF superconductors, pressure drives the superconducting state toward a magnetically ordered one. This observation is counter-intuitive to our understanding of conventional superconductivity and further points to the possibility of a highly unusual superconducting state in these compounds.

A few specific examples of our findings are given in the following paragraphs.

Scaling Law for the Electrical Resistance. The transition from "high"-temperature behavior to coherent low-temperature behavior often results in a maximum in the electrical resistivity at a temperature T_{max}, which can be a strong function of pressure. One important observation from our resistance/pressure studies has been the observation of a "scaling law" in the electrical resistance as the characteristic temperature scales are increased by pressure. That is, plots of ρ/ρ_{max} versus T/T_{max}, where ρ_{max} is the resistivity at T_{max}, are invariant with respect to pressure. Such a "law," if it exists universally, has fundamental implications for any theory that may be developed. An aspect of our research has been the establishment of such universality. From investigations of nearly 20 HF compounds, we have found scaling to hold over a large low-temperature interval in all these materials provided phase transitions or crystalline electric fields do not strongly perturb the electronic scattering.

Pressure Dependence of Electrical Resistance in URu_2Si_2. The compound URu_2Si_2 was discovered recently to exhibit two phase transitions, a superconducting one at $T_c \sim 1.5$ K and a second one at $T_0 \sim 17.5$ K, whose natures have not been established conclusively. Because of the shape of the specific heat anomaly at T_0, we have interpreted this transition as arising from the formation of a spin- or charge-density wave that produces a gap ~11 meV wide over ~40% of the Fermi surface. The magnitude of the electronic specific heat (~112 mJ/mole-K^2 above T_0 and ~66 mJ/mole-K^2 near $T = 0$) implies an effective mass $m^* \sim (25\text{-}50)m_e$, where m_e is the free-electron mass.

We have studied the effect of hydrostatic pressures to over 15 kbar on the transitions T_c and T_0 through electrical resistance measurements from 300 K to 20 mK. For $P < 12$ kbar, T_0 increases +0.125 K/kbar, whereas T_c decreases −0.095 K/kbar and extrapolates to zero at ~15.5 kbar. This rate of T_c depression with P is two to nine times larger than the rate found in other heavy-electron superconductors. The nearly equal but opposite P-dependences of T_c and T_0 suggest an increase in the fraction of the Fermi surface that is removed by the transition at T_0, i.e., a pressure-induced competition for electron density-of-states at the Fermi energy. These observations support our interpretation for the nature of the transition at T_0.

The temperature-dependent resistivity $\rho(T)$ of URu_2Si_2 is typical of Kondo-lattice behavior, namely, a region of negative $\delta\rho/\delta T$ above 75 K, followed by a sharp drop in resistivity below ~70 K. Although pressure produces relatively large changes in the shape of ρ versus T, we find that the resistivity may be scaled onto a single curve for all pressures over a wide temperature interval, except in the immediate vicinity of T_0. That scaling persists both above and below T_0 suggests the dominance of coherent Kondo spin scattering in determining the overall shape of $\rho(T)$ in this temperature regime.

Kondo-Lattice Behavior. Despite extensive searches during the last decade, only a relatively small handful of materials may yet be classified as Kondo lattices. Two notable series of compounds that have been found to show Kondo-lattice behavior are those of general formulae CeM_3 and CeM_2Si_2, where M is one of several transition elements. We have discovered a new series of Kondo-lattice compounds Ce_3M, where M = Al, In, and Sn, and have studied these through magnetic susceptibility and resistivity measurements at ambient and elevated pressures.

Most unusual is the behavior of Ce_3Al and Ce_3In. Ce_3Al orders magnetically near 2 K but under pressure undergoes a phase transition that appears similar to the γ-α transition seen in pure Ce. In pure Ce, the γ-α transition is one from a magnetic to a nonmagnetic state accompanied by a 15% volume collapse. Only one compound (CeNi) shows similar behavior so far. However, Ce_3Al also retains the magnetic transition even in the α-like state! If our speculation as to the nature of the first-order transition in Ce_3Al is supported by neutron-scattering experiments planned for the near future, Ce_3Al will have proved to be a truly unique material. Ce_3In shows comparable behavior: however, it does not order magnetically at ambient pressure, although it may do so under pressure. More experiments are required for clarification of these most interesting observations.

Superconductivity in UBe_{13}. This heavy-fermion superconductor has been the subject of intense experimental and theoretical research since its discovery in 1983. Much of the excitement has been generated by the strong possibility of odd-parity superconductivity and the unusual temperature dependence of the electrical resistivity ρ. The resistivity increases below room temperature, reaches a plateau near 10 K, and passes through a sharp maximum at $T_M \sim 2.5$ K before superconductivity sets in at 0.9 K. A T^2-dependence of ρ is not observed above T_c, contrary to behavior expected from the Fermi-liquid model.

We have determined $\rho(T)$ from 1 to 300 K at pressures up to 16 kbar. We find that with pressure T_M moves rapidly to higher temperatures and that $\rho(T_M)$ grows substantially so that the plateau region is obscured, as in the case for UBe_{13} doped with small amounts of Th or Lu. For $P > 4.4$ kbar, a clearly defined T^2 variation in ρ appears, the T^2 interval increasing with applied pressure. Taking $\rho = \rho_o + AT^2$, we find $A \sim 25\ \mu\Omega$-cm/K^2 at 4.4 kbar and that $1/\sqrt{A}$, which theoretically should be proportional to a characteristic temperature of the heavy-Fermi liquid, increases linearly with P, as does T_M. Extrapolating $1/\sqrt{A}$ versus P to $P = 0$ gives $A \sim 29\ \mu\Omega$-cm/K^2, a value consistent with the very large electronic specific heat of UBe_{13} ($\gamma \propto \sqrt{A}$). These results add to the evidence that superconductivity in UBe_{13} is mediated by spin fluctuations and is likely to be other than s-wave pairings.

Nonlinear Transport Properties in $NbSe_3$ (P-10, Princeton University)

In a one-dimensional metal, a periodic lattice distortion (PLD) spontaneously occurs at a critical temperature. The PLD is stabilized by a modulation of the electronic density known as a charge-density wave (CDW). Depending on the Fermi surface caliper dimension ($2k_F$) existing in the high-temperature pretransition phase, the CDW may be commensurate or incommensurate with the original host lattice. In the incommensurate case, CDWs are pinned by impurities. The possibility that CDWs may become depinned and move through the lattice was suggested by Frohlich in 1954 as a model for a one-dimensional superconductor. The moving CDWs transport electrons, and if there were no dissipation, the current would persist in time. However, it is now known that a moving CDW can result if the applied electric field exceeds the threshold E_T, giving rise to the non-ohmic dc conductivity. One of the most spectacular transport phenomena is the appearance of very sharp frequency components in the voltage spectrum.

$NbSe_3$ is a quasi-one-dimensional system and has two phase transitions at T_1 (142 K) and T_2 (58 K). Figure VI-6 displays the noise spectrum below T_1. When the area under the noise signal $\int V(\omega)d\omega/I_{CDW}$ is plotted against 1/T, the data can be fitted to the Arrhenius law $\int V(\omega)d\omega/I_{CDW} \propto \exp(-1400/T)$, indicating an activation energy of ~2800 K. When the CDW portion of the conductivity, σ_{CDW}, is plotted against 1/T, as displayed in Fig. VI-7, we find approximately $\sigma_{CDW} \exp(-1385/T)$. Again, the activation energy is approximately 2800 K. To date, we know neither the origin of the noise nor the source of this large value of the activation energy. Work on this effort has been discontinued at Los Alamos but is still pursued at a number of other laboratories to elucidate these complex yet fundamental transport properties.

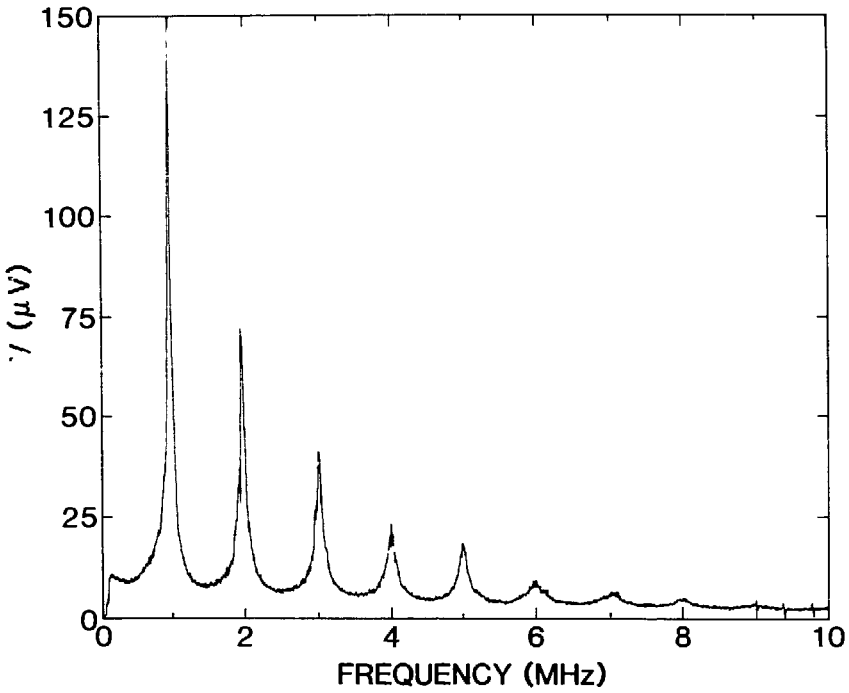

Fig. VI-6. The noise power spectrum of $NbSe_3$ at 110 K.

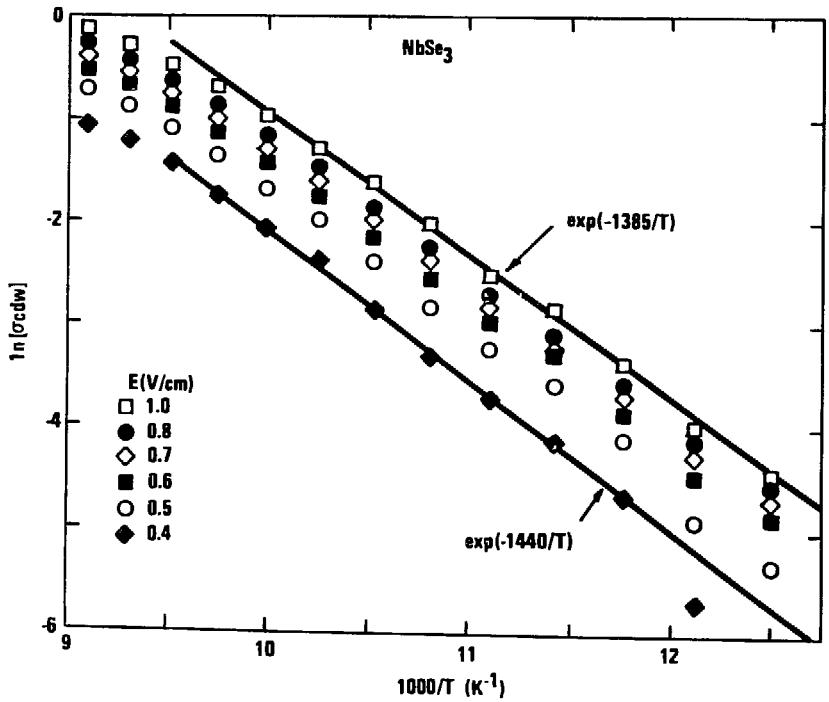

Fig. VI-7. The charge-density conductivity versus 1/T.

Muon Spin Relaxation Study of Exchange Coupling in Dilute AgMn Alloys (P-10, MP-3, Rice University, University of California at Riverside)

Potential scattering due to the presence of a magnetic impurity in a metal causes both charge- and spin-density oscillations (SDO) of the conduction electrons. The SDO are caused by the spin dependence of the potential, which is a consequence of the conduction-electron local-moment exchange interaction. This exchange has both direct and mixing contributions (covalent s-d mixing here). We have used μSR to examine some single-ion properties of manganese local moments in silver. We find that the coupling between muons and manganese moments is partially mediated by SDO, so we can determine the exchange constant average J_{SDO} appropriate to SDO coupling. Our value for J_{SDO}, 2.8 eV, is larger but more reliable than values found from NMR or electron-spin-resonance (ESR) experiments. This constitutes the first observation of SDO by μSR and the first unambiguous determination of J_{SDO} for AgMn.

$Ag_{1-c}Mn_c$ samples with c = 0.003, 0.016, and 0.030 were prepared by arc-melting the weighed constituents, followed by a 10-hour annealing at 800°C and a quench. Concentrations were verified by ac susceptibility and by determination of the residual resistance.

Muon spin relaxation in a transverse field H is dominated by the spread in manganese dipole fields at the muon site (inhomogeneous broadening). The inhomogeneous linewidth $1/T_2^*$ is proportional to c and to the manganese spin polarization (S_z). In the high-temperature limit the manganese polarization follows a Curie law, so one expects $1/T_2^* \propto cH/T$. Experimentally, the constants of proportionality are (0.270 ± 0.007), (0.276 ± 0.016), and (0.267 ± 0.013) μs^{-1} Oe^{-1} K for c = 0.003, 0.016, and 0.030, respectively. We note that these values are essentially constant over a decade of variation of c.

The constant of proportionality can be calculated assuming a muon-Mn coupling consisting of both dipolar and SDO terms. Using the measured μSR linewidths $1/T_2^*$ and magnetization measurements to determine the effective manganese moments, we find that the measured linewidths exceed those expected for dipolar coupling alone by a factor of 1.7. Using existing formalism for both dipolar and SDO coupling, we then find that the SDO amplitude exceeds the dipolar amplitude by a factor of about 1.8.

The exchange interaction is characterized by a wave-vector dependent exchange parameter $J(\vec{k},\vec{k}')$, which includes both atomic and covalent-mixing contributions. One can extract J_{SDO}, which is an appropriate average of $J(\vec{k},\vec{k}')$ over the Fermi surface, from our measurements; we obtain $|J_{SDO}| = 2.8 \pm 0.3$ eV. Values of $|J_{SDO}|$ in AgMn obtained by NMR and ESR are considerably smaller than this; but the NMR experiments may have been affected by metallurgical problems, and the interpretation of the ESR data may have been affected by a failure to break the bottleneck fully. The present determination of J_{SDO} is free of these problems.

One may also extract a different exchange constant J_K from quasi-elastic neutron scattering. Here J_K characterizes the relaxation of the manganese spin by spin-flip conduction-electron scattering and is a different average of $J(\vec{k},\vec{k}')$ over the Fermi surface than is J_{SDO}. It is found to be $|J_K| = 0.85$ eV.

One may ask whether the exchange constant averages J_{SDO} (μSR) and J_K (neutron scattering) are consistent with a reasonable set of exchange parameters. If the covalent mixing contribution to $J(\vec{k},\vec{k}')$ is assumed to be completely dominant, then $|J_{SDO}/J_K| = \sqrt{5}$, which is less than the measured ratio of 3.3 ± 0.6. This may indicate that direct exchange contributions are also important; but for a proper evaluation of the additional terms, we must have the potential-scattering phase shifts, which are not reliably known. Alternatively, recent photoemission results suggest that the Schrieffer-Wolf transformation, which underlies our analysis, may be inadequate to describe the strong mixing in AgMn.

Ferromagnetic and Reentrant Spin Glass Transitions in *Pd*FeMn (P-10, MP-3, Rice University, University of California at Riverside, University of Leiden)

One of the unsolved problems in spin-glass research is the nature of the double transition seen in some materials. These systems exhibit a transition to a ferromagnetic state at a Curie temperature T_c and a transition to a spin-glass-like state, where the magnetic spins freeze in random orientations, at a lower temperature T_g. The wide variety of materials exhibiting a reentrant phase diagram suggests that the double transition is a common feature of magnetic systems with competing interactions. Verbeek et al. discovered that small amounts of iron added to *Pd*Mn (few at.%) produced such a double-transition system. Two models have been proposed to explain this behavior. The separate transition model assumes that the iron spins order ferromagnetically at T_c and that the manganese spins freeze randomly and separately at the lower spin-glass temperature T_g. The Sherrington-Kirkpatrick (SK) mean-field model assumes that both the manganese and the iron spins participate in the transition at T_c by forming a percolative, infinite cluster of ferromagnetically coupled manganese and iron spins. On cooling to T_g, the antiferromagnetic near-neighbor interactions break the cluster at its weak links. The spin-glass phase would then be due to randomly oriented clusters of manganese and iron spins.

We have performed zero-field μSR measurements to delineate the local-field distribution at the μ^+ site in *Pd*$Fe_{0.0035}Mn_{0.05}$, for which $T_c \simeq 8$ K and $T_g \simeq 2$ K. For dilute atomic species, the theoretical field distribution separates into a sum of contributions from each of the two magnetic ions. Measured in terms of the static μSR rate for dipolar coupling between the μ^+ and the magnetic ions, the iron spins are calculated to contribute a rate of 3.3 μs^{-1}, and the manganese spins yield 68 μs^{-1}, giving a total theoretical linewidth of 71 μs^{-1}. Our experimental data for the inhomogeneous field distributions give a linewidth of 8.7 $\pm$ 1.5 μs^{-1} at T = 7.5 K and a larger linewidth at low temperatures, showing unambiguously that both the iron and the manganese moments contribute to the transition at T_c. This finding negates the separate-transition model.

We also measured the muon spin-lattice relaxation rate caused by fluctuating iron and manganese spins in the temperature range 0.5 to 16 K. In earlier work we carried out similar measurements on ferromagnetic *Pd*$Mn_{0.02}$ and on spin-glass $PdMn_{0.07}$, to which the current data can be compared. At T_c in *Pd*FeMn, one sees the same characteristic cusp in the temperature dependence of the linewidth (produced by the critical slowing down of the magnetic ions) as was seen in $PdMn_{0.02}$ (Fig. VI-8). Furthermore, the application of a longitudinal field completely suppressed the μSR rate for $T \geq T_c$, as was the case for ferromagnetic $PdMn_{0.02}$. By contrast, a field has only a modest effect on μ^+ relaxation in a spin glass. It is therefore reasonable that the transition seen at T_c in *Pd*FeMn is to a ferromagnetic-like state.

The transition to the spin-glass state, although showing a definite signature in the ac susceptibility, shows no comparable signal in the muon relaxation (Fig. VI-8). Instead, the μSR rate only gradually decreases below T_g. A nonreentrant spin glass, such as *Pd*$Mn_{0.07}$, shows a definite cusp at T_g; thus, the spin-glass transition in PdFeMn is unusual. A further difference in the relaxation rate in this system appears at temperatures between T_c and T_g. In an ordinary disordered ferromagnet like $PdMn_{0.02}$, the μSR rate falls off to nearly zero below T_c, whereas in *Pd*FeMn the rate remains substantially elevated. This indicates the continuing presence of slow fluctuations (with correlation times 10^{-10} to 10^{-11} s) in this intermediate temperature regime.

Our main conclusions can be summarized as follows: 1) The static muon linewidth in the ferromagnetic phase shows that the manganese spins participate in the spin freezing at T_c. This effect rules out the possibility that the ferromagnetic-to-spin-glass transition at T_g might represent a simple spin-glass freezing of the manganese spins. 2) The field and temperature dependence of the muon spin-lattice relaxation rate near T_c is consistent with a ferromagnetic transition at T_c involving the manganese spins. Below T_c, slow fluctuations persist to the lowest temperatures measured, but there is no strong dynamic signature of the transition at T_g. This result indicates that the spin dynamics in this reentrant system are significantly different from the dynamics in either disordered ferromagnets or canonical spin-glasses.

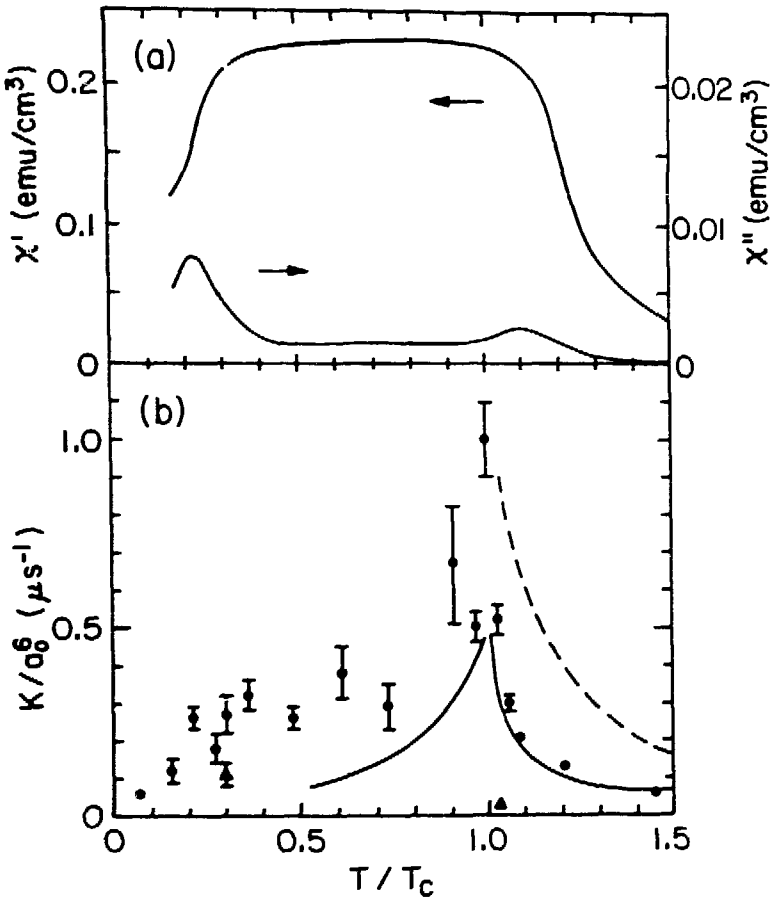

Fig. VI-8. (a) Temperature dependence of the real (χ') and imaginary (χ'') parts of the low-field ac susceptibility of the $\underline{Pd}$FeMn μSR sample, showing $T_g \approx 1.9$ K from the peak of μ''. (b) Temperature dependence of the zero-field muon spin-lattice relaxation parameter scaled by the Pd lattice parameter. $T_c = 8.25$ K, from the peak of the μSR relaxation rate. Circles, zero applied field. Triangles: 1-kOe longitudinal field. The solid line represents muon relaxation rates in ferromagnetic $\underline{Pd}Mn_{0.02}$ with temperature scaled by $T_c = 5.8$ K. The dashed line represents muon relaxation rates in spin-glass $\underline{Pd}Mn_{0.07}$ with temperatures scaled by $T_g = 5.0$ K.

Some Aspects of the Interplay Between Magnetism and Superconductivity (P-10)

The origin of itinerant ferromagnetism has been a mystery. We have conjectured that it is related to those lattice vibrations which involve no spins but are responsible for the occurrence of superconductivity. The best known itinerant magnets are transition metals, X = Fe, Co, Mn, while V_6X compounds are superconductors. In order to help untangle the complex interrelationship between superconductivity and magnetism, we have begun to measure some of the electromagnetic properties in these compounds. We have measured the penetration depths, λ, of the compounds and their alloys by observing the frequency shift of a Gunn oscillator arising from the change in the penetration depth of a superconductor that forms a part of the LC circuit. Interestingly, λ^{-1} is proportional to the superconductivity transition temperature. We have also found that λ^{-1} is correlated with the saturation magnetic moment of pure-element X. This unexpected correlation

between superconductivity and magnetism has bolstered our earlier speculations that the origins of superconductivity and itinerant magnetism are strongly related, even though they also seem to exclude each other.

It has been shown that superconductivity and ferromagnetism do not coexist in the bulk ferromagnetic superconductor, $ErRh_4B_4$; but this conclusion does not apply to the surface properties of that material. We have again measured λ, which can be shown to be proportional to $(1 + 4\pi\chi)^{1/2}$, where the magnetic susceptibility, χ, should vary with temperature as $1/(T - T_s)$, with T_s the surface ferromagnetic Curie temperature. Figure VI-9 shows our results, which are consistent with that prediction. Here T_s is higher than the reentrant temperature T_{c2}, below which superconductivity disappears. This is the first observation of surface ferromagnetism that coexists with superconductivity.

Another system of interest is Y_9Co_7, which becomes itinerant-ferromagnetic at ~6.5 K but superconducting below $T_c \sim 3.5$ K. We have employed the zero-field longitudinal muon spin relaxation technique to study this compound. From the relaxation data, we have obtained a fast component below T_c, which can be interpreted as a fast-decay oscillatory component attributable to disturbed weak ferromagnetism. This result suggests the coexistence of superconductivity and weak ferromagnetism and hence would contradict the mean-field theory, which predicts the mutual exclusion of these two possible ground states.

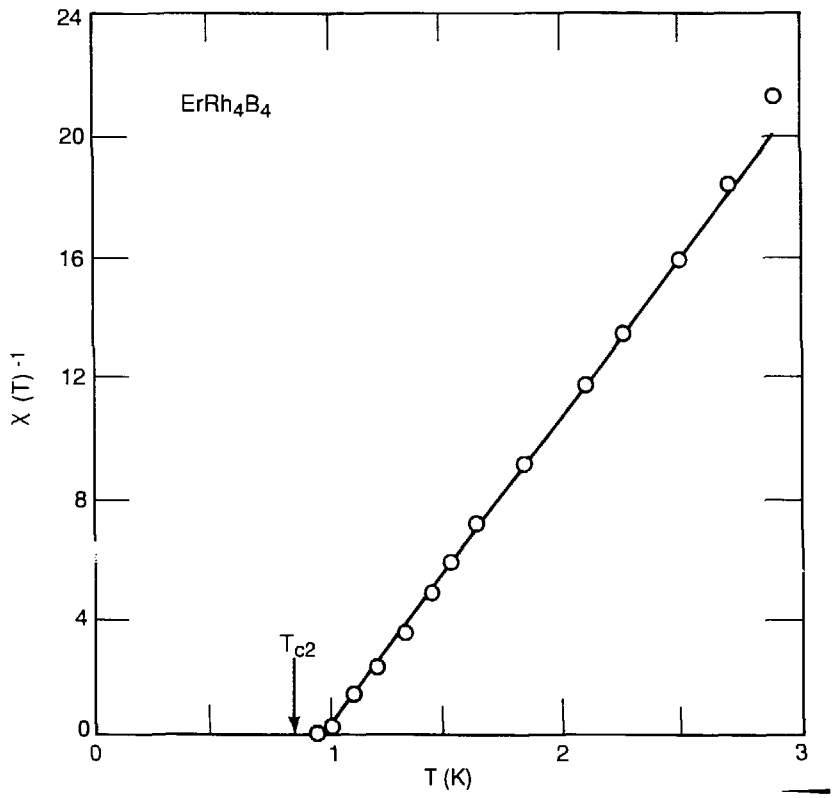

Fig. VI-9. Surface magnetic susceptibility χ as a function of temperature.

Time-Resolved Picosecond Spectroscopy of Laser-Excited Semiconductors and Graphite (P-10, Harvard University)

The time-resolved reflectivity and transmission of semiconductor surfaces excited by picosecond laser pulses provide direct information on the evolution of the photogenerated electron-hole plasma and the heating and melting of the lattice. The optimum conditions for probing the plasma occur near the plasma resonance, where the real part of the dielectric constant approaches zero and a sharp rise of the reflectivity of the material occurs, determining the carrier density.

We have performed time-resolved spectroscopy measurements, with 20-ps, 0.532-μm laser pulses, specifically to study excitation conditions reached in silicon and germanium just before the surface melts. Because the photon energy is large compared to the band-gap in germanium, we can preclude such complicating features as saturation of the absorption and intravalence band transitions. The delayed probe beam is obtained by Raman-shifting the fundamental frequency, 1.06 μm, in high-pressure H_2 and CH_4 gas cells.

The reflectivity and transmission at 1.9 μm have been measured as a function of the pump fluence. The experimental data were compared with the calculated response derived from numerical simulations of the carrier density and temperature made on the basis of the thermal model, which assumes the Auger effect as the main carrier recombination mechanism. Under degenerate conditions, a higher fraction of available energy is routed to the carrier gas rather than directly to the lattice. Thus, significant heating of the lattice, by recombination and subsequent phonon emission, occurs at later times.

Our data also show a saturation of the transmission and only a small rise of the reflectivity with fluence. This behavior is even more evident at the longer delays, where an increase in transmission indicates that a progressive reduction of the plasma density with increasing fluence takes place as soon as the plasmon energy becomes comparable with the thermally reduced band-gap of germanium. When these conditions are met at the surface, this new mechanism gives rise to strong recombination, reducing the total number of carriers that can diffuse into the bulk of the sample, as the trend of the transmission at 200-ps delay shows. A similar, although less pronounced, behavior is observed in the measurements on silicon at 1.9 μm.

More recently, we investigated the optical properties of highly oriented pyrolytic graphite (HOPG) by picosecond pump-and-probe techniques. Our results at 1.9, 1.06, and 0.532 μm have shown that a new phase occurs as soon as a critical fluence, $F^{th} = 140$ mJ/cm^2, is exceeded. Above this value, the reflectivity drops considerably from the original value. Contrary to the behavior of silicon and other semiconductors, which exhibit metallic reflectivities after surface melting, the new phase in graphite is characterized by lower reflectivities in a wide wavelength range. As displayed, the reflectivity drops to $\sim$0.05, which is about that of ordinary glass, indicating a decrease in both the real and the imaginary parts of the index of refraction. In consequence, more light can penetrate into the material, heating further layers. This process can provide a considerable depth of transformed material, much thicker than the initial absorption depth. Moreover, the thermal diffusion, which is intrinsically lower than in the metallic case, is slowed down by the lower gradients so that surface evaporation will be a major cooling channel at later times. We suggest that the new phase consists of carbon microcrystallites behaving like a liquid.

Velocity of Propagation of the ^{3}He A-B Interface in Hypercooled ^{3}He-A (P-10)

Liquid ^{4}He becomes a superfluid at temperatures below 2.17 K and remains a liquid even at absolute zero temperature, except when subjected to considerable pressure. Liquid ^{3}He behaves similarly, but becomes superfluid at much lower temperatures (below about 0.003 K) and, in addition, as shown in Fig. VI-10, has two superfluid phases, A and B, in the absence of a magnetic field. (In a field, a third phase, A^1, develops, the A-B and A-A^1 phase boundaries shifting with field intensity.) The A and B phases differ in magnetic and mechanical properties.

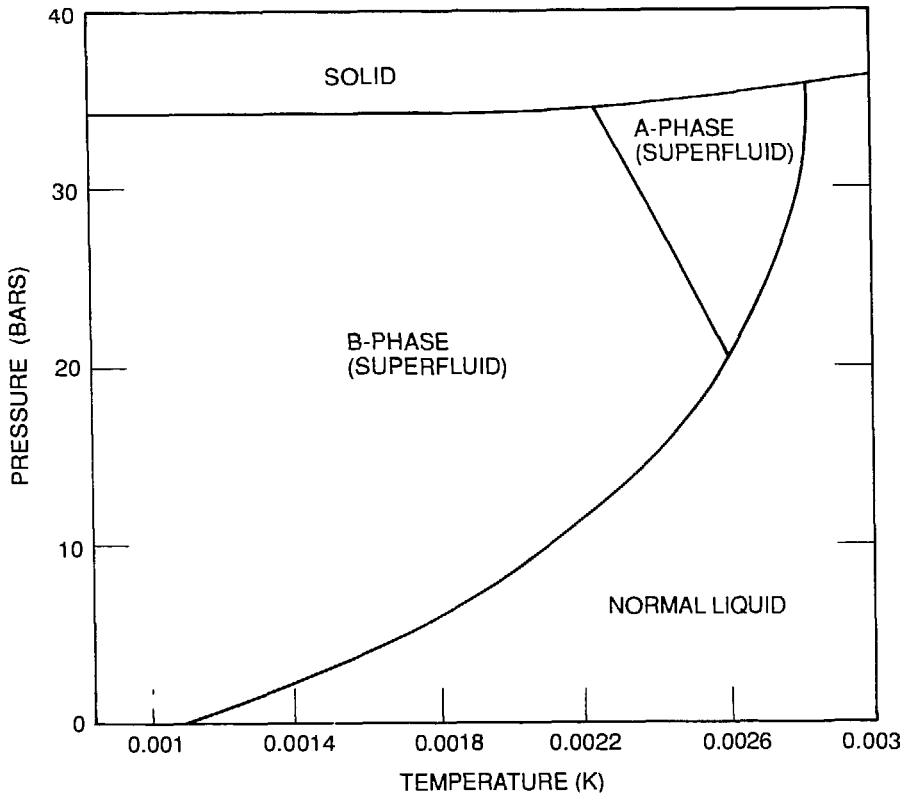

Fig. VI-10. Low-temperature phase diagram for liquid and solid ^{3}He at zero magnetic field.

Of all the first-order phase transitions that occur in nature, those in superfluid ^{3}He, and particularly the transition between ^{3}He-A and ^{3}He-B are among the most remarkable. The ^{3}He A→B transition is remarkable insofar as the interfacial energy is a consequence of the existence of different quantum mechanical order parameters in each of the two phases, an accommodation between the two order parameters taking place in the interface. The A→B transition is also remarkable in that it takes place at all in view of the small bulk free-energy difference between the two phases. This small free-energy difference makes the probability of homogeneous nucleation of the B-phase vanishingly small. Also, the A→B transition occurs at a very low reduced temperature T_n/T_{AB}, where T_n is the temperature at which nucleation occurs, and T_{AB} is the thermodynamic transition temperature. Indeed, over most of the range of cooling, the ^{3}He-A is in a hypercooled state. A substance is hypercooled when the latent heat released during the transition is insufficient to raise the temperature of the sample above the thermodynamic transition temperature. In this study of the A→B transition, we have measured the velocity of propagation, V_{AB}, of the A-B interface in a hypercooled sample of ^{3}He-A for T/T_{AB} between 0.99 and 0.77 and at pressures of 2.45, 2.96, and 3.36 MPa.

When ^{3}He undergoes the A→B transition, the magnetic susceptibility changes. We took advantage of this change in order to follow the interface as it moved up a column of ^{3}He. The tube containing the column was wound with a series of pickup coils, spaced a known distance apart and hooked to the input terminals of a superconducting quantum interference device (SQUID). As the interface passed through each pickup coil, the flux through the coil changed because of the susceptibility change generating a signal in the SQUID. By measuring the time of passage of the interface between succeeding pickup coils, we could determine the velocity of the interface.

Using this technique, we measured velocities of propagation as high as 67 cm/s. Calculations performed before the experiment was conducted had indicated that we should expect velocities on the order of 0.06 cm/s. The discrepancy arose because the calculations did not account for the possibility that the ^{3}He is hypercooled when the transition takes place. If it were not hypercooled, but merely supercooled, then thermal diffusion of the released latent heat away from the interface would limit the velocity; but because thermal processes do not play a role in the hypercooled state, we see velocities as high as 67 cm/s. One explanation proposed for this result suggests that partial reflection of quasi-particles from the interface is the only mechanism limiting the velocity.

Another important result of our investigation is the observation that the temperature at which the B-phase nucleates from the A-phase is dependent on cell geometry. We observed that this temperature was different for two different parts of our cell. We believe that this is an important clue in the attempt to understand exactly how the B-phase nucleates from the A-phase.

NONLINEAR DYNAMICS: SCALING AT THE ONSET OF OSCILLATORY RAYLEIGH-BÉNARD CONVECTION (P-10, CNLS, University of California at San Diego)

Dilute solutions of ^{3}He in superfluid ^{4}He undergoing Rayleigh-Bénard convection have proven to be model systems for studying and testing concepts of theoretical nonlinear dynamics and could be the bases for a better understanding of fully developed fluid turbulence in general. The immediate application of these concepts to a wide variety of physical systems has already been highly productive. We have previously observed the period-doubling cascade to chaos; quasi-periodicity (two or more incommensurate frequencies); mode-locking, where two incommensurate frequencies entrain to a rational frequency ratio; and chaotic intermittence, a state characterized by intermittent bursts of aperiodic sequences interspersed with periodic or "laminar" intervals. Another transition that we have explored in detail is the onset of periodic oscillations from a time-independent convective state. Here, we describe the interesting and provocative analogy between that transition and an equilibrium phase transition, such as the ferromagnetic ordering of magnetic spins at low temperature. Theoretical and experimental work reveals a general scaling relation at any continuous transition to periodic oscillations (often referred to as a Hopf bifurcation).

Convection is a thermally driven nonequilibrium state in which a temperature difference maintained across a thin fluid layer causes a competition between buoyant forces arising from the thermal expansion of the fluid and the dissipative forces of viscosity and thermal diffusion. For small temperature differences, the fluid is motionless and heat conduction is diffusive. At some critical temperature difference ΔT_c, the fluid will begin to convect. A time-independent velocity field develops in the form of counter-rotating pairs of simple two-dimensional rolls, the characteristic size determined by the thickness of the fluid layer. For fluids that diffuse heat rapidly compared to the diffusion time for vorticity (i.e., a low-Prandtl-number fluid), a secondary instability to time-dependent oscillations occurs at higher temperature differences. It is this second transition that we describe here. At still greater temperature differences, complex states and transitions to chaos (states characterized by aperiodic time dependences) are common.

The experiment consists of a convection cell having top and bottom copper boundaries and low thermal conductance sidewalls defining the cell geometry. The convective motion of the fluid is sensed in several ways. For diffusive heat transport, by measuring heater power and temperature difference across the cell, we can detect and characterize the time-independent convective motion. In the case of time-dependent fluid flow, the motion is detected by a local temperature probe located in the top plate of the cell. This highly sensitive SQUID thermocouple can resolve temperature differences of 10^{-7} K, compared to a mean temperature of about 1 K, and is very insensitive to thermal noise common to the entire cell. The time-dependent periodic oscillations have a characteristic frequency of about 0.5 Hz at 0.85 K, compared to the probe's response time of approximately 15 ms.

The analogy between continuous equilibrium phase transitions and nonequilibrium instabilities, such as convection, is useful and may also be of deep theoretical interest. The transition between an ordered and a disordered state induced by changing the temperature is denoted by T_c, and the scaling variable measuring the effective distance from the transition is $t = (T - T_c)/T_c$. In addition, we consider β, the order parameter, which takes on a zero value in the disordered state and a nonzero value in the ordered state and which depends continuously on the scaling variable t. For a mean-field or fluctuation-free regime, β varies as $t^{1/2}$ for $t < 0$. Finally, the characteristic relaxation time over which changes in the order parameter can occur diverges as t^{-1} as T_c is approached: this behavior is often referred to as critical slowing-down.

The onset of continuous growth of the amplitude of spontaneous periodic oscillations can be described in an analogous fashion. The scaling variable analogous to the reduced temperature t is the quantity $\eta = (\Delta T - \Delta T_o)/\Delta T_o$, where ΔT_o is the temperature difference at the oscillatory onset. The order parameter is the rms amplitude of the fundamental frequency (higher harmonics are considered below). Changes in the order parameter are described by a characteristic time τ. In previous work on the oscillatory onset in dilute solutions of ^{3}He in superfluid ^{4}He, we established that the scaling of the order parameter was indeed $\eta^{1/2}$ (exponent 0.495 ± 0.01) and that τ exhibited critical slowing-down with an exponent of -1.003 ± 0.005, in agreement with the predictions. This result suggests that any nonequilibrium system that undergoes a continuous transition to periodic time dependence will exhibit the same scaling relations but with the asymptotic scaling regime depending on the particular system being studied. We note that the nonequilibrium transition seems to be mean-field, perhaps because fluctuations in the order parameter are exceedingly small and thus do not contribute substantially to the critical exponents, in contrast with equilibrium phase transitions, where mean-field scaling is rather uncommon.

For a very general nonlinear system describable by a series of coupled ordinary differential equations, the scaling of the amplitude of the pth harmonic is $A_p \sim \eta^{p/2}$ in the limit $\eta \rightarrow 0$. Here we use the convention that the pth harmonic refers to the frequency pf, where f is the fundamental. Figure VI-11 shows experimental verification of the predicted scaling for the first four harmonics. The scaling exponents obtained by least-squares fits to the curves are 0.495 ± 0.01, 1.01 ± 0.01, 1.44 ± 0.1, and 2.05 ± 0.10 for the first four harmonics, respectively. Predictions, from the theory of transient dynamics, of the different harmonics and the dynamics of the oscillatory frequency appear to be supported by the experiments.

The significance of the theoretical and experimental verification of these scaling properties is that any nonlinear system exhibiting this type of continuous transition to spontaneous periodic oscillations should behave according to these scaling laws. In the language of phase transition theory, we have a universality class in which the critical exponents do not depend on the specific details of the system: the system could be a convecting fluid as illustrated here, a nonlinear electronic circuit, a complex biological structure, or a large-scale geophysical system.

THERMAL PHYSICS—HEAT ENGINES

Magnetic Refrigeration with External Regeneration (P-10)

In the fall of 1985, the magnetic refrigerator (MR) research and development project, the project manager, and three other staff members were transferred to the Astronautics of America, Inc., Laboratories in Madison, Wisconsin. The purpose of the transfer was to expand the project and work toward commercialization of magnetic refrigeration. This move is considered an excellent example of direct technology transfer from the Laboratory to industry, as strongly encouraged by Department of Energy and Los Alamos policy. Through the early part of 1986, Los Alamos continued to receive support for concluding some MR studies, the results of which are reported here.

Although work on the Los Alamos MR project had led to the belief that an MR system employing regeneration could provide refrigeration from 77 K down to 4 K, system configurations were not

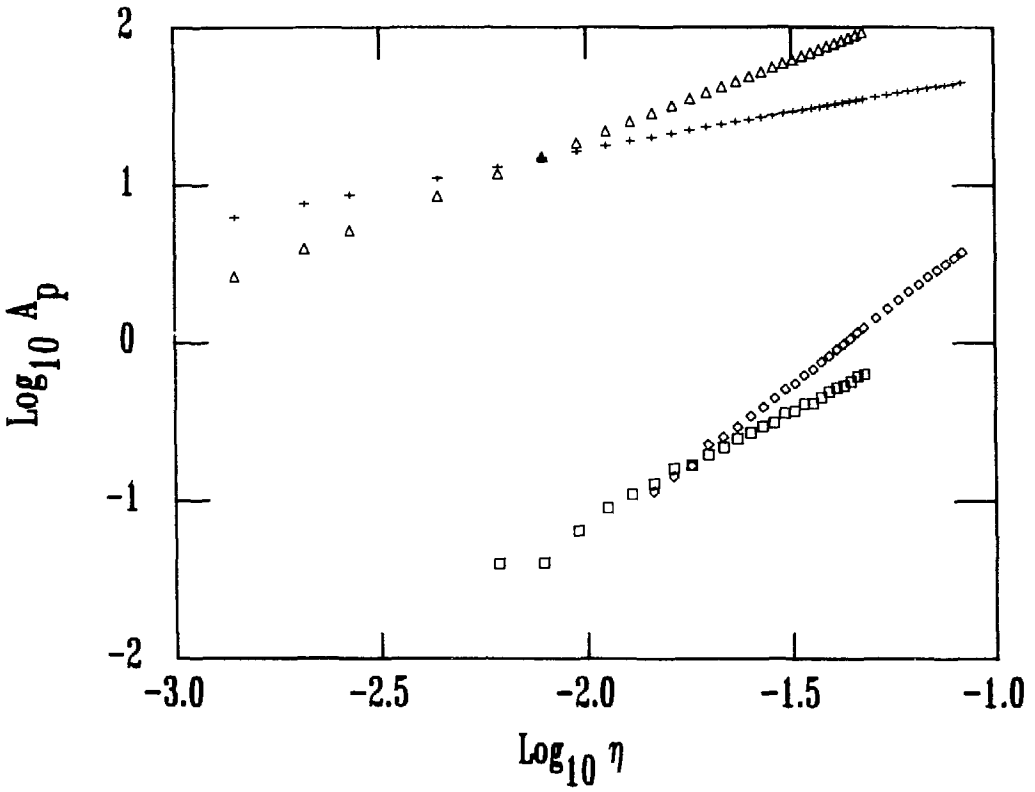

Fig. VI-11. Log-log plot of rms amplitudes of first four harmonics of oscillatory temperature versus reduced scaling parameter η. Data symbols: plus sign indicates p = 1; triangle, p = 2; square, p = 3; and diamond, p = 4.

well defined, and there was no basis for estimating either the lowest temperatures that could be attained or the system's performance under heat load. The need for a quantitative study of various system configurations was clear.

A reasonable (and workable) configuration was postulated for an MR in which the magnetic material would exchange heat with various stages of a regenerator. By proper cyclic operation of a system of valves and manifolds linking the magnetized (or demagnetized) magnetic material to the regenerator stages (copper) by exchange gas, we showed that we could achieve significant refrigeration. Systems with five to ten regenerator stages were studied in detail. A linearized model was assumed for the entropy-versus-temperature function of the magnetic material for zero field and for high magnetic fields. This model indicates very well how a real refrigerator might operate if GdNi above its Curie temperature of 70.5 K were used as the working material, but it is less accurate at lower temperatures. Using this model, we performed a theoretical thermodynamic analysis of the cyclic operations of systems with five to ten stages. The hot heat exchanger was assumed to exchange heat with a sink at temperatures between 50 K and 130 K but was typically at 75 K, the liquid-N_2 boiling point. The enthalpy of the magnetic material plus the internal energy of the regenerator stage material were assumed to be conserved during the heat exchange between them. The small gas-flow hydrodynamic losses were neglected in this first analysis.

The results of the study for regenerative magnetic refrigerators with five to ten regenerator stages show the lowest temperature achieved at the cold heat exchanger (after cyclic equilibrium had been achieved) as a function of the number of stages in the regenerator, the mass of each stage, and the refrigeration heat load at the cold heat exchanger. For example, a system with ten regenerator stages and a single magnetic stage could provide refrigeration from 75 K down to 34 K (no heat load) and from 75 K down to 46 K (200-J/cycle load). The thermodynamic cycle of these systems

was analyzed in detail, was compared with the familiar Brayton cycle and other cycles, and was found to be unique. The coefficient of performance was evaluated, and the system efficiency was compared to the ideal Carnot cycle. We found that with large refrigeration loads the efficiency approached 35% of Carnot; typical refrigeration systems have efficiencies of 2% to 8%.

This work, the first quantitative analysis of high-temperature magnetic refrigeration systems, has led to a better understanding of regenerative magnetic refrigeration systems and of other types of systems in general. It will serve as a guideline for the analysis of various types of MR systems.

Use of Liquids in Heat Engines (P-10)

In the most familiar heat engines – the internal combustion engine, the steam turbine, and the household refrigerator – the working substances undergo some chemical or physical change of state to produce useful work or to pump heat. Many less familiar conventional engines use gaseous working substances in cycles that do not change the state of the substance. We are currently investigating the use of liquids, also without change of state, as working substances in heat engines. A common misconception is that liquids behave much like an idealized hydraulic fluid, with density independent of temperature and pressure. In fact, especially near the critical point, a typical real liquid is somewhat compressible, has a large thermal expansion coefficient (comparable to or larger than that of an ideal gas), and possesses other attractive thermophysical properties. We believe that heat engines using liquid working substances are potentially important in applications involving the transfer of large amounts of heat across small temperature differences (on the order of 30°C); such an application might be pumping heat from ground water into buildings.

To study the use of liquids in heat engines, we built a laboratory Stirling-cycle heat pump in which liquid propylene (C_3H_6) is the working substance. For this engine, an electric motor supplies work for pumping heat from a heat source (an electric heater, for convenience of measurement) at or below room temperature to a heat sink (flowing water) at or above room temperature. The engine can pump large amounts of heat; in Fig. VI-12 we plot the heat pumped across zero temperature

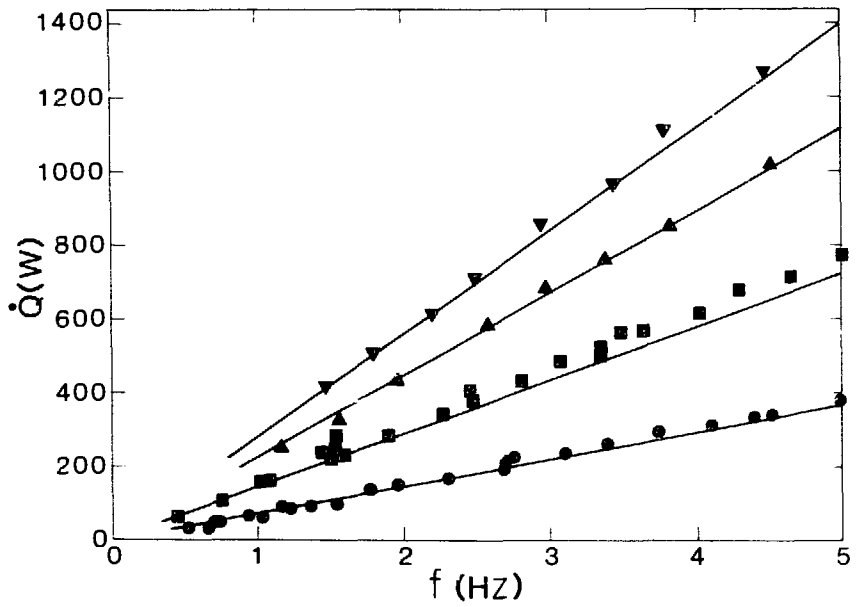

Fig. VI-12. The heat-pumped Q versus crankshaft frequency f is shown for four peak pressure amplitudes: circles, 13 bar; squares, 26 bar; erect triangles, 41 bar; and inverted triangles, 52 bar.

difference versus crankshaft speed for four pressure amplitudes. The points are measured heat flows; the lines, which match the data extremely well, were calculated directly from physical properties of propylene and the geometry of the engine.

One advantage of using a liquid working substance is that liquids have a large heat capacity per unit volume; consequently, the thermal elements (heat exchangers and regenerators) in a liquid engine can be very efficient and compact. Figure VI-13 shows the propylene-to-water heat exchanger developed at Los Alamos. It consists of hundreds of chemically milled, stainless-steel sheets, copper-brazed together. When the system is in operation, propylene flows in and down through one propylene duct, across through the propylene manifolds and channels, and up and out through the other propylene duct. Water flows in and up through one water duct, across through the water manifolds and channels, and down and out through the other water duct. The exchanger is only 4 by 4 by 9 cm and entrains only a few cubic centimeters of propylene, yet it transfers heat between the two fluid streams at a rate of 230 W/°C.

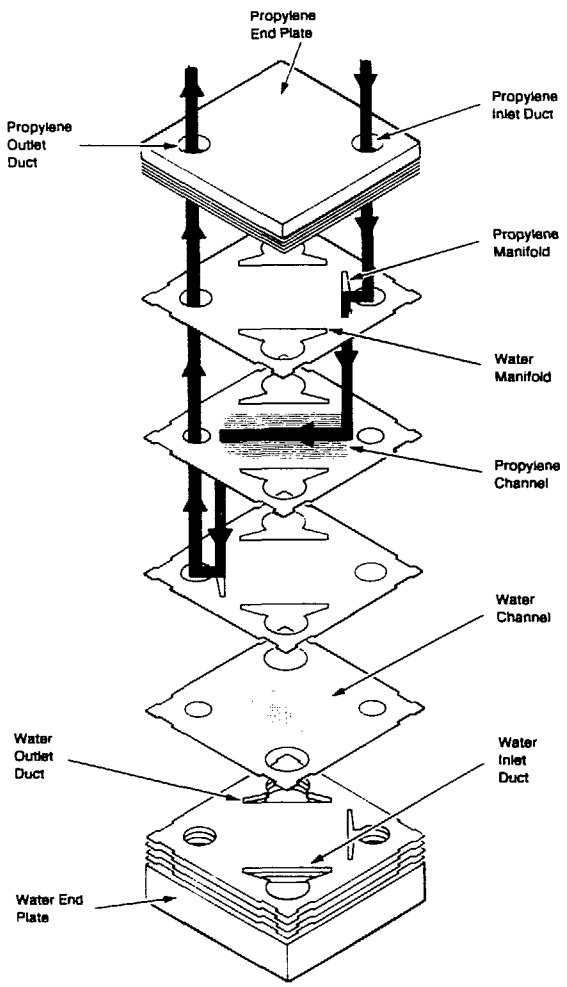

Fig. VI-13. The propylene-to-water heat exchanger is 4 by 4 by 9 cm. A typical dimension in this exploded view is the thickness of the propylene sheets, 50 μm. The arrows indicate one typical path followed by propylene. Water follows a similar path through the water ducts, manifold, and channels.

Another advantage of using a liquid working substance is that the typical liquid is much less compressible than is an ideal gas; as a result, the large pressure amplitudes required for pumping large amounts of heat can be achieved with small piston motions, even for a substantial volume of entrained liquid in the thermal elements. This characteristic allowed us to build our high-power engine with extremely efficient, short-stroke mechanical elements without compromising the size and efficiency of the thermal elements.

We are continuing to measure the efficiency (heat pumped per unit of work input) of the laboratory engine. Although we have only preliminary results, they indicate that the efficiency is usefully high, as we expected, and that engines using liquid working substances may ultimately be of great technological importance.

Liquid-Metal Thermoacoustic Engine (P-10)

We are studying a liquid-metal thermoacoustic engine both theoretically and experimentally. This type of engine promises to produce large quantities of electrical energy from heat, at modest efficiency, with no moving parts except the acoustic oscillations in the liquid metal. It is a new concept in energy conversion. Our objectives are to make a working model and to obtain a thorough understanding of the principles and details of its operation.

A sound wave is usually thought of as consisting of pressure oscillations. Always attendant on the pressure oscillations, however, are temperature oscillations, and the combination produces a rich variety of "thermoacoustic" effects. These effects are so small that they are never noticed in everyday life; nevertheless, under the right circumstances they can be harnessed to produce powerful heat-engine, heat-pumping, and refrigeration devices. In our liquid-metal thermoacoustic engine, heat flow from a high-temperature source to a low-temperature sink amplifies a standing acoustic wave in liquid sodium. This acoustic power is simply converted to electric power by means of a magnetohydrodynamic (MHD) effect at the acoustic oscillation frequency.

We have developed a detailed thermoacoustic theory applicable to this engine and find that a reasonably designed liquid-sodium engine operating between 700°C and 100°C can generate about 60 W/cm^2 of acoustic power at about one-third of Carnot's efficiency. Imperfect efficiency results equally from three sources: the viscosity of the sodium; the nonzero thermal conductivity of the sodium and the metal parts of the engine; and the intrinsic irreversibility characteristic of this kind of engine, caused by an oscillatory diffusion of heat across a temperature difference at the acoustic frequency. Construction of a 3000-W-thermal laboratory-model engine has been completed, and we have exciting preliminary results showing, basically, that the engine works. We have also designed and built a 1-kHz liquid-sodium MHD generator and have completed extensive measurements on it. It is now very well characterized, both experimentally and theoretically. The first generator of its kind, it already converts acoustic power to electric power with 40% efficiency; in addition, we understand the electrode resistance and end effects responsible for nearly all the losses.

Accurate Acoustic Power Measurements and Acoustic Refrigeration (P-10, University of California at San Diego)

We have developed an acoustic driver apparatus that is capable of driving various closed resonant systems containing gases at mean pressures ranging from 1 to 10 bar and at frequencies ranging from 400 to 700 Hz. Maximum acoustic powers attained are in excess of 13 W for systems with appropriate impedance. The driver apparatus has been instrumented and calibrated for the absolute measurement of acoustic power, acoustic impedance, and dynamic pressure, with results giving an absolute acoustic impedance accuracy of $\pm 1\%$ in magnitude and $\pm 1°$ in phase and an absolute acoustic power accuracy of $\pm 3\%$. (Acoustic impedance is the complex ratio of dynamic pressure to

volume velocity, and the volume velocity is the local fluid velocity multiplied by an effective area such as the cross-sectional area of a driven tube. The phase of this complex ratio is then the phase between the local dynamic pressure and velocity.)

We are using this sophisticated driver in an experimental investigation of the efficiency of thermoacoustic refrigerators. Our latest refrigerator apparatus, as opposed to that used in our earlier proof-of-principle experimental tests, is a completely functional refrigerator. Our acoustic driver is the motor, and one-half of the refrigerator efficiency measurement is accomplished by the acoustic power measurement. The other one-half of the efficiency measurement is simply the electrical ohmic heat load on the cold end of the refrigerator. It is our intent not only to measure the efficiency of this particular refrigerator but also to infer the efficiency inherent in refrigerators within this general class.

A modified high-power loudspeaker driver was used for the acoustic motor. This device enabled us to obtain reasonably high acoustic powers as well as simply adjustable frequencies and amplitudes, and it simplified construction. A calibrated dynamic pressure transducer was installed close to the driver piston, and a highly miniaturized accelerometer was mounted on the piston. The accelerometer signal was calibrated as a volume velocity by measurements made on an acoustic load with calculable impedance. The acoustic power was then merely the product of the volume velocity amplitude and the dynamic pressure amplitude and a factor for phases other than zero.

The driver apparatus and power measurement method is a very effective means of determining the efficiency of the acoustic refrigerator, and this in turn is a valuable check on our theoretical understanding of thermoacoustics. Also, acoustic impedance measurement is of great interest to the acoustics community, and our method offers advantages over classical methods in common use. The accuracy of our method could be rather easily improved, if necessary.

Resonant Reciprocity Calibration of an Ultra-Compliant Transducer (P-10, Naval Postgraduate School)

It is well known that the turns ratio of an ordinary transformer can be obtained by making measurements of voltage and current at two terminals of the transformer when a known electrical impedance is connected to the other two terminals, as in Fig. VI-14a. The same principles can be applied to a reversible electroacoustic transducer, as shown schematically in Fig. VI-14b, to obtain an *absolute* calibration of the transducer. Since the 1940s this technique, called reciprocity calibration, has been the primary method used for calibrating microphones, loudspeakers, and other acoustic transducers. If the acoustic impedance, Z_{ac}, of the acoustic load on the transducer can be calculated and if various other conditions are met, one can obtain the transducer sensitivity, in V/bar or V/(cm/s), for example, from measurements of electric voltage and current only. But conventional reciprocity calibrations have required that the transducer be noncompliant; that is, the transducer must be so stiff that it does not move appreciably in response to the acoustic wave.

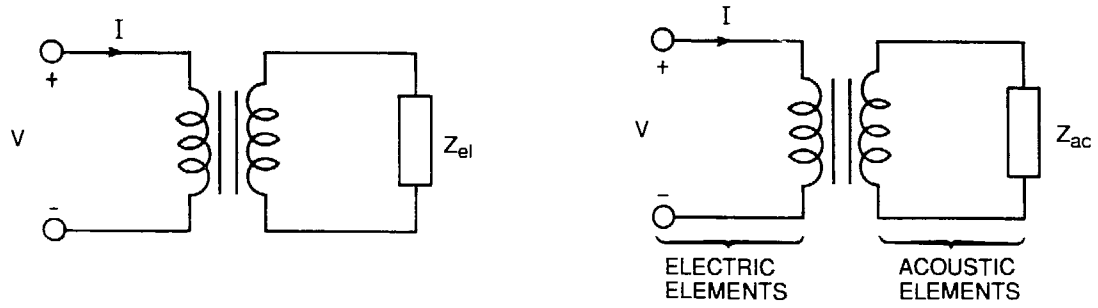

Fig. VI-14. (a) An ordinary transformer with electrical load Z_{el}; the turns ratio N is given by $N_2 = VZ_{el}/I$. (b) A reversible electroacoustic transducer with acoustic load Z_{ac}; the transducer sensitivity β is given by $\beta_2 = VZ_{ac}/I$.

Our contribution in this work is to show how to apply reciprocity calibration techniques to an ultracompliant transducer, one that is so flexible and lightweight that it does not appreciably perturb the oscillations of the acoustic medium. We have demonstrated the success of our ultracompliant reciprocity calibration theory and procedure by applying the technique to a MHD transducer we built for use in mercury or salt water. The MHD transducer is simple enough that we can use it to compare our reciprocity calibration with another absolute calibration technique. We find excellent agreement between the two.

We began this work because we needed to calibrate the MHD acoustic-to-electric power converter we made for our liquid-sodium thermoacoustic engine. But the reciprocity technique we developed will enable us to perform simple, extremely accurate calibrations of technologically important transducers, such as hydrophones and accelerometers, as well as MHD transducers.

FACILITIES DEVELOPMENT—ION-BEAM MATERIALS LABORATORY (P-10, CMS, CLS-2, E-11, INC-7, MST-7)

The Ion-Beam Materials Laboratory (IBML) is devoted to the characterization and modification of surfaces through the use of ion beams. When completed, the IBML will provide a wide range of capabilities, which will be readily available to both Laboratory and outside users, for surface science research. At present, the IBML is under construction, and only a 200-kV ion implanter is operational. Delivery of the 3-MV tandem electrostatic accelerator is expected later in 1986. The Center for Materials Science (CMS), Group P-10 (Condensed Matter and Thermal Physics Group), and materials science researchers from many other Laboratory divisions have contributed to the construction of the IBML. A steering committee composed of selected research staff from the Laboratory has greatly aided this effort.

Construction of the IBML has proceeded through a number of stages: preparing and modifying the laboratory area in the basement of SM-34, placing the implanter in operation, planning and implementing improvements to the implanter, and designing and constructing the various instruments that will make up the laboratory. Since we acquired the implanter, we have made several modifications to the research end-station so that hot (to 500°C) and cold (liquid-N_2 temperatures) implants can be performed. More recently, we installed a vaporizer source so that many metals can be used as source materials, greatly enhancing the variety of ions available for implantation.

The planned IBML instruments and their status are described in the following paragraphs.

General Purpose—National Security Programs (NSP) Chamber. The NSP chamber will provide the general user with both Rutherford backscattering (RBS) and particle-induced x-ray emission (PIXE) capabilities. High-energy implants with beams from the tandem will also be available. The chamber and detector systems are on order. The chamber should be ready when the tandem arrives. Groups E-11 and P-10 are responsible for this system.

Ultrahigh-Vacuum, Medium-Energy Surface-Science Chamber. This system will provide sophisticated surface modification and analysis under ultrahigh-vacuum conditions. Analysis techniques such as Auger and electron diffraction will be available. This chamber will be connected to both the implanter and the tandem accelerator for increased versatility. Groups CLS-2 and E-11 are responsible for this system.

Surface Modification Chamber. The surface modification chamber will be the primary research station for the implanter. Implantation and ion-beam mixing experiments will be the primary types of research performed here. This chamber is also connected to the tandem so that a quick analysis of the modified surface can be made. Group MST-7 has the responsibility for this system.

Nuclear Microprobe. This instrument is currently located at the Ion-Beam Facility (IBF). It will be moved to the IBML when the tandem accelerator is operational. The microprobe is used for surface analyses where small areas (linear dimension less than 10 μm) are of interest. Groups INC-7 and E-11 are responsible for this system.

Radiation Damage Chamber. This chamber was formerly located at the IBF and has recently been moved into the IBML. It will be the first external chamber to be attached to the implanter and will be used primarily for the modification of powders by radiation damage. Group MST-7 is responsible for this chamber.

Many research programs for which the IBML will be used are currently being carried out at the IBF. The programs for which the implanter will be used are relatively new. Most of these are ion-beam mixing experiments of metal-ceramic and metal-carbon interfaces, which are being conducted by Group MST-7. Other experiments including the implantation (or mixing) of Mössbauer nuclei into surfaces and the modification of polymers are being developed.

VII. BIOPHYSICS

CURRENT ROLE OF THE PHYSICS DIVISION IN BIOPHYSICS

Expertise that has evolved from other parts of the Physics Division currently supports a number of significant research projects in important areas of biophysics. In particular, techniques and experience derived from nuclear physics and solid-state or low-temperature physics are being applied to biological problems. These efforts are often carried out in collaboration with other divisions within the Laboratory—most notably the Life Sciences Division—and with experts outside the Laboratory.

A subject of increasing interest, and of special importance to the widely publicized human genome project, is the analysis of protein expression by means of two-dimensional gel studies. Here, we are applying nuclear and weapons physics techniques—developed within the Division for determining, with high spatial resolution, the source and strength of radioactivity—to the analysis of proteins in which radiolabeled amino acids have been incorporated. The results are also considered in relation to the effects of low-level radiation exposure on humans and other organisms, but they have significantly broader potential applications.

Similarly, we are applying nuclear physics data-acquisition methods to the study of magnetic fields from the brain—a technique called magnetoencephalography (MEG). With MEG, and our expertise in low-temperature physics and other areas, we are at the forefront in our understanding of the functioning of the human brain.

In another study that has emanated from ongoing programs within the Physics Division, we are using neutron scattering to explore the structure of biological molecules. This program takes advantage of the vast amount of expertise on neutron scattering available here and of the Laboratory's neutron detectors and the LANSCE facility, a combination that may well make Los Alamos the country's leading laboratory in this field of research. Details of this project are not reported here, but the development of appropriate instrumentation (still under way) is described in Chapter V.

ANALYSIS OF PROTEINS BY DIRECT COUNTING OF β-RAYS IN TWO-DIMENSIONAL GELS AND APPLICATION TO LOW-LEVEL RADIATION EFFECTS (P-DO, Eleanor Roosevelt Institute for Cancer Research)

Protein Analysis

Proteins play such a fundamental role in every living process that the knowledge of which proteins given cells produce and how the proteins are regulated is essential to an understanding of what goes on in living organisms. To this end, two-dimensional electrophoresis has become an important tool in molecular biology. A large fraction of the thousands of proteins each cell produces is physically separated into an array of spots in a thin gel (2-D gel) over an area—in our case, some 16 by 19 cm^2—according to isoelectric point, or pH, in the horizontal dimension and to molecular weight in the vertical dimension. The amount of protein in each spot can be determined from a measurement of its radioactivity, obtained by using radiolabeled amino acids in the medium used to grow the cells. Conventionally, the readout is provided by autoradiography, with an optical densitometer supplying the quantitative information. Our method differs in that the β-rays are counted directly.

Our measurement is linear, and it is more precise and better adapted to automated analysis by computer than are previously used techniques.

The β-rays from the gel are counted directly with a position-sensitive multiwire proportional chamber. A strong magnetic field is used to keep the β-rays from spreading away from their point of origin. The β-rays from the ^{14}C or ^{35}S used in the radiolabel are of such low energy that they follow the magnetic lines of force in tight spirals, keeping the displacement from the point of origin to within 400 μm. Figure VII-1 is a schematic representation showing the helical path taken by the β-rays as they emerge from the gel and ionize the gas within the chamber. The figure also shows how the two-dimensional readout is obtained. The result is a "spot-graph" of the proteins found in the gel. The amount of protein on a given spot is indicated by the blackness of the spot. The location of the spot is determined according to pH (values decreasing with x) and molecular weight (values increasing with y). The spot-graphs are useful for visualizing the separation and checking the peak-finding algorithms against autoradiographs. For each protein, the actual values of pH, molecular weight, and amount are recorded as tables.

It is well known that many cell lines cease to divide when a monolayer has been formed. This effect is an inhibition by contact, a density-dependent form of regulation. A typical limiting value is 10^6 cells on a 6-cm culture dish. To discover which proteins are involved in this regulatory process, we attempted to determine the point at which cell density causes an increase or decrease in each protein as a percentage of total protein. To this end, we measured gels prepared from cultures of 2×10^4, 2×10^5, and 2×10^6 cells, measuring four gels in each case to obtain a more reliable result.

The increase in cell density from 2×10^4 to 2×10^5 had only a small effect on protein abundance, but for the increase to 2×10^6, the results were striking. At the 2×10^6 level, 37 proteins were diminished and 22 were increased by a factor of 2 or more; at the 2×10^5 level, only 8 proteins showed such a reduction and 4 such an increase. Clearly, there are many proteins whose abundance is strongly modulated by cell-density regulation, and we can specify their molecular weights and isoelectric points. Finding out more about their structure and function will require additional research.

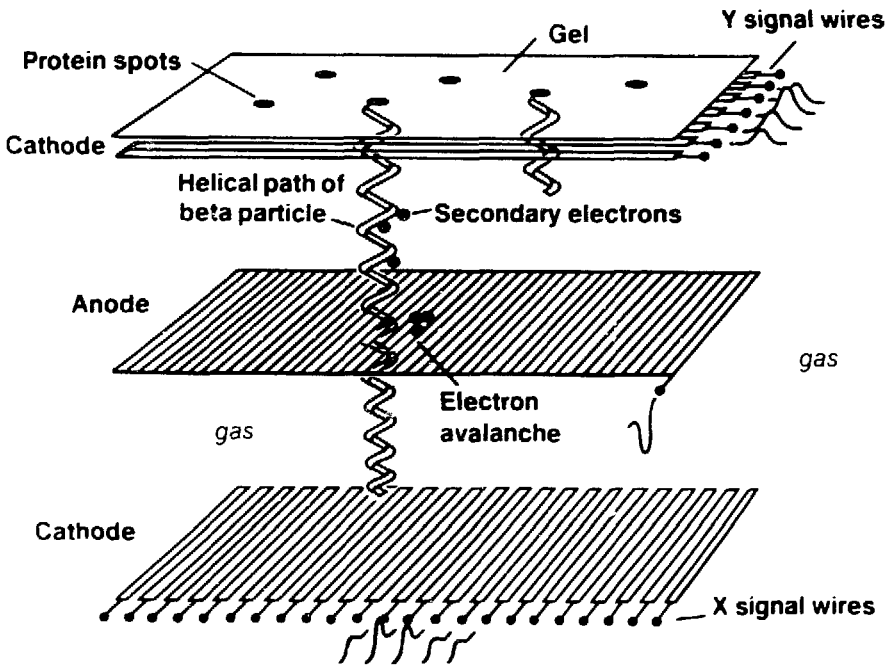

Fig. VII-1. Schematic representation of method used to count β-ray position and number from radioisotope-tagged proteins deposited on a 2-D gel in a multiwire proportional chamber

Effects of Radiation at Low Levels

Although a great deal is known about the effects of radiation, most of our information is about what happens at high levels—100 rad or more. At such levels a measurable fraction of organisms or their cells die, and it is practical to measure survival curves for all manner of cells and organisms by different kinds of radiation. Extrapolation from high to low radiation levels leads us to believe that exposures of less than that required to produce the acute radiation syndrome may still result in genetic effects or in effects on growth and development, on the incidence of neoplasm, and on the life span. At still lower levels, 10 rad or less, what happens is not so clear, and it is difficult to say how dangerous low-level radiation is.

In the United States, the estimated annual dose equivalent from all types of natural radiation (cosmic rays plus terrestrial radiation plus internal radionuclides) is about 125 mrem. It is unlikely to be less than 100 mrem for any individual and unlikely to be more than 400 mrem for any significant number of people. This estimate establishes the level of radiation at which man has been living throughout his history. The question is, how harmful are additional amounts of radiation exposure and what are the long-term effects of low levels of radiation.

The need for better data was emphasized recently by the accident at Chernobyl, where the fallout of radioactive fission products covered vast areas of crop and pasture lands in many countries. In the absence of reliable data, it was difficult to assess the danger and to determine what food and what cattle should be withheld from the market. The public was greatly concerned about the possible health effects of consuming contaminated food and, in the end, the financial loss due to the withholding of agricultural produce from the market was enormous.

The proper disposal of low-level radioactive wastes (many of them by-products of nuclear medicine) is another major problem of our time. Until we have more reliable information about the effects of low-level radiation, it will be difficult to decide at what point advantage outweighs risk.

The protein-analysis technique we have developed in the Physics Division shows promise as a new and more sensitive means of measuring radiation effects. Following a procedure similar to the one we used to demonstrate cell-density effects, we propose to measure the influence of radiation on protein production by irradiating cells over the range from high to low levels. Each protein will serve as a marker for the effect of the radiation on the production of that protein. Because we can measure the effect on several hundred proteins at the same time, our measurement is correspondingly more sensitive than are single-target experiments. Some proteins will be more sensitive to the radiation, others less; but because we are able to distinguish one protein from another, we should be able to develop a more reliable basis for making the extrapolation from high to low levels of radiation. A pilot study carried out by Puck and his collaborators at the Eleanor Roosevelt Institute has already shown that, according to the behavior of one marker, the effects of low-level radiation increase more rapidly than linearly and are much greater than linear extrapolation from high levels has led us to believe.

NEUROMAGNETOMETRY (P-DO, LS-7)

Much of the neuroscience research at Los Alamos is focused on the processing of information and the sensory control performed by the central nervous system. Our purpose is not only to increase our basic understanding of the relevant neural processes but also to identify and test potential cognitive strategies and neural "signatures" that would enable us to enhance human performance. Although traditional animal experiments may be employed for some aspects of this work, the ability to examine noninvasively the neural basis of sensory and cognitive processes in human subjects is very important. To this end, we have developed advanced neuromagnetometry (NM) systems.

Neuromagnetometry enables us to monitor and map the weak magnetic fields associated with the electrical activity of neurons in the brain. NM does not require the administration of radionuclides, as does positron emission tomography (PET scanning). Unlike electroencephalography (EEG), NM does not require sensor contact with the subject, nor is it sensitive to the electrical properties of

the tissue intervening between the signal source and the magnetic sensor. Because of the well-defined relationship between an observed magnetic field and its source, it is possible to localize the field source precisely. Our current practical resolution is better than 1 cm, and we may eventually achieve a resolution of better than 0.1 cm.

We have completed a detailed neural source mapping study of the auditory-evoked responses elicited by a long tone-burst stimulus. Measurements were carried out on four human subjects in a magnetically shielded room. We used auditory stimuli of two different frequencies, 250 and 2500 Hz, presented binaurally by means of standard plastic airline headsets. The magnetic field was measured with a second-order gradiometer with a 2.4-cm diameter and a 3.2-cm baseline between adjacent coils coupled to a dc superconducting quantum interference device (SQUID). The superconducting circuitry was contained in a superinsulated fiberglass Dewar oriented so that the magnetic field perpendicular to the scalp was monitored by the gradiometer. The output voltage from the SQUID electronics was applied to a bandpass filter with cutoffs at 10.01 and 50 Hz; subsequently, averaged waveforms were digitally filtered from 0 to 25 Hz. Extensive field maps were obtained over the auditory cortex region in each of the subjects. The latency and amplitude of the evoked response for each tone were measured at about 40 positions. Magnetic responses were averaged on-line for approximately 50 trials per stimulus, with at least two replications to achieve satisfactory signal-to-noise ratios.

In all subjects, good-quality auditory evoked fields (AEFs) were obtained. The amplitudes of the P1m (first positive magnetic response), N1m (first negative magnetic response), P2m, and SF (sustained field occurring throughout the duration of the stimulus) had two clear extrema of opposite polarity located at the estimated ends of the Sylvian fissure (auditory cortex). Figure VII-2 illustrates the AEF waveform obtained from the N1m extrema of one subject. To determine the source location of the cortically evoked neural activity, we used a current dipole in a conducting sphere as a theoretical model. The five parameters determining the dipole were then adjusted by computer until the sum of the squared deviations between the observed and theoretical fields was minimized. It was found that these four major components (P1m, N1m, P2m, SF) evoked by a tone burst can be attributed to equivalent dipole sources whose lateral positions for a given subject are tightly grouped within a small area, amounting in this case to a circle with a radius of less than 2 cm. The span of distance for source positions is consistent with the lateral extent of the human primary auditory cortex. To elicit functional differences in sources, tones of 250 and 2500 Hz were presented. For our four subjects, the positions of the N1m and P2m were invariant with tone frequency. However, the positions of the P1m and SF sources showed clear shifts with increasing frequency. These results demonstrate the feasibility of using the NM technique to isolate functional differences in cortical organization.

Studies in progress are aimed at defining the neural basis of selective attentional enhancement of stimulus-evoked activity. The N1m component is increased in amplitude when attention is directed to the sensory channel in which the stimulus occurs. This enhancement of the N1m appears to be caused by the superimposition of a separate negative process, termed the negative displacement (Nd). The onset and duration of the Nd depends on the complexity of the perceptual processing that is required by the task and upon the time pressure under which such processing is performed. Using the NM technique, we are examining the distribution of neural sources for these negative processes to determine the locus of cortical activation when selective attention is recruited for achievement of a task. An understanding of the neural basis of this cognitive activity is important not only in a basic neuroscience context but also in the application to empirical problems, such as characterizing brain states underlying "peak performance." Such considerations could have an impact on personnel selection and training strategies.

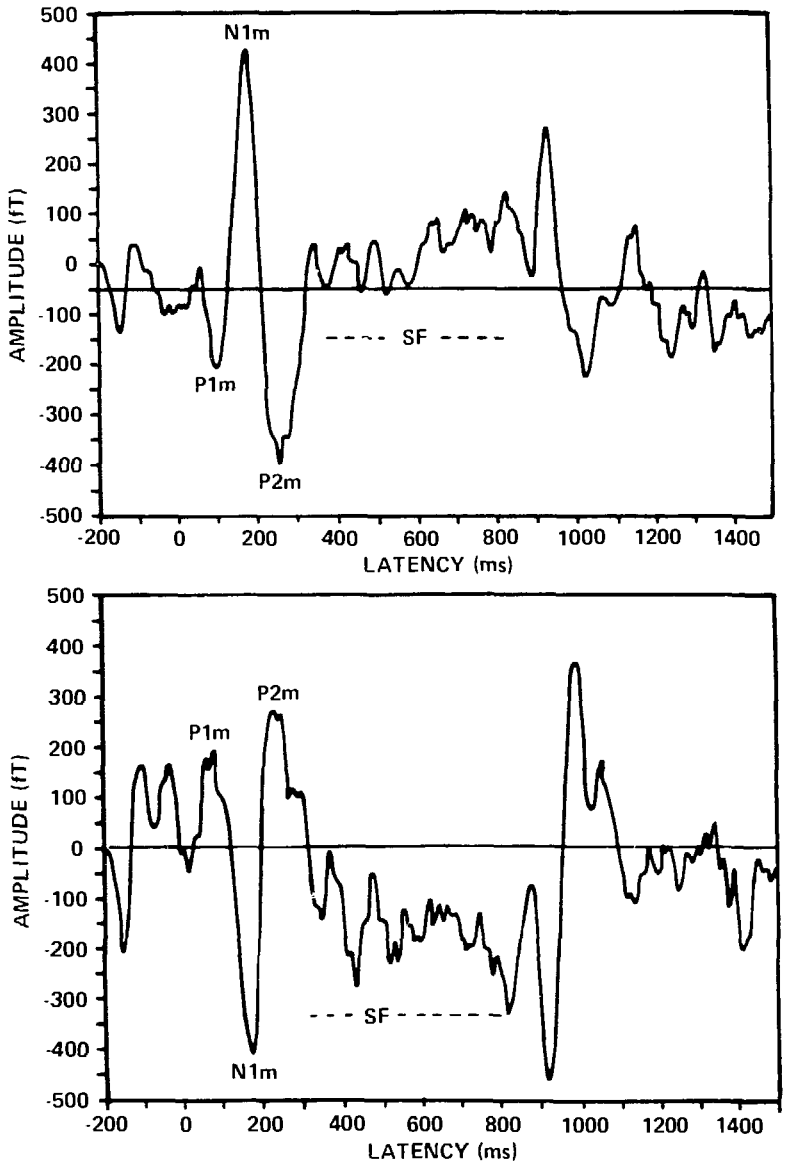

Fig. VII-2. Auditory evoked waveform obtained from the N1m extrema of one subject (SW) to the 250-Hz tone. The top panel represents activity recorded at the anterior extrema (close to C4); the bottom panel shows activity recorded at the parietal end of the Sylvian fissure. Note the reversal in polarity of each of the elicited components P1m, N1m, P2m, and the SF at the two opposite sides of the Sylvian fissure.

VIII. PHYSICS DIVISION DATA, FY86

PHYSICS DIVISION GROUPS, PRINCIPAL MISSIONS AND ACTIVITIES, BUDGETS, AND SIZES

P-1—Experimental High-Energy-Density Physics

Allocation:	$4.2 million
Staff Members:	14.7 FTE
Graded Employees:	13.0 FTE

P-2—Basic Applied Accelerator-Based Nuclear and Particle Physics

Allocation:	$2.7 million
Staff Members:	11.7 FTE
Graded Employees:	4.5 FTE

P-3—Basic and Applied Research in Nuclear and Particle Physics; Support of Weapons Test Program

Allocation:	$6.0 million
Staff Members:	20.0 FTE
Graded Employees:	14.2 FTE

P-4—Inertial Confinement Fusion Experiments

Allocation:	$4.2 million
Staff Members:	8.7 FTE
Graded Employees:	13.4 FTE

P-5—Free-Electron Laser and Inertial Confinement Fusion Optical Systems

Allocation:	$6.4 million
Staff Members:	14.0 FTE
Graded Employees:	11.7 FTE

P-7—Pulsed Power Systems Design and Research

Allocation:	$3.7 million
Staff Members:	10.4 FTE
Graded Employees:	19.5 FTE

P-8—Neutron-Scattering Research at WNR/PSR/LANSCE

Allocation:	$3.1 million
Staff Members:	9.6 FTE
Graded Employees:	10.6 FTE

P-9—WNR/PSR and Van de Graaff Operations

Allocation:	$4.0 million
Staff Members:	13.2 FTE
Graded Employees:	16.5 FTE

P-10—Condensed-Matter and Thermal Physics Research

Allocation:	$2.8 million
Staff Members:	10.9 FTE
Graded Employees:	6.2 FTE

P-12—Mechanical Engineering

Allocation:	$3.5 million
Staff Members:	8.4 FTE
Graded Employees:	13.6 FTE

P-14—Weapons Physics with an Emphasis on Electromagnetic Measurements

Allocation:	$9.1 million
Staff Members:	28.0 FTE
Graded Employees:	27.0 FTE

P-15—Weapons Physics Experiments; Basic and Applied Atomic and Nuclear Physics Research and Development

Allocation:	$9.3 million
Staff Members:	30.5 FTE
Graded Employees:	24.5 FTE

P-16—Laser Physics and Applications

Allocation:	$3.1 million
Staff Members:	9.5 FTE
Graded Employees:	8.6 FTE

P-DIVISION FUNDING FY-86

($K)

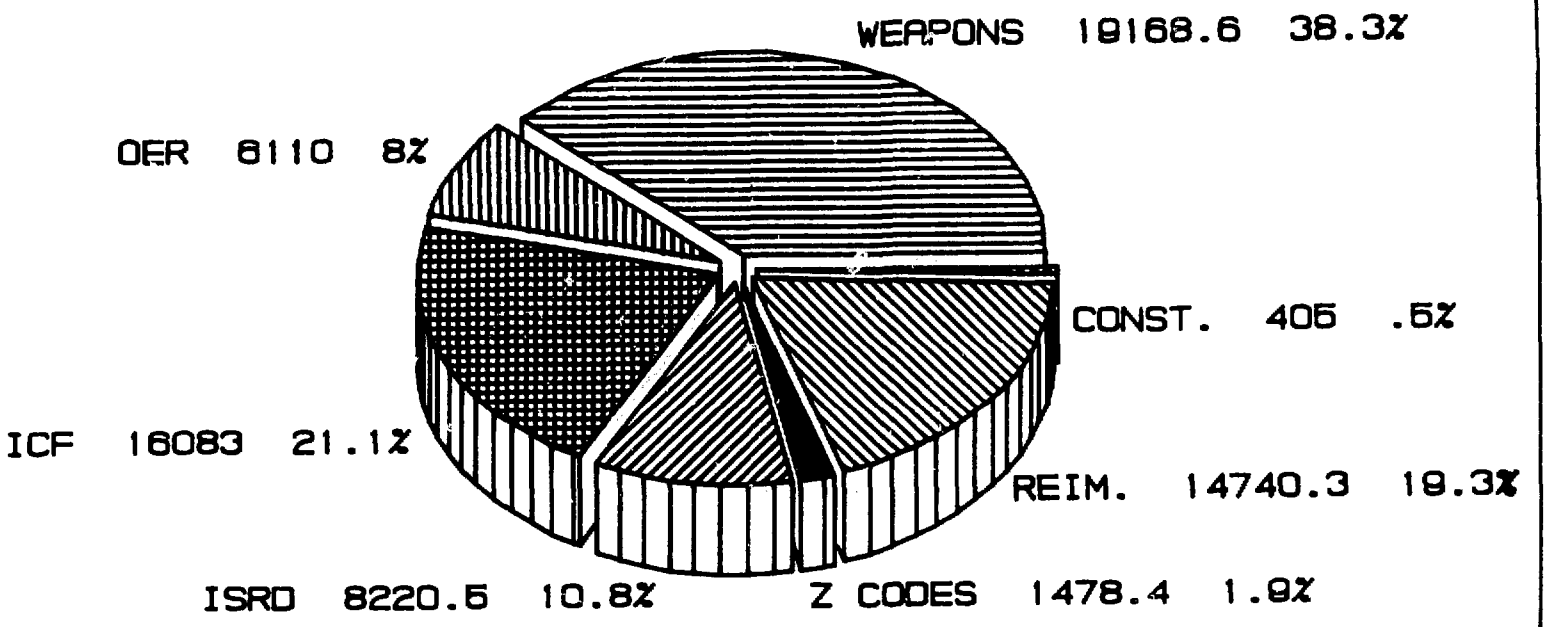

PUBLICATIONS, TALKS, AND PATENTS*

JOURNAL ARTICLES

B. Aas, M. V. Hynes, A. Picklesimer, P. C. Tandy, and R. M. Thaler, "Spin Observables in Elastic Proton Scattering," *Phys. Rev. C* **32**, 1985, pp. 231-237.

S. F. Agnew, B. I. Swanson, L. H. Jones, and R. L. Mills, "Disproportionation of Nitric Oxide at High Pressure," *J. Chem. Phys.* **89**, 1985, pp. 1678-1682.

F. Ajzenberg-Selove, R. E. Brown, E. R. Flynn, and J. W. Sunier, "Experimental Location of Gamow-Teller Strength for Astrophysical Calculations in the Region of A = 54-58," *Phys. Rev. C* **30**, 1984, pp. 1850-1854.

F. Ajzenberg-Selove, R. E. Brown, E. R. Flynn, and J. W. Sunier, "(t,^{3}He) Reactions on ^{56}Fe, ^{58}Fe, and ^{58}Ni," *Phys. Rev. C* **31**, 1985, pp. 777-786.

F. Ajzenberg-Selove, R. E. Brown, E. R. Flynn, and J. W. Sunier, "(t,^{3}He) Reactions on ^{40,42,44}Ca, ^{46,48,50}Ti, ^{54}Cr, and ^{54}Fe," *Phys. Rev. C* **32**, 1985, pp. 756-780.

D. M. Alde, F. Binon, D. Boget, C. Bricman, S. V. Donskov, G. Dromby, J. Defournaud, P. Duteil, M. Gouanere, V. A. Kachanov, D. B. Kakauridze, G. V. Khaustov, E. A. Knapp, C. D. Lac, J. P. Lagnaux, A. A. Lednev, D. Michotte, "Acquisition System for the Hodoscopic Spectrometer GAMS-4000," *Nucl. Instrum. & Methods Phys. Res. Sect. A* (Netherlands) **A240**, 1985, pp. 343-350.

D. M. Alde, F. Binon, C. Bricman, S. V. Donskov, P. Duteil, M. Gouanere, A. V. Inyakin, D. B. Kakauridze, V. A. Kachanov, G. V. Khaustov, A. V. Kulik, J. P. Lagnaux, A. A. Lednev, V. A. Maisheev, Yu. M. Melnik, Yu. V. Rodnov, S. A. Sadovsky, P. M. Shagin, D. Sillou, A. V. Singavsky, J. P. Stroot, V. P. Sugonyaev, "Neutral Decays of the η-Meson," *Z. Phys. C* (Germany) **25**, 1984, pp. 225-229.

D. M. Alde, F. Binon, C. Bricman, S. V. Donskov, J. Dufournaud, P. Duteil, M. Gouanere, A. V. Inyakin, V. A. Kachanov, D. B. Kakauridze, G. V. Khaustov, E. A. Knapp, A. V. Kulik, C. D. Lac, J. P. Lagnaux, A. A. Lednev, Y. V. Mikhailov, T. Mouthuy, V. F. Obraztsov, J. P. Peigneux, A. Possoz, Y. D. Prokashkin, Y. V. Rodnov, S. A. Sadovsky, P. M. Shagin, D. Sillou, A. V. Singovsky, J. P. Stroot, V. P. Sugonyaev, "Production of G(1590) and Other Mesons Decaying into Eta Pairs by 100 GeV/$c\pi^-$ on Protons," *Nucl. Phys. B, Part. Phys.* (Netherlands) **B269**, 1986, pp. 485-508.

J. P. Aldridge, E. G. Brock, H. Filip, K. Fox, H. W. Galbraith, R. F. Holland, K. C. Kim, B. J. Krohn, D. W. Magnuson, W. B. Maier II, R. S. McDowell, C. W. Patterson, W. B. Person, D. F. Smith, and G. K. Werner, "Measurement and Analysis of the Infrared-Active Stretching Fundamental (NU 3) of Uranium Hexaflouride," *J. Chem. Phys.* **83**, 1985, pp. 34-37.

R. W. Alkire, A. C. Larson, and P. J. Vergamini, "The Structures of Trithallium Tetraselenophosphate and Trithallium Tetrathioarsenate at 65 K," *Acta Crystallogr. Sect. C: Cryst. Struct. Commun.* **41**, 1985, pp. 1709-1714.

R. W. Alkire, A. C. Larson, P. J. Vergamini, J. E. Schirber, and B. Morosin, "High-Pressure Single-Crystal Neutron Diffraction (to 20 kbar) Using a Pulsed Source - Preliminary Investigation of Ti_3PSe_4," *J. Appl. Crystallogr.* **18**, 1985, pp. 145-149.

R. C. Allen, V. Bharadwaz, G. A. Brooks, H. H. Chen, P. J. Doe, R. Hausammann, W. P. Lee, H. H. Mahler, M. E. Potter, A. M. Rushton, K. C. Wang, T. J. Bowles, R. L. Burman, R. D. Carlini, D. R. F. Cochran, J. S. Frank, E. Piasetzky, V. D. Sandberg, D. A. Krakauer, and R. L. Talaga,

* Names of Physics Division authors underlined. List includes only unclassified material.

"First Observation and Cross Section Measurement of $\nu_e + e^- \rightarrow \nu_e + e^-$," *Phys. Rev. Lett.* **55**, 1985, pp. 2401 2404.

J. Anandan, "Gauge Fields, Quantum Interference and Holonomy Transformations," *Phys. Rev. D* **33**, April 1986, pp. 2280 2287.

H. L. Anderson, "Scientific Uses of the Maniac," *J. Stat. Phys.* **43**, 1986, pp. 731 738.

E. J. Ansaldo, D. R. Noakes, J. H. Brewer, R. Keitel, D. R. Harshman, M. Senba, C.-Y. Huang and B. V. B. Sarkissian, "Study of the Hybrid State of Y_9Co_7 ($2.0 < T < 6K$) by Means of Zero-Field Muon Spin Relaxation," *Sol. Stat. Commun.* **55**, 1985, p. 193.

G. F. Auchampaugh, G. de Saussure, D. K. Olsen, R. W. Ingle, R. B. Perez, and R. L. Macklin, "Resolution of the Nature of the Coupling in Subthreshold Fission in $^{238}U + n$," *Phys. Rev. C* **33**, 1986, pp. 125 129.

N. Auerbach, A. S. Goldhaber, M. B. Johnson, L. D. Miller, A. Picklesimer, "Probing for DIRAC Vacuum Structure in Nuclei," *Phys. Lett.* **182B**, 1986, pp. 221 225.

J. N. Bahcall, B. T. Cleveland, R. Davis, Jr., and J. K. Rowley, "Chlorine and Gallium Solar Neutrino Experiments," *Astrophys. J. Lett. Ed.* **292**, 1985, pp. 79 82.

G. C. Baldwin and M. S. Feld, "Kinetics of Nuclear Super-Radiance," *J. Appl. Phys.* **59** (11), 1986, pp. 3665 3671.

G. C. Baldwin, M. S. Feld, J. P. Hannon, T. Hutton, and G. T. Trammell, "Mössbauer/Borrmann Super-Radiance," *J. Phys.* **47**, pp. C-6-229 308.

R. J. Bartlett, D. R. Kania, W. J. Trela, E. Kallne, P. Lee, and E. Spiller, "Performance of Multilayer Dispersion Elements from 80 to 500 eV," *Opt. Eng.* **23**, 1985, p. 667.

R. J. Bartlett, W. J. Trela, D. R. Kania, M. Y. Hockaday, T. Barbee, and P. Lee, "Soft X-Ray Measurements of Solid Fabry-Perot Etalons," *Opt. Commun.* **55**, 1985, pp. 229 234.

T. Bergeman, C. Harvey, K. B. Butterfield, H. C. Bryant, D. A. Clark, P. A. M. Gram, D. W. MacArthur, M. Davis, J. B. Donahue, J. Dayton, and W. W. Smith, "Shape Resonances in the Hydrogen Stark Effect in Fields Up to 3 MV/cm," *Phys. Rev. Lett.* **53**, 1984, pp. 775 778.

J. Birchall, W. T. H. van Oers, J. W. Watson, H. E. Conzett, R. M. Larimer, B. Leemann, E. J. Stephenson, P. Von Rossen, and R. E. Brown, "Analyzing Power Measurements for $^3He(\vec{p}, p)^3He$ Elastic Scattering Between 20 and 50 MeV," *Phys. Rev. C* **29**, 1984, pp. 2009 2012.

R. L. Blake, R. D. Cowan, H. Felthauser, E. E. Fenimore, M. P. Hockaday, F. Bely-Dubau, R. Faucher, and L. Steenman-Clark, "Analysis of Magnesium XI Profiles from Solar Active Regions," *Astrophys. J.* **282**, July 1984, pp. 784 792.

T. J. Bowles, J. D. Moses, J. Sunier, R. E. Brown, P. Lisowski, W. Mampe, and P. Liaud, "Time Reversal Invariance in Polarized Neutron Beta Decay," *J. Phys. Colloq.* (France) **45**, March 1984, pp. 27 30.

P. S. Bowling, L. Burczyk, R. D. Dingler, and R. B. Shurter, "Aurora Inertial Confinement Fusion Laser Control and Data Acquisition System," *Fusion Technol.*, May 1987.

R. D. Bolton, J. D. Bowman, M. D. Cooper, J. S. Frank, A. L. Hallin, P. Heusi, C. M. Hoffman, G. E. Hogan, F. G. Mariam, H. S. Matis, R. E. Mischke, D. E. Nagle, L. Piilonen, V. D. Sandberg, G. H. Sanders, U. Sennhauser, R. D. Werbeck, R. A. Williams, S. L. Wilson, R. Hofstadter, E. B. Hughes, M. W. Ritter, D. Grosnick, S. C. Wright, V. L. Highland, and J. McDonough, "Search for the Decay $\mu^+ \rightarrow e^+\gamma$," *Phys. Rev. Lett.* **56**, 1986, pp. 2461 2464.

H. C. Britt, D. C. Hoffman, J. van der Plicht, J. B. Wilhelmy, E. Cheifetz, R. J. Dupzyk, and R. W. Lougheed, "Fission of $^{255,256}Es$, $^{255,256,257}Fm$ and ^{258}Md at Moderate Excitation Energies," *Phys. Rev. C* **30**, 1984, pp. 559 565.

R. E. Brown, R. A. Hardekopf, N. Jarmie, F. D. Correll, J. M. Lambert, P. A. Treado, I. Slaus, P. Schwandt, W. W. Jacobs, H. O. Meyer, E. J. Stephenson, J. Q. Yang, W. T. H. van Oers, P. Doleschall, and J. Tjon, "Polarization in Three-Nucleon Breakup Experiment and Theory," *Nucl. Instrum. & Methods Phys. Res. Sect. B* **10-11**, 1985, pp 356 360.

W. K. Brown, "Approximate Rotation Curve Solutions for the Evolution of a Viscous Protogalactic Disk," *Astrophys. Space Sci.* **111**, 1985, pp. 139 155.

W. K. Brown, "Comparison of a Theory of Sequential Fragmentation with the Initial Mass Function of Stars," *Astrophys. Space Sci.* **122**, 1986, pp. 287 298.

W. K. Brown, "Flat Rotation Curves According to the Fragmentation/Shear Flow Model of Galaxy Formation," *Astrophys. Space Sci.* **105**, 1984, pp. 109–130.

W. K. Brown, "High Explosive Simulations of Supernovae," accepted by *Astrophys. Space Sci.*, Los Alamos National Laboratory document LA-UR-86-1876.

W. K. Brown, "An Indicator of Galactic Violence," *Astrophys. Space Sci.* **126**, 1986, pp. 255–267.

W. K. Brown, "Model of Protogalactic Cloud Collapse," *Astrophys. Space Sci.* **113**, 1985, pp. 143–153.

W. K. Brown, "Possible Mass Distributions in the Solar Nebulae of Other Solar Systems," *Earth, Moon and Planets* **37**, 1987, pp. 225–239.

W. K. Brown, "Possible Protogalactic Role of Eddies in a Turbulent Early Universe," *Astrophys. Space Sci.* **115**, 1985, pp. 257–265.

W. K. Brown, "Universal Fragmentation," *Astrophys. Space Sci.* **121**, 1986, pp. 351–355.

W. K. Brown and L. A. Gritzo, "The Supernova Fragmentation Model of Solar System Formation," *Astrophys. Space Sci.* **123**, 1986, pp. 161–181.

R. M. Brugger and P. A. Seeger, "Mass Spectrometry of Light Elements by eV Neutron Spectroscopy," *Nucl. Instrum. & Methods Phys. Res. Sect. A* **236**, 1985, pp. 423–425.

D. S. Buchanan, G. W. Swift, and J. C. Wheatley, "Velocity of Propagation of the ^{3}He A-B Interface in Hypercooled ^{3}He A," *Phys. Rev. Lett.* **57**, 1986, pp. 341–344.

S. Buchsbaum, R. L. Mills, and D. Schiferl, "Phase Diagram of N_2 Determined by Raman Spectroscopy from 5 to 300 K at Pressures to 52 GPa," *J. Phys. Chem.* **88**, 1984, pp. 2522–2525.

D. G. Burke, W. F. Davidson, J. A. Cizewski, R. E. Brown, E. R. Flynn, and J. W. Sunier, "Nuclear Structure of ^{168}Er Studied with the ^{170}Er(p,t)^{168}Er and ^{166}Er(t,p)^{168}Erbium Reactions," *Can. J. Phys.* **63**, 1985, pp. 1309–1319.

D. G. Burke, W. F. Davidson, J. A. Cizewski, R. E. Brown, and J. W. Sunier, "Two-Quasiproton States in ^{168}Er Studied by the ^{169}Tm($\vec{t}$,α)^{168}Er Reaction," *Nucl. Phys.* **A445**, 1985, pp. 70–92.

T. N. Buti, J. Kelly, W. Bertozzi, J. M. Finn, F. W. Hersman, C. Hyde-Wright, M. V. Hynes, M. A. Kovash, S. Kowalski, R. W. Lourie, B. Murdock, B. E. Norum, B. Pugh, C. P. Sargent, W. Turchinetz, and B. L. Berman, "Electroexcitation of Isoscalar States in ^{16}O," *Phys. Rev. C* **33** (3), March 1986, pp. 755–775.

T. A. Carey, K. W. Jones, J. B. McClelland, J. M. Moss, L. Rees, N. Tanaka, and A. D. Bacher, "Complete Polarization Transfer Measurements in Inclusive Scattering of 500-MeV Protons and Pionic Enhancement of the Nuclear Sea-Quark Distribution," *Phys. Rev. Lett.* **53**, 1984, pp. 133–147.

J. M. Carpenter, R. A. Robinson, A. D. Taylor, and D. J. Picton, "Measurement and Fitting of Spectrum and Pulse Shapes of a Liquid Methane Moderator at IPNS," *Nucl. Instrum. & Methods* **A234**, 1985, pp. 542–551.

F. E. Cecil, D. M. Cole, R. Philbin, N. Jarmie, and R. E. Brown, "Reaction ^{2}H(^{3}He,γ)^{5}Li at Center-of-Mass Energies Between 25 and 60 keV," *Phys. Rev. C* **32**, 1985, pp. 690–693.

W. A. Challener and J. D. Thompson, "Far-Infrared Spectroscopy in Diamond Anvil Cells," *Appl. Spectrosc.* **40** (3), 1986, pp. 298–303.

J. S. Chalmers, W. R. Ditzler, T. Shima, H. Shimizu, H. Spinka, R. Stanek, D. Underwood, R. Wagner, A. Yokosawa, J. E. Simmons, G. Burleson, C. Fontenla, T. S. Bhatia, G. Glass, and L. C. Northcliffe, "Measurement of K_{LL} and K_{NN} in $\vec{p}$d → n$\vec{p}$p at 500, 650 and 800 MeV," *Phys. Lett.* **153B**, 1985, p. 235.

G. G. Christoph, C. E. Corbato, and R. T. Tettenhorst, "Space Group and Structure Refinement of Boehmite," *Clay and Clay Minerals*, 1984.

N. Cindro, D. Pocanic, D. M. Drake, J. D. Moses, J. C. Peng, N. Stein, and J. W. Sunier, "Elastic Scattering of ^{28}Si on ^{24}Mg and ^{26}Mg," *Nucl. Phys.* **A459**, 1986, p. 438.

M. D. Cohler, R. Wadsworth, S. M. Lane, D. L. Watson, M. J. Smithson, R. E. Brown, D. M. Drake, N. Stein, J. C. Peng, and J. W. Sunier, "Investigation of a Possible Abrupt Change in Structure at N = 58–60 Using Two-Proton Transfer," *Z. Phys. A* **322**, 1985, pp. 491–493.

M. D. Cohler, D. L. Watson, R. Wadsworth, S. M. Lane, M. J. Smithson, R. E. Brown, J. C. Peng, N. Stein, J. W. Sunier, and D. M. Drake, "Measurement of the Mass of ^{110}Pd and ^{114}Pd Using the (^{14}C, ^{16}O) Reaction," *Zeit. fur Physik* **A319**, 1984, p. 107.

S. A. Colgate and A. G. Petschek, "Angular Momentum The Cosmic Pollutant," *Los Alamos Science* **13**, 1986, p. 61.

D. W. Cooke, R. H. Heffner, R. L. Hutson, M. E. Schillaci, J. L. Smith, J. O. Willis, H. Daniel, and D. E. MacLaughlin, "Muon Spin Relaxation and Knight Shift in the Heavy-Fermion Superconductor UPt_3," to be published in *Hyperfine Int.*.

D. W. Cooke, J. K. Hoffer, M. A. Maez, W. A. Steyert, and R. H. Heffner, "Dilution Refrigeration for Muon Spin Relaxation Experiments," *Rev. Sci. Instrum.* **57**, 1986, pp. 336 340.

W. W. Daehnick, R. E. Brown, E. R. Flynn, R. A. Hardekopf, and J. C. Peng, "Analyzing Powers for ^{207}Pb($\vec{t}$, $\vec{p}$)^{209}Pb at 17 MeV as Evidence for Multistep Contributions," *Phys. Rev. C* **34**, 1986, pp. 815 824.

S. Datz, B. B. Berman, B. A. Dahling, M. V. Hynes, H. Park, J. O. Kephart, R. K. Klein, and R. H. Pantell, "On the Dependence of Electron Planar Channeling Radiation Upon Lattice Vibration Amplitude," *Nucl. Instrum. & Methods Phys. Res. Sect. B* (Netherlands) **B13** (1-3), March 1986, pp. 19 22.

H. A. Davis, R. R. Bartsch, L. E. Thode, E. G. Sherwood, and R. M. Stringfield, "High-Power Microwave Generation from a Virtual Cathode Device," *Phys. Rev. Lett.* **55** (21), 1985, pp. 2293 2296.

R. H. Day and T. W. Barbee, "Application of Layered Synthetic Microstructures to High-Temperature Plasma Diagnostics," *Rev. Sci. Instrum.* **56**, 1985, pp. 791 795.

R. H. Day, R. L. Blake, G. L. Stradling, W. J. Trela, and R. J. Bartlett, "Los Alamos X-Ray Characterization Facilities for Plasma Diagnostics," *SPIE X-Ray Calibration: Techniques, Sources, and Detectors* **689**, 1986, pp. 208 217.

C. W. De Jager, P. H. M. Keizer, E. A. Offermann, H. De Vries, M. V. Hynes, S. Kowalski, C. N. Rad, and C. F. Williamson, "Electroexcitation of the First Excited State in ^{39}K," *Phys. Lett. B* (Netherlands) **150B**, January 1985, pp. 421 424.

J. L. Dersch, R. Beckmann, G. Feige, T. Lund, P. Vater, R. Brandt, E. Ganssauge, K. Aleklett, E. M. Friedlander, P. L. McGaughey, G. T. Seaborg, W. Loveland, J. Hermann, and N. T. Porile, "Unusual Behaviour of Projectile Fragments from the Interaction of Copper with Relativistic Argon Ions," *Phys. Rev. Lett.* **55**, 1985, p. 1176.

N. J. DiGiacomo and M. R. Clover, "Significance of Positive Kaon Production in Low-Energy p-Nucleus Annihilations," *J. Phys. G* **10**, 1984, pp. L119 L125.

N. J. DiGiacomo, M. R. Clover, R. M. DeVries, J. C. Dousse, J. S. Kapustinsky, P. L. McGaughey, W. E. Sondheim, J. W. Sunier, M. Buenerd, and D. Lebrun, "Pion Production in 330, 400, and 500 MeV Proton-Nucleus Collisions," *Phys. Rev. C* **31**, 1985, pp. 292 294.

J. C. Dousse, E. D. Arthur, D. M. Drake, J. C. Gursky, J. D. Moses, N. Stein, and J. W. Sunier, "Coincident Neutron-Proton Emission from Proton Bombardment of ^{87}Sr and ^{91}Zr," *Phys. Rev. C* **32**, July 1985, pp. 92 102.

P. Dyer, G. C. Baldwin, A. M. Sabbas, C. Kittrell, E. L. Schweitzer, E. Abramson, and D. G. Imre, "Isomerically Selective Photoionization of ^{197}Hg," *J. Appl. Phys.* **58**, 1985, pp. 2431 2436.

P. Dyer, A. M. Sabbas, and S. A. Wender, "Laser Spectroscopy of the Transitional Nucleus ^{151}Sm," *Phys. Rev. C* **31**, 1985, pp. 240 241.

R. E. Ecke, H. Haucke, Y. Maeno, and J. C. Wheatley, "Critical Dynamics at a Hopf Bifurcation to Oscillatory Rayleigh-Bénard Convection," *Phys. Rev. A* **33** (3), 1986, pp. 1870 1878.

R. E. Ecke, Y. Maeno, H. Haucke, and J. C. Wheatley, "Critical Dynamics Near the Oscillatory Instability in Rayleigh-Bénard Convection," *Phys. Rev. Lett.* **53**, 1984, pp. 1567 1570.

R. E. Ecke, Y. Maeno, H. Haucke, and J. C. Wheatley, "Noise-Induced Intermittency in a Converting ^{3}He-Superfluid ^{4}He Solution," *Phys. Rev. Lett.* **53**, 1984, pp. 2090 2093.

J. Eckert, "Neutron Vibrational Spectroscopy: The Use of Hydrogen as a Structural and Dynamical Probe," *Physica* **136B**, 1986, pp. 150 155.

W. C. Feldman and D. M. Drake, "Doppler Filter Technique to Measure the Hydrogen Content of Planetary Surfaces," *Nucl. Instrum. & Methods.* **A245**, 1986, pp. 182–190.

D. H. Fitzgerald, H. W. Baer, J. D. Bowman, M. D. Cooper, F. Irom, N. S. P. King, M. J. Leitch, E. Piasetzky, W. J. Briscoe, M. E. Sadler, K. J. Smith, and J. N. Knudson, "Forward-Angle Cross Sections for Pion-Nucleon Charge Exchange Between 100 and 150 MeV/c," *Phys. Rev. C* **34**, August 1986, p. 619.

G. Flik, J. N. Bradbury, D. W. Cooke, L. Melvin, M. A. Paciotti, M. E. Schillaci, R. H. Heffner, K. Maier, C. Boekema, and H. Daniel, "Muon Channeling in Semiconductors—Evidence for Pionium Formation," *Phys. Rev. Lett.* **57**, 1986, pp. 563–567.

Z. Fraenkel, E. Piasetzky, and M. R. Clover, "Pion-Nucleus Absorption via the Delta-Nucleon Intermediate State," *Phys. Rev. C* **30**, 1984, pp. 720–722.

W. S. Freeman, D. F. Geesaman, R. J. Holt, J. R. Specht, B. Zeidman, E. J. Stephenson, J. D. Moses, M. Farkhondeh, S. Gilad, and R. P. Redwine, "Tensor Polarization in Pion-Deuteron Elastic Scattering," *Phys. Rev. C* **31**, March 1985, pp. 934–945.

A. I. Gavron, J. G. Boissevain, H. C. Britt, K. A. Eskola, P. L. Eskola, M. M. Fowler, H. Ohm, J. B. Wilhelmy, T. Awes, R. L. Ferguson, F. E. Obenshain, F. Plasil, G. R. Young, and S. Wald, "Fission Cross Sections up to 20 MeV/Nucleon," *Phys. Rev. C* **30**, 1984, pp. 1550–1560.

A. I. Gavron, A. Gayer, J. Boissevain, H. C. Britt, T. C. Awes, J. R. Beene, B. Cheynis, D. Drain, R. L. Ferguson, F. E. Obenshain, F. Plasil, G. R. Young, G. A. Petitt and C. Butler, "Neutron Emission in the Fissioning ^{158}Er Composite System," *Phys. Rev. C* **35**, 1987, p. 579.

A. I. Gavron, A. Gayer, J. G. Boissevain, H. C. Britt, J. R. Nix, A. J. Sierk, P. Grange, S. Hassani, H. Weidenmuller, J. R. Beene, B. Cheynis, D. Drain, R. L. Ferguson, F. E. Obenshain, F. Plasil, G. R. Young, G. A. Petitt, and C. Butler, "Neutron Emission Prior to Fission," *Phys. Rev. Lett.* **176**, 1986, p. 312.

G. A. Gist, S. A. Dodds, D. E. MacLaughlin, D. W. Cooke, R. H. Heffner, R. L. Hutson, M. Leon, M. E. Schillaci, C. Boekema, J. A. Mydosh, and G. J. Nieuwenhuys, "Ferromagnetism in Reentrant *Pd*FeMn," *J. Appl. Phys.* **51**, April 1985, p. 3491.

S. J. Gitomer, R. D. Jones, F. Begay, W. A. Ehler, J. F. Kephart, and R. Kristal, "Fast Ions and Hot Electrons in the Laser Plasma Interaction," *Phys. Fluids* **29** (8), August 1986, pp. 2679–2688.

G. Glass, T. S. Bhatia, J. C. Hiebert, R. A. Kenefick, S. Nath, L. C. Northcliffe, W. B. Tippens, D. Barlow, A. Saha, K. K. Seth, J. G. Boissevain, J. J. Jarmer, J. E. Simmons, R. H. Jeppesen, and G. E. Tripard, "Measurement of Spin-Correlation Parameters A^{LL} and A^{SL} for $p_{pol}p_{pol} \rightarrow d\pi^+$ Between 500 and 800 MeV," *Phys. Rev. C* **31**, 1985, p. 288.

G. Glass, T. S. Bhatia, J. C. Hiebert, R. A. Kenefick, L. C. Northcliffe, W. B. Tippens, J. G. Boissevain, J. J. Jarmer, J. E. Simmons, D. H. Fitzgerald, J. Holt, A. Mokhtari, and G. E. Tripard, "Measurements of Spin Correlation Parameter A_{NN} and Analyzing Power at 90 Degrees for $\vec{p}\vec{p} \rightarrow \pi d$ Between 500 and 800 MeV," *Phys. Rev. Lett.* **53**, 1984, p. 1984.

T. J. Goldman, M. V. Hynes, and M. M. Nieto, "The Gravitational Acceleration of Antiprotons," *Gen. Relativ. Gravitation* **18**, 1986, pp. 67–70.

T. Goldman, and G. J. Stephenson, "Quark Tunneling in Nuclei," *Phys. Lett.* **146B**, 1984, p. 143.

J. A. Goldstone, J. Eckert, P. M. Richards, and E. L. Venturini, "Temperature and Concentration Dependence of Hydrogen Site Occupancy in Several Rare Earth Dihydrides," *Physica* **136B**, 1986, pp. 183–186.

P. Grange, S. Hassani, H. Weidenmuller, A. I. Gavron, J. R. Nix, and A. J. Sierk, "Effects of Nuclear Dissipation on Neutron Emission Prior to Fission," *Phys. Rev. C* **34**, 1986, p. 209.

B. H. Grier, L. Passell, J. Eckert, H. Patterson, D. Richter, and R. J. Rollefson, "Neutron Scattering Study of Ethylene Motions on Graphite Surfaces," *Phys. Rev. Lett.* **53**, August 1984, pp. 814–817.

J. A. Hanlon and J. McLeod, "Aurora Laser Optical System," *Fusion Technol.* **11**, May 1987, pp. 634–653.

J. S. Hanspal, K. I. Pearce, N. M. Clarke, R. J. Griffiths, R. E. Brown, R. A. Hardekopf, and W. Gruebler, "The Interaction of 17 MeV Polarized Tritons with $^{3(}$ [illegible]," *Nucl. Phys.* **A444**, 1986, pp. 494–524.

H. Haucke and R. Ecke. "Mode-Locking and Chaos in Rayleigh-Bénard Convection." *Physica D* **24**, 1987.

H. Haucke, R. Ecke, Y. Maeno, and J. C. Wheatley. "Noise-Induced Intermittency in a Convecting Dilute Solution of ^{3}He in Superfluid ^{4}He." *Phys. Rev. Lett.* **53**. 1984. pp. 2090 2092.

A. Hauer and R. D. Cowan. "Absorption Spectroscopy Diagnosis of Pusher Conditions in Laser-Driven Implosions." *Phys. Rev. A* **34** (1). 1986. pp. 411 420.

A. Hauer, J. D. Kilkenny, and O. L. Landen. "Toroidally Curved Crystal for Time-Resolved X-Ray Spectroscopy." *Rev. Sci. Instrum.* **56**. 1985. pp. 803 804.

A. Hauer, J. D. Kilkenny, and J. S. Wark. "Studies of X-Ray Switching and Shuttering Techniques." *Rev. Sci. Instrum.* **57** (8). 1986. pp. 2168 2170.

A. Hauer, W. C. Mead, O. Willi, J. D. Kilkenny, D. Bradley, S. D. Tabatabaei, and C. Hooker. "Measurement and Analysis of Near-Classical Thermal Transport in One-Micron Laser Irradiated Spherical Plasmas." *Phys. Rev. Lett.* **53**. 1984. pp. 2563 2566.

R. H. Heffner, D. W. Cooke, Z. Fisk, R. L. Hutson, M. E. Schillaci, J. L. Smith, J. O. Willis, D. E. MacLaughlin, C. Boekema, R. L. Lichti, A. B. Denison, and J. Oostens. "Muon Knight Shift in the Heavy Fermion Superconductor $U_{1-x}Th_xBe_{13}$, $x = 0$ and 0.033." *Phys. Rev. Lett.* **57**. 1986. pp. 1255 1259.

R. H. Heffner, D. W. Cooke, R. L. Hutson, M. E. Schillaci, S. A. Dodds, G. A. Gist, and D. E. MacLaughlin. "Muon Spin Relaxation Study of Exchange Coupling in Dilute AgMn Alloys." *J. Magn. & Magn. Mat.* **54-57**. 1986. pp. 1103 1104.

J. Helffrich, M. Maley, M. Krusius, and J. C. Wheatley. "Hydrogen Dissociation Below 1 K." *J. Low Temp. Phys.* **66**. 1987. pp. 277 304.

J. Helffrich, M. P. Maley, M. F. Krusius, and J. C. Wheatley. "Measurement of Thermal Accommodation of Spin-Polarized Hydrogen on a Saturated ^{4}He Film at 0.18 0.4 K." *Phys. Rev. B* **34**. 1986. pp. 6550 6553.

F. W. Hersman, W. Bertozzi, T. N. Buti, J. M. Finn, C. E. Hyde-Wright, M. V. Hynes, J. Kelly, M. A. Kovash, S. Kowalski, J. Lichtenstadt, R. Lourie, B. Murdock, B. Pugh, F. N. Rad, C. P. Sargent, and J. B. Bellicard. "Inelastic Electron Scattering from Collective Levels of ^{154}Gd." *Phys. Rev. C* **33** (6). June 1986. pp. 1905 1916.

M. Hillman and A. C. Larson. "Structural Consequences of Oxidation of Ferrocene Derivatives II. 1,1',2,2',4,4' Tris(Trimethylene) Ferrocenium Perchlorate." *J. Organometallic Chemistry* **280**. 1985. pp. 389 396.

M. V. Hoehn, E. B. Shera. "Energies of the Muonic L and M Transitions of the Even-A Lead Isotopes." *Phys. Rev. C* **30**. 1984. pp. 704 707.

J. K. Hoffer and D. N. Sinha. "Dynamics of Binary Phase Separation in Liquid ^{3}He-^{4}He Mixtures." *Phys. Rev. A* **33** (3). 1986. pp. 1918 1939.

C. L. Hollas, D. J. Cremans, K. H. McNaughton, P. J. Riley, R. F. Rodebaugh, S. W. Xu, B. E. Bonner, M. W. McNaughton, H. Ohnuma, O. B. van Dyck, S. Tsu-Hsun, S. E. Turpin, B. Aas, and G. S. Weston. "D_{SS}, D_{LL}, D_{SL}, D_{LS}, and P for pp→pp at 600 to 800 MeV." *Phys. Rev. C* **30**. 1984. pp. 1251 1255.

C. L. Hollas, K. H. McNaughton, P. J. Riley, S. W. Xu, B. E. Bonner, O. B. van Dyck, J. A. McGill, M. W. McNaughton, J. C. Peng, R. R. Silbar, J. F. DuBach, and W. M. Kloet. "Wolfenstein Polarization Observables for the Reaction $p_{pol}p \rightarrow p_{pol}\pi n$ at 800 MeV." *Phys. Rev. Lett.* **55**. 1985. p. 29.

Y. S. Horowitz, M. Moscovitch, J. M. Mack, Jr., H. H. Hsu, and E. Kearsley. "Incorporation of Monte Carlo Electron Interface Studies into Photon General Cavity Theory." *Nucl. Sci. & Eng.* **94**. 1986. pp. 233 240.

M. Hoshi, D. Goodhead, D. J. Brenner, D. A. Bance, J. J. Chmielewski, M. A. Paciotti, and J. N. Bradbury. "Dosimetry Comparison and Characterization of an Al K Ultrasoft X-Ray Beam from an MRC Cold-Cathode Source." *Phys. Med & Biol.* **30**. October 1985. pp. 1029 1041.

M. K. Hou, C.-Y. Huang, M. B. Maple, M. S. Torikachvili, and H. C. Hamaker. "Surface Impedance of Several Magnetic Superconductors." *J. Magn. & Magn. Mater.* **59**. 1986. p. 247.

J. Howard, J. M. Nicol, B. C. Boland, J. Tomkinson, J. Eckert, J. A. Goldstone, and A. D. Taylor, "Debye-Waller Factors in Incoherent Inelastic Neutron Scattering Spectra of Molecular Polycrystals," *Mol. Phys.* **53**, 1984, p. 323.

S. D. Howe, P. W. Lisowski, G. J. Russell, N. S. P. King and H. J. Donnert, "Determination of the Absolute Efficiency of an Organic Scintillator for Neutrons with Energies Between 0.5 and 800 MeV," *Nucl. Instrum. & Methods Phys. Res. Sect. A* **227**, December 1984, pp. 565 570.

H. H. Hsu, "Interpolation Method for Functions of Two Variables," *Nucl. Sci. & Eng.* **94**, 1986, pp. 199 205.

C.-Y. Huang, "Interplay Among Charge Density Waves Superconductivity, and Magnetism," *CRC Crit. Rev. Solid State & Mater. Sci.* **12**, 1984, p. 75.

C.-Y. Huang, "Some Experimental Aspects of Spin Glasses A Review," *J. Magn. & Magn. Mater.* **51**, 1985, pp. 1 74.

C.-Y. Huang, A. M. Malvezzi, J. M. Liu, and N. Bloembergen, "Time-Resolved Picosecond Optical Study of Laser-Excited Graphite," *Phys. Rev. Lett.* **57**, 1986, p. 146.

C.-Y. Huang, C. E. Olsen, G. Kozlowski, H. Matsumoto, H. Umezawa, F. Mancini, M. B. Maple, H. C. Hamaker, M. S. Torikachvili, J. P. Whitehead, and F. E. Wang, "Anomalous Surface Impedance in Reentrant Ferromagnetic Superconductors," *J. Appl. Phys.* **57**, 1985, pp. 3104 3106.

G. S. Hurst, C. H. Chen, S. D. Kramer, *B. T. Cleveland*, R. Davis, Jr., J. K. Rowley, F. Gabbard, and J. J. Schima, "Feasibility of a $^{81}Br(\nu, e^-)^{81}Kr$ Solar Neutrino Experiment," *Phys. Rev. Lett.* **53**, 1984, pp. 1116 1119.

M. V. Hynes, J. L. C. Ford, Jr., T. P. Sjoreen, J. L. Blankenship, and F. E. Bertrand, "Design and Performance of a Vertical Drift Chamber for Heavy Ion Applications," *Nucl. Instrum. & Methods Phys. Res. Sect. A* (Netherlands) **224** (1-2), July 1984, pp. 89 96.

M. V. Hynes, A. Picklesimer, P. C. Tandy, and R. M. Thaler, "Characteristic Dirac Signature in Elastic Proton Scattering at Intermediate Energies," *Phys. Rev. Lett.* **52** (12), March 1984, pp. 978 981.

M. V. Hynes, A. Picklesimer, P. C. Tandy, and R. M. Thaler, "Relativistic (Dirac Equation) Effects in Microscopic Elastic Scattering Calculations," *Phys. Rev. C* **31**, 1985, pp. 1438 1463.

J. H. Jacob, M. Rokni, R. E. Klinkowstein, and S. Singer, "Expanding Beam Concept for Building Very Large Excimer Laser Amplifiers," *Appl. Phys. Lett.* **48**(5), 1986, pp. 318 320.

N. Jarmie and R. E. Brown, "Low-Energy Nuclear Reactions with Hydrogen Isotopes," *Nucl. Instrum. & Methods Phys. Res. Sect. B* **10-11**, 1985, pp. 405 410.

N. Jarmie, R. E. Brown, and R. A. Hardekopf, "Fusion-Energy Reaction $^2H(t,\alpha)n$ from E_t = 12.5 to 117 keV," *Phys. Rev. C* **29**, 1984, pp. 2031 2046.

N. Jarmie, G. Hale, and P. A. Young, "Summary of the International Conference on Nuclear Data for Basic and Applied Science, Santa Fe, New Mexico, May 13 17, 1985," *Fusion Technol.* **9**, 1986, p. 366.

R. J. Jensen, "Los Alamos Krypton Fluoride Laser Program," *Lasers & Part. Beams*, 1986, pp. 3 16.

W. M. Johnson, E. B. Shera, M. V. Hoehn, R. A. Naumann, J. D. Zumbro, and C. E. Bemis, "^{241}Am and ^{243}Am Charge Distributions from Muonic X-Ray Spectroscopy and the Quadrupole Moment of the ^{240}Am Fission Isomer," *Phys. Lett. B* **161**, 1985, pp. 75 78.

K. W. Jones, C. Glashausser, R. DeSwiniarski, S. Nanda, T. A. Carey, W. D. Cornelius, J. M. Moss, J. B. McClelland, J. R. Comfort, J. L. Escudie, M. Gazzaly, N. M. Hintz, G. Igo, M. Haji-Saeid, and C. A. Whitten, Jr., "Energy Dependence of Deformation Parameters in the $^{12}C(\vec{p}, p')^{12}C$ Reaction," *Phys. Rev. C* **33**, 1986, pp. 17 21.

L. A. Jones, E. Kallne, D. R. Kania, M. D. Maestas, J. S. McGurn, and R. L. Shepherd, "Technique for In-Situ Calibration of an X-Ray Streak Camera in the Nanosecond Regime Using a High Density Z-Pinch," *J. Appl. Phys.* **58** 1985, pp. 1711 1714.

L. A. Jones and D. R. Kania, "Temporally and Spatially Resolved X-Ray Emission from a Collapsing-Gas-Shell Z-Pinch Plasma," *Phys. Rev. Lett.* **55** (19), 1985, pp. 1993 1996.

D. R. Kania, R. J. Bartlett, and P. Pianetta, "Subnanosecond Time Resolved Measurements of Synchrotron X-Ray Pulses Using Photoconductive Detectors," *Nucl. Instrum. & Methods Phys. Res. Sect. A* **246**, 1986, pp. 534 536.

D. R. Kania and L. A. Jones. "Observation of an Electron Beam in an Annular Gas-Puff Z-Pinch Plasma Device." *Phys. Rev. Lett.* **53**, 1984, pp. 166 169.

D. R. Kania, E. L. Zimmermann, R. J. Trainor, L. R. Veeser, and L. A. Jones. "Experimental Tests of a Moving Foil as a High Current Vacuum Opening Switch." *Appl. Phys. Lett.* **45**, 1984, pp. 26 28.

R. D. Kaplan and R. B. Gibson. "Metal Halide Saturable Absorbers at 248 nm." *Appl. Phys. Lett.* **49** (5), 1986, pp. 251 252.

J. S. Kapustinsky, R. M. DeVries, N. J. DiGiacomo, W. E. Sondheim, J. W. Sunier, and H. Coombes. "A Fast Timing Light Pulser for Scintillation Detectors." *Nucl. Instrum. & Methods Phys. Res. Sect. A* **241**, 1985, pp. 612 613.

A. I. Katz, D. Schiferl, and R. L. Mills. "New Phases and Chemical Reactions in Solid Carbon Monoxide Under Pressure." *J. Phys. Chem.* **88**, 1984, pp. 3176 3179.

J. Kelly, W. Bertozzi, T. N. Buti, J. M. Finn, F. W. Hersman, M. V. Hynes, C. Hyde-Wright, B. E. Norum, A. D. Bacher, G. T. Emery, C. C. Foster, W. P. Jones, D. W. Miller, B. L. Berman, J. A. Carr, and F. Petrovich. "Neutron Transition Density for the Lowest 2^+ State of ^{18}O." *Phys. Lett. B* (Netherlands) **169B** (2-3), March 1986, pp. 157 160.

R. E. Kelly, P. B. Lyons, and L. D. Looney. "Radiation Induced Time Dependent Attenuation in a Fiber." *SPIE Optical Fiber Characteristics and Standards* **584**, 1985, pp. 61 70.

K. C. Kim and H. Filip. "Molecular Density Measurements Using Tunable Semiconductor Lasers in a Supersonic Flow." *Appl. Spectrosc.* **39**, 1985, pp. 167 169.

W. D. Kimura and E. T. Salesky "Kr_2F^* Fluorescence Measurements of Electron Beam Pumped KrF Laser Mixtures." *Appl. Phys. Lett.* **48**, April 1986, pp. 897 899.

N. S. P. King, G. L. Morgan, P. W. Lisowski, C. A. Goulding, P. Craig, R. G. Jeppesen, D. A. Lind, J. R. Shepard, J. L. Ullmann, C. D. Zafiratos, and C. D. Goodman. "Observation of Fermi and Gamow-Teller Strength in the 800 MeV (p,n) Reaction." *Phys. Lett. B* **175**, (3), 1986, pp. 279 283.

P. E. Koehler, H. D. Knox, D. A. Resler, R. O. Lane, and G. F. Auchampaugh. "Structure of ^{19}O from Measurement and R-Matrix Analysis of $\sigma(\theta)$ for $^{18}O(n,n)^{18}O$ and $^{18}O(n,n')^{18}O^*$ (1.98 MeV)." *Nucl. Phys.* **A453**, 1986, pp. 429 462.

P. E. Koehler, S. A. Wender, and J. S. Kapustinsky. "Improvements in the Energy Resolution and High-Count-Rate Performance of Bismuth Germanate." *Nucl. Instrum. & Methods Phys. Res. Sect. A* **242**, 1986, pp. 369 372.

B. L. Kortegaard. "Position Alignment Control System, Multi-Variable, Self-Adaptive Through the Use of Noise." *Fusion Technol.* **11**, May 1987, pp. 671 684.

G. Kovacs, J. R. Buchler, and C. G. Davis "Application of Time-Dependent Fourier Analysis to Nonlinear Pulsational Stellar Models." *Astrophys. J.* **319**, August 1987.

G. Kozlowski, H. Matsumoto, H. Umezawa, C.-Y. Huang, C. E. Olsen, M. B. Maple, H. C. Hamaker, M. S. Torikachvili, and F. E. Wang. "Anomalies in the Surface Impedance Penetration Depth in Ferromagnetic Superconductors." *Sol. Stat. Commun.* **54**, 1985, p. 221.

R. H. Kraus, Jr., W. Loveland, K. Aleklett, P. L. McGaughey, T. T. Sugihara, G. T. Seaborg, T. Lund, Y. Morita, E. Hagebo, and I. R. Haldorsen. "Target-Fragment Angular Distributions for the Interaction of 86 MeV/A ^{12}C with ^{197}Au." *Nucl. Phys.* **A432**, 1985, p. 525.

G. A. Kyrala. "Simulation of Bent Crystal Spectrometers." *Rev. Sci. Instrum.* **56**, 1985, pp. 815 817.

G. A. Kyrala, J. S. McGurn, J. Calligan, and J. Pallone. "Fast Framing Camera with Independent Frame Adjustments." *SPIE High Speed Photography, Videography, and Photonics III* **569**, 1985, pp. 36 40.

E. M. Larson, P. G. Eller, and A. C. Larson. "Single Crystal Structure of Ethyoxytetrakis-Perfluoro-T-Butoxyethanol Uranium (V), U OC(CF3) 4 (OC2 H5) (HOC2 H5)." *Lanthanide and Actinide Research*, in press.

J. M. Lawrence, J. D. Thompson, Z. Fisk, and B. Batlogg. "Low Temperature Resistivity of Cerium-Lanthanium-Thorium Under Pressure." *J. Appl. Phys.* **57**, 1985, pp. 3131 3133.

J. M. Lawrence, J. D. Thompson, and Y. Chen. "Lawrence, Thompson, and Chen Respond." *Phys. Rev. Lett.* **55**, 1985, p. 1702.

J. M. Lawrence, J. D. Thompson, and Y. Chen, "Two Energy Scales in $CePd_3$," *Phys. Rev. Lett.* **54**, 1985, pp. 2537 2540.

A. C. Lawson, A. C. Larson, R. B. von Dreele, A. T. Ortiz, J. L. Smith, J. Faber, R. L. Hitterman, and M. H. Muller, "Rhombohedral Phase at the Cubic-Orthorhombic Transformation of UMn_2," *J. Less-Common Metals*, in press.

A. C. Lawson, A. Williams, and J. G. Huber, "Field Induced Ordering of Local Moments in Ferromagnetic $CeRh_3B_2$," *J. Less-Common Metals* **120**, 1986, pp. 147 152.

A. C. Lawson, A. Williams, J. G. Huber, and R. B. Roof, Jr., "Magnetic Structure of UPt," *J. Less-Common Metals* **120**, 1986, pp. 113 122.

A. C. Lawson, A. Williams, J. L. Smith, P. A. Seeger, J. A. Goldstone, J. A. O'Rourke, and Z. Fisk, "Magnetic Neutron Diffraction Study of UGa_3 and UGa_2," *J. Magn. & Magn. Mater.* **50**, 1985, pp. 83 87.

P. Lee, R. J. Bartlett, and D. R. Kania, "Soft X-Ray Optics Using Multilayer Mirrors," *Opt. Eng.* **24**, 1985, p. 197.

P. H. Y. Lee, "On Relativistic Self Focusing," *Laser & Part. Beams* **5**, 1987, p. 15.

P. H. Y. Lee, R. H. Price, J. Reay, J. F. Pecos, J. D. Seagrave, J. S. McGurn, J. C. Cochrane, and B. G. Anderson, "Optical and UV/X-Ray Imaging Diagnostics for Imploding Plasma Experiments," *Rev. Sci. Instrum.* **9**, 1986, p. 2227.

P. H. Y. Lee and O. Willi, "A Model for Inhibition of Thermal Transport in Laser Produced Plasmas," *Laser & Part. Beams* **3**, 1985, p. 263.

P. H. Y. Lee, and Z. Z. Xu, "Scaling Laws of Self Focusing Mechanisms in Laser Plasmas," *Scientia Sinica A* **26**, 1986, p. 889.

B. E. Lehnert and C. R. Tech, " Quantitative Evaluation of Opsonin-Independent Phagocytosis by Alveolar Macrophages in Monolayer Using Polystyrene Microspheres," *J. Immunol. Methods* **78** (2), 1985, pp. 337 344.

M. J. Leitch, R. L. Burman, R. Carlini, S. Dam, V. Sandberg, M. Blecher, K. Croton, R. Ng, R. Auble, F. E. Bertrand, E. E. Gross, F. E. Obenshain, J. Wu, G. S. Blanpied, B. M. Preedom, B. G. Ritchie, W. Bertozzi, M. V. Hynes, M. A. Kovash, and R. P. Redwine, "Pion-Nucleus Scattering at 80 MeV," *Phys. Rev. C* **29**, 1984, pp. 561 575.

K. Liapis, U. A. Jayasooriya, S. F. Kettle, J. Eckert, J. A. Goldstone, and A. D. Taylor, "Solid State Studies Part XXIX: Crystalline Urea Evidence for Vibrational Delocalization," *Physical Chemistry* **89**, 1985, p. 4560.

J. W. Lillberg, "Time Projection Chamber Data Acquisition System," *Nucl. Instrum. & Methods Phys. Res. Sect. A* **240**, 1985, pp. 122 129.

J. W. Lillberg, W. W. Kinnison, R. J. McKee, and H. L. Anderson, "A Multiwire Proportional Chamber Based System for Digitizing Electrophoretic Gels," *Nucl. Instrum. & Meth.* **A252**, 1986, pp. 251 254.

P. W. Lisowski, S. A. Wender, G. F. Auchampaugh, "The WNR/PSR Facility – Neutron Physics Capabilities From Sub-Thermal to 800 MeV," *Radiat. Eff.* **95**, 1986, pp. 239–252.

T. R. Loree, R. R. Showalter, T. M. Johnson, B. S. Birmingham, and W. M. Hughes, "Lasing XeO in Liquid Ar," *Opt. Lett.*, August 1986, pp. 510 512.

D. W. MacArthur, K. Butterfield, D. Clark, J. Donahue, P. A. M. Gram, H. Bryant, C. Harvey, W. W. Smith, and G. Comtet, "Energy Measurement of the Lowest $^1P^o$ Feshbach Resonance in H^-," *Phys. Rev. A* **32**, September 1985, pp. 1921 1923.

D. W. MacArthur, K. Butterfield, D. Clark, J. Donahue, P. A. M. Gram, H. Bryant, C. Harvey, W. W. Smith, and G. Comtet, "Test of the Special-Relativistic Doppler Formula at $\beta = 0.84$," *Phys. Rev. Lett.* **56**, 1986, pp. 282 285.

Y. Maeno, H. Haucke, R. E. Ecke, and J. C. Wheatley, "Oscillatory Convection in a Dilute ^3He Superfluid ^4He Solution," *J. Low Temp. Phys.* **59**, 1985, pp. 305 344.

Y. Maeno, H. Haucke, and J. C. Wheatley, "Transition to Oscillatory Convection in a ^3He Superfluid-^4He Mixture," *Phys. Rev. Lett.* **54**, 1985, pp. 340 342.

A. M. Malvezzi, N. Bloembergen, and C.-Y. Huang, "Time-Resolved Picosecond Optical Measurements of Laser-Excited Graphite," *Phys. Rev. Lett.* **57** (1), 1986, pp. 146 149.

A. Mandl, and E. T. Salesky, "Electron Beam Deposition Studies of the Rare Gases," submitted for publication in *J. Appl. Phys.*.

D. M. Manley, B. L. Berman, W. Bertozzi, J. M. Finn, F. W. Hersman, C. E. Hyde-Wright, M. V. Hynes, J. J. Kelly, M. A. Kovash, S. Kowalski, R. W. Lourie, B. Murdock, B. E. Norum, B. Pugh, and C. P. Sargent, "Electroexcitation of M4 Transitions in ^{17}O and ^{18}O," *Phys. Rev. C* **34**, 1986, pp. 34 50.

M. B. Maple, J. W. Chen, Y. Dalichaouch, T. Kohara, C. Rossel, M. S. Torikachvili, M. W. McElfresh, and J. D. Thompson, "Partially Gapped Fermi Surface in the Heavy Electron Superconductor URu_2Si_2," *Phys. Rev. Lett.* **56**, 1986, p. 185.

R. H. McCamis, P. J. T. Verheijen, W. T. H. van Oers, P. Drakopoulos, C. Lapointe, G. R. Maughan, N. T. Okumusoglu, and R. E. Brown, "$^{3}\overrightarrow{\text{He}}$(p,p)^{3}He Analyzing Powers Between 25 and 35 MeV," *Phys. Rev. C* **31**, 1985, pp. 1651 1655.

D. K. McDaniels, J. R. Tinsley, J. Lisantii, D. M. Drake, I. Bergqvist, L. W. Swenson, F. E. Bertrand, E. E. Bross, D. J. Horen, T. P. Sjoreen, R. Liljestrand, and H. Wilson, "Cross Section and Analyzing Power Measurements for the Giant Resonance Region in ^{208}Pb with 200 MeV Protons," *Phys. Rev. C* **33** (6), 1986, pp. 1943 1954.

M. W. McElfresh, J. D. Thompson, J. O. Willis, M. B. Maple, M. S. Torikachvili, and T. Kohara, "Effect of Pressure on Competing Electronic Correlations in the Heavy Fermion System URu_2Si_2," *Phys. Rev. B* **35**, 1987, pp. 43 47.

W. K. McFarlane, L. B. Auerbach, F. C. Gaille, V. L. Highland, E. Jastrzembski, R. J. Macek, F. H. Cverna, C. M. Hoffman, G. E. Hogan, R. E. Morgado, J. C. Pratt, and R. D. Werveck, "Measurement of the Rate for Pion Beta Decay," *Phys. Rev. D* **32** (3), 1985, p. 547.

P. L. McGaughey, K. D. Bol, M. R. Clover, R. M. DeVries, N. J. DiGiacomo, J. S. Kapustinsky, W. E. Sondheim, G. R. Smith, J. W. Sunier, Y. Yariv, M. Buenerd, J. Chauvin, D. Lebrun, P. Martin, and J. C. Dousse, "Dynamics of Low-Energy Antiproton Annihilation in Nuclei as Inferred from Inclusive Proton and Pion Measurements," *Phys. Rev. Lett.* **56** (20), 1986, pp. 2156 2159.

P. L. McGaughey, M. R. Clover, and N. J. DiGiacomo, "Antiproton Annihilations in Nuclei May Not Produce High Nuclear Temperatures," *Phys. Rev. Lett.* **56B**, 1986, pp. 2156 2159.

P. L. McGaughey, N. J. DiGiacomo, W. E. Sondheim, J. W. Sunier, and Y. Yariv, "Low Energy Antiproton-Nucleus Annihilation Ra Selection Using an Active Si Detector/Target," *Nucl.Instrum. & Methods* **A249**, 1986, p. 361.

P. L. McGaughey, W. Loveland, D. J. Morrissey, K. Aleklett, and G. T. Seaborg, "Uranium Target Fragmentation by Intermediate and High Energy ^{12}C and ^{20}Ne Ions," *Phys. Rev. C* **31**, 1985, p. 896.

B. H. J. McKellar, and G. J. Stephenson Jr., "Remarks on the Nature of Confining Potentials," submitted for publication in Brief Reports section of *Phys. Rev. C*.

K. F. McKenna, W. T. Armstrong, D. C. Barnes, R. R. Bartsch, R. E. Chrien, J. C. Cochrane, P. L. Klingner, W. N. Hugrass, R. K. Linford, D. J. Rej, J. L. Schwarzmeier, E. G. Sherwood, R. E. Siemon, R. L. Spencer, and M. Tuszewski, "Field-Reversed Configuration Research at Los Alamos," *Nucl. Fusion* **25**, September 1985, pp. 1317 1319.

J. McLeod, "Output Optics for Aurora: Beam Separation, Pulse Stacking and Focusing," *Fusion Technol.* **11**, May 1987, pp. 654 670.

M. McNaughton, B. Bonner, H. Ohnuma, O. B. Van Dyck, S. Tsu-Hsun, C. L. Hollas, D. J. Cremans, K. H. McNaughton, P. J. Riley, R. F. Rodebaugh, S. W. Xu, S. E. Turpin, A. Bjorne, and G. Weston, "P-C Analyzing Power Between 100 and 750 MeV," *Nucl. Instrum. & Methods Phys. Res. Sect. A* **241**, 1985, pp. 435 440.

F. D. Michaud, "Estimating Thermal Distortion of Monochromator Crystals," *Nucl. Instrum. & Methods Phys. Res. Sect. A* **246**, May 1986, pp. 444 449.

R. Mills, B. Olinger, and D. Cromer, "Structures and Phase Diagrams of Nitrogen-2 and Carbon Monoxide to 13 GPa by X-Ray Diffraction," *J. Chem. Phys.* **84**, 1986, pp. 2837 2845.

R. L. Mills, D. Schiferl, A. I. Katz, B. W. Olinger, and I. Allen, "New Phases and Chemical Reactions in Solid Carbon Monoxide Under Pressure," *J. Phys. Colloq.* **8**, 1984, pp. 187 190.

C. Milner, M. Barlett, G. W. Hoffman, S. Bart, R. E. Chrien, P. Pile, P. D. Barnes, G. B. Franklin, R. Grace, H. S. Plendl, J. F. Amann, T. S. Bhatia, T. Kozlowski, J. C. Peng, R. R. Silbar, H. A. Thiessen, C. Glashausser, J. A. McGill, R. Hackenburg, E. V. Hungerford, and R. L. Stearns, "Observation of Λ-Hypernuclei in the $^{12}C(\pi^+,K^+)^{12}_{\Lambda}C$," *Phys. Rev. Lett.* **54**, March 1985, pp. 1237 1240.

C. S. Mishra, B. G. Ritchie, R. S. Moore, M. Blecher, K. Gotow, R. L. Burman, M. V. Hynes, E. Piasetzky, P. G. Roos, F. E. Bertrand, T. P. Sjoreen, F. E. Obenshain, and E. E. Gross, "Isospin Effect in $\pi^{\pm}$ ^{14}C Elastic Scattering at 50 MeV," *Phys. Rev. C* **32**, 1985, pp. 995 998.

M. S. Moore, L. Calabretta, F. Corvi, and H. Weighmann, "Analysis of Intermediate Structure in the Fission and Capture Cross Sections of ($^{235}U + n$) *Phys. Rev. C* **30**, 1984, pp. 214 216.

G. L. Morgan, P. W. Lisowski, S. A. Wender, R. E. Brown, N. Jarmie, J. F. Wilkerson, and D. M. Drake, "Measurement of the Branching Ratio $^3H(d,\gamma)/^3H(d,n)$ Using Thick Tritium Gas Targets," *Phys. Rev. C* **33**, 1986, pp. 1224 1227.

B. T. Murdoch, D. K. Hasell, A. M. Sourkes, W. T. H. van Oers, P. J. T. Verheijen, and R. E. Brown, "$^3He(p,p)^3He$ Scattering in the Energy Range 19 to 48 MeV," *Phys. Rev. C* **29**, 1984, pp. 2001 2008.

B. E. Newnam, R. W. Warren, R. L. Sheffield, W. E. Stein, M. T. Lynch, J. S. Fraser, J. C. Goldstein, J. E. Sollid, T. A. Swann, J. M. Watson, and C. A. Brau, "Optical Performance of the Los Alamos Free-Electron Laser," *IEEE J. Quantum Electron.* **QE-21**, July 1985, pp. 867 881.

R. J. Newport, P. A. Seeger, and W. G. Williams, "Test Measurements on a Resonance Filter Spectrometer Using Electron Volt Neutrons," *Nucl. Instru. & Methods Phys. Res. Sect. A* **238**, 1985, pp. 177 179.

D. R. Noakes, E. J. Ensaldo, J. H. Brewer, C.-Y. Huang, and D. R. Harshman, "Muon Spin Relaxation in $ErRh_4B_4$," *J. App. Phys.* **57**, 1985, p. 3197.

B. W. Olinger, R. L. Mills, and R. B. Roof, Jr., "Structures and Transitions in Solid Oxygen to 13 GPa at 298 K by X-Ray Diffraction," *J. Chem. Phys.* **81**, 1984, pp. 5068 5073.

D. M. Parkin, J. A. Goldstone, H. M. Simpson, and J. W. Hemsky, "Point Defect-Dislocation Interactions in Copper Following Pulsed Neutron and Electron Irradiations," *J. Phys. F: Met. Phys.* **17**, 1987, pp. 577 592.

M. Pasternak, J. N. Farrell, and R. D. Taylor, "Mössbauer Effect of Iodine at Pressures to 30 GPa," *Hyperfine Interact.* **28**, 1986, pp. 837 842.

M. Pasternak, J. N. Farrell, and R. D. Taylor, "The Isomer Shift of Elemental Iodine Under High Pressure," *Solid State Commun.* **61** (7), 1987, pp. 409 411.

M. Pasternak, J. N. Farrell, and R. D. Taylor, "Metallization and Structural Transformation of Iodine under Pressure: A Microscopic View," *Phys. Rev. Lett.* **58** (6), February 1987, pp. 575 578.

J. C. Peng, "Associated Production of Hypernuclei," *Nucl. Phys.* **A450**, 1986, pp. 129c 146c.

A. G. Petschek, "Letter to the Editor," *Physics Today*, July 1986.

A. Picklesimer and P. C. Tandy, "Interpretation of Relativistic Dynamical Effects in Proton-Nucleus Scattering," *Phys. Lett. C*, in press.

A. Picklesimer and P. C. Tandy, "Relativistic Scattering Operators for DIRAC Particles Structure, Symmetries and Reconstruction," *Phys. Rev. C* **34**, 1986, pp. 1860 1894.

A. Picklesimer and J. W. Van Orden, "Formal Framework for the Electroproduction of Polarized Nucleons from Nuclei," *Phys. Rev. C* **35**, 1987, pp. 266 279.

G. Pien, M. C. Richardson, P. D. Goldstone, G. E. Eden, R. H. Day, and F. P. Ameduri, "Computerized 3-GHz Multi-Channel Soft X-Ray Diode Spectrometer for High Density Plasma Diagnosis," *Nucl. Instrum. & Methods Phys. Res. Sect. B* **18**, 1986, p. 101.

C. E. Ragan III, "Shock-Wave Experiments at Threefold Compression," *Phys. Rev. A* **29**, 1984, pp. 1391 1402.

S. Raman, R. F. Carlton, J. C. Wells, Jr., E. T. Jurney, and J. E. Lynn, "Thermal Neutron Capture Gamma Rays from Sulfur Isotopes Experiment and Theory," *Phys. Rev. C* **32**, 1985, pp. 18 69.

S. Raman, W. Ratynski, E. T. Jurney, and M. E. Bunker, "$^{36}S(n,\gamma)^{37}S$ Reaction with Thermal Neutrons and Decay ^{37}S to Levels in ^{37}Cl," *Phys. Rev. C* **30**, 1984, pp. 26 30.

L. B. Rees, J. M. Moss, T. A. Carey, K. W. Jones, J. B. McClelland, N. Tanaka, A. D. Bacher, and H. Ebensen, "Continuum Polarization Transfer in 500 MeV Proton Scattering and Pionic Collectivity in Nuclei," *Phys. Rev. C* **34** (2), 1986, pp. 627 636.

G. Reiter and R. N. Silver, "Measurement of Interionic Potentials in Solids Using Deep-Inelastic Neutron Scattering," *Phys. Lett.* **54**, 1985, pp. 1047 1050.

W. Reuter, J. C. Gursky, E. B. Shera, and M. W. Johnson, "Thick Osmium Targets," *Nucl. Instrum. & Methods* **220**, 1984, p. 288.

W. Reuter, E. B. Shera, M. V. Hoehn, F. W. Hersman, T. Milliman, J. Finn, C. Hyde-Wright, R. Lourie, B. Pugh, and W. Bertozzi, "Ground-State and Transition Charge Densities in ^{192}Os," *Phys. Rev. C* **30**, 1984, pp. 1465 1478.

W. Reuter, E. B. Shera, M. V. Hoehn, F. W. Hersman, T. Milliman, J. Finn, C. Hyde-Wright, R. Lourie, B. Pugh, and W. Bertozzi, "Nuclear Charge Densities in the Transition Region: ^{192}Os," *Phys. Lett. B* **137**, 1984, pp. 32.

R. G. H. Robertson and P. E. Koehler, "Calorimetric Measurement of Thermal Neutron Flux," *Nucl. Instrum. & Methods* **A251**, 1986, pp. 307 312.

R. A. Robinson, J. D. Axe, A. I. Goldman, Z. Fisk, J. L. Smith, and H. R. Ott, "Measurement of Acoustic Phonons in UBe_{13}," *Phys. Rev. B* **33** (9), 1986, pp. 6488 6490.

R. A. Robinson, R. Pynn, and J. Eckert, "An Improved Constant-Q Spectrometer for Pulsed Neutron Sources," *Nucl. Instrum. & Methods Phys. Res. Sect. A* **241**, 1985, pp. 312 324.

L. A. Rosocha, P. S. Bowling, M. D. Burrows, M. Kang, J. A. Hanlon, J. McLeod, and G. W. York, "An Overview of Aurora A Multi-Kilojoule Krypton-Fluoride Laser System for Inertial Confinement Fusion," *Laser & Part. Beams* **4**, 1986, pp. 55 70.

L. A. Rosocha, J. A. Hanlon, J. McCleod, M. Kang., G. L. Kortegaard, M. D. Burrows, and P. S. Bowling, "Aurora Multikilojoule KrF Laser System Prototype for Inertial Confinement Fusion," *Fusion Technol.* **11**, May 1987, p. 497.

L. A. Rosocha, J. McLeod, and J. A. Hanlon, "Beam Propagation Considerations in the Aurora Laser System," *Fusion Technol.* **11**, May 1987, pp. 624 633.

E. T. Salesky and W. D. Kimura, "Electron-Beam Pumped KrF Laser Extraction Measurements for High Kr Concentration Gas Mixtures," *IEEE J. Quantum Electron.* **QE-21**, November 1985, pp. 1761 1765.

E. T. Salesky and W. D. Kimura, "Energy Extraction Measurements on an Electron-Beam Pumped, High Kr Concentration KrF Laser at Elevated Temperatures," *Appl. Phys. Lett.* **47**, October 1985, pp. 774 776.

E. T. Salesky and W. D. Kimura, "Gain and Absorption Measurements of Electron Beam Pumped, High Krypton Concentration Krypton Fluoride Gas Mixtures," *Appl. Phys. Lett.* **46**, 1985, pp. 927 929.

D. Schiferl, S. Buchsbaum, and R. L. Mills, "Phase Transitions in Nitrogen Observed by Raman Spectroscopy from 0.4 to 27.4 GPa at 15 K," *J. Phys. Chem.* **89**, 1985, pp. 2324 2330.

J. E. Schirber, B. Morosin, R. W. Alkire, A. C. Larson, and P. J. Vergamini, "Structure of ReO_3 Above the 'Compressibility Collapse Transition'," *Phys. Rev. B* **29**, 1984, p. 4150.

A. G. Seamster, W. B. Norman, D D. Leach, P. Dyer, and D. Bodansky, "Cross Sections Relevant to Gamma-Ray Astronomy," *Phys. Rev. C* **29** (2), 1984, pp. 394 402.

P. A. Seeger, "Comparison of Collimation Systems for Small-Angle Neutron Scattering," *Physica* **136B**, 1986, pp. 106 109.

P. A. Seeger, A. D. Taylor, and R. M. Brugger, "Double-Difference Method to Improve the Resolution on an eV Neutron Spectrometer," *Nucl. Instrum. & Methods Phys. Res. Sect. A* **240**, 1985, pp. 98 114.

P. A. Seeger and R. Pynn, "Resolution of Pulsed-Source Small-Angle Neutron Scattering," *Nucl. Instrum. & Methods Phys. Res. A* **245**, 1986, pp. 115 124.

S. J. Seestrom-Morris, C. L. Morris, J. M. Moss, T. A. Carey, D. M. Drake, J. C. Dousse, L. C. Bland, and G. S. Adams, "Measurement of π^-/π^- Cross Section Ratio for the Giant Quadrupole Resonance in ^{208}Pb," *Phys. Rev. C* **33**, 1986, pp. 1847 1849.

R. L. Sheffield, W. E. Stein, R. W. Warren, J. S. Fraser, and A. H. Lumpkin, "Electron-Beam Diagnostics and Results for the Los Alamos Free-Electron Laser," *IEEE J. Quantum Electron.* **QE-21**, 1985, pp. 895 903.

E. R. Siciliano, M. D. Cooper, M. B. Johnson, and M. J. Leitch, "Effects of Nuclear Correlations on Low-Energy Pion Charge-Exchange Scattering," *Phys. Rev. C* **34**, 1986, p. 267.

R. E. Siemon, W. T. Armstrong, D. C. Barnes, R. R. Bartsch, R. E. Chrien, J. C. Cochrane, W. N. Hugrass, R. W. Kewish, Jr., P. L. Klingner, H. R. Lewis, Jr., R. K. Linford, K. F. McKenna, R. D. Milroy, D. J. Rej, J. L. Schwarzmeier, C. E. Seyler, Jr., E. G. Sherwood, R. L. Spencer, and M. Tuszewski, "Review of the Los Alamos FRX-C Experiment," *Fusion Technol.* **9**, 1986, pp. 13 35.

R. N. Silver, "The Los Alamos Neutron Scattering Center," *Physica* **137B**, 1986, pp. 359 372.

R. N. Silver and G. Reiter, "Structure Dependence of Final-State Effects in Deep Inelastic Neutron Scattering: Quasiclassical Theory," *Phys. Rev. B* **35**, March 1987, pp. 3647 3650.

D. N. Sinha and J. K. Hoffer, "Study of Dynamical Light Scattering in Phase Separating ^{3}He-^{4}He Mixtures Using Linear Photodiode Arrays," *Rev. Sci. Instrum.* **55**, 1984, pp. 875 878.

T. P. Sjoreen, J. L. C. Ford, Jr., J. L. Blankenship, R. L. Auble, F. E. Bertrand, E. E. Gross, D. C. Hensley, D. Schull and M. V. Hynes, "The Vertical Drift Chamber as a High Resolution Focal Plane Detector for Heavy Ions," *Nucl. Instrum. & Methods Phys. Res. Sect. A* (Netherlands) **224** (3), July 1984, pp. 421 431.

E. F. Skelton, A. W. Webb, S. B. Qadri, S. A. Wolf, R. C. Lacoe, J. L. Feldman, W. T. Elam, E. R. Carpenter, Jr., and C.-Y. Huang, "Energy-Dispersive X-Ray Diffraction with Synchrotron Radiation at Cryogenic Temperatures," *Rev. Sci. Instrum.* **55**, 1984, p. 849.

E. Sklar, "Advantages of a Negative Branch Regenerative Unstable Resonator for Use with Free-Electron Lasers," *IEEE J. Quantum Electron.* **QE-22** (7), July 1986, pp. 1088 1094.

S. H. Southworth, A. C. Parr, J. E. Hardis, and J. L. Dehmer, "Channel Coupling and Shape Resonance Effects in the Photoelectron Angular Distributions of the $3\sigma_g^{-1}$ and $2\sigma_u^{-1}$ Channels of N_2," *Phys. Rev. A* **33** (2), 1986, pp. 1020 1023.

S. H. Southworth, A. C. Parr, J. E. Hardis, J. L. Dehmer, and D. M. P. Holland, "Calibration of a Monochromator/Spectrometer System for the Measurement of Photoelectron Angular Distributions and Branching Ratios," *Nucl. Instrum. & Methods Phys. Res. Sect. A* **246**, 1986, pp. 782 786.

R. Stine, W. Leland, C. Mansfield, L. Rosocha, J. Jansen, R. Gibson, and G. Allen, "Development of the Antares Electron Gun," *IEEE Trans. Electr. Insul.* **EI-20**, August 1985, pp. 781 788.

G. L. Stradling, "Workshop on Standards for Photonic Streak Camera Characterization," *SPIE: High Speed Photography, Videography, and Photonics III* **569**, 1985, pp. 136 140.

J. A. Sullivan, "Design of a 100-kJ KrF Power Amplifier Module," *Fusion Technol.* **11** (3), May 1987, pp. 684 704.

J. A. Sullivan and C. W. Von Rosenberg Jr., "High Energy KrF Amplifiers for Laser-Induced Fusion," *Laser & Part. Beams* **4**, Part I, 1986, pp. 91 205.

J. W. Sunier, K. D. Bol, M. R. Clover, R. M. DeVries, N. J. DiGiacomo, J. S. Kapustinsky, P. L. McGaughey, and W. E. Sondheim, "Calliope A Large Acceptance Multiparticle Magnetic Spectrometer for Intermediate Energy Physics," *Nucl. Instrum. & Methods Phys. Res. Sect. A* **241**, 1985, pp. 139 152.

G. W. Swift and S. L. Garrett, "Resonant Reciprocity Calibration of an Ultracompliant Transducer," accepted by *J. Acoust. Soc. Am.*.

G. W. Swift, A. Migliori, T. Hofler, and J. C. Wheatley, "Theory and Calculations for an Intrinsically Irreversible Acoustic Prime Mover Using Liquid Sodium as Primary Working Fluid," *J. Acoust. Soc. Am.* **78**, 1985, pp. 767 781.

G. W. Swift, A. Migliori, and J. Wheatley, "Construction of and Measurements with an Extremely Compact Cross-Flow Heat Exchanger," *Heat Transfer Eng.* **6**, 1985, pp. 39 46.

Y. Tanaka, R. M. Steffen, E. B. Shera, W. Reuter, M. V. Hoehn, and J. D. Zumbro, "Measurement and Analysis of the Muonic X Rays of ^{151}Eu and ^{153}Eu," *Phys. Rev. C* **29**, 1984, pp. 1897 1904.

Y. Tanaka, R. M. Steffen, E. B. Shera, W. Reuter, M. V. Hoehn, and J. D. Zumbro, "Measurement and Analysis of Muonic X Rays of ^{176,177,178,179,180}Hf," *Phys. Rev. C* **30**, 1984, pp. 350 359.

Y. Tanaka, R. M. Steffen, E. B. Shera, W. Reuter, M. V. Hoehn, and J. D. Zumbro, "Pionic M X-Rays of ^{166,168}Er and ^{176}Hf." *Phys. Lett. B* **143**, 1984, pp. 347–350.

Y. Tanaka, R. M. Steffen, E. B. Shera, W. Reuter, M. V. Hoehn, and J. D. Zumbro, "Systematics of Ground-State Quadrupole Moments of Odd-*A* Deformed Nuclei Determined with Muonic *M* X Rays." *Phys. Rev. C* **29**, 1984, p. 1830.

S. Tang, H. H. Hsu, J. E. Simmons, J. S. Kapustinsky, and J. C. Peng, "Energy Resolutions of a Position-Sensitive NaI Detector by Monte Carlo Simulations." *Nucl. Instrum. & Methods Phys. Res. Sect. A* **254**, 1987, p. 129–134.

J. D. Thompson and Z. Fisk, "Kondo-Lattice Mixed-Valence Resistance Scaling in Heavy-Fermion $CeCu_6$ Under Pressure," *Phys. Rev. B* **31**, 1985, pp. 389–391.

J. D. Thompson, Z. Fisk, Y. Y. Chen, and J. M. Lawrence, "Pressure Investigations of the New Kondo-Lattice Systems Ce_3Sn, Ce_3In, and Ce_3Al." *J. Less-Common Metals* **127**, 1987, pp. 385–390.

J. D. Thompson, Z. Fisk, and L. C. Gupta, "Magnetic Ordering in URh_2Ge_2 A Resistivity Investigation at Ambient and Elevated Pressures," *Phys. Lett. A* **110**, 1985, p. 470.

J. D. Thompson, Z. Fisk, and H. R. Ott, "Response of Uranium-Based Heavy-Fermion Magnets to Hydrostatic Pressure." *J. Magn. & Magn. Mater.* **54-57**, 1986, p. 393.

J. D. Thompson, J. M. Lawrence, and Y. Y. Chen, "Two Energy Scales in $CePd_3$." *Phys. Rev.* **54**, 1985, p. 2537.

J. D. Thompson, R. D. Parks, and H. Borges, "Effect of Pressure on the Neel Temperature of Kondo-Lattice Systems." *J. Magn. & Magn. Mater.* **54-57**, 1986, pp. 377–378.

J. D. Thompson, J. O. Willis, C. Godart, D. E. MacLaughlin, and L. C. Gupta, "Heavy Fermion State and Pressure-Induced Resistive Behavior in $CeRu_2Si_2$." *Solid State Commun.* **56**, 1985, p. 169.

J. D. Thompson, J. O. Willis, C. Godart, D. E. MacLaughlin, and L. C. Gupta, "Pressure-Induced Variation in the Resistive Behavior of the Kondo-Lattice System $CeRu_2Si_2$." *J. Magn. & Magn. Mater.* **47-48**, 1985, p. 281.

J. Tomkinson, A. D. Taylor, J. Howard, J. Eckert, and J. A. Goldstone, "Inelastic Neutron Scattering Spectrum of Chromous Acid at High Energy Transfers." *J. Chem. Phys.* **82**, 1985, pp. 1112–1114.

J. Trewhella and J. Eckert, "Inelastic Neutron Scattering in Biology." *Physica* **136B**, 1986, pp. 507–511.

M. Tuszewski, W. T. Armstrong, R. E. Chrien, P. L. Klingner, K. F. McKenna, D. J. Rej, E. G. Sherwood, and R. E. Siemon, "Confinement of Translated Field-Reversed Configurations." *Phys. Fluids* **29**, 1986, pp. 863–870.

J. L. Ullmann, J. J. Kraushaar, T. G. Masterson, R. J. Peterson, R. S. Raymond, C. L. Morris, R. A. Ristenen, N. S. P. King, R. L. Boudrie, C. L. Christopher, R. E. Anderson, and E. R. Siciliano, "Pion Inelastic Scattering to Giant Resonances and Low-Lying Collective States in ^{118}Sn and ^{40}Ca." *Phys. Rev. C* **31**, 1985, pp. 177–188.

E. Ungricht, W. S. Freeman, D. F. Geesaman, R. J. Holt, J. R. Specht, B. Zeidman, E. J. Stephenson, J. D. Moses, M. Farkhondeh, S. Gilad, and R. P. Redwine, "Tensor Polarization in Pion-Deuteron Elastic Scattering." *Phys. Rev. Lett.* **52**, 1984, pp. 333–336.

D. B. van Hulsteyn and T. W. Barbee, "Monochromatic X-Ray Imaging with a Metal Multilayer Camera." *J. Appl. Opt.* **24**, 1985, p. 2526.

D. B. van Hulsteyn, and L. O. Sillerud, "Transverse Relaxation Time Constraints on Resolution in One-Dimensional, Phase- and Frequency-Encoded Nuclear Magnetic Resonance Imaging." *J. Magn. Resonance* **71**, 1987, p. 14–23.

P. J. Vergamini, R. W. Alkire, G. G. Christoph, and A. C. Larson, "Time-of-Flight Single-Crystal Diffraction at the Los Alamos Pulsed Neutron Source." *Nucl. Instrum. & Methods Phys. Res.*, in press.

W. K. Wang, Y. J. Wang, S. A. He, J. H. Huang, J. D. Boyer, C.-Y. Huang, and H. Iwazaki, "Superconductivity and Phase Compositions in Annealed Amorphous Ni-Si Alloys Under High Pressure." *Solid State Commun.* **58** (5), 1986, pp. 285–288.

J. Wheatley, S. Buchanan, G. W. Swift, A. Migliori, and T. Hofler, "Nonlinear Natural Engine Model for Thermodynamic Processes in Mesoscale Systems," *Proc. Nat. Acad. Sci.* (USA) **82**, 1985, pp. 7805–7809.

J. C. Wheatley and A. N. Cox, "Natural Engines," *Phys. Today* **38**, 1985, pp. 50–58.

J. C. Wheatley, T. Hofler, G. W. Swift, and A. Migliori, "Understanding Some Simple Phenomena in Thermoacoustics with Applications to Acoustical Heat Engines," *Am. J. Phys.* **53**, 1985, pp. 147–162.

O. Willi and P. H. Y. Lee, "Filamentation of an Annular Laser Beam in a Short Wavelength Laser Produced Plasma," *Opt. Commun.* **55**, 1985, p. 120.

O. Willi, P. H. Y. Lee, and Z. Lin, "Non-Uniform Shock Break-Through of Laser Irradiated Targets," *Opt. Commun.* **53**, 1985, p. 225.

J. O. Willis, J. D. Thompson, J. L. Smith, and Z. Fisk, "Magnetoresistance and Upper Critical Magnetic Field of ^{13}CBe Under Pressure," accepted for publication by *J. Magn. & Magn. Mater.*

J. O. Willis, J. D. Thompson, Z. Fisk, A. DeVisser, J. J. M. Franse, and A. Menovsky, "Effect of Pressure on Spin Fluctuations and Superconductivity in Heavy-Fermion UPt_3," *Phys. Rev. B* **31**, 1985, pp. 1654–1656.

M. S. Wire, J. D. Thompson, and Z. Fisk, "Influence of Spin Fluctuations on the Electrical Resistance of UAl_2 and UPt_3 at High Pressures and Low Temperatures," *Phys. Rev. B* **30**, 1984, pp. 5591–5595.

S. A. Wood, J. L. Matthews, G. A. Rebka, P. A. M. Graan, H. J. Ziock, and D. A. Clark, "Inclusive Pion Double Charge Exchange in ^{16}O and ^{40}Ca," *Phys. Rev. Lett.* **54**, 1985, pp. 635–638.

J. D. Zumbro, R. A. Naumann, M. V. Hoehn, W. Reuter, E. B. Shera, C. E. Bemis, and Y. Tanaka, "E2 and E4 Deformations in ^{232}Th and ^{239,240,242}Pu," *Phys. Lett.* **167B**, 1986, pp. 383–387.

J. D. Zumbro, E. B. Shera, M. V. Hoehn, W. Reuter, Y. Tanaka, R. M. Steffen, C. E. Bemis, and R. A. Naumann, "E2 and E4 Deformations in ^{233,234,235,238}U," *Phys. Rev. Lett.* **53**, 1984, p. 1888.

PROCEEDINGS AND BOOK CHAPTERS

P. R. Akkapeddi, P. Glenn, A. Fuschetto, Q. D. Appert, and V. K. Viswanathan, "Grazing Incidence Beam Expander," *Proceedings from the Southwest Conference on Optics*, SPIE **540**, 1985, pp. 94–103.

M. Aldissi, M. K. Hou, and J. N. Farrell, "Physical Characteristics of Diblock Polyacetylene Copolymers: Processability-Conductivity Correlation," Proceedings, ICSM '86 Conference, Kyoto, Japan, June 1–6, 1986, to be published in *Synthetic Materials*.

D. L. Arthur, G. Sullivan, E. R. Flynn, and S. J. Williamson, "Source Localization of the Long Latency Auditory Event-Related Magnetic Fields," 10th Annual Meeting of the Society for Neuroscience, in *Sc. Neurosci. Abstr.* **23**, 1986, p. 1278.

D. L. Arthur, G. Sullivan, E. R. Flynn, and S. J. Williamson, "Source Localization of the Long Latency Auditory Evoked Magnetic Field in Human Temporal Cortex," Proceedings, 8th International Conference on Event-Related Potentials of the Brain (EPIC VIII), to be published as a supplement to *Journal of Electroencephalography and Clinical Neurophysiology*.

D. R. Bach, M. A. Yates, S. C. Evans, D. W. Forslund, H. Kochler, and R. A. Zacharias, "Microwave and X-Ray Generation from CO_2 Laser Irradiated Targets," in *Laser Interaction and Related Plasma Phenomena* **7**, H. Horn and G. Miley, Eds., 1986, pp. 213–224.

G. C. Baldwin, *AIP Conference Proceedings* **146**, W. Stwalley and M. Lapp, Eds., 1986, pp. 6–9.

G. C. Baldwin, *X Ray Lasers*, P. Vaegli, and A. Sweare, Eds., Editions de Physique, Les Ulis Cedek, France, 1986, pp. 299–308.

G. C. Baldwin and M. S. Feld, *AIP Conference Proceedings* **146**, W. Stwalley and M. Lapp, Eds., 1986, pp. 26–30.

J. A. Barclay and S. Surangi, "Selection of Regenerator Geometry for Magnetic Refrigerator Applications," in *Proceedings, 5th Intersociety Cryogenics Symposium*, ASME, 1984, pp. 51–58.

R. J. Bartlett, W. J. Trela, S. H. Southworth, F. D. Michaud, R. Rothe, and R. W. Alkire, "VUV-Soft X-ray Beamline for Spectroscopy and Calibration," in *Proceedings, Optical & Optoelectronic Applied Sciences & Engineering* **689**, pp. 200 207.

W. Bauke, D. A. Clark, and P. B. Trujillo, "Optical Alignment to Set a Skewed Beamline for Neutrino Research at the LAMPF Accelerator," *Optical Alignment II*, SPIE, 1984, pp. 131 138.

W. Bauke and E. W. Cross, "Optical Tooling for the Functional Alignment of Tilted and Decentered Optical Trains," *Optical Alignment II*, SPIE, 1984, pp. 104 112.

W. Bauke and D. B. Stahl, "Installation Alignment of a Multi-Beam ICF Target Illumination System," *Proceedings from the Southwest Conference on Optics*, SPIE **540**, 1985, pp. 205 211.

S. C. Bender and Q. D. Appert, "Operational Performance of the Antares Alignment System," *Optical Alignment II*, SPIE, 1984, pp. 113 119.

T. M. Benjamin, P. S. Z. Rogers, J. C. Duffy, C. J. Maggiore, and J. R. Tesmer, "Development and Application of the Los Alamos Nuclear Microprobe Hardware, Software, and Calibration," in proceedings, *Microbeam Analysis*, San Francisco Press, 1985, pp. 235 239.

B. L. Berman, S. Datz, J. O. Kephart, R. K. Klein, R. H. Pantell, H. Park, R. L. Swent, M. J. Alguard, and M. V. Hynes, "Channeling Radiation from LiH and LiD," in *Bull. Am. Phys. Soc.* **30**, 1985, p. 373.

I. O. Bohachevsky, V. Viswanathan, and G. L. Woodlin, "Intelligent Optical Design Program," *Intelligence*, SPIE, 1984, pp. 104 112.

T. J. Bowles, "Time Reversal Invariance in Polarized Neutron Beta Decay," Investigation of Fundamental Interactions with Cold Neutrons, in *NBS Special Publication 711*, 1986, pp. 69 74.

T. J. Bowles, J. C. Browne, J. Helffrich, D. A. Knapp, M. P. Maley, R. G. H. Robertson, and J. F. Wilkerson, "Beta Decay of Free Molecular Tritium," in *Proceedings of the International Symposium on Weak and Electromagnetic Interactions in Nuclei*, H. V. Klapdor, Ed., Springer-Verlag, Berlin, 1986, pp. 782 785.

R. E. Brown, "An Experiment to Measure the Gravitational Force of the Antiproton," in *Low Energy Antimatter (Workshop on the Design of a Low-Energy Antimatter Facility in the USA)*, D. B. Cline, Ed., World Scientific, Singapore, 1986, pp. 105 119.

R. E. Brown, "Proposed Measurement of the Gravitational Acceleration of the Antiproton," in *Intersections Between Particle and Nuclear Physics*, D. F. Geesaman, Ed., AIP Conference Proceedings No. 150, American Institute of Physics, New York, 1986, pp. 436 444.

R. E. Brown and N. Jarmie, "Hydrogen Fusion-Energy Reactions," International Conference on Nuclear Data for Basic and Applied Science, in *Radiation Effects* **92-96**, 1986, p. 45.

R. R. Brown and J. R. Parker, "High Speed Electronic Imaging Application in Aeroballistic Research," in *Proceedings of the 2nd Conference on High Speed Photography, Videography, and Photonics* SPIE, 1984, pp. 95 108.

G. H. Canavan, "Strategic Defense Concepts for Europe," and "Quantitative Issues in Theater Missile Defense," *Swords & Shields*, Yost, Wohlstetter, and Hoffman, Eds., European/American Institute, Lexington Books, Boston, Spring 1987.

G. H. Canavan, "Theater Applications of Strategic Defense Concepts," in *Swords & Shields*, Yost, Wohlstetter, and Hoffman, Eds., European/American Institute, Lexington Books, Boston, Spring 1987.

S. Clearwater, G. J. V. Papcun, D. A. Clark, and P. Clout, "Developing an Expert System to Control a Beam Line at the Los Alamos Meson Physics Facility," Proceedings, 2nd International Workshop in Accelerator Control Systems, in *Nucl. Instrum. & Methods Phys. Res.* **A247**, June 1986.

B. T. Cleveland, R. Davis, Jr., and J. K. Rowley, "The Chlorine and Bromine Solar Neutrino Experiments," in *Proceedings of the Second International Symposium on Resonance Ionization Spectroscopy and Its Applications*, G. S. Hurst and M. G. Payne, Eds., Institute of Physics Conference Series (71), 1984.

G. Cort and D. M. Barrus, "Configuration Management for Mission-Critical Software The Los Alamos Solution," in *Proceedings, Softool Users Group*, Santa Barbara, California, September 10 11, 1984, pp. 85 94.

G. Cort, J. A. Goldstone, R. O. Nelson, R. B. Poore, L. B. Miller, and D. M. Barrus, "Development Methodology for Scientific Software," 4th Biennial Conference on Real-Time Computer Applications in Nuclear & Particle Physics, in *IEEE Transactions on Nuclear Science* **NS-32**, 1985, pp. 1439–1443.

G. Cort and R. O. Nelson, "Los Alamos Software Development Tools," in *Proceedings, DECUS*, Anaheim, California, January 1986, pp. 391–394.

G. Cort and R. O. Nelson, "Los Alamos Tool-Oriented Software Development Methodology," in *Proceedings, DECUS*, Anaheim, California, January 1986, pp. 395–402.

G. Cort and R. O. Nelson, "Modular, Automated Software Testing Environment," in *Proceedings, Softool User's Group Meeting*, Culver City, California, March 1986, pp. 21–30.

R. Davis, Jr., B. T. Cleveland, J. C. Evans, Jr., and J. K. Rowley, "Results from the Chlorine Solar Neutrino Experiment," in *Bull. Am. Phys. Soc.* **29**, 1984, p. 731.

R. Davis, Jr., B. T. Cleveland, and J. K. Rowley, "Report on Solar Neutrino Experiments," in *Am. Inst. of Phys. Conf. Proc.* **123**, 1984, pp. 1037–1050.

R. H. Day, R. L. Blake, G. L. Stradling, W. J. Trela, and R. J. Bartlett, "Los Alamos X-Ray Characterization Facilities for Plasma Diagnostics," in *Proceedings, Optical & Optoelectronic Applied Sciences & Engineering* **689**.

J. L. Dehmer, A. C. Parr, and S. H. Southworth, "Resonances in Molecular Photoionization," *Handbook on Synchrotron Rad.*, Vol. II, G. V. Marr, Ed., North-Holland, Amsterdam, in press.

T. W. Dombeck, "The Production of Slow Neutrons Using Doppler-Shifting from a High Speed Rotor and Their Applications in Fundamental Research," *Proceedings, Conference on Cold Neutrons*, G. L. Greene, Ed., NBS Special Publication No. 711, 1985.

P. Dyer, "Nuclear Isomer Separation," *Proceedings, First International Laser Science Conference*, W. C. Stradley and M. Lapp, Eds., AIP Conference Series, 1986, pp. 33–36.

E. L. Fireman, B. T. Cleveland, R. Davis, Jr., and J. K. Rowley, "Cosmic-Ray Depth Studies at the Homestake Mine with ^{39}K-^{37}Ar Detectors," in *Am. Inst. Phys. Conf. Proc.* **126**, M. L. Cherry, W. A. Fowler, and K. Lande, Eds., 1985, pp. 22–31.

C. M. Fowler, E. L. Zimmerman, C. E. Cummings, R. F. Davidson, E. Foley, R. S. Hawke, J. F. Kerrisk, J. V. Parker, W. M. Parsons, D. R. Peterson, N. M. Schnurr, and P. M. Stanley, "Railguns Powered by Explosive Driven Flux Compression Generators," 3rd Symposium on Electromagnetic Launch Technology, 1986, published in *IEEE Transactions on Magnetics*.

T. J. Goldman, K. E. Schmidt, and G. J. Stephenson, Jr., "Nuclear-Like States of Quark Matter," in *Intersections Between Particle and Nuclear Physics*, D. F. Geesaman, Ed., AIP Conference Proceedings No. 150, American Institute of Physics, New York, 1986, p. 773.

L. Golub, E. Spiller, R. J. Bartlett, M. Hockaday, D. R. Kania, W. J. Trela, "X-Ray Tests of Multilayer Coated Optics," *Proceedings, 3rd Topical Meeting on Optical Interference Coatings*, Optical Society of America, 1984, pp. TUA-B3-1–B3-4.

J. A. Hanlon, J. McLeod, J. E. Sollid, W. W. Horn, R. E. Carmichael, B. L. Kortegaard, G. L. Woodfin and L. A. Rosocha, "Aurora Project Optical Design for a Kilojoule Class Krypton Fluoride Laser," *Proceedings from the Southwest Conference on Optics*, SPIE **540**, 1985, pp. 284–289.

W. C. Haxton and G. J. Stephenson, Jr., "Double Beta Decay," in *Progress in Particle and Nuclear Physics*, Vol. 12, Sir Denys Wilkinson, Ed., Pergamon Press, New York, 1984, pp. 409–479.

W. C. Haxton and G. J. Stephenson, Jr., "Nuclear Structure Problems in Double Beta Decay," in *Neutrino Mass and Low Energy Weak Interactions*, World Scientific, Philadelphia, 1985, pp. 149–155.

R. H. Heffner, "Muon Spin Relaxation," in *1987 Yearbook of Science and Technology*, McGraw Hill, New York, 1986.

M. P. Hockaday, R. L. Blake, J. S. Grosso, M. M. Selph, M. M. Klein, W. Matuska, M. A. Palmer, and R. J. Liefeld, "Preliminary Investigation of Changes in X-Ray Multilayer Optics Subjected to High Radiation Flux," in *Proceedings, Applications of Thin-Film Multilayered Structures to Figured X-Ray Optics*, SPIE, 1985, pp. 61–64.

A. Hopkins, R. E. Kelly, L. D. Looney, and P. B. Lyons, "Transient Attenuation in Optical Fibers," *Proceedings of 2nd Fiber Optics in Adverse Environments*, SPIE **506**, pp. 209–216.

S. D. Howe and M. V. Hynes, "Antimatter Propulsion: Status and Prospects," in *Manned Mars Missions Working Group Papers*, NASA M002, Vol. II, June 1986, pp. 836-855.

J. A. Howell and R. M. Wright, "Language Features That Aid the Development of Reliable, Maintainable Control System Software," Proceedings, 2nd International Workshop in Accelerator Control Systems, published in *Accelerator Control Systems*, P. N. Clout and M. Crowley-Milling, Eds., North-Holland, Amsterdam, 1986, pp. 239-241.

M. V. Hynes, "Physics with Low Temperature Antiprotons," *Proceedings of the 3rd Lear Workshop, Tignes, France, January 19-26, 1985*, Los Alamos National Laboratory document LA-UR-85-1060.

N. Jarmie, "Low-Energy Nuclear Reactions with Hydrogen Isotopes," Application of Accelerators in Research & Industry, in *Bull. Am. Phys. Soc.* **29**, 1984, p. 1087.

N. Jarmie, "A Measurement of the Gravitational Acceleration of the Antiproton - An Experimental Overview," Application of Accelerators in Research and Industry, in *Bull. Am. Phys. Soc.* **31**, 1986, p. 1275.

N. Jarmie, R. E. Brown, I. Slaus, J. M. Lambert, P. A. Treado, T. A. Treado, and F. D. Correll, "Some Quasifree and Final-State Interactions in ^{2}H(t,pt)n Reaction at 18 and 24 MeV," in *Bull. Am. Phys. Soc.* **29**, 1984, p. 701.

N. Jarmie and R. E. Brown, "D(d,p)T and D(d,n)^{3}He Reactions for Ed = 20-117 keV," in *Bull. Am. Phys. Soc.* **31**, 1986, p. 1275.

L. A. Jones, "Non-Thermal Effects in a Hot Dense Plasma," 3rd International Conference/Workshop on the Radiative Properties of Hot Dense Matter, published in *Radiative Properties of Hot Dense Matter III*, World Scientific, 1987.

N. Kalantar-Nayestanaki, H. Baghaei, W. Bertozzi, S. Dixit, C. Hyde-Wright, S. Kowalski, R. W. Lourie, C. P. Sargent, P. Ulmer, L. Weinstein, J. M. Finn, M. V. Hynes, and B. L. Berman, "Magnetic Structure of ^{17}O at High Momentum," in *Bull. Am. Phys. Soc.* **31**, 1986, p. 876.

P. W. Keaton, "Can the U.S. Afford a Lunar Base?" in Proceedings, NASA Workshop on Astronomical Observations from a Lunar Base, Houston, Texas, January 10, 1986, in press.

P. W. Keaton, "A Moon Base/Mars Base Transportation Depot," *Lunar Bases and Space Activities of the 21st Century*, W. W. Mendell, Ed., Lunar and Planetary Institute, Houston, Texas, 1985, pp. 141-154.

P. W. Keaton and M. B. Duke, "A Lunar Laboratory," in Proceedings, XXVI Meeting of the Committee on Space Research (COSPAR), Toulouse, France, June 30-July 12, 1986.

P. W. Keaton and D. J. Tubb, "Nuclear Elective Propulsion," in *Manned Mars Missions Working Group Papers*, NASA M002, Vol. I, June 1986, pp. 129-141.

R. E. Kelly, P. B. Lyons, and L. D. Looney, "Radiation Induced Time Dependent Attenuation in a Fiber," *Proceedings of Optical Fiber Characteristics and Standards*, 2nd International Technical Symposium on Optical and Electro-Optical Applied Sciences and Engineering, 1985, pp. 61-69.

W. W. Kinnison, J. W. Lillberg, E. C. Milner, R. J. McKee, H. J. Ziock, H. L. Anderson, M. J. Yang, and A. Zehnder, "A High-Statistics Normal Muon Decay Experiment," in *Proceedings of the Workshop in Fundamental Muon Physics: Atoms, Nuclei, and Particles, Los Alamos National Laboratory, Los Alamos, New Mexico, January 20-22, 1986*, Los Alamos National Laboratory report LA-10714-C.

D. A. Knapp, T. J. Bowles, J. C. Browne, T. H. Burritt, R. G. H. Robertson, S. T. Staggs, and J. F. Wilkerson, "Status of the Los Alamos National Laboratory Free Atomic Tritium Beta Decay Experiment," in *Bull. Am. Phys. Soc.* **30**, 1985, p. 1272.

D. A. Knapp, T. J. Bowles, J. F. Wilkerson, T. H. Burritt, R. G. H. Robertson, J. C. Browne, J. S. Cohen, R. L. Martin, M. P. Maley, and J. A. Helfrich, "Los Alamos Free Atomic Tritium Beta Decay Experiment," *Neutrino Mass and Low Energy Weak Interactions*, V. Barger and D. Cline, Eds., World Scientific, Singapore, 1985, pp. 57-62.

P. E. Koehler, S. A. Wender, and J. S. Kapustinsky, "Improvements in the Energy Resolution and High-Count-Rate Performance of Bismuth Germanate," 6th Symposium on X- and Gamma-Ray Sources and Applications, published in *Nucl. Instrum. & Methods* **A242**, 1986, p. 369.

G. A. Kyrala, J. S. McGurn, J. H. Calligan, and J. Pallone, "Fast Framing Camera with Independent Frame Adjustments," *Proceedings of High Speed Photography, Videography, and Photonics III*, SPIE, 1985, pp. 36–40.

J. W. Lillberg, W. W. Kinnison, R. J. McKee, and H. L. Anderson, "A Multiwire Proportional Chamber-Based System for Digitizing Electrophoretic Gels," Proceedings, 4th Wire Chamber Conference, published in *Nucl. Instrum. & Methods Phys. Res. Sect. A* **252**, 1986, pp. 251–254.

T. R. Loree, R. R. Showalter, T. M. Johnson, J. M. Telle, R. A. Fisher, and W. M. Hughes, "E-Beam-Induced Fluorescence of Excimers in Cryogenic Solutions," *Proceedings from the Southwest Conference on Optics*, SPIE **540**, 1985, pp. 279–283.

D. M. Manley, B. L. Berman, W. Bertozzi, J. M. Finn, F. W. Hersman, C. Hyde-Wright, M. V. Hynes, J. Kelly, M. A. Kovash, S. Kowalski, R. W. Lourie, B. Murdock, B. E. Norum, B. Pugh, and C. P. Sargent, "Inelastic Electron Scattering from ^{17}O and ^{18}O," in *Bull. Am. Phys. Soc.* **31**, 1986, p. 877.

W. C. Mead, S. Coggeshall, S. R. Goldman, E. K. Stover, P. D. Goldstone, J. Cobble, A. Hauer, G. Stradling, J. M. Kindel, L. Montierth, C. Richardson, O. Barnouin, F. Marshall, R. Marjoribanks, P. Joanimagi, R. L. Kauffman, H. N. Kornblum, and B. F. Lasinski, "Analysis, Modeling, and Design of Short-Wavelength Laser-Plasma Experiments," in *Laser Interaction and Related Plasma Phenomena* **7**, H. Horn and G. Miley, Eds., 1986, pp. 723–744.

E. L. Miller, S. C. Bender, Q. D. Appert, A. C. Saxman, and T. A. Swann, "Long-Base Free Electron Laser Resonant Cavity," *Proceedings from the Southwest Conference on Optics*, SPIE **540**, 1985, pp. 235–239.

R. L. Mills, D. Schiferl, A. I. Katz, and B. W. Olinger, "New Phases and Chemical Reactions in Solid Carbon Monoxide Under Pressure," in *J. Physics Colloq.*, No. 8, 1984, pp. 187–190.

C. S. Mishra, B. M. Preedom, J. Escalante, M. Blecher, K. Gotow, W. Burger, R. L. Burman, M. V. Hynes, E. Piasetsky, and G. Giangaru, "Isospin Dependence of $\pi^{\pm}$ Elastic Scattering from Nickel Isotopes at 50 MeV," in *Bull. Am. Phys. Soc.* **29**, 1984, p. 131.

J. M. Moss, "Polarization Transfer in Inelastic Scattering and Pionic Models of the EMC Effect," in *Antinucleon- and Nucleon-Nucleus Interactions*, G. E. Walker, C. D. Goodman, and C. Olmer, Eds., Plenum Publishing Corp., 1985, pp. 249–260.

J. M. Moss, "Review of Proton Scattering and Reactions," International Nuclear Physics Conference, published in *Inst. Phys. Conf. Ser. No. 86*, IOP Publishing Ltd, 1987, pp. 41–60.

R. O. Nelson, D. M. Barrus, G. Cort, J. A. Goldstone, D. E. McMillan, R. V. Poore, and D. R. Machen, "FASTBUS Data Acquisition System for Neutron Time-of-Flight Measurements," in *IEEE Transactions on Nuclear Science* **NS-32**, 1985, p. 1.

R. O. Nelson, D. M. Barrus, G. Cort, J. A. Goldstone, D. E. McMillan, L. B. Miller, D. R. Machen, and R. B. Poore, "Configuration for the WNR Data Acquisition System for Neutron Measurements," 4th Biennial Conference on Real-Time Computer Applications in Nuclear & Particle Physics, in *IEEE Transactions on Nuclear Science* **NS-32**, 1985, p. 4.

J. W. Ogle, L. D. Looney, and R. T. Peterson, "Characterization of Fiber Optic Cables Under Large Tensile Loads," *Proceedings of 2nd Fiber Optics in Adverse Environments*, SPIE **506**, pp. 156–164.

J. W. Ogle, R. C. Smith, M. Ward, R. Ramsey, and J. S. Hollabaugh, "100 MHz Fiber Optic Single Transient Gamma Ray Detection System," in *Fiber Optics – Short-Haul and Long-Haul Measurements and Applications*, SPIE, 1984.

H. Park, J. O. Kephart, R. K. Klein, R. H. Pantell, M. V. Hynes, B. L. Berman, B. A. Dahling, S. Datz, R. L. Swent, and M. J. Alguard, "Temperature Dependence of Channeling Radiation," in *Bull. Am. Phys. Soc.* **30**, 1985, p. 374.

J. V. Parker and W. M. Parsons, "Experimental Measurement of Ablation Effects in Plasma Armature Railguns," 3rd Symposium on Electromagnetic Launch Technology, 1986, published in *IEEE Transactions on Magnetics*.

J. R. Parker, V. K. Viswanathan, and G. L. Woodfin, "Performance Evaluation of the Antares Reference Telescope System," *Proceedings from the Southwest Conference on Optics*, SPIE **540**, 1985, pp. 212–218.

W. M. Parsons, J. V. Parker, and J. R. Simms, "Lethality Test System," 3rd Symposium on Electromagnetic Launch Technology, 1986, published in *IEEE Transactions on Magnetics*.

J. C. Peng, "η-Meson Production Experiments at LAMPF," in *Intersections Between Particle and Nuclear Physics*, D. F. Geesaman, Ed., AIP Conference Proceedings No. 150, American Institute of Physics, New York, 1986, p. 630.

J. C. Peng, "Experiments on η-Meson Production," AIP Conference Proceedings No. 133, American Institute of Physics, New York, 1985, pp. 255–270.

J. C. Peng, "P-Nucleus Interaction," in *Intersections Between Particle and Nuclear Physics*, D. F. Geesaman, Ed., AIP Conference Proceedings No. 150, American Institute of Physics, New York, 1986, p. 499.

A. G. Petschek, "Neutrino Measurements on the Moon," *Lunar Bases and Space Activities of the 21st Century*, W. W. Mendell, Ed., Lunar and Planetary Institute, Houston, Texas, 1985, pp. 345–347.

R. B. Poore, D. M. Barrus, G. Cort, J. A. Goldstone, L. B. Miller, and R. O. Nelson, "Data Acquisition Command Interface Using VAX/VMS DCL," 4th Biennial Conference on Real-Time Computer Applications in Nuclear & Particle Physics, in *IEEE Transactions on Nuclear Science* **NS-32**, 1985, p. 4.

R. E. Prael, M. V. Hynes, S. D. Howe, and J. D. Stewart, "Potential Applicability of the Los Alamos Antiproton Research Program to Advanced Propulsion," *Proceedings of the 15th International Symposium for Space Technology and Science, Tokyo, Japan, May 19–23, 1986.*

C. E. Ragan III, B. C. Diven, M. Rich, W. A. Teasdale, and E. E. Robinson, "Precise Ultrahigh-Pressure Experiments," in *Proceedings of the American Physical Society 1983 Topical Conference on Shock Waves in Condensed Matter*, J. R. Asay, G. K. Straub, and R. A. Graham, Eds., North-Holland, Amsterdam, 1984, pp. 77–80.

M. C. Richardson, G. Gregory, R. L. Keck, S. A. Letzring, R. S. Marjoribanks, F. Marshall, G. Pien, J. S. Wark, B. Yaakobi, P. D. Goldstone, A. Hauer, G. L. Stradling, B. L. Henke, and P. A. Jaanimagi, "Time-Resolved X-Ray Diagnostics for High Density Plasma Physics Studies," in *Laser Interactions and Related Plasma Phenomena* **7**, H. Hora and G. Miley, Eds., 1986, pp. 179–211.

R. G. H. Robertson, "Measurements of Neutrino Mass," Aspen Winter Physics, published in *Ann. N. Y. Acad. Sci.* **461**, 1986, pp. 564–581.

R. G. H. Robertson, "Review of the Physics of the Neutrino," in *Intersections Between Particle and Nuclear Physics*, D. F. Geesaman, Ed., AIP Conference Proceedings No. 150, American Institute of Physics, New York, 1986, pp. 115–126.

H. Robinson, G. J. Russell, K. D. Williamson, Jr., and F. J. Edeskuty, "Los Alamos Liquid Hydrogen Neutron-Moderator System," in *Proceedings, Symposium on Cryogenic Properties, Processes and Applications 1986* **82**, AIChE, 1986, pp. 172–176.

J. K. Rowley, B. T. Cleveland, and R. Davis, Jr., "The Chlorine Solar Neutrino Experiment," AIP Conference Proceedings No. 126, M. L. Cherry, W. A. Fowler, and K. Lande, Eds., American Institute of Physics, New York, 1985, pp. 1–21.

S. Sarangi and J. A. Barclay, "Analysis of Compact Heat Exchanger Performance," *American Society of Mechanical Engineers, Winter Meeting*, 1984, pp. 37–44.

K. E. Schmidt, T. J. Goldman, and G. J. Stephenson, Jr., "Quark Tunneling Effects in He," in *Bull. Am. Phys. Soc. Ser. II* **29**, 1984, p. 1984.

N. M. Schnurr, J. F. Kerrisk, and J. V. Parker, "Numerical Predictions of Railgun Performance Including the Effects of Ablation and Arc Drag," 3rd Symposium on Electromagnetic Launch Technology, 1986, published in *IEEE Transactions on Magnetics*.

P. A. Seeger, "Comparison of Collimation Systems for Small-Angle Neutron Scattering," International Conference on Neutron Scattering, published in *Physica* **136B**, 1986, pp. 106–109.

P. A. Seeger and J. Trewhella, "New Low-Q Diffractometer at the Los Alamos Scattering Center," Biophysical Society, published in *Biophys. J.* **49**, 1986, p. 473a.

W. O. Sellers and P. W. Keaton, "The Budgetary Feasibility of a Lunar Base," in *Lunar Bases and Space Activities of the 21st Century*, W. W. Mendell, Ed., Lunar and Planetary Institute, Houston, Texas, 1985, pp. 711–716.

R. N. Silver. "Goals of the HEEC'M Workshop." *Proceedings of the 1984 Workshop on High-Energy Excitations in Condensed Matter*. Vol. I. Los Alamos National Laboratory report LA-10227-C.

I. Slaus, I. Supek, Y. Koike, J. M. Lambert, P. A. Treado, F. D. Correll, R. E. Brown, R. A. Hardekopf, and N. Jarmie, " The Sensitivity of the d+α Breakup to n-p Forces," in *Tenth International Conference on Few Body Problems in Physics*. Vol. II. B. Zeitnitz, Ed., North-Holland, Amsterdam, 1984, pp. 565 566.

V. Smiley, B. M. Whitcomb, M. Perrassini, D. Whitaker, R. L. Flurer, C. W. Colburn, P. B. Lyons, J. W. Ogle, and L. D. Looney, "Optical Characterization of Radiation-Resistant Fibers," in *Proceedings of 2nd Fiber Optics in Adverse Environments*, SPIE **506**, pp. 22 28.

G. J. Stephenson, Jr., T. J. Goldman, and K. E. Schmidt, "Exchange Corrections to the Quark Basis Calculation of ^{4}He," in *Bull. Am. Phys. Soc. Ser. II* **130**, 1985, p. 1260.

R. D. Stine, W. T. Leland, C. R. Mansfield, L. A. Rosocha, J. Jansen, R. B. Gibson, and G. R. Allen, "Development of the Antares Electron Gun," in Proceedings, International Symposium on Discharges and Electrical Insulation in Vacuum, published in *IEEE Transactions on Electrical Insulation* **EI-20** (4), August 1985, pp. 781 788.

G. L. Stradling, "Workshop on Standards for Photonic Streak Camera Characterization," *Proceedings of High Speed Photography, Videography, and Photonics III* SPIE **159**, 1985, pp. 136 140.

G. L. Stradling, T. R. Hurry, E. R. Denbow, M. M. Selph, and F. P. Ameduri, "Forge A Short Pulse X-Ray Diagnostic Development Facility," in *Proceedings of High Speed Photography, Videography, and Photonics III*, SPIE **159**, 1985, pp. 196 200.

G. L. Stradling and J. C. Riordan, "Pulsed X-Ray Sources," in *X-Ray Data Booklet*, D. Vaughan, Ed., Lawrence Berkeley Laboratory Publication No. PUB-490 Rev., University of California, Berkeley, April 1986, pp. 4 18.

J. W. Sunier, K. D. Bol, M. R. Clover, R. M. DeVries, N. J. Digiacomo, J. S. Kapustinsky, P. L. McGaughey, G. R. Smith, W. E. Sondheim, M. Buenerd, J. Chauvin, D. Lebrun, P. Martin, and J. C. Dousse, "PS187 A Good Statistics Study of Antiproton Interactions with Nuclei: Preliminary Results," *Proceedings of the 7th European Symposium on Antiproton Interactions*, Adam Hilger, Ed., Durham, England, 1984, pp. 195 200.

L. R. Veeser, G. I. Chandler, and G. W. Day, "Fiber Optic Sensing of Pulsed Currents," Chapter 14 in *Photonics: High Bandwidth Analog Applications*, Jim Wang, Ed., SPIE Advanced Institute Series on Broadband Photonic Sensors, SPIE, Bellingham, Washington, 1986.

V. K. Viswanathan, A. C. Saxman, and G. L. Woodfin, "Resonator Optical Designs for Free Electron Lasers," *Proceedings from the Southwest Conference on Optics*, SPIE **540**, 1985, pp. 227 231.

P. B. Weiss, P. Black, H. Oona, and L. B. Sprouse, "Characterization of Electronic Streak Tubes Including One with Internal CCD Readout," *Proceedings, 16th International Conference on High Speed Photography and Photonics*, SPIE **491**, pp. 679 684.

S. A. Wender, H. R. Reiss, and G. C. Baldwin, "Predicted Changes in the Internal Conversion Rates of ^{119}Sn Due to Admixtures of Lower Multipole Order," in *Advances in Laser Science*, W. C. Stwally and M. Lapp, Eds., American Institute of Physics Press, 1986.

M. D. Wilke, N. S. P. King, N. T. Gray, D. Johnson, D. Esquibel, P. Nedrow, and S. P. Ishiwata, "Imaging Techniques Utilizing Optical Fibers and Tomography," *Proceedings, Fiber Optics and Laser Sensors III*, E. L. Moore and O. G. Ramer, Eds., SPIE **566**.

J. F. Wilkerson, T. J. Bowles, T. H. Burritt, D. A. Knapp, R. G. H. Robertson, J. C. Browne, J. C. Cohen, R. L. Martin, M. P. Maley, and J. A. Helffrich, "Status of the Los Alamos Free Atomic Tritium Beta-Decay Experiment," in *Proceedings of the Santa Fe Meeting*, T. Goldman and M. M. Nieto, Eds., World Scientific, Philadelphia, 1985, pp. 247 248.

S. L. Wipf, "Dipole Aperture and Superconductor Requirements," in *Accelerator Physics Issues for a Superconducting Super Collider*, UMHE 84-1, University of Michigan, 1984, pp. 167 170.

G. L. Woodfin and M. L. Feind, "Comparison of Four Methods of Interferogram Reduction and Interpretation," *Proceedings from the Southwest Conference on Optics*, SPIE **540**, 1985, pp. 69 75.

R. Woods, J. R. Tesmer, L. J. Rowton, W. B. Ingalls, G. A. Chaparro, G. R. Goosney, D. H. Shadel, and L. F. Hunt, "Status Report on the Los Alamos National Laboratory Ion Beam

Facility." Proceedings, Symposium of North-Eastern Accelerator Personnel, published in *Rev. Sci. Instrum.* **57** (5), May 1986, p. 815.

E. L. Zimmermann, C. M. Fowler, E. Foley, J. V. Parker, and P. M. Stanley, "Himass Electromagnetic Launcher at Los Alamos," 3rd Symposium on Electromagnetic Launch Technology, 1986, published in *IEEE Transactions on Magnetics*.

REPORTS

G. J. Berzins, A. H. Lumpkin, and H. L. Smith, *Inorganic Fluorescent Screen Properties Important for MeV Radiation Imagery*, Los Alamos National Laboratory report LA-10290-MS, November 1984.

R. R. Brown and J. R. Parker, *Conceptual Design and Analysis of High Speed Electronic Imaging*, Los Alamos National Laboratory report LA-10072-MS, March 1984.

M. Drosg, G. A. Haouat, W. Stoeffel, and D. M. Drake, *Differential Cross Sections of $^3H(p,n)^3He$ and of $^6Li(N,T)^4He$ By Using Triton Beams Between 5.95 and 19.15 MeV and a Reevaluation of the p-T Neutron Production Cross Sections up to 12 MeV*, Los Alamos National Laboratory report LA-10444-MS, October 1985.

M. Drosg, S. M. Muellner, P. W. Lisowski, D. M. Drake, and R. A. Hardefopf, *Cross Sections for Neutron-Producing Reactions Induced by 6 and 10 MeV Neutrons Incident*, Los Alamos National Laboratory report LA-10665-MS.

M. B. Duke, W. W. Mendell, and P. W. Keaton, *Report of the Lunar Base Working Group April 23–27, 1984*, Los Alamos National Laboratory publication LALP-84-43, August 1984.

W. C. Feldman, W. P. Aiello, D. M. Drake, and M. W. Herrin, *BDD II — An Improved Electron Dosimeter for the Global Positioning System*, Los Alamos National Laboratory report LA-10453-MS, May 1985.

M. V. Hoehn, J. F. Amann, H. S. Butler, W. K. Dawson, E. W. Hoffman, J. Hofteizer, M. Kaletka, W. W. Kinnison, T. Kozlowski, M. W. McNaughton, R. E. Mischke, M. A. Oothoudt, R. V. Poore, E. B. Shera, S. E. Turpin, and J. M. Wouters, *Long Range Planning Committee for LAMPF Computing Needs Report*, Los Alamos National Laboratory report LA-10103-MS, April 1984.

N. Jarmie, *Antimatter Gravitation Newsletters, March 18, 1986 and May 14, 1986*, Los Alamos National Laboratory publication LALP-86-20.

J. S. Kapustinsky, W. E. Sondheim, K. D. Bol, M. R. Clover, R. M. DeVries, N. J. DiGiacomo, and J. W. Sunier, *Position Sensitive Gas Counter Readout System*, Los Alamos National Laboratory report LA-10494-MS, July 1985.

P. W. Keaton, *Low-Thrust Rocket Trajectories*, Los Alamos National Laboratory report LA-10265-MS, December 1985.

P. W. Keaton and M. B. Duke, Eds., *Manned Mars Missions*, National Aeronautics and Space Administration report NASA M001, May 1986.

J. B. McClelland, A. Bacher, R. L. Boudrie, T. A. Carey, J. Donahue, C. D. Goodman, M. W. McNaughton, N. Tanaka, O. B. Van Dyck, and R. Werbeck, *Development Plan for the Nucleon Physics Laboratory Facility at LAMPF*, Los Alamos National Laboratory report LA-10278-MS, October 1984.

A. F. McGirt and J. F. Wilkerson, *C Compiler Relative Performance Benchmarks for the IBM Personal Computer*, Los Alamos National Laboratory report LA-10535-MS, August 1985.

J. D. Moses, D. B. Holtkamp, J. D. King, P. W. Lisowski, and J. E. Simmons, *Angular Distribution of Neutral Hydrogen Following Collisional Electron Detachment from Negative Hydrogen*, Los Alamos National Laboratory report LA-10326-MS, December 1984.

W. C. Overton, Jr., *Analysis of Magnetic Refrigeration Systems with Staged Regenerators Based on an Idealized Magnetic Material Entropy Model*, Los Alamos National Laboratory report LA-10676-MS, July 1986.

R. N. Silver, Comp., *Proceedings of the 1984 Workshop on High-Energy Excitations in Condensed Matter — Held at Los Alamos, New Mexico — February 13–15, 1984*, Los Alamos National Laboratory report LA-10227-C, Vol. 1, February 1985.

M. D. Wilke, K. R. Alrick, and S. Egdorf, *Subnanosecond Relative Timing System and Cable Measurements on the Atrisco Event*, Los Alamos National Laboratory report LA-10031-MS, November 1984.

G. J. Yates, B. H. Vine, I. Aeby, D. L. Dunbar, N. S. P. King, S. A. Jaramillo, N. N. Thayer, and B. W. Noel, *High-Resolution SIT TV Tube for Subnanosecond Image Shuttering*, Los Alamos National Laboratory report LA-9771-MS, November 1984.

TALKS AND PRESENTATIONS

S. F. Agnew, B. I. Swanson, L. H. Jones, R. L. Mills, and D. Schiferl, "Disproportionation of Nitric Oxide at High Pressure," Research at High Pressure, Meriden, New Hampshire, June 25–29, 1984, Los Alamos National Laboratory document LA-UR-84-1886.

M. Aldissi, S. F. Agnew, J. W. White, and J. N. Farrell, "Resonance Raman Scattering of Polyacetylene Vs. Finite Polyenes—Filling the Gap," American Chemical Society, Anaheim, California, September 7–13, 1986, Los Alamos National Laboratory document LA-UR-86-1303.

R. W. Alkire, A. C. Larson, P. J. Vergamini, J. E. Schirber, and B. Morosin, "High Pressure Single Crystal Neutron Diffraction (up to 20 kbar) Using a Pulsed Source—Preliminary Investigation of Tl_3PSe_4 at 15 kbar," Neutron Scattering Symposium, Berlin, West Germany, August 5–7, 1984, Los Alamos National Laboratory document LA-UR-84-735.

R. W. Alkire, A. C. Larson, P. J. Vergamini, J. E. Schirber, and B. Morosin, "Single Crystal Structure Determination of ReO_3 at 15 kbar," International Union of Crystallography, Hamburg, West Germany, August 9–18, 1984, Los Alamos National Laboratory document LA-UR-84-1889.

R. C. Allen, V. Bharadwaz, G. A. Brooks, H. H. Chen, F. J. Doe, R. Hausammann, H. J. Mahler, A. M. Rushton, K. C. Wang, T. J. Bowles, R. L. Burman, R. D. Carlini, D. R. F. Cochran, J. S. Frank, E. Piasetzky, V. D. Sandberg, D. A. Krakauer, and R. L. Talaga, "Preliminary Results of Electron Neutrino Electron Minus Scattering at LAMPF," Neutrino Physics and Astro-Physics, Dortmund, West Germany, June 1984, Los Alamos National Laboratory document LA-UR-84-2764.

Q. D. Appert, S. C. Bender, E. L. Miller, A. C. Saxman, and T. A. Swann, "Long Base Free Electron Laser Resonant Cavity," Southwest Conference on Optics '85, Albuquerque, New Mexico, March 4–8, 1985, Los Alamos National Laboratory document LA-UR-84-3376.

Q. D. Appert, E. L. Miller, A. C. Saxman, T. A. Swann, and V. K. Viswanathan, "High Energy Free Electron Laser Resonant Cavity," Quantum Electronics, Anaheim, California, June 18–24, 1984, Los Alamos National Laboratory document LA-UR-84-513.

D. L. Arthur, "Mapping of Cognitive Processing," Magnetoencephalography Conference: Applications to Cognitive Processing and Polygraphy, Washington, D.C., February 27–28, 1986.

D. L. Arthur, G. W. Sullivan, E. R. Flynn, and S. J. Williamson, "Source Localization of the Long Latency Auditory Evoked Magnetic Field in Human Temporal Cortex," Magnetoencephalography Conference: Applications to Cognitive Processing and Polygraphy, Washington, D.C., February 27–28, 1986, Los Alamos National Laboratory document LA-UR-86-1409.

D. R. Bach, D. E. Casperson, D. W. Forslund, F. B. Harrison, J. S. Ladish, K. R. Winn, and M. A. Yates, "Search for Very High Energy Electrons in an Underdense CO_2 Laser Plasma," Anomalous Absorption Conference, Charlottesville, Virginia, May 6–11, 1984, Los Alamos National Laboratory document LA-UR-84-697.

D. R. Bach, S. C. Evans, D. W. Forslund, M. A. Yates, H. Koehler, and R. A. Zacharias, "CO_2 Laser Generated Microwave Experiment," American Physical Society, Division of Plasma Physics, San Diego, California, November 3–8, 1985, Los Alamos National Laboratory document LA-UR-85-2661.

D. R. Bach, D. W. Forslund, and M. A. Yates, "High Power High Frequency Microwaves from CO_2 Laser Targets," American Physical Society, Division of Plasma Physics, Boston, Massachusetts, October 29–November 2, 1984, Los Alamos National Laboratory document LA-UR-84-3435.

G. C. Baldwin, "Present Status and Potential Applications for Gamma-Ray Lasers," International Congress of Pacific-Basin Chemical Societies, Symposium on Applications of the Mössbauer Effect, Honolulu, Hawaii, December 10–14, 1984.

G. C. Baldwin. "Critical Review of Gamma-Ray Laser Proposals." International Conference on Laser Science. Dallas, Texas. November 18–22, 1985. Los Alamos National Laboratory document LA-UR-85-2952.

G. C. Baldwin. "Kinetics of Proposed Gamma-Ray Lasers." 7th International Workshop on Laser Interaction. Monterey, California. October 28–November 1, 1985. Los Alamos National Laboratory document LA-UR-85-2951.

G. C. Baldwin. "Superradiance Approach to Coherent Gamma-Ray Sources." American Physical Society. Washington, D.C. April 23–26, 1984. Los Alamos National Laboratory document LA-UR-84-312.

G. C. Baldwin, M. S. Feld, J. P. Hannon, J. T. Hutton, and G. T. Trammell. "Mössbauer-Borrman Superradiance." X-Ray Lasers. Aussois, France. April 14–17, 1986. Los Alamos National Laboratory document LA-UR-86-2010.

E. O. Ballard, A. W. Ehler, E. A. Meyer, K. B. Riepe, and H. L. Rutkowski. "Ion Source Extractor Development for Heavy Ion Fusion." IEEE Conf. on Plasma Science. St. Louis, Missouri. February 7, 1984. Los Alamos National Laboratory document LA-UR-84-473.

E. O. Ballard, E. A. Meyer, and G. M. Brennan. "Brazing of Large Diameter, 85% Al_2O_3 Rings to Niobium Using an Active Metal Ticusil Process." 66th Annual AWS Convention. Las Vegas, Nevada. April 30, 1985. Los Alamos National Laboratory document LA-UR-85-1456.

E. O. Ballard, E. A. Meyer, H. Oona, K. B. Riepe, H. L. Rutkowski, R. P. Shurter, F. W. Van Haaften, D. C. Wilson, and S. Humphries. "Design Status of Heavy Ion Injector Program." Particle Accelerator Conference. Vancouver, Canada. May 13–16, 1985; 6th International Conference on High Power Particle Beam. Kobe, Japan. June 9–12, 1986. Los Alamos National Laboratory document LA-UR-85-4431.

J. A. Barclay. "Comparison of Efficiency of Gas and Magnetic Refrigerators." ASME/AICHE Heat Transfer. Niagara Falls, New York. August 5–8, 1984. Los Alamos National Laboratory document LA-UR-84-212.

J. A. Barclay. "Magnetic Refrigeration for Low Temperature Applications." Cryo-Cooler Conference. Boulder, Colorado. September 17–18, 1984. Los Alamos National Laboratory document LA-UR-84-2138.

J. A. Barclay. "Magnetic Refrigeration—The Promise and the Problems." Twenty-First Space Congress. Orlando, Florida. April 24–26, 1984. Los Alamos National Laboratory document LA-UR-84-745.

J. A. Barclay, W. C. Overton, and C. B. Zimm. "Thermomagnetic Properties of GdPd." Low Temperature Physics. Karlsruhe, West Germany. August 15–22, 1984. Los Alamos National Laboratory document LA-UR-84-1053.

J. A. Barclay, R. Chesebrough, M. Van Novat, W. C. Overton, Jr., S. Sarangi, W. F. Stewart, and C. B. Zimm. "Apparatus and Methods for Heat Capacity and Adiabatic Temperature Change Measurements on Soft Magnetic Materials from 4 to 600 K and in Magnetic Fields to 9 T." Calorimetry Conference. Asilomar, California. August 25–30, 1985. Los Alamos National Laboratory document LA-UR-85-1875.

J. A. Barclay, W. F. Stewart, W. C. Overton, R. D. Candler, and O. D. Harkleroad. "Experimental Results on a Low-Temperature Magnetic Refrigerator." Cryogenics Materials. Cambridge, Massachusetts. August 12–16, 1985. Los Alamos National Laboratory document LA-UR-85-2987.

R. J. Bartlett. "Session 4—Experimental Capabilities and Prospects." New Directions in Soft X-Ray Photoabsorption. Livermore, California. April 11–18, 1984. Los Alamos National Laboratory document LA-UR-84-2157.

R. J. Bartlett, D. R. Kania, and W. J. Trela. "Reflectance Measurements of Layered Synthetic Microstructures in the Soft X-Ray Regime." Materials Research Society Meeting. San Francisco, California. April 15–18, 1985. Los Alamos National Laboratory document LA-UR-84-3574.

R. R. Bartsch and H. A. Davis. "Observations of High-Power Microwave Emission from a Virtual Cathode Device." American Physical Society, Division of Plasma Physics. Boston, Massachusetts. October 29–November 1, 1984. Los Alamos National Laboratory document LA-UR-84-2141.

R. R. Bartsch, M. H. Baron, G. L. Bell, H. A. Davis, R. E. Kribel, E. G. Sherwood and R. M. Stringfield. "Calorimeter for Evaluation of an Intense Relativistic Electron Beam Microwave

Source," American Physical Society, Division of Plasma Physics, San Diego, California, November 4–8, 1985, Los Alamos National Laboratory document LA-UR-85-2690.

R. R. Bartsch, H. A. Davis, and R. E. Kribel, "Power and Mode Diagnostics for High-Power Microwave Sources with Over-Moded Output," High Temperature Plasma Diagnostics, Tahoe City, California, September 16–20, 1984, Los Alamos National Laboratory document LA-UR-84-2442.

R. R. Bartsch, H. A. Davis, E. G. Sherwood, and R. M. Stringfield, "Magnetically Insulated Transmission Line Pulse-Risetime Sharpener," 6th International Conference on High-Power Particle Beam, Kobe, Japan, June 9–12, 1986, Los Alamos National Laboratory document LA-UR-85-4053.

W. Bauke, "Application for Surveying Technology for the Alignment of Large Optical Systems," 1984 ASP-ACSM Convention, Washington, D.C., March 11–16, 1984, Los Alamos National Laboratory document LA-UR-84-34.

W. Bauke, D. A. Clark, and P. B. Trujillo, "Surveying and Optical Tooling Technologies Combined to Align a Skewed Beamline at the LAMPF Accelerator," ASP-ACSM Convention, Washington, D.C., March 10–15, 1985, Los Alamos National Laboratory document LA-UR-85-61.

W. Bauke and D. B. Stahl, "Optical Tooling for the Alignment of Large Multi-Beam Laser Support Structures," ASCM-ASPRS Convention, Washington, D.C., March 16–23, 1985, Los Alamos National Laboratory document LA-UR-85-3433.

F. Begay, "Technical Issues in SDI," University of Nebraska, March 19, 1986, Los Alamos National Laboratory document LA-UR-86-1079.

F. Begay, R. J. Faehl, D. R. Kania, and L. A. Jones, "Acceleration of Ions by Intense MeV Electron Beams," American Physical Society, Division of Plasma Physics, San Diego, California, November 4–8, 1985, Los Alamos National Laboratory document LA-UR-85-2711.

P. Bergem, M. Boschung, T. Q. Phan, G. Piller, A. Ruetschi, L. A. Schaller, L. Schellenberg, H. Schneuwly, M. V. Hoehn, and E. B. Shera, "New Evaluation of Muonic X-Ray Energies in ^{208}Pb," Heidelberg Conference on Nuclear Structure, Heidelberg, Germany, August, 1984.

T. Bergeman, C. Harvey, K. B. Butterfield, H. C. Bryant, G. Comtet, D. A. Clark, P. A. M. Gram, D. W. MacArthur, M. Davis, J. B. Donahue, J. Dayton, C. T. Stoors, and W. W. Smith, "Observation of the Stark Effect in n = 4 Level of Hydrogen in Fields up to 3 MV/cm," American Physical Society, Washington, D.C., April 23–26, 1984, Los Alamos National Laboratory document LA-UR-84-490.

B. S. Birmingham, R. R. Showalter, T. R. Loree, T. M. Johnson, and W. M. Hughes, "Molecular Xenon and Krypton Lasing in a Liquid Argon Host," CLEO/IQEC Conference on Lasers and Electro-Optics, XIV International Conference on Quantum Electronics, San Francisco, California, June 12, 1986, Los Alamos National Laboratory document LA-UR-86-1742.

I. O. Bohachevsky, T. P. Cotter, and V. K. Viswanathan, "Development of an Autonomous Design Program," Artificial Intelligence – From Outer Space Down to Earth, Huntsville, Alabama, October 15–16, 1985, Los Alamos National Laboratory document LA-UR-85-3616.

I. O. Bohachevsky, V. K. Viswanathan, and D. R. Rossbach, "Generalized Simulated Annealing in the Construction of 'Intelligent' Design Programs," Seminar on Stochastic Optimization, Oberlech, Austria, Los Alamos National Laboratory document LA-UR-86-1312.

B. E. Bonner, "Physics with Cold Antiprotons," American Physical Society, Houston, Texas, March 8–9, 1985.

H. Borges, J. D. Thompson, S. Horn, and R. D. Parks, "Variation of the Characteristic Temperature with Pressure in the Kondo Lattice Systems $CePt_2$ and $CeIr_2Si_2$," American Physical Society, Las Vegas, Nevada, March 31–April 4, 1986, Los Alamos National Laboratory document LA-UR-86-27.

C. D. Bowman, "Spallation Sources for Neutron Nuclear Physics," IAEA Advisory Group Meeting on Properties of Neutron Sources, Radium Khlopin Institute, Leningrad, USSR, June 9–13, 1986, Los Alamos National Laboratory document LA-UR-86-1874.

C. D. Bowman, J. D. Bowman, and V. Yuan, "Proposal for a High Sensitivity Search for T-Violation in Slow Neutron Resonances," Weak and Electromagnetic Interactions in Nuclei, Heidelberg, West Germany, July 1–5, 1986, Los Alamos National Laboratory document LA-UR-86-1873.

C. D. Bowman, S. A. Wender, and G. F. Auchampaugh, "Nuclear Physics in the 10-300 MeV Energy Range Using a Pulsed White Neutron Source," Neutron-Nucleus Collisions, Nuclear Structure

Probe, Glouster, Ohio, September 5–8, 1984, Los Alamos National Laboratory document LA-UR-84-3506.

J. D. Boyer and C.-Y. Huang, "Temperature Dependence of the Narrow Band Noise Integrated Intensity and Non-Linear Conductivity in $NbSe_3$ Between 77-144 K," American Physical Society, Baltimore, Maryland, March 25–29, 1985, Los Alamos National Laboratory document LA-UR-84-3974.

J. H. Brewer, M. Celio, D. R. Harshman, R. Kettel, S. R. Kreitzman, G. M. Luke, D. R. Noakes, R. E. Turner, E. J. Ansaldo, C. W. Clawson, K. M. Crowe, S. E. Kohn, S. R. Rosenblum, J. Smith, and C.-Y. Huang, "Determination of Very Slow Positive Muon Hop Rates in Copper by Longitudinal Field-Muon Spin Relaxation," 4th International Conference on Muon Spin Rotation, Relaxation, and Resonance, Uppsala, Sweden, June 23–27, 1986, Los Alamos National Laboratory document LA-UR-86-1851.

J. H. Brewer, D. P. Spencer, C.-Y. Huang, Y. J. Uemura, and H. S. Chen, "Muon Spin Relaxation in Amorphous Spin Glasses Palladium Iron Silside and Palladium Iron Phosphide," 4th International Conference on Muon Spin Rotation, Relaxation, and Resonance, Uppsala, Sweden, June 23–27, 1986, Los Alamos National Laboratory document LA-UR-86-1852.

J. H. Brewer, D. P. Spencer, C.-Y. Huang, Y. J. Uemura, and H. S. Chen, "Muon Relaxation in Amorphous Spin Glass $Pd_{75}Fe_5Si_{20}$," American Physical Society, Detroit, Michigan, March 26–30, 1984.

R. E. Brown, "Cold Antiprotons and Gravity," Colloquium: University of Manitoba Physics Department, Winnipeg, Canada, September 17, 1986; Seminar: University of Minnesota Physics Department, Minneapolis, Minnesota, September 19, 1986.

R. E. Brown, R. A. Hardekopf, and N. Jarmie, "Final Data and Thermonuclear Reactivities for the D(t,α)n Reaction at Low Energies," American Physical Society, Washington, D.C., April 23–26, 1984, Los Alamos National Laboratory document LA-UR-84-247.

R. E. Brown, N. Jarmie, and G. M. Hale, "Low Energy Fusion Reactions," LANL/LLNL Weapons Nuclear Physics Workshop, Livermore, California, September 25–27, 1984, Los Alamos National Laboratory document LA-UR-84-3429.

J. H. Brownell, I. R. Lindemuth, T. A. Oliphant, Jr., A. E. Greene, D. L. Weiss, R. F. Benjamin, D. J. Erickson, J. H. Goforth, H. Oona, A. Williamson, P. H. Y. Lee, R. H. Price, R. J. Trainor, and L. R. Veeser, IEEE Conference on Plasma Science, Pittsburgh, Pennsylvania, July 3–5, 1985, LA-UR-85-916.

R. M. Brugger, J. M. Carpenter, M. Loewenhaupt, and R. N. Silver, "High Energy Excitations," Scientific Opportunities with Advanced Facilities for Neutron Scattering, Shelter Island, New York, October 23–26, 1984, Los Alamos National Laboratory document LA-UR-85-1382.

M. D. Burrows, "No($A \rightarrow X$) Laser," Short Wavelength Chemical Laser Workshop, Charleston, South Carolina, November 13–15, 1984, Los Alamos National Laboratory document LA-UR-84-3400.

M. D. Burrows and S. J. Thomas, "Generation and Amplification of Single 5-ns Krypton Fluoride Pulses," CLEO '85 Meeting, Baltimore, Maryland, May 21–24, 1985.

K. B. Butterfield, H. C. Bryant, D. A. Clark, G. Comtet, J. B. Donahue, P. A. M. Gram, C. J. Harvey, D. W. MacArthur, and W. W. Smith, "H^-_{po} Shape Resonance in up to 2.5 MV/cm Electric Fields," Atomic Physics, Seattle, Washington, July 22–27, 1984, Los Alamos National Laboratory document LA-UR-84-1798.

K. B. Butterfield, D. A. Clark, J. B. Donahue, P. A. M. Gram, D. W. MacArthur, H. C. Bryant, C. Harvey, and W. W. Smith, "Stark Broadening of H^- Resonances in Large Electric fields," American Physical Society Meeting, University of Connecticut, May 30–June 1, 1984

R. S. Caird, Jr., D. J. Erickson, C. M. Fowler, R. F. Benjamin, A. H. Williams, J. G. Goforth, B. L. Freeman, L. R. Veeser, and F. S. Felber, "Tests of an Explosive-Driven Coaxial Generator," 5th IEEE Pulsed Power Conference, Arlington, Virginia, June 10–12, 1985, Los Alamos National Laboratory document LA-UR-85-1993.

S. E. Caldwell, R. A. Gentry, R. W. White, and S. W. Allison, "Measurement of Gas Density and Temperature Profiles in Uranium Hexafluoride Using Laser Induced Fluorescence," 6th Workshop on Gases in Strong Rotation, Tokyo, Japan, August 19–23, 1985, Los Alamos National Laboratory document LA-UR-85-2266.

S. E. Caldwell and S. K. Silson, "Scope Trace Centroid Determination," Seventh International Conference on Pattern Recognition, Montreal, Canada, July 30 August 2, 1984.

L. J. Campbell, D. B. Holtkamp, S. D. Howe, M. H. Holzscheiter, M. V. Hynes, N. S. P. King, and W. W. Saylor, "Potential Development of Advanced Power Sources Resulting from Current Antiproton Technology Research," 21st Intersociety Energy Conversion Engineering Conference, San Diego, California, August 25 29, 1986.

G. H. Canavan, "Areas of Agreement in Strategic Defense," Practical & Political Implications of BMD, Ditchley Park, England, June 28 30, 1985, Los Alamos National Laboratory document LA-UR-85-2277.

G. H. Canavan, "Centralization and Public Sector Approaches to Defense Technology," 1984 U.S. Military Academy Senior Conference, West Point, New York, May 31 June 2, 1984, Los Alamos National Laboratory document LA-UR-85-1855.

G. H. Canavan, "Comments on Strategic Defense," Ditchley Conference on Strategic Defense, Ditchley Park, England, June 28 30, 1985; International Symposium on Space Defense and Deterrence: The Security of Europe and the Alliance, National Assembly, Paris, France, October 18 19, 1985, Los Alamos National Laboratory document LA-UR-85-2972.

G. H. Canavan, "Comments on the Role of Scientists in Policy," Panel on Role of Scientist in Nuclear Age, California Institute of Technology, Pasadena, California, July 28, 1985, Los Alamos National Laboratory document LA-UR-85-2734.

G. H. Canavan, "Concepts for Strategic Defense," 5th International Seminar on Nuclear War, Erice, Italy, August 19 24, 1985, Los Alamos National Laboratory document LA-UR-85-2972.

G. H. Canavan, "Mathematics of Strategic Defense," Seminar at CNLS, Los Alamos, New Mexico, November 26, 1985, Los Alamos National Laboratory document LA-UR-85-4114.

G. H. Canavan, "Physics and Mathematics of Strategic Defense," UC-Physics Division Colloquium, Riverside, California, January 30, 1986, Los Alamos National Laboratory document LA-UR-86-303.

G. H. Canavan, "Theater Applications of Strategic Defense Concepts," DNA New Alternatives Workshop, San Francisco, California, May 15 16, 1985, Los Alamos National Laboratory document LA-UR-85-2245.

T. A. Carey, "Discussion Session Nucleon- and Antinucleon-Nucleus Inelastic Scattering and Charge Exchange," International Conference on Antinucleon- and Nucleon-Nucleus Interactions, Telluride, Colorado, March 17 21, 1985, Los Alamos National Laboratory document LA-UR-85-1512.

T. A. Carey, "Overview of Polarization in Intermediate Energy Nucleon-Nucleus Inelastic Scattering," 6th International Symposium on Polarization Phenomena in Nuclear Physics, Osaka, Japan, August 26 30, 1985, Los Alamos National Laboratory document LA-UR-85-2909.

T. A. Carey, K. W. Jones, J. B. McClelland, J. M. Moss, L. Rees, N. Tanaka, and A. D. Bacher, "Comparison of Pb and ^{2}H$\rightarrow \sigma \rightarrow q/\rightarrow \sigma x \rightarrow q$ Quasielastic Responses at $Q = 350$ MeV/c and the Low EMC Effect," American Physical Society, Washington, D.C., April 23 26, 1984, Los Alamos National Laboratory document LA-UR-84-356.

T. A. Carey, K. W. Jones, J. B. McClelland, J. M. Moss, L. Rees, N. Tanaka, and A. D. Bacher, "Polarization Transfer in Inelastic Scattering and Pionic Models of the EMC Effect," 6th International Symposium on Polarization Phenomena in Nuclear Physics, Osaka, Japan, August 26 30, 1985, Los Alamos National Laboratory document LA-UR-85-2047.

M. L. Cherry, B. T. Cleveland, R. Davis, Jr., and K. Lande, "A Program of Radiochemical Solar Neutrino Experiments," Summer Study on the Physics of the Superconducting Super Collider, Snowmass, Colorado, July 1986.

G. G. Christoph, P. G. Eller, J. D. Purson, R. A. Penneman, and G. H. Rinehard, "Crystal Structure Determination of Barium Plutonate by TOF Neutron Diffraction," International Conference on Neutron Scattering, Santa Fe, New Mexico, August 19 23, 1985, Los Alamos National Laboratory document LA-UR-85-1917.

G. G. Christoph, P. J. Vergamini, R. W. Alkire, and A. C. Larson, "Crystallography Using LAUE Time-of-Flight Neutrons," 11th International Conference on Crystallography, Erice, Italy, May 24 June 6, 1985, Los Alamos National Laboratory document LA-UR-85-2003.

J. A. Cizewski, D. G. Burke, R. E. Brown, E. R. Flynn, and J. W. Sunier, "Systematics of Proton Strength in Gold Nuclei," American Physical Society, Washington, D.C., April 23 26, 1984, Los Alamos National Laboratory document LA-UR-84-591.

D. A. Clark, K. B. Butterfield, J. B. Donahue, P. A. M. Gram, D. W. McArthur, H. C. Bryant, C. J. Harvey, and W. W. Smith, "Observation of Decay of $H^-(N = 2)$ Resonances to $H^0(n = 2) + e$ Using Stepwise Laser Excitations," XV DEAP, Division of Electron and Atomic Physics, May 30 June 1, 1984.

B. T. Cleveland, R. Davis, Jr., E. L. Fireman, and J. K. Rowley, "Status of Potassium Experiment to Measure Cosmic-Ray Background for Radiochemical Solar Neutrino Experiments," Workshop on Solar Neutrinos, Moscow, U.S.S.R., October 1 2, 1985.

M. R. Clover, "Calculation of Deuteron, Triton, Helion, and Alpha Spectra in Heavy Ion Collisions Within an INC Framework," American Physical Society Meeting, Washington, D.C., April 23 26, 1984.

M. R. Clover and N. J. Digiacomo, "Examination of Various Physical Effects on INC-Generated Pion Spectra in $P^- + {}^{40}Ca$ Annihilations at 175 MeV," American Physical Society, Washington, D.C., April 23 27, 1984. Los Alamos National Laboratory document LA-UR-84-355.

M. R. Clover, N. J. Digiacomo, and P. L. McGaughey, "Comparison of an INC Calculation of Pion and Kaon Spectra in $P^- + {}^{128}S$ Annihilations at 175 MeV to Recent Lear Data," American Physical Society, Washington, D.C., April 23 29, 1984. Los Alamos National Laboratory document LA-UR-84-351.

M. R. Clover and P. L. McGaughey, "Intra-Nuclear Cascade Results and Data for Composite Particle Production in Anti-Proton Annihilations," American Physical Society, Washington D.C., April 28 May 5, 1986. Los Alamos National Laboratory document LA-UR-86-429.

J. C. Cobble, P. D. Goldstone, A. Hauer, S. R. Goldman, W. C. Mead, G. Stradling, M. C. Richardson, and E. Kowaluk, "Gold X-Ray Spectra From UV-Laser-Produced Plasmas," American Physical Society, Division of Plasma Physics, San Diego, California, November 3 8, 1985, Los Alamos National Laboratory document LA-UR-85-3890.

S. A. Colgate and A. G. Petschek, "Expansion Degradation of Ultraviolet Photons in Supernova Ejecta," 167th Meeting of the American Astronomical Society, Houston, Texas, January 5 9, 1986, Los Alamos National Laboratory document LA-UR-85-3624.

S. A. Colgate and A. G. Petschek, "Gamma Ray Burst Model," 165th Meeting of the American Astronomical Society, Tucson, Arizona, January 13 16, 1985. Los Alamos National Laboratory document LA-UR-84-3358.

S. A. Colgate, A. G. Petschek, and P. D. Noerdlinger, "Gamma Burst from Field Free Neutron Stars," Stanford Workshop on Gamma Bursts, Stanford, California, July 1984, Los Alamos National Laboratory document LA-UR-84-3216.

D. W. Cooke, R. H. Heffner, R. L. Hutson, M. E. Schillaci, J. L. Smith, J. O. Willis, D. E. MacLaughlin, C. Boekema, R. L. Lichti, A. B. Denison, and J. Oostens, "Muon Spin Relaxation and Knight Shift in the Heavy-Fermion Superconductor UPt_3," 4th International Conference on Muon Spin Rotation, Relaxation, and Resonance, Uppsala, Sweden, June 23 27, 1986.

G. Cort, "Los Alamos Documentation Generation Tools," Fall 1985 U.S. DECUS Symposium, Anaheim, California, December 9 13, 1985, Los Alamos National Laboratory document LA-UR-85-3842.

G. Cort, "Los Alamos Hybrid Environment An Integrated Development/Configuration Management System," ACM Conference on Software Tools, New York City, April 15 17, 1985, Los Alamos National Laboratory document LA-UR-84-3935.

G. Cort, "Performance Programming with the Los Alamos Macro Accelerator," Softool User's Group, Santa Barbara, California, September 30 October 1, 1985, Los Alamos National Laboratory document LA-UR-85-3129.

G. Cort and J. A. Goldstone, "The Los Alamos Automated Configuration Accounting System: A Proposal," Softool User's Group Dallas, Texas, March 25 26, 1985 .

G. Cort and R. O. Nelson, "The Los Alamos Tool-Oriented Software Development System," Fall 1985 U.S. DECUS Symposium, Anaheim, California, December 9 13, 1985, Los Alamos National Laboratory document LA-UR-85-3843.

G. Cort, J. A. Goldstone, R. O. Nelson, R. V. Poore, and D. W. Barrus, "Dynamic Data Structures and Concurrency in a Real-Time Data Acquisition System," Real-Time Computer Applications in Nuclear and Particle Physics, Chicago, Illinois, May 20–24, 1985, Los Alamos National Laboratory document LA-UR-85-331.

G. Cort and R. O. Nelson, "A Modular, Automated Software Testing Environment," Softool Users' Group Meeting, Culver City, California, April 14–15, 1986, Los Alamos National Laboratory document LA-UR-86-964.

C. G. Davis, "Theoretical Study of Cepheid Light Curves," IAU Colloquium '82, Toronto, Canada, May 29–June 1, 1984, Los Alamos National Laboratory document LA-UR-84-1640.

C. G. Davis, "Radiative Transfer and Hydrodynamics in Pulsating Stars," IAU Colloquium '89, Copenhagen, Denmark, June 10–20, 1985, Los Alamos National Laboratory document LA-UR-85-1680.

C. G. Davis, G. Kovacs, and J. R. Buchler, "Time-Dependent Fourier Analysis, Application to Nonlinear Pulsations of Stellar Models," Stellar Pulsation, Los Alamos, New Mexico, August 11–15, 1986, Los Alamos National Laboratory document LA-UR-86-2479.

H. A. Davis and R. R. Bartsch, "Observations of High-Power Microwave Emission from a Virtual Cathode Device," IEEE Conference on Plasma Science, St. Louis, Missouri, May 14–16, 1984, Los Alamos National Laboratory document LA-UR-84-479.

H. A. Davis, R. R. Bartsch, E. G. Sherwood, and R. M. Stringfield, "Observation of High-Power Microwave Emission from Strongly Magnetized Virtual Cathode Sources," 13th IEEE International Conference on Plasma Science, Saskatoon, Canada, May 19–21, 1986, Los Alamos National Laboratory document LA-UR-86-550.

H. A. Davis, G. L. Bell, E. G. Sherwood, and R. M. Stringfield, "High-Power Microwave Emission from a Virtual Cathode Device," American Physical Society, Division of Plasma Physics, San Diego, California, November 4–8, 1985, Los Alamos National Laboratory document LA-UR-85-2691.

H. A. Davis, R. R. Bartsch, T. J. T. Kwan, E. G. Sherwood, and R. M. Stringfield, "Design of a Magnetized Virtual Cathode Microwave Generator," 13th IEEE International Conference on Plasma Science, Saskatoon, Canada, May 19–21, 1986, Los Alamos National Laboratory document LA-UR-86-551.

H. A. Davis, R. R. Bartsch, E. G. Sherwood, and R. Stringfield, "Observation of High-Power Microwave Emission From a Virtual Cathode Device," IEEE Conference on Plasma Science, Pittsburgh, Pennsylvania, June 3–5, 1985, Los Alamos National Laboratory document LA-UR-85-492.

H. A. Davis, R. R. Bartsch, E. G. Sherwood, and R. Stringfield, "Observation of High-Power Microwave Emission from Magnetized and Unmagnetized Virtual Cathode Sources," 6th International Conference on High-Power Particle Beam, Kobe, Japan, June 9–12, 1986, Los Alamos National Laboratory document LA-UR-85-4052.

G. W. Day, J. D. O. McFadden, L. R. Veeser, G. I. Chandler, and R. W. Cernosek, "Optical Fiber Sensors for the Measurement of Pulsed Electric Currents," NATO Advisory Group for Aerospace Research and Development, Ankara, Turkey, September 9–12, 1985, Los Alamos National Laboratory document LA-UR-85-2789.

G. W. Day, L. R. Veeser, G. I. Chandler, and R. W. Cernosek, "Progress in the Design of Optical Fiber Sensors for the Measurement of Pulsed Electric Currents," Measurement of Electrical Quantities in Pulsed Power Systems II, Gaithersburg, Maryland, March 5–7, 1986, Los Alamos National Laboratory document LA-UR-86-923.

R. H. Day, "Fiber Optics in X-Ray Diagnostics Applications," NATO Meeting, Castelvecchio Pascoli, Italy, July 10–24, 1985, Los Alamos National Laboratory document LA-UR-85-227.

R. H. Day, "High Energy X-Ray Diagnostics of Short Lived Plasmas," NATO Meeting, Castelvecchio Pascoli, Italy, July 10–24, 1985, Los Alamos National Laboratory document LA-UR-85-226.

R. H. Day, "Techniques of Absolute Low Energy X-Ray Calibration," SPIE '86, International Technical Symposium, San Diego, California, August 17–22, 1986, Los Alamos National Laboratory document LA-UR-86-2255.

R. H. Day and T. W. Barbee, "Application of Layered Synthetic Microstructures to High Temperature Plasma Diagnostics," High Temperature Plasma Diagnostics, Tahoe City, California, September 16–20, 1984, Los Alamos National Laboratory document LA-UR-84-2460.

R. H. Day and T. W. Barbee, "Application of Layered Synthetic Microstructures to High Temperature Plasma Diagnostics." Full paper submitted for proceedings at the 5th Topical Conference on High Temperature Diagnostics, Tahoe City, California, September 16–20, 1984.

N. J. Digiacomo, M. R. Clover, R. M. DeVries, J. S. Kapustinsky, P. L. McGaughey, W. E. Sondheim, and J. W. Sunier, "On a Discrepancy Between Pion Production on Nuclei at Low (E_p = 330, 400, 500 MeV) Proton Bombarding Energies & Predictions of an Intranuclear Cascade Calculation." American Physical Society, Washington, D.C., April 23–26, 1984. Los Alamos National Laboratory document LA-UR-84-353.

N. J. Digiacomo, R. M. DeVries, P. L. McGaughey, W. E. Sondheim, J. W. Sunier, J. Chauvin, M. Buenerd, D. Lebrun, P. Martin, and J. C. Dousse, "Low Energy Antiproton Annihilation in Nuclei." American Physical Society, Santa Fe, New Mexico, October 31–November 3, 1984. Los Alamos National Laboratory document LA-UR-84-2995.

R. S. Dingus and S. R. Goldman, "A Model for Optical-Laser-Induced Impulse in Vacuo." AIAA Laser Effects and Target Response Meeting, Stanford Research Institute, Menlo Park, California, November 5–7, 1985.

R. S. Dingus, T. R. King, W. Z. Osborne, and C. R. Phipps, Jr., "Single-Pulse Laser Effects Measurements at 248 nm." AIAA Laser Effects and Target Response Meeting, Stanford Research Institute, Menlo Park, California, November 5–7, 1985. Los Alamos National Laboratory document LA-UR-85-3901.

T. Dombeck, "Accelerator Based Neutrino Sources." Workshop on Cryogenic Detectors for Neutrinos and Dark Matter Candidates, Institute for Theoretical Physics, Santa Barbara, California, January 1986.

T. Dombeck, "Muon-Neutrino-Carbon Interactions Near the Muon Production Threshold." Division of Nuclear Physics Meeting, American Physical Society, Vancouver, Canada, 1986.

M. Drosg, P. W. Lisowski, R. A. Hardekopf, D. M. Drake, and K. Treitl, "Double Differential Neutron Emission Cross Sections of ^{10}Be and ^{11}Be at 6, 10, and 14 MeV and of ^{6}Li, ^{7}Li, and ^{12}C." International Conference on Nuclear Data for Basic and Applied Science, Santa Fe, New Mexico, May 13–17, 1985. Los Alamos National Laboratory document LA-UR-85-1743.

D. L. Dunbar, G. J. Yates, and J. P. Black, "Gated SIT Vidicon Streak Tube." SPIE's International Technical Symposium, San Diego, California, August 18–23, 1985. Los Alamos National Laboratory document LA-UR-85-2928.

P. Dyer, "Nuclear Isomer Separation and Resonance Ionization Spectroscopy." 3rd International Symposium on Resonance Ionization Spectroscopy and its Applications, Swansea, Wales, September 7–13, 1986. Los Alamos National Laboratory document LA-UR-86-1673.

R. Ecke, "Dimension and Entropy for Quasiperiodic and Chaotic Systems." Dimensions and Entropies in Chaotic Systems, Pecos, New Mexico, September 11–16, 1985. Los Alamos National Laboratory document LA-UR-85-3411.

R. Ecke, "Quasiperiodicity, Mode-Locking and Chaos in Rayleigh-Bénard Convection." University of California, Santa Cruz, February 10, 1986; Los Angeles, February 12, 1986. Los Alamos National Laboratory document LA-UR-86-452.

R. Ecke, H. Haucke, and J. C. Wheatley, "Nonlinear Dynamics and Chaos in Oscillatory Rayleigh-Bénard Convection." Perspectives on Nonlinear Dynamics Workshop, Silver Spring, Maryland, May 30, 1985. Los Alamos National Laboratory document LA-UR-85-2791.

R. Ecke, D. Umberger, and J. D. Farmer, "Fat Fractal Scaling in the Circle Map." Dynamics Day, La Jolla Workshop, La Jolla, California, January 6–10, 1985. Los Alamos National Laboratory document LA-UR-85-4081.

J. Eckert, "High Energy Phonons: Overview." 1984 Energy Excitations in Condensed Matter workshop, Los Alamos National Laboratory, February 13–15, 1984.

J. Eckert, "Neutron Vibrational Spectroscopy—The Use of Hydrogen as a Structural and Dynamical Probe." International Conference on Neutron Scattering, Santa Fe, New Mexico, August 19–23, 1985. Los Alamos National Laboratory document LA-UR-85-2649.

J. Eckert, "Program for International Conference on Neutron Scattering." Neutron Scattering, Santa Fe, New Mexico, August 19–23, 1985. Los Alamos National Laboratory document LA-UR-85-2650.

J. Eckert, "Studies of Surface Adsorbed Molecules and Hydrogen-Bonded Systems by Inelastic Neutron Scattering," Western Spectroscopy Association, Asilomar, California, January 30 February 1, 1985, Los Alamos National Laboratory document LA-UR-85-170.

J. Eckert, T. O. Brun, A. J. Dianoux, J. Howard, J. J. Rush, and J. W. White, "Chemical Spectroscopy," Scientific Opportunities with Advanced Facilities for Neutron Scattering, Shelter Island, New York, October 23 26, 1984, Los Alamos National Laboratory document LA-UR-85-783.

J. Eckert, B. H. Grier, L. Passell, H. Patterson, D. Richter, and R. Rollefson, "Structures and Dynamics of Ethylene Surface Layers on Graphite," Structure of Surfaces, Berkeley, California, August 13 16, 1984, Los Alamos National Laboratory document LA-UR-84-1366.

J. Eckert and J. Howard, "Neutron Spectroscopy of Molecules Adsorbed in Zeolites," American Crystallographic Association, Lexington, Kentucky, May 21 25, 1984, Los Alamos National Laboratory document LA-UR-84-799.

D. J. Erickson, B. L. Barthell, R. F. Benjamin, J. H. Brownell, C. A. Fenstermacher, J. H. Goforth, A. E. Greene, P. H. Y. Lee, I. R. Lindemuth, T. A. Oliphant, Jr., H. Oona, R. H. Price, B. R. Suydam, R. J. Trainor, L. R. Veeser, D. L. Weiss, and A. H. Williams, "Pioneer I Experiments Plasma Implosions from Explosive Pulsed Power," Megagauss Magnetic Field Generation, Santa Fe, New Mexico, July 14 17, 1986, Los Alamos National Laboratory document LA-UR-86-1452.

D. J. Erickson, J. H. Brownell, R. J. Trainor, and C. A. Fenstermacher, "High Energy Foil Implosions from Explosive Pulsed Power," 5th IEEE Pulsed Power Conference, Arlington, Virginia, June 10 12, 1985, Los Alamos National Laboratory document LA-UR-84-3895.

D. J. Erickson, R. S. Caird, Jr., B. L. Freeman, C. M. Fowler, J. H. Goforth, H. Oona, A. H. Williams, B. L. Barthell, D. V. Duchane, J. H. Brownell, A. E. Greene, I. R. Lindemuth, T. A. Oliphant, Jr., D. L. Weiss, R. H. Price, J. B. Van Marter, B. R. Suydam, W. T. Leland, and R. J. Trainor, "Design of FOIL Implosion System for Pioneer I Experiments," 5th IEEE Pulsed Power Conference, Arlington, Virginia, June 10 12, 1985, Los Alamos National Laboratory document LA-UR-85-2078.

J. N. Farrell and R. D. Taylor, "High Pressure Mössbauer Study of Intermediate Valence in Europium Oxide and Europium Metals," American Physical Society, Las Vegas, Nevada, March 31 April 4, 1986, Los Alamos National Laboratory document LA-UR-85-4313.

M. S. Fee, R. L. Blake, D. R. Kania, L. A. Jones, and M. D. Maestas, "Design and Application of a Doubly Curved Crystal Spectrograph To Obtain Imaged, Time Resolved Spectra of 3 4-keV X Rays," American Physical Society, Division of Plasma Physics, San Diego, California, November 4 9, 1985, Los Alamos National Laboratory document LA-UR-85-2591.

D. W. Feldman, R. W. Warren, J. S. Fraser, J. M. Watson, B. E. Carlsten, W. E. Stein, G. Spalek, A. H. Lumpkin, H. Takeda, T.-S. F. Wang, "Energy Recovery in the Los Alamos Free-Electron Laser," 8th International Free Electron Laser Conference, September 1 5, 1986, Glasgow, Scotland, Los Alamos National Laboratory document LA-UR-86-3490.

D. W. Feldman, R. W. Warren, B. E. Newnam, A. H. Lumpkin, W. E. Stein, M. T. Lynch, R. Lohsen, L. M. Young, B. D. McVey, J. C. Goldstein, H. Takeda, T. Wang, R. B. Feldman, S. C. Bender, J. M. Watson, and C. A. Brau, "Los Alamos Free-Electron Laser Experiment Current Status," 14th International Conference on Quantum Electronics, IQEC '86, San Francisco, California, June 9 13, 1986, Los Alamos National Laboratory document LA-UR-86-575.

J. F. Figueira, S. R. Foltyn, L. A. Rosocha, R. C. Sze, C. R. Tallman, J. M. Telle, and D. E. Watkins, "Recent Advances in Ultraviolet Laser Technology," Trends in Quantum Electronics, Bucharest, Hungary, September 2 6, 1985, Los Alamos National Laboratory document LA-UR-85-3560.

R. B. Fiorito, D. W. Rule, S. G. Iversen, P. A. Zagarino, P. E. Nash, J. S. Ladish, C. S. Young, S. E. Caldwell, H. H. Hsu, and J. M. Mack, Jr., "Transition Radiation Diagnostics for Intense Charged Particle Beams," High Power Particle Beam, Kobe, Japan, June 9 12, 1986, Los Alamos National Laboratory document LA-UR-86-677.

D. H. Fitzgerald, H. W. Baer, J. D. Bowman, F. Irom, N. S. P. King, M. J. Leitch, E. Piasetzky, W. J. Briscoe, M. E. Sadler, K. Smith, and J. N. Knudson, "Forward-Angle Cross Sections for Pion Nucleon Charge-Exchange Scattering at Momenta Between 100 and 150 MeV," American

Physical Society, Washington, D.C., April 23–26, 1984. Los Alamos National Laboratory document LA-UR-84-287.

G. Flik, K. Maier, H. Rempp, J. N. Bradbury, D. W. Cooke, M. Leon, M. A. Paciotti, M. E. Schillaci, R. H. Heffner, J. J. Reidy, C. Boekema, and H. Daniel, "Muon Channeling in Ge: Evidence for Pionium Formation," 4th International Conference on Muon Spin Rotation, Relaxation, and Resonance, Uppsala, Sweden, June 23–27, 1986. Los Alamos National Laboratory document LA-UR-86-2158.

R. L. Flurer, A. J. Cordi, C. W. Colburn, B. M. Whitcomb, and J. W. Ogle, "Characteristics of 850 nm Single Mode Fiber," SPIE '86, Optoelectronics and Fiber Optic Applications, Cambridge, Massachusetts, September 21–26, 1986. Los Alamos National Laboratory document LA-UR-86-1210.

E. R. Flynn and G. W. Sullivan, "Human Function Monitoring," Lunar Bases and Space Activities of the 21st Century, Washington, D.C., October 29–31, 1984. Los Alamos National Laboratory document LA-UR-84-2885.

C. M. Fowler, C. E. Cummings, R. F. Davidson, E. Foley, W. E. Fox, J. F. Kerrisk, J. V. Parker, W. M. Parsons, N. M. Schnurr, P. M. Stanley, and E. L. Zimmermann, "Rail Guns Driven by Helical Flux Compression Generators," Megagauss Magnetic Field Generation, Santa Fe, New Mexico, July 14–17, 1986. Los Alamos National Laboratory document LA-UR-86-388.

C. M. Fowler, C. E. Cummings, E. Foley, R. S. Hawke, J. F. Kerrisk, J. V. Parker, D. R. Peterson, W. M. Parsons, N. M. Schnurr, P. M. Stanley, and E. L. Zimmermann, "Explosively Driven Flux Compression Generators as Railgun Power Sources," 3rd Symposium on Electromagnetic Launch Technology, Austin, Texas, April 20–24, 1986. Los Alamos National Laboratory document LA-UR-85-4227.

C. M. Fowler, E. L. Zimmerman, C. E. Cummings, R. F. Davidson, W. E. Fox, J. F. Kerrisk, J. V. Parker, W. M. Parsons, N. M. Schnurr, P. M. Stanley, and J. P. Barber, "Rail Guns Driven by Helical Flux Compression Generators," 4th International Conference on Megagauss Magnetic Field Generation, Santa Fe, New Mexico, July 14-17, 1986. Los Alamos National Laboratory document LA-UR-86-2352.

M. M. Fowler, W. B. Ingalls, P. Lysaght, J. R. Tesmer, and J. B. Wilhelmy, "Accelerator Based Mass Spectrometry of Molecules," American Chemical Society, Chicago, Illinois, September 1985. Los Alamos National Laboratory document LA-UR-85-1177.

J. S. Frank, T. J. Bowles, R. L. Burman, R. D. Carlini, D. R. F. Cochran, E. Piasetzky, V. D. Sandberg, R. C. Allen, Jr., V. Bharadwaj, H. H. Chen, P. J. Doe, R. Hausammann, H. J. Mahler, K. C. Wang, and R. L. Talaga, "Observation of Neutrino Electron Elastic Scattering," High Energy Physics, Leipzig, East Germany, July 19–25, 1984. Los Alamos National Laboratory document LA-UR-84-2325.

B. L. Freeman, D. J. Erickson, C. M. Fowler, R. F. Hoeberling, J. C. King, P. J. Kruse, A. L. Peratt, D. G. Rickel, L. E. Thode, and J. W. Toevs, "Magnetic Flux Compression Generator Powered Electron Beam Experiments," 4th International Conference on Megagauss Magnetic Field Generation, Santa Fe, New Mexico, July 14–17, 1986. Los Alamos National Laboratory document LA-UR-86-2412.

B. L. Freeman, C. M. Fowler, J. C. King, A. R. Martinez, J. B. Van Marter, L. R. Veeser, and J. E. Vorthman, "Testing of the Mark 101 Magnetic Flux Compression Generator," 4th International Conference on Megagauss Magnetic Field Generation, Santa Fe, New Mexico, July 14–17, 1986. Los Alamos National Laboratory document LA-UR-86-2507.

Z. Gacsi, J. Sa, J. L. Weil, E. T. Jurney, and S. Raman, "Energy Levels of ^{116}Sn from (n,n'γ) and (n,γ) Reactions," American Physical Society, Nashville, Tennessee, October 18–20, 1984. Los Alamos National Laboratory document LA-UR-84-2495.

J. S. Gaffney, J. H. Hall, R. S. Rundberg, and B. R. Erdal, "Peroxyacyl Nitrates—Their Physical and Chemical Properties," American Chemical Society, Anaheim, California, September 7–13, 1986. Los Alamos National Laboratory document LA-UR-86-1220.

F. R. Gallegos, L. J. Morrison, and A. A. Browman, "Development of a Wide Dynamic Range Pulsed Beam Current Monitor System," Particle Accelerator, Vancouver, Canada, May 5, 1985. Los Alamos National Laboratory document LA-UR-84-3865.

A. I. Gavron, A. Gayer, J. G. Boissevain, H. C. Britt, J. R. Nix, A. J. Sierk, P. Grange, S. Hassani, H. Weidenmuller, J. R. Beene, B. Cheynis, D. Drain, R. L. Ferguson, F. E. Obenshain, F. Plasil, G. R. Young, and G. A. Petit, "Neutron Emission Prior to Fission," and "Heavy Ion Fission An Experimentalist's View," Winter Workshop on Nuclear Dynamics IV, Copper Mountain, Colorado, February 24 28, 1986; Argonne National Laboratory Symposium on the Many Facets of Heavy-Ion Fusion Reactions, March 24 26, 1986, Los Alamos National Laboratory document LA-UR-86-1045.

J. S. George, C. J. Aine, and E. R. Flynn, "Visual Processing of Spatial Frequency: Neuromagnetic Studies," The Association for Research in Vision and Opthamology, Sarasota, Florida, May 4 8, 1987, Los Alamos National Laboratory document LA-UR-86-4272.

R. B. Gibson, "Breakdown Processes in Large-Area Cold-Cathode Vacuum Triodes," Discharges & Electrical Insulation in Vacuum, Berlin, Germany, September 24 28, 1984, Los Alamos National Laboratory document LA-UR-84-2037.

R. B. Gibson, "High-Power Gas Laser Research at Los Alamos," Seminar at the University of Illinois, Urbana, Illinois, August 6, 1984, Los Alamos National Laboratory document LA-UR-84-2469.

R. B. Gibson, "High-Power Pulsed Gas Lasers for Inertial Fusion," Physics Department, United States Military Academy, West Point, New York, April 25, 1986, Los Alamos National Laboratory document LA-UR-86-1381.

R. B. Gibson, "Subpicosecond High-Brightness UV Laser System," SPIE Topical Meeting on High-Intensity Laser Processes, Quebec City, Canada, June 2 6, 1986, Los Alamos National Laboratory document LA-UR-86-1499.

S. J. Gitomer, J. F. Kephart, R. Kristal, and G. E. Eden, "Laser Plasma Interfaction Research with Antares," IEEE Conference on Plasma Science, St. Louis, Missouri, 1984, Los Alamos National Laboratory document LA-UR-84-867.

D. W. Glasgow, M. S. Moore, G. L. Morgan, N. S. P. King, K. R. Alrick, M. L. Sheppard, J. R. Streetman, G. M. Hale, J. H. Norman, L. R. Fawcett, C. D. Bowman, J. A. Harvey, N. W. Hill, and R. R. Spencer, "Los Alamos National Laboratory Neutron-Neutron Scattering Program," International Conference on Nuclear Data for Basic and Applied Science, Santa Fe, New Mexico, May 13 17, 1985, Los Alamos National Laboratory document LA-UR-85-1675.

R. P. Godwin, F. B. Harrison, and A. R. Larson, "Transient Absorption of Light Induced by Radiation," High-Power Laser Optical Components, Boulder, Colorado, May 1986, Los Alamos National Laboratory document LA-UR-86-1202.

J. H. Goforth, S. P. Marsh, I. R. Lindemuth, and H. W. Kruse, "Experiments with Multi-Megampere Explosively Formed Fuses in Cylindrical Geometry," 4th International Conference on Megagauss Magnetic Field Generation, Santa Fe, New Mexico, July 14 17, 1986, Los Alamos National Laboratory document LA-UR-86-2378.

J. H. Goforth and A. H. Williams, "Plasma Compression Opening Switch Experiment," IEEE Conference on Plasma Science, St. Louis, Missouri, February 7, 1984, Los Alamos National Laboratory document LA-UR-84-210.

S. R. Goldman, G. H. Canavan, R. S. Dingus, and M. Mahaffy, "Simulation of the Interaction of Single-Pulsed Optical Lasers with Targets in a Vacuum," Gas Flow and Chemical Lasers, Oxford, England, August 20 24, 1984, Los Alamos National Laboratory document LA-UR-84-2555.

S. R. Goldman, J. A. Cobble, N. Delamater, P. D. Goldstone, P. Jaanimagi, R. D. Jones, R. S. Marjoribanks, F. J. Marshall, W. C. Mead, M. C. Richardson, S. Skupsky, and G. L. Stradling, "High-Z Laser Target Interaction at $\lambda = 0.35$ μm," Anomalous Absorption, Lake Luzerne, New York, July 13 18, 1986, Los Alamos National Laboratory document LA-UR-86-1426.

S. R. Goldman, J. A. Cobble, N. Delamater, P. D. Goldstone, W. C. Mead, and G. L. Stradling, "Physics of High-Z Laser Target Interactions at $\lambda = 0.35$ μm," American Physical Society, Division of Plasma Physics, San Diego, California, November 4 8, 1985, Los Alamos National Laboratory document LA-UR-85-2657.

S. R. Goldman, S. L. Gitomer, R. A. Kopp, J. S. Saltzman, and R. S. Dingus, "Simulation of Laser-Target Interactions in a Vacuum," AIAA Laser Effects and Target Response Meeting, Stanford Research Institute, Menlo Park, California, November 5 7, 1985, Los Alamos National Laboratory document LA-UR-85-4047.

S. R. Goldman, P. D. Goldstone, W. C. Mead, and M. Richardson, "Energy Penetration and Profile Steepening in High-Z Plasmas," American Physical Society, Division of Plasma Physics, Boston, Massachusetts, October 29–November 2, 1984, Los Alamos National Laboratory document LA-UR-84-2150.

S. R. Goldman, P. D. Goldstone, W. C. Mead, and M. C. Richardson, "Energy Transport and Spatial Structure in High-Z Targets," Anomalous Absorption, Banff, Canada, June 1985, Los Alamos National Laboratory document LA-UR-85-1455.

T. J. Goldman, G. J. Stephenson, Jr., and G. B. West, "Effects of Quark Tunnelling on High Energy Lepton-Nucleus Scattering," American Physical Society, Washington, D.C., April 23–26, 1984, Los Alamos National Laboratory document LA-UR-84-252.

J. A. Goldstone, J. Eckert, E. L. Venturini, and P. M. Richards, "Temperature and Concentration Dependence of Hydrogen Site Occupancy in Several Rare Earth Dihydrides," Neutron Scattering, Santa Fe, New Mexico, August 19–23, 1985, Los Alamos National Laboratory document LA-UR-85-1714.

P. D. Goldstone, "Laser-Accelerator Physics at Los Alamos," 2nd Workshop on Laser Acceleration of Particles, Malibu, California, January 1985, Los Alamos National Laboratory document LA-UR-84-4041.

P. D. Goldstone, F. P. Ameduri, R. H. Day, G. E. Eden, S. R. Goldman, R. L. Keck, J. Knauer, R. L. McCrory, W. C. Mead, G. Pien, M. C. Richardson, W. Seka, J. M. Soures, "Interaction Physics and X-Ray Emission in High-Z Plasmas at 351 nm," American Physical Society, Division of Plasma Physics, Boston, Massachusetts, October 29–November 2, 1984, Los Alamos National Laboratory document LA-UR-84-2160.

P. D. Goldstone, O. Barnouin, J. A. Cobble, S. R. Goldman, A. Hauer, P. Jaanimagi, R. Marjoribanks, W. C. Mead, G. Pien, M. Richardson, G. L. Stradling, and B. Yaakobi, "X-Ray Emission and Energy Transport in Ultra Violet-Laser-Produced High-Z Plasmas," American Physical Society, Division of Plasma Physics, San Diego, California, November 3–8, 1985, Los Alamos National Laboratory document LA-UR-85-3889.

P. D. Goldstone, R. H. Day, S. R. Goldman, and W. C. Mead, "X-Ray Conversion and High-Z Plasma Dynamics at 351 nm," CLEO '85, Conference on Lasers and Electro-Optics, Baltimore, Maryland, May 21–24, 1985, Los Alamos National Laboratory document LA-UR-85-1770.

C. A. Goulding, N. S. P. King, G. L. Morgan, P. W. Lisowski, R. G. Jeppesen, D. A. Lind, J. L. Ullmann, C. D. Zafiratos, and C. D. Goodman, "(p,n) Reaction to Th Delta Region at 800 MeV," American Physical Society, Arlington, Virginia, April 24–27, 1985, Los Alamos National Laboratory document LA-UR-85-616.

A. E. Greene, J. H. Brownell, D. J. Erickson, J. H. Goforth, I. R. Lindemuth, T. A. Oliphant, Jr., L. R. Veeser, and D. L. Weiss, "Computational Simulations of Magnetic Flux Compression Generator Driven Imploding Plasmas," American Physical Society, Division of Plasma Physics, San Diego, California, November 4–8, 1985, Los Alamos National Laboratory document LA-UR-85-2594.

B. H. Grier, L. Passell, J. Eckert, H. Patterson, D. Richter, and R. Rollefson, "Structure and Dynamics of Ethylene Adsorbed on Graphite," American Physical Society, Detroit, Michigan, March 26–30, 1984, Los Alamos National Laboratory document LA-UR-84-1059.

L. C. Gupta and J. D. Thompson, "Pressure Effects on the Resistivity of $CeRu_2Si_2$: A Kondo-Lattice System," Fourth International Conference on Valence Fluctuations, August 27–30, 1984, Cologne, West Germany, Los Alamos National Laboratory document LA-UR-84-1364.

J. C. Gursky, "Capabilities of the Los Alamos National Laboratory in Nuclear Target Technology," Nuclear Target Development Society, Antwerp, Belgium, September 25–28, 1984, Los Alamos National Laboratory document LA-UR-84-2951.

R. F. Haglund, Jr., "Spin-Polarized Nuclei in Surface Physics," Physics and Astronomy Colloquium, Brigham Young University, March 10, 1984; Colloquium at Vanderbilt University, April 30, 1984, Los Alamos National Laboratory document LA-UR-84-1410.

R. F. Haglund, Jr., E. Beckmann, D. Fick, B. Horn, and E. Koch, "Spin-Polarized Nuclei – A Novel Probe of Surface Electromagnetic Fields," American Vacuum Society, Albuquerque, New Mexico, June 22, 1984, Los Alamos National Laboratory document LA-UR-84-567.

R. F. Haglund, Jr., B. Horn, D. Fick, E. Koch, E. Beckmann, and N. H. Tolk. "Spin Relaxation Experiments on Surfaces." Polarized Targets in Storage Rings, Argonne, New York, May 1984. Los Alamos National Laboratory document LA-UR-84-1588.

R. F. Haglund, Jr. and N. H. Tolk. "Experimental Studies of Photon-Surface Interaction Dynamics in the Alkali." SPIE Symposium on X-Rays in Mail Analysis, Nashville, Tennessee, July 1986. Los Alamos National Laboratory document LA-UR-86-2369.

R. F. Haglund, Jr. and N. H. Tolk. "Stimulated Desorption as a Source of Damage Mechanisms in Excimer-Laser Optics." Desorption Induced by Electronic Transitions, Schloss Elmau, Bavaria, West Germany, October 14 17, 1984. Los Alamos National Laboratory document LA-UR-84-2089.

R. F. Haglund, Jr. and N. H. Tolk. "Stimulated Desorption in Surface Spectroscopy with Nuclear-Spin Polarized Atomic Beams." Desorption Induced by Electronic Transitions, Schloss Elmau, Bavaria, West Germany, October 14 17, 1984, Los Alamos National Laboratory document LA-UR-84-2090.

R. F. Haglund, Jr., N. H. Tolk, W. T. Pinkston, and G. W. York. "Fundamental Mechanisms of Optical Damage in Short-Wavelength High-Power Lasers." High-Power Laser Optical Components, Boulder, Colorado, October 28 30, 1985. Los Alamos National Laboratory document LA-UR-85-3678.

S. F. Hahn, G. J. Berzins, A. C. Rose, J. E. Valencia, H. E. Flethauser, J. E. Lenberg, J. G. Garsow, P. G. Beck, C. I. Westmark, and C. T. Fuller. "XDS Status." AFTAC Satellite Working Group, Patrick AFB, Florida, March 12 14, 1985. Los Alamos National Laboratory document LA-UR-86-10.

R. C. Haight. "Quadrupole Spectrometer Measurements of (N, Charged Particle) Cross Sections of Be, N, and O at E_n = 14 MeV." Fast Neutron Physics, Dubrovnik, Yugoslavia, May 26 31, 1986. Los Alamos National Laboratory document LA-UR-86-1794.

R. C. Haight and G. C. Baldwin. "Assessment of a Method Proposed for Finding Transfer Levels for Isomeric Deexcitation." International Conference on Laser Science, Dallas, Texas, November 18 22, 1985.

A. L. Hallin, H. W. Baer, J. D. Bowman, F. Irom, M. J. Leitch, J. C. Peng, J. R. Comfort, and J. N. Knudson. "Angular Distributions for the $^{15}N(\pi^+, \pi^o)O^{15}$ Reaction to the Isobaric Analog State at 100 and 295 MeV." American Physical Society, Washington, D.C., April 23 26, 1984.

A. D. Hancock, R. Hilko, N. S. P. King, A. W. Obst, K. G. Boyer, and Q. Klingler. "Permanent Magnet Proton Spectrometer." American Physical Society Meeting, Washington, D.C., April 28 May 2, 1986. Los Alamos National Laboratory document LA-UR-86-317.

J. A. Hanlon, J. McLeod, J. E. Sollid, W. W. Horn, R. E. Carmichael, and B. L. Kortegaard. "Optical Design for a Kilojoule Class Krypton Flouride Laser." Optical Society of America, San Diego, California, February 13 14, 1985. Los Alamos National Laboratory document LA-UR-84-1908.

D. A. Hardwick, C. J. Maggiore, J. R. Tesmer, and R. W. Meier. "Use of Nuclear Reaction Analysis for Tritium and ^3He Profiling," 47th DAMSUL Committee, Miamisburg, Ohio, July 1986. Los Alamos National Laboratory document LA-UR-86-151.

D. B. Harris, R. A. Berggren, N. A. Kurnit, D. D. Lowenthal, R. G. Berger, J. M. Eggleston, J. J. Ewing, and M. J. Kushner. "Krypton Fluoride Lasers as Inertial Fusion Drivers." 11th Symposium on Fusion Engineering, Austin, Texas, November 18 23, 1985, Los Alamos National Laboratory document LA-UR-85-4019.

F. B. Harrison. "Transient Absorption of Light Induced by Radiation." High-Power Laser Optical Components, Boulder, Colorado, May 1986. Los Alamos National Laboratory document LA-UR-85-3769.

H. Hauke. "Oscillatory Convection in Dilute Solutions of ^3He Solution." American Physical Society, Baltimore, Maryland, March 25 29, 1985.

H. Haucke, R. Ecke, and J. C. Wheatley. "Dimension and Entropy for Quasiperiodic and Chaotic Convection." Dimensions and Entropies in Chaotic Systems, Pecos, New Mexico, September 11 16, 1985. Los Alamos National Laboratory document LA-UR-85-3766.

H. Haucke, R. Ecke, and J. C. Wheatley, "Quantum Vortex Turbulence in Rayleigh-Bénard Convection," American Physical Society, Las Vegas, Nevada, March 31 April 4, 1986, Los Alamos National Laboratory document LA-UR-85-4314.

H. Haucke, Y. Maeno, and J. C. Wheatley, "Period-Doubling Two-Torus State in A Convecting ^{3}He-Superfluid ^{4}He Solution," Low Temperature Physics, Karlsruhe, West Germany, August 15 22, 1984, Los Alamos National Laboratory document LA-UR-84-1052.

A. Hauer, D. R. Bach, S. R. Goldman, P. D. Goldstone, and W. C. Mead, "Short Wavelength Laser Fusion Experiments at Los Alamos," University of Rochester, New York, 1985, Los Alamos National Laboratory document LA-UR-85-2143.

A. Hauer, D. Duston, J. D. Kilkenny, W. Mead, and O. Willi, "Spectroscopic Evaluation of the Heat Front Profile in Laser Plasma Transport Experiments," Anomalous Absorption Conference, Charlottesville, Virginia, May 6 11, 1984, Los Alamos National Laboratory document LA-UR-84-1383.

A. Hauer and S. J. Gitomer, "Development of Diagnostics of Shell Break Up in Laser Driven Implosions," American Physical Society, Division of Plasma Physics, Boston, Massachusetts, October 29 November 2, 1984.

A. Hauer, P. D. Goldstone, and W. C. Mead, "Summary of Comparison of Time Integrated and Time Resolved Measurements of Thermal Transport in 351 nm Laser Experiments," American Physical Society, Division of Plasma Physics, San Diego, California, November 3 8, 1985, Los Alamos National Laboratory document LA-UR-85-3799.

A. Hauer and J. D. Kilkenny, "Torodially Curved Crystal Spectrograph for Laser Plasma Measurements," 5th Topical Conference on High Temperature Plasma Diagnostics, Tahoe City, California, September 16 20, 1984, Los Alamos National Laboratory document LA-UR-84-2408.

R. H. Heffner, D. W. Cooke, R. L. Hutson, M. E. Schillaci, Z. Fisk, J. L. Smith, J. O. Willis, D. E. MacLaughlin, C. Boekema, R. L. Lichti, A. B. Denison, and J. Oostens, "Muon Knight Shift and Zero-Field Relaxation in (U,Th)Be_{13}," 4th International Conference on Muon Spin Rotation, Relaxation, and Resonance, Uppsala, Sweden, June 23 27, 1986, Los Alamos National Laboratory document LA-UR-86-2251.

R. H. Heffner, D. W. Cooke, R. L. Hutson, M. E. Schillaci, J. L. Smith, Z Fisk, J. O. Willis, D. E. MacLaughlin, J. Oostens, C. Bockema, and A. B. Denison, "Micro SR Relaxation and Knight Shifts in $U_{1-X}Th_X$ Be_{13} ($X = 0, 0.033$)," American Physical Society, Las Vegas, Nevada, March 31 April 1, 1986, Los Alamos National Laboratory document LA-UR-86-30.

J. A. Helffrich, M. F. Krusius, M. P. Maley, and J. C. Wheatley, "High Flux Hydrogen Dissociator Operating at 0.2-0.5 K," Gordon Research, Antrim, New Hampshire, July 22 26, 1985, Los Alamos National Laboratory document LA-UR-85-2407.

J. A. Helffrich, M. F. Krusius, M. P. Maley, and J. C. Wheatley, "Hydrogen Dissocation Below 1 K," American Physical Society, Las Vegas, Nevada, March 31 April 4, 1986, Los Alamos National Laboratory document LA-UR-85-4315.

J. Helffrich, M. F. Krusius, M. P. Maley, and J. C. Wheatley, "Production and Cooling of Spin-Polarized Hydrogen," Symposium on Rotating Superfluids, ROTA 1986, Helsinki University of Technology, Finland, June 2 6, 1986, Los Alamos National Laboratory document LA-UR-86-2533.

J. Helffrich, M. P. Maley, M. F. Krusius, and J. C. Wheatley, "Thermal Accommodation of Spin-Polarized Hydrogen on the Liquid Helium Surface," University of Turku, Finland, May 30, 1986, Los Alamos National Laboratory document LA-UR-86-2532.

P. R. Higbie and P. W. Lisowski, "Spallation Fragment Measurements at 800 MeV Using the WNR Facility," AFTAC Satellite Working Group, Patrick AFB, Florida, March 12 14, 1985, Los Alamos National Laboratory document LA-UR-85-49.

D. L. Hjeresen, J. M. O'Donnell, J. S. George, D. L. Arthur, M. M. Whalen, E. R. Flynn, and J. C. Fowler, "Los Alamos National Laboratory Bioelectromagnetics Research Program," Bioelectromagnetics Society, Madison, Wisconsin, June 1 5, 1986, Los Alamos National Laboratory document LA-UR-86-547.

R. F. Hoeberling, F. W. Van Haaften, and C. M. Fowler, "Plate Motion Uniformity Detection Using Triboluminescence," Megagauss Magnetic Field Generation, Santa Fe, New Mexico, July 14 17, 1986, Los Alamos National Laboratory document LA-UR-86-493.

J. K. Hoffer and D. N. Sinha, "Dynamical Scaling in ^{3}He ^{4}He Liquid Mixtures," Low Temperature Physics, Karlsruhe, West Germany, August 15 22, 1984, Los Alamos National Laboratory document LA-UR-84-905.

C. M. Hoffman, R. D. Bolton, M. D. Cooper, J. S. Frank, A. L. Hallin, P. Heusi, G. E. Hogan, L. Piilonen, F. G. Mariam, H. S. Matis, R. E. Mischke, D. E. Nagle, V. D. Sandberg, G. H. Sanders, U. Sennhauser, R. D. Werbeck, A. Williams, S. L. Wilson, R. Hofstadter, E. B. Hughes, M. W. Ritter, D. Grosnick, S. C. Wright, V. L. Highland, and J. McDonough, "Search for Rare Muon-Number-Nonconserving Decays of the Mu Plus," High Energy Lepton and Photon Interactions, Kyoto, Japan, August 19 24, 1985, Los Alamos National Laboratory document LA-UR-85-2828.

B. M. Hogan, R. B. Walton, T. F. Covert, G. A. Reeves, S. Armstrong, D. B. Court, and R. L. Rhorer, "Improved Resolution with a Tapered Pinhole," American Vacuum Society, Albuquerque, New Mexico, April 12 19, 1984, Los Alamos National Laboratory document LA-UR-84-1005.

M. H. Holzscheiter, "Antiproton Storage in Ion Traps A New Concept in Low Energy Antimatter Physics," Atomic Physics, Tokyo, Japan, August 24 30, 1986, Los Alamos National Laboratory document LA-UR-86-1437.

M. H. Holzscheiter, M. V. Hynes, and N. S. P. King, "Measurement of the Gravitational Acceleration of the Antiproton," GR 11, Stockholm, Sweden, July 6 12, 1986, Los Alamos National Laboratory document LA-UR-86-976.

S. Horn, H. Borges, J. D. Thompson, and R. D. Parks, "Evolution of the Structural Phase Transition in CeAg in the Low Pressure Range," Magnetism, San Francisco, California, August 26 30, 1985, Los Alamos National Laboratory document LA-UR-85-2551.

M. K. Hou, H. C. Hamaker, C.-Y. Huang, M. B. Maple, and M. S. Torikachvili, "Surface Impedence of Several Magnetic Superconductors," International Conference on Magnetism, San Francisco, California, August 26 30, 1985, Los Alamos National Laboratory document LA-UR-85-2142.

M. K. Hou, C.-Y. Huang, and C. E. Olsen, "Penetration Depths of Superconducting U_6 (X = Cobalt, Iron, and Manganese)," American Physical Society, Las Vegas, Nevada, March 31 April 4, 1986, Los Alamos National Laboratory document LA-UR-86-29.

J. Howard, J. M. Nicol, and J. Eckert, "Infrared and Neutron Scattering Studies of Ethene Adsorbed Onto Partially Exchanged Zinc A Zeolite," Structure of Surfaces, Berkeley, California, August 1984, Los Alamos National Laboratory document LA-UR-84-2728.

H. H. Hsu, G. D. Doolen, W. L. Talbert, Jr., and J. M. Mack, Jr., "Is it Possible to Induce a Fast De-excitation of the 16 Plus Isomeric State in ^{178}Hf?" IUCF Workshop, Bloomington, Indiana, October 21 23, 1985, Los Alamos National Laboratory document LA-UR-85-3664.

H. H. Hsu, M. C. Lucas, J. M. Mack, and C. E. Moss, "A Semiempirical Method for Calculating Detector Efficiency as a Function of Distance," IEEE Nuclear Science Symposium, Orlando, Florida, October 31 November 2, 1984.

C.-Y. Huang, "Some Aspects of Laser-Solid Interactions and Related Problems," Invited Colloquia: Lawrence Livermore National Laboratory, January 27, 1986; Buffalo, New York, February 11, 1986; Case Western Reserve University, February 13, 1986; Lockheed Research Center, March 20, 1986, Los Alamos National Laboratory document LA-UR-86-537.

C.-Y. Huang, "Some Aspects of the Interplay Between Magnetism and Superconductivity," Case Western Reserve University, February 18, 1986; University of California, Berkeley, March 21, 1986, Los Alamos National Laboratory document LA-UR-86-909.

C.-Y. Huang, "Superconductivity and Lasers," Engineering Society, Houston, Texas, February 28, 1986; University of Texas, Austin, March 4, 1986, Los Alamos National Laboratory document LA-UR-86-735.

C.-Y. Huang, "Time-Resolved Picosecond Optical Measurements of Laser-Excited Graphite," University of Texas, Austin, March 3, 1986; University of California, Berkeley, March 21, 1986; University of Maryland, April 21, 1986; Sandia National Laboratories, May 16, 1986; Los Alamos National Laboratory document LA-UR-86-1745.

C.-Y. Huang, A. M. Malvezzi, and N. Bloembergen, "Phase Transformations in Picosecond Laser-Irradiated Graphite," Quantum Electronics, San Francisco, California, June 9 13, 1986, Los Alamos National Laboratory document LA-UR-86-257.

C.-Y. Huang, A. M. Malvezzi, N. Bloembergen, and J. M. Liu, "Time-Resolved Picosecond Optical Study of Laser-Excited Graphite," Symposium on Beam-Solid Interactions & Phase Transformations, Boston, Massachusetts, December 3, 1985. Los Alamos National Laboratory document LA-UR-85-4272.

C.-Y. Huang, C. E. Olsen, G. Kozlowski, H. Matsumoto, H. Umezawa, J. P. Whitehead, and F. Mancini, "Penetration Depths in Some Magnetic Superconductors," American Physical Society, Detroit, Michigan, March 26 30, 1984.

C.-Y. Huang, C. E. Olsen, G. Kozlowski, H. Matsumoto, H. Umezawa, J. P. Whitehead, F. Mancini, and M. B. Maple, "Anomalous Surface Impedance in Reentrant Ferromagnetic Superconductors," Magnetism and Magnetic Materials, San Diego, California, November 27 30, 1984; Conference on Low Temperature Physics, Karlsruhe, West Germany, August 15 22, 1984. Los Alamos National Laboratory document LA-UR-84-2151.

R. L. Hutson, D. W. Cooke, M. E. Schillaci, R. H. Heffner, and S. A. Dodds, "Beam Chopper Development at LAMPF," 4th International Conference on Muon Spin Rotation, Relaxation, and Resonance, Uppsala, Sweden, June 23 27, 1986. Los Alamos National Laboratory document LA-UR-86-969.

M. V. Hynes and L. Campbell, "Physics with Bottled Antiprotons," First Workshop on Antimatter Physics at Low Energy, Fermilab, Batavia, Illinois, April 10 12, 1986. Los Alamos National Laboratory document LA-UR-86-2138.

B. V. Jacak, H. C. Britt, A. E. Gavron, J. B. Wilhelmy, G. Claesson, K. G. Doss, H. A. Gustafsson, H. H. Gutbrod, K. H. Kampert, B. Kolb, A. M. Poskanzer, H. G. Ritter, H. R. Schmidt, H. Wieman, J. W. Harris, "Multifragmentation in Intermediate Energy Heavy Ion Collisions," Nuclear Dynamics IV, Copper Mountain, Colorado, February 23 28, 1986; Local Equilibrium in Strong Interaction Physics, Santa Fe, New Mexico, April 9 12, 1986; National Meeting of the American Chemical Society, New York City, April 14 17, 1986. Los Alamos National Laboratory document LA-UR-86-4164.

S. A. Jaramillo and G. J. Yates, "Quantitative Comparison of Different MCPTs as Nanosecond Light Shutters in Coupled Video Systems," SPIE International Technical Symposium, San Diego, California, August 18 23, 1985. Los Alamos National Laboratory document LA-UR-86-1736.

R. J. Jensen, "KrF Laser Program," Princeton University, July 29, 1985, Los Alamos National Laboratory document LA-UR-85-2685.

R. J. Jensen, "Los Alamos Investigation of Laser Fusion with Collaboration of the Entire Los Alamos Fusion Team," Workshop on Magnetic and Inertial Fusion, University of Naples, Italy, May 24 25, 1984.

R. J. Jensen, "Los Alamos KrF Laser Program," CLEO '85 on Lasers and Electro-Optics, Baltimore, Maryland, May 21 24, 1985. Los Alamos National Laboratory document LA-UR-84-3909.

R. J. Jensen and D. C. Cartwright, "KrF Laser as a Fusion Driver," Workshop on Laser Interaction, Monterey, California, October 28 November 1, 1985. Los Alamos National Laboratory document LA-UR-85-3244.

R. J. Jensen, L. A. Rosocha, and J. A. Sullivan, "High Power KrF Lasers for Fusion," SPIE OE/LASE '86 Conference, Los Angeles, California, January 19 24, 1986. Los Alamos National Laboratory document LA-UR-85-4471.

L. A. Jones and D. R. Kania, "Nonthermal Effects on the Diagnostics of a Collapsing Gas Shell Z-Pinch," Dense Z-Pinches for Fusion, Washington, D.C., March 29 30, 1984. Los Alamos National Laboratory document LA-UR-84-1077.

L. A. Jones, D. R. Kania, M. D. Maestas, and R. L. Shepherd, "Infrared Emission as a Diagnostic for a Collapsing Gas Shell Z-Pinch," High Temperature Plasma Diagnostics, Tahoe City, California, September 16 20, 1984. Los Alamos National Laboratory document LA-UR-84-2424.

L. A. Jones, D. R. Kania, M. D. Maestas, and R. L. Shepherd, "Temporally and Spatially Resolved X-Ray Emission from a Collapsing Gas Shell Z-Pinch Plasma," American Physical Society, Division of Plasma Physics, San Diego, California, November 4 8, 1985. Los Alamos National Laboratory document LA-UR-85-2592.

M. Kang, L. A. Rosocha, V. O. Romero, F. W. Van Haaften, and J. P. Brucker, "Design and Performance of Large Area Monolithic Electron Guns for the Aurora KrF Laser System," 5th IEEE

Pulsed Power Conference, Arlington, Virginia, June 10 12, 1985. Los Alamos National Laboratory document LA-UR-85-2077.

D. R. Kania, "Effects of X-Ray Heat Loading on Low Z Flourescers, X-Ray Mirrors, and Layered Synthetic Microstructures," JOWOG-37, Aldermaston, England, April 30 May 4, 1984. Los Alamos National Laboratory document LA-UR-84-109.

D. R. Kania, "Flat Response Detectors from UV to X-Ray Region," 6th Topical Conference on High Temperature Plasma Diagnostics, American Physical Society, Hilton Head Island, South Carolina, March 9 13, 1986, Los Alamos National Laboratory document LA-UR-86-597.

D. R. Kania, R. J. Bartlett, R. H. Day, and W. J. Trela, "Design of Synchrotron Based Crossed Ion and Photon Beam Experiments for Photoionization Studies of Ionized Species," American Physical Society, Storrs, Connecticut, May 30 June 1, 1985. Los Alamos National Laboratory document LA-UR-84-548.

D. R. Kania, R. J. Bartlett, R. B. Hammond, and D. L. Smith, "Measurements of the Temperature & Intensity Dependence of Transient Photoconductivity in InP:Fe," Topical Meeting on Picosecond Electronics & Optoelectronics, Incline Village, Nevada, March 13 15, 1986. Los Alamos National Laboratory document LA-UR-84-3542.

D. R. Kania, R. J. Bartlett, R. B. Hammond, R. S. Wagner, and P. J. Walsh, "Measurement of the Soft X-Ray Temporal and Spectral Response of Indium Phosphorus Iron Photoconductors," Optical Society, Ultrafast Phenomena, Monterey, California, June 12 15, 1984, Los Alamos National Laboratory document LA-UR-84-564.

D. R. Kania, R. J. Bartlett, and W. J. Trela, "Synchrotron Based Measurements of the Soft X-Ray Performance of Thin Film Multilayer Structures," SPIE's 29th Annual International Technical Symposium, San Diego, California, August 18 23, 1985, Los Alamos National Laboratory document LA-UR-85-2349.

D. R. Kania, R. J. Bartlett, W. J. Trela, E. Eberhard, and L. Golub, "Performance of Transition Metal Carbon Multilayer Mirrors from 80 to 350 eV," Laser Techniques in the Extreme Ultraviolet, Boulder, Colorado, March 5 7, 1984, Los Alamos National Laboratory document LA-UR-84-720.

D. R. Kania, F. Begay, R. C. Hammock, L. A. Jones, and D. T. Nothwang, "Relativistic Electron Beam Heating of a High Density Carbon Plasma," American Physical Society, Division of Plasma Physics, San Diego, California, November 4 8, 1985, Los Alamos National Laboratory document LA-UR-85-2589.

D. R. Kania, J. M. Bradley, R. B. Hammond, L. A. Jones, M. D. Maestas, R. L. Shepherd, S. Wagner, "Application of Indium Phosphorus Photoconductors as a Fast and Sensitive Soft X-Ray Detector and Bolometer," High Temperatire Plasma Diagnostics, Tahoe City, California, September 16 20, 1984, Los Alamos National Laboratory document LA-UR-84-2395.

D. R. Kania and L. A. Jones, "Diagnostics of a High Current Capillary Discharge," Dense Z-Pinches for Fusion, Washington, D.C., March 29 30, 1984, Los Alamos National Laboratory document LA-UR-84-1249.

D. R. Kania and L. A. Jones, "Experimental Study of a Capillary Discharge," IEEE Conference on Plasma Science, St. Louis, Missouri, May 14 16, 1984, Los Alamos National Laboratory document LA-UR-84-476.

D. R. Kania, L. A. Jones, and R. L. Shepherd, "Solid Density, Low Temperature Plasma Formation in a Capillary Discharge," 3rd International Conference on Radiative Properties of Hot Dense Matter, Williamsburg, Virginia, October 14 18, 1985, Los Alamos National Laboratory document LA-UR-85-3201.

J. S. Kapustinsky, R. M. DeVries, N. J. Digiacomo, W. E. Sondheim, and J. W. Sunier, "Fast Timing Light Pulser for Scintillation Detectors," Optical Society of America, San Diego, California, October 29 November 2, 1984, Los Alamos National Laboratory document LA-UR-84-1856.

P. W. Keaton, "Settlement of the Moon and Ventures Beyond," Second Symposium on Space Nuclear Power Systems, Albuquerque, New Mexico, January 1985, Los Alamos National Laboratory document LA-UR-85-366.

G. L. Keller, M. L. Scott, and K. B. Mitchell, "Performance of Oblique Angle of Incidence Collection Systems in the VUV," SPIE '86, International Technical Symposium, San Diego, California, August 17 22, 1986, Los Alamos National Laboratory document LA-UR-86-2330.

W. E. Keller, "Some Super Properties of Liquid Helium," 60th Annual Meeting, American Association for the Advancement of Science, Southwestern and Rocky Mountain Division, Lubbock, Texas, March 27 31, 1984.

J. F. Kephart, D. R. Bach, G. E. Eden, S. J. Gitomer, P. D. Goldstone, R. Kristal, C. R. Mansfield, and M. A. Yates, "Energy Balance Experiments on Antares," American Physical Society, Division of Plasma Physics, Boston, Massachusetts, October 29 November 1, 1984; Anomalous Absorption Conference, Charlottesville, Virginia, May 6 11, 1984, Los Alamos National Laboratory document LA-UR-84-2252.

J. F. Kephart, M. M. Mueller, H. L. Halbig, and M. J. Kellum, Jr., "Temporally Unfolded Bremsstrahlung Spectra for Long Pulse Irradiation of Spherical Targets with a Carbon Dioxide Laser," American Physical Society, Division of Plasma Physics, San Diego, California, November 3 8, 1985, Los Alamos National Laboratory document LA-UR-85-2575.

W. D. Kimura and E. T. Salesky, "Elevated Temperature Extraction Measurements of a High Kr Concentration KrF Laser," CLEO '85 on Lasers and Electro-Optics, Baltimore, Maryland, May 21 24, 1985, Los Alamos National Laboratory document LA-UR-84-4045.

W. D. Kimura and E. T. Salesky, "Temperature Dependence Measurements of Kr_2F Fluorescence in KrF_2 Mixture," CLEO '85 on Lasers and Electro-Optics, Baltimore, Maryland, May 21 24, 1985, Los Alamos National Laboratory document LA-UR-84-3992.

W. D. Kimura, J. F. Seamans, G. P. Quigley, and E. T. Salesky, "Experimental Comparison of Electron-Beam Pumped XeF Laser Performance Using Ne and Ar Diluents," CLEO/IQEC Conference on Lasers and Electro-Optics, XIV International Conference on Quantum Electronics, San Francisco, California, June 10, 1986, Los Alamos National Laboratory document LA-UR-86-1970.

N. S. P. King, C. C. Goodman, R. G. Jeppesen, D. A. Lind, P. W. Lisowski, G. L. Morgan, J. R. Shepard, J. R. Ullmann, and C. D. Zafiratos, "Angular Distribution for Spin Flip Transitions in the 800 MeV (Proton, Neutron) Reaction," American Physical Society, Toronto, Canada, January 21 24, 1985, Los Alamos National Laboratory document LA-UR-85-248.

N. S. P. King, S. A. Jaramillo, G. J. Yates, "Nanosecond Optical Shutters," High Speed Photography and Photonics, Strasbourg, France, August 27 31, 1984, Los Alamos National Laboratory document LA-UR-84-1078.

N. S. P. King, G. J. Yates, S. A. Jarmillo, T. S. Pagano, and J. P. Black, "Nanosecond Optical Shutters," SPIE's 29th Annual International Technical Symposium, San Diego, California, August 18 23, 1985, Los Alamos National Laboratory document LA-UR-85-3022.

T. R. King, D. M. Barrus, R. S. Dingus, W. Z. Osborne, and C. R. Phipps, Jr., "Measurements of Laser Generated Impulse," Intense Dynamic Loading and Its Effects, Beijing, China, June 1986, Los Alamos National Laboratory document LA-UR-86-634.

P. L. Klingner, S. J. Levings, and R. W. Wilkins, "General Distributed Control System for Fusion Experiments," High Temperature Plasma Diagnostics, Hilton Head Island, South Carolina, March 9 13, 1986, Los Alamos National Laboratory document LA-UR-86-80.

C. E. Knapp, V. K. Viswanathan, S. C. Bender, Q. D. Appert, G. Lawrence, and C. C. Barnard, "Analysis of FEL Optical Systems with Grazing Incidence Mirrors," SPIE, Optics and Optoelectric Systems, Orlando, Florida, March 31 April 4, 1986, Los Alamos National Laboratory document LA-UR-86-1298.

D. A. Knapp, T. J. Bowles, J. C. Browne, T. H. Burritt, J. A. Helffrich, M. P. Maley, R. G. H. Robertson, R. K. Sander, M. L. Stelts, and J. F. Wilkerson, "Diagnostics in the Los Alamos Free Tritium Beta Decay Experiment," American Physical Society, Washington, D.C., April 23 26, 1984, Los Alamos National Laboratory document LA-UR-84-189.

P. E. Koehler, C. D. Bowman, F. J. Steinkruger, D. C. Moody, S. A. Wender, R. C. Haight, P. W. Lisowski, and W. L. Talbert, "Measurement of the ^{7}Be(Neutron, Proton)^{7}Li Cross Section from 0.03 eV to Approximately 300 eV," American Physical Society, Washington, D.C., April 18 May 1, 1986, Los Alamos National Laboratory document LA-UR-86-275.

B. L. Kortegaard, "Superfine Laser Position Control Using Statistically Enhanced Resolution in Real Time," Architectures and Algorithms for Digital Image Processing II, SPIE, Los Angeles, California, January 23, 1985.

R. Kristaly, J. F. Kephart, A. Hauer, and H. Oona, "Preheat Inhibition in CO_2 Laser Illuminated Targets," American Physical Society, Division of Plasma Physics, Boston, Massachusetts, October 29 November 1, 1984; 8th International Conference on Quantum Electronics, Anaheim, California, June 18 21, 1984, Los Alamos National Laboratory document LA-UR-84-2197.

H. W. Kruse, L. D. Looney, R. C. Taylor, R. S. Medina, J. S. Baumgart, G. T. Baca, and D. E. Dominguez, "Attempts to Characterize Microballoon Sensors for Shock Velocity and Material Motion Studies," 11th International Pyrotechnics Seminar, Vail, Colorado, July 7 11, 1986, Los Alamos National Laboratory document LA-UR-86-1704.

G. J. Kubas, R. J. Ryan, P. J. Vergamini, H. J. Wasserman, and B. I. Swanson, "Characterization of $W(CO)_2(PPr^i_3)_2$ (η^2-H_2). The First Example of a Molecular Hydrogen Complex," XXIII International Conference on Coordination Chemistry, Boulder, Colorado, July 29 August 3, 1984.

T. J. T. Kwan, H. A. Davis, R. R. Bartsch, R. M. Stringfield, and E. G. Sherwood, "Design of a Magnetized Virtual Cathode Microwave Generator," IEEE Conference on Plasma Physics, Saskatchewan, Canada, May 19 21, 1986, Los Alamos National Laboratory document LA-UR-86-551.

G. A. Kyrala, "Simulation of Bent Crystal Spectrometers," 5th Topical Conference on High Temperature Plasma Diagnostics, Tahoe City, California, September 16 20, 1984, Los Alamos National Laboratory document LA-UR-84-2441.

G. A. Kyrala, "T_{hot} studies with Defocused Laser Beams and Large Spots," Anomalous Absorption Conference, Charlottesville, Virginia May 6 11, 1984, Los Alamos National Laboratory document LA-UR-84-837.

G. A. Kyrala, D. B. Stahl, V. K. Viswanathan, and G. L. Woodfin, "Effect of Modifying the Laser Beam Profile on the Interaction of Carbon Dioxide Lasers with Spherical Targets," Quantum Electronics, Anaheim, California, June 18 21, 1984, Los Alamos National Laboratory document LA-UR-84-19.

J. S. Ladish, J. W. Toevs, and C. S. Young, "Observation of the 16.7 MeV D-T Fusion Gamma Using a Gas Cerenkov Detector," IEEE Nuclear Science Symposium, San Francisco, California, October 23 25, 1985, Los Alamos National Laboratory document LA-UR-85-3674.

A. C. Larson, "Comments Concerning the Crystal Structure of Boron Carbide," International Conference on Physics and Chemistry of Boron and Borium-Rich Borides, Albuquerque, New Mexico, July 29 31, 1985, Los Alamos National Laboratory document LA-UR-85-2833.

A. C. Larson and R. B. VonDreele, "Generalized Crystal Structure Analysis System GSAS," IPNS User's Group Meeting, Argonne, Illinois, April 15 16, 1985, Los Alamos National Laboratory document LA-UR-85-1454.

G. Lawrence, C. C. Barnard, and V. K. Viswanathan, "Global Coordinates and Exact Aberration Calculations Applied to Physical Optics Modeling of Complex Optical Systems," SPIE, Optics and Optoelectronic Systems, Orlando, Florida, March 31 April 4, 1986, Los Alamos National Laboratory document LA-UR-86-1027.

J. M. Lawrence, Y. Chen, and J. D. Thompson, "Low Temperature Coherence in $CeSn_3$," American Physical Society, Las Vegas, Nevada, March 31 April 4, 1986, Los Alamos National Laboratory document LA-UR-85-4410.

A. C. Lawson, A. Williams, J. G. Huber, and R. B. Roof, Jr., "Magnetic Structure of UPt," International Conference on Magnetism, San Francisco, California, August 25 30, 1985, Los Alamos National Laboratory document LA-UR-85-782.

C. Y. Lee, J. M. Lawrence, and J. D. Thompson, "Susceptibility and Resistivity of Ce_3Al, Ce_3Sn, Ce_3In," American Physical Society, Las Vegas, Nevada, March 31 April 4, 1986, Los Alamos National Laboratory document LA-UR-85-4409.

P. H. Y. Lee, B. Anderson, J. C. Cochrane, J. S. McGurn, J. F. Pecos, R. Price, J. Reay, and J. D. Seagrave, "Optical and UV/X-Ray Imaging Diagnostics for Imploding Foil Experiments," 6th Topical Conference on High-Temperature Plasma Diagnostics, Hilton Head Island, South Carolina, March 9 13, 1986, Los Alamos National Laboratory document LA-UR-86-1985.

P. H. Y. Lee, R. F. Benjamin, J. H. Brownell, D. J. Erickson, J. H. Goforth, A. E. Greene, J. S. McGurn, J. F. Pecos, R. H. Price, H. Oona, J. L. Reay, R. M. Stringfield, R. J. Trainor, L. R. Veeser, and A. H. Williams, "Diagnostics for Pioneer I Imploding Plasma Experiments,"

5th IEEE Pulsed Power Conference, Arlington, Virginia, June 10–12, 1985. Los Alamos National Laboratory document LA-UR-85-2042.

P. H. Y. Lee, J. C. Cochrane, G. A. Kyrala, R. Price, J. D. Seagrave, A. R. Stringfield, R. J. Trainor, and L. R. Veeser, "Diagnostics for Fast Opening Switch & Imploding Foil Experiments at the HEDP Facility," American Physical Society, Division of Plasma Physics, Boston, Massachusetts, October 29–November 2, 1984, Los Alamos National Laboratory document LA-UR-84-2025.

P. H. Y. Lee, C. L. Wang, and O. Willi, "Time Resolved Measurements of Ablation Velocity and Acceleration of Laser Irradiated Thin Foil Targets," IEEE Conference on Plasma Science, St. Louis, Missouri, May 14–16, 1984, Los Alamos National Laboratory document LA-UR-84-466.

P. H. Y. Lee, O. Willi, and R. J. Trainor, "Convective Mechanism for Inhibition of Heat Conduction in Laser Produced Plasmas," International Conference on Plasma Physics, Lausanne, Switzerland, June 27–July 3, 1984, Los Alamos National Laboratory document LA-UR-84-1154.

M. J. Leitch, H. W. Baer, R. L. Burman, M. D. Cooper, F. Irom, C. L. Morris, J. N. Knudson, J. R. Comfort, D. H. Wright, and R. Gilman, "Energy Dependence for Low-Energy-Pion Double Charge Exchange on ^{14}C," American Physical Society, Washington, D.C., April 28–May 1, 1986, Los Alamos National Laboratory document LA-UR-86-338.

M. J. Leitch, H. W. Baer, R. L. Burman, M. D. Cooper, F. Irom, C. L. Morris, J. N. Knudson, J. R. Comfort, D. H. Wright, and R. Gilman, "Measurement of the $^{48}Ca(^{+},^{-})^{48}Ti$ Reaction at 35 and 50 MeV," American Physical Society Washington, D.C., April 28–May 1, 1986, Los Alamos National Laboratory document LA-UR-86-339.

S. A. Letzring, M. C. Richardson, P. D. Goldstone, G. Gregory, and G. E. Eden, "Coronal Conditions in High-Z Spherical Targets Irradiated by Multibeam 351-nm Radiations," American Physical Society, Division of Plasma Physics, Boston, Massachusetts, October 29–November 2, 1984, Los Alamos National Laboratory document LA-UR-84-2162.

P. W. Lisowski, R. E. Brown, J. C. Gursky, S. D. Howe, N. Jarmie, and G. L. Morgan, "Cross Sections for the $^{6}Li(t, n)_2$ Alpha Reaction," American Physical Society, Washington, D.C., April 23–26, 1984, Los Alamos National Laboratory document LA-UR-84-312.

P. W. Lisowski, S. A. Wender, and G. F. Auchampaugh, "WNR/PSR Facility—Neutron Physics Capabilities from Sub-Thermal to 800 MeV," International Conference on Nuclear Data for Basic and Applied Science, Santa Fe, New Mexico, May 13–17, 1985, Los Alamos National Laboratory document LA-UR-85-2272.

A. H. Lumpkin, "Comments on the Possible Roles of Volatile Fission Products (Cesium) in Cabri Tests," Science and Technology of Fast Reactor Safety, Isle of Guernsey, England, May 12–16, 1986, Los Alamos National Laboratory document LA-UR-86-1634.

A. H. Lumpkin and D. W. Feldman, "Diagnostics of the Los Alamos Free-Electron Laser Using Streak Systems," 8th International Free Electron Laser Conference, Glasgow, Scotland, September 1–5, 1986, Los Alamos National Laboratory document LA-UR-86-2984.

A. H. Lumpkin and R. B. Feldman, "On-Line Extraction Efficiency Analyses for the Los Alamos Free-Electron Laser," 8th International Free Electron Laser Conference, Glasgow, Scotland, September 1–5, 1986, Los Alamos National Laboratory document LA-UR-86-2983.

P. B. Lyons, "Fiber Optic Radiation Sensors," Optical Society of America, San Diego, California, February 13–14, 1985, Los Alamos National Laboratory document LA-UR-85-517.

Y. Maeno, H. Haucke, R. Ecke, and J. C. Wheatley, "Onset of Oscillations in Symmetric Convective States in a Superfluid ^{3}He-^{4}He Mixture," Low Temperature Physics, Karlsruhe, West Germany, August 15–22, 1984, Los Alamos National Laboratory document LA-UR-84-1020.

M. D. Maestas, R. L. Shepherd, D. R. Kania, and L. A. Jones, "Experimental Studies of High Density Plasma Formation in a 20 μm Diameter Polyurethane Capillary," American Physical Society, Division of Plasma Physics, San Diego, California, November 4–8, 1985, Los Alamos National Laboratory document LA-UR-85-2593.

M. P. Maley, T. J. Bowles, J. C. Browne, T. H. Burritt, J. A. Helffrich, D. A. Knapp, R. G. H. Robertson, M. L. Stelts, and J. F. Wilkerson, "Preparation of an Intense Source of Atomic Hydrogen Isotopes," American Physical Society, Washington, D.C., April 23–26, 1984, Los Alamos National Laboratory document LA-UR-84-188.

A. M. Malvezzi, C.-Y. Huang, H. Kurz, and N. Bloembergen, "Observation of Plasmon-Aided Recombination in Silicon and Germanium Under Picosecond Laser Irradiation," Quantum Electronics, San Francisco, California, June 9–13, 1986, Los Alamos National Laboratory document LA-UR-86-1756.

A. M. Malvezzi, N. Bloembergen, C.-Y. Huang, and H. Kurtz, "Time-Resolved Spectroscopy of Plasma Resonances in Highly Excited Silicon and Germanium," Materials Research Society Conference, Boston, Massachusetts, December 2–7, 1985, Los Alamos National Laboratory document LA-UR-85-3987.

A. Mandl, D. Klimek, and E. T. Salesky, "KrF Intrinsic Laser Efficiency as a Function of Kr Concentration," CLEO '85 on Lasers and Electro-Optics, Baltimore, Maryland, May 21–24, 1985, Los Alamos National Laboratory document LA-UR-84-4037.

C. R. Mansfield, "Review of the Antares Laser Fusion Facility," CLEO '84, Anaheim, California, June 19–24, 1984, Los Alamos National Laboratory document LA-UR-84-832.

R. S. Marjoribanks, G. Stradling, M. C. Richardson, A. Hauer, O. Barnouin, B. Yaakobi, S. A. Letzring, and P. D. Goldstone, "Spectral and Temporal Characteristics of X-Rays from Spherical High-Z Targets Irradiated with 351-nm Laser Light," American Physical Society, Division of Plasma Physics, Boston, Massachusetts, October 29–November 2, 1984, Los Alamos National Laboratory document LA-UR-84-2161.

P. L. Mascheroni, J. L. Norton, M. M. Mueller, J. F. Kephart, and C. R. Mansfield, "Different Turbulent Regimes in Antares Long Pulse Experiments," American Physical Society, Division of Plasma Physics, San Diego, California, November 4–8, 1985, Los Alamos National Laboratory document LA-UR-85-2656.

R. S. McDowell, R. F. Holland, J. P. Aldridge, H. Filip, H. J. Flicker, K. C. Kim, B. J. Krohn, W. B. Maier, D. W. Magnuson, and W. B. Person, "Measurement of the Infrared-Active Stretching Fundamental (NU 3) of UF_6," Symposium on Molecular Spectroscopy, Columbus, Ohio, June 17–21, 1985, Los Alamos National Laboratory document LA-UR-85-189.

M. W. McElfresh, J. D. Thompson, J. O. Willis, M. S. Torikachvili, and M. B. Maple, "Influence of Pressure on Competing Electronic Correlations in Heavy-Fermion URu_2Si_2," American Physical Society, Las Vegas, Nevada, March 31–April 4, 1986, Los Alamos National Laboratory document LA-UR-85-4121.

P. L. McGaughey, K. D. Bol, M. R. Clover, R. M. DeVries, N. J. Digiacomo, J. S. Kapustinsky, G. R. Smith, J. W. Sunier, W. E. Sondheim, Y. Yariv, M. Buenerd, J. Chauvin, D. Lebrun, P. Martin, and J. C. Dousse, "Antiproton Annihilations in Nuclei," Hadronic Probes and Nuclear Interactions, Tempe, Arizona, March 10–14, 1985, Los Alamos National Laboratory document LA-UR-85-1481.

W. C. Mead, D. Duston, A. Hauer, J. D. Kilkenny, M. A. Mahaffy, O. Willi, "Electron Transport and Plasma Profiles in 1.06-Micrometer Multilayer Spherical Transport Experiment," Anomalous Absorption Conference, Charlottesville, Virginia, May 6–11, 1984, Los Alamos National Laboratory document LA-UR-84-812.

W. C. Mead, A. Hauer, M. A. Mahaffy, and O. Willi, "Time-Dependence, Refraction, and Brillouin Scatter in 1.05-Micrometer Multilayer Spherical Transport Experiment," American Physical Society, Division of Plasma Physics, Boston, Massachusetts, October 29–November 2, 1984, Los Alamos National Laboratory document LA-UR-84-2149.

M. M. Meier, D. B. Holtkamp, G. L. Morgan, H. Robinson, G. J. Russell, E. R. Whitaker, W. Amian, and N. Paul, "800 and 318 MeV (p,xn) Cross Sections," American Physical Society, Washington, D.C., April 28–May 1, 1986, Los Alamos National Laboratory document LA-UR-86-375.

M. M. Meier, D. B. Holtkamp, G. L. Morgan, H. Robinson, G. J. Russell, E. R. Whitaker, W. Amian, and N. Paul, "Thin Target (Proton, Neutron) Cross Sections at 318 and 800 MeV," Nuclear Data for Basic and Applied Science, Santa Fe, New Mexico, May 13–17, 1985, Los Alamos National Laboratory document LA-UR-85-469.

A. Migliori, D. S. Buchanan, and J. C. Wheatley, "Experimental Search for Localized States," Seminar, University of California, Los Angeles, November 13, 1985, Los Alamos National Laboratory document LA-UR-85-3956.

R. L. Mills, D. Schiferl, and S. Buchsbaum, "Phase Diagram of Nitrogen from 15 to 300 K and 5 to 500 kbar by Raman Spectroscopy," Gordon Conference on Orientational Disorder in Crystals, Oxnard, California, January 9–13, 1984, Los Alamos National Laboratory document LA-UR-84-205.

M. M. Minor, E. B. Shera, and J. W. Lillberg, "Loss-Free Gamma-Ray Counting on the VMebus," CERN Conference on the VMebus in Physics, Geneva, Switzerland, October 7–8, 1985, Los Alamos National Laboratory document LA-UR-85-2048.

F. A. Morse, "Status of the Commissioning of the Los Alamos Neutron Scattering Center, LANSCE," ICANS, London, England, September 22–26, 1986, Los Alamos National Laboratory document LA-UR-85-2246.

J. M. Moss, "Intermediate Energy Studies of Polarization Transfer, Polarized Deuteron Scattering, and (p,π^{pm}) Reactions," 6th International Symposium on Polarization Phenomena in Nuclear Physics, Osaka, Japan, August 1985, Los Alamos National Laboratory document LA-UR-85-3339.

M. M. Mueller, J. F. Kephart, R. Kristal, C. R. Mansfield, and E. K. Stover, "Comparison of Long-Versus-Short-Pulse Carbon Dioxide Laser Irradiation of Solid Spherical Targets," American Physical Society, Division of Plasma Physics, San Diego, California, November 3–8, 1985, Los Alamos National Laboratory document LA-UR-85-3891.

M. M. Mueller, P. L. Mascheroni, J. F. Kephart, and C. R. Mansfield, "First Look at Results from the Carbon Dioxide Long-Pulse Experiment," Anomalous Absorption, Banff, Canada, June 24–28, 1985, Los Alamos National Laboratory document LA-UR-85-2258.

B. E. Newnam, R. W. Warren, R. L. Sheffield, W. M. Parsons, J. V. Parker, and P. Thullen, "Optical Performance of the Los Alamos Free-Electron Laser," 5th IEEE Pulsed Power Conference, Arlington, Virginia, June 10–12, 1985, Los Alamos National Laboratory document LA-UR-85-262.

J. M. Nicol, J. Howard, and J. Eckert, "IR and Neutron Spectroscopy of Hydrogen and Ethylene Adsorbed on Type A Zeolites," Structure of Surfaces, Berkeley, California, August 13–16, 1984, Los Alamos National Laboratory document LA-UR-84-1365.

D. R. Noakes, E. J. Ansaldo, J. H. Brewer, D. R. Harshman, C.-Y. Huang, M. S. Torikachile, S. E. Lambert, and M. B. Maple, "Muon Spin Relaxation in $ErRh_4B_4$," Magnetism and Magnetic Materials, San Diego, California, November 26–30, 1984, Los Alamos National Laboratory document LA-UR-84-3159.

M. J. Nutter, L. Lewis, S. Tepper, R. N. Silver, and R. H. Heffner, "Neutron Chopper Development at LANSCE," 8th Meeting of International Collaboration of Advanced Neutron Sources, Oxford, England, July 7–12, 1985, Los Alamos National Laboratory document LA-UR-85-2650.

J. W. Ogle, F. Cverna, C. Iverson, L. D. Looney, S. S. Lutz, M. A. Nelson, D. R. Thayer, B. M. Whitcomb, and G. J. Yates, "Radiation Induced Imaging System over Long Fiber Optic Bundles," Fiber Lase '86, Cambridge, Massachusetts, September 21–26, 1986, Los Alamos National Laboratory document LA-UR-86-1514.

H. Oona, P. H. Y. Lee, A. H. Williams, J. L. McGurn, and L. R. Veeser, "Radiation Diagnostics in Extremely Harsh Environments," 4th International Conference on Megagauss Magnetic Field Generation, Santa Fe, New Mexico, July 14–17, 1986, Los Alamos National Laboratory document LA-UR-86-2377.

W. C. Overton and H. Weinstock, "Dynamics of Normal-Zone Propagation in TA at Small Currents," Low Temperature Physics, Karlsruhe, Germany, August 15–22, 1984, Los Alamos National Laboratory document LA-UR-84-1051.

J. V. Parker, "Investigation of Plasma Armature Voltage Gradients Using a Static Discharge," 1986 IEEE International Conference on Plasma Science, Saskatoon, Canada, May 19–21, 1986, Los Alamos National Laboratory document LA-UR-86-549.

J. V. Parker, C. E. Cummings, W. E. Fox, and W. M. Parsons, "Performance Loss Due to Wall Ablation in Plasma Armature Railguns," AIAA 18th Annual Fluid Dynamics and Plasma Dynamics and Lasers Conference, Cincinnati, Ohio, July 16–18, 1985, Los Alamos National Laboratory document LA-UR-85-2455.

J. V. Parker, C. E. Cummings, W. E. Fox, and W. M. Parsons, "Plasma Armature Railgun Studies," 12th IEEE Conference on Plasma Science, Pittsburgh, Pennsylvania, June 3–5, 1985, Los Alamos National Laboratory document LA-UR-85-573.

J. V. Parker and W. M. Parsons, "Arc Damage to Railgun Insulators- Mechanisms and Consequences," IEEE Conference on Plasma Science, St. Louis, Missouri, February 7, 1984, Los Alamos National Laboratory document LA-UR-84-472.

J. V. Parker and W. M. Parsons, "Foil Fuses as Opening Switches for Slow Discharge Circuits," 5th IEEE Pulsed Power Conference, Arlington, Virginia, June 10–12, 1985, Los Alamos National Laboratory document LA-UR-85-2021.

D. M. Parkin, J. A. Goldstone, H. M. Simpson, and J. W. Hemsky, "Kinetic Analysis of Diffusion of Point Defects to Dislocations Following Pulsed Neutron and Electron Irradiations," 8th International Conference on Internal Friction and Ultrasonic Attenuation in Solids, Urbana, Illinois, June 3–6, 1985, Los Alamos National Laboratory document LA-UR-85-1828.

R. D. Parks, J. D. Thompson, and H. Borges, "Change in Nature of Antiferromagnetic Transition with Pressure in the Kondo Lattice System $CePd_2Si_2$," American Physical Society, Las Vegas, Nevada, March 31–April 4, 1986, Los Alamos National Laboratory document LA-UR-86-28.

W. M. Parsons, J. V. Parker, and N. M. Schnurr, "Insulator Studies in the Midi-2 Railgun," 2nd Electromagnetic Launcher, Pomona, California, July 1986, Los Alamos National Laboratory document LA-UR-86-2358.

W. M. Parsons, J. V. Parker, and P. Thullen, "Railgun Power Supply System Utilizing Traction Motors and Vacuum Interrupters," 5th IEEE Pulsed Power Conference, Arlington, Virginia, June 10–12, 1985, Los Alamos National Laboratory document LA-UR-85-2022.

M. Pasternak, J. N. Farrell, and R. D. Taylor, "Mössbauer Effect Studies of Elemental Iodine to 35 GPa," Gordon Research Conference, Research at High Pressure, Meriden, New Hampshire, June 23–27, 1986, Los Alamos National Laboratory document LA-UR-86-2186.

D. C. Pease, D. R. Kania, and L. A. Jones, "Correlation of Optical and X-Ray Emissions in a Dense Gas Puff Z-Pinch," High Temperature Plasma Diagnostics, Tahoe City, California, September 16–20, 1984, Los Alamos National Laboratory document LA-UR-84-2450.

J. C. Peng, "Recent Results of η Meson Production in Nuclei," American Physical Society, Washington, D.C., April 28–May 1, 1986, Los Alamos National Laboratory document LA-UR-86-83.

J. C. Peng, P. Birien, G. Bruge, A. Chaumeaux, D. M. Drake, D. Garreta, S. Janouin, D. Legrand, M. C. Mallet-Lemaire, M. Mayer, J. Pain, M. Berrada, J. P. Bocquet, E. Monnand, J. Mouget, J. Perrin, E. Aslanides, O. Bing, A. Erell, J. Lichtenstadt, and A. I. Yavin, "Measurements of Antiproton Elastic and Inelastic Scattering on ^{12}C," American Physical Society, Washington, D.C., April 23–26, 1984, Los Alamos National Laboratory document LA-UR-84-382.

J. C. Peng, P. Birien, G. Bruge, A. Chaumeaux, D. M. Drake, D. Garreta, S. Janouin, D. Legrand, M. C. Mallet-Lemaire, B. Mayer, J. Pain, M. Berrada, J. P. Bocquet, E. Monnand, J. Mougey, P. Perrin, E. Aslanides, O. Bing, A. Erell, and J. Lichtenstadt, "Search for Antiproton-Nucleus States with the (Proton, Proton) Reactions on ^{12}C, ^{63}Cu, and ^{209}Bi," American Physical Society, Washington, D.C., April 23–26, 1984, Los Alamos National Laboratory document LA-UR-84-383.

A. L. Peratt, B. L. Freeman, R. F. Hoeberling, L. E. Thode, and J. W. Toevs, "High-Power Reflex Triode," IEEE Conference on Plasma Science, St. Louis, Missouri, 1984, Los Alamos National Laboratory document LA-UR-84-486.

A. G. Petschek and S. A. Colgate, "Accretion Model of Gamma Ray Bursts," American Astronomical Society, Tucson, Arizona, January 13–16, 1985, Los Alamos National Laboratory document LA-UR-84-3490.

A. G. Petschek and S. A. Colgate, "Confinement of Radiation in Expanding Ejecta," 167th Meeting of the American Astronomical Society, Houston, Texas, January 5–9, 1986, Los Alamos National Laboratory document LA-UR-85-3624.

L. Piilonen, R. C. Bolton, J. D. Bowman, M. D. Cooper, J. S. Frank, A. L. Hallin, P. Heusi, C. M. Hoffman, G. E. Hogan, F. G. Mariam, H. S. Matis, R. E. Mischke, D. E. Nagle, V. E. Sandberg, G. H. Sanders, U. Sennhauser, R. Werbeck, R. A. Williams, S. L. Wilson, R. Hofstadter, E. B. Hughes, M. Ritter, D. Grosnick, S. C. Wright, V. L. Highland, and J. McDonough, "Search for Rare Muon and Pion Decay Modes with the Crystal Box Detector," 2nd Conference on Intersections Between Particle & Nuclear Physics, Lake Louise, Canada, May 26–31, 1986, Los Alamos National Laboratory document LA-UR-86-2197.

R. Price, P. H. Y. Lee, J. C. Cochrane, J. L. Reay, A. M. Laird, Jr., J. F. Pecos, and R. Showalter, "Fuse Driven Dielectric Switches for Pulsed Power Applications," 5th IEEE Pulsed Power Conference, Arlington, Virginia, June 10–12, 1985, Los Alamos National Laboratory document LA-UR-84-3907.

R. H. Price, P. H. Y. Lee, J. C. Cochrane, R. J. Trainor, J. D. Seagrave, J. L. Reay, A. M. Laird, Jr., J. F. Pecos, L. R. Veeser, and R. M. Stringfield, "Progress in Railgun Opening Switches," IEEE Conference on Plasma Science, Pittsburgh, Pennsylvania, June 3–5, 1985, Los Alamos National Laboratory document LA-UR-85-871.

C. E. Ragan III, "Hermosa Results on Pin Hardness Test," Experimental Review Group, Los Alamos National Laboratory, New Mexico, May 24, 1985.

C. E. Ragan III, "High Pressure Equation-of-State Experiments at the NTS (and Related Matters)," Physics Division Colloquium, Los Alamos National Laboratory, New Mexico, May 24, 1984.

C. E. Ragan III, "Hypervelocity Projectile Experiments." Sandia National Laboratories, Albuquerque, New Mexico, March 8, 1984.

M. R. Raju, S. G. Carpenter, J. J. Chmielewski, J. P. Freyer, M. E. Wilder, D. Goodhead, D. J. Brenner, M. Hoshi, M. E. Schillaci, "Radiobiology of Ultrasoft X Rays," Radiation Research Society, Las Vegas, Nevada, April 12–13, 1986, Los Alamos National Laboratory document LA-UR-85-3993.

W. H. Reichelt, "Quality Assurance in the Antares Laser Fusion Construction Project," ASQC, Eleventh Annual National Energy Division Conference, Las Vegas, Nevada, September 16–19, 1984.

K. B. Riepe, E. O. Ballard, E. A. Meyer, D. C. Wilson, and S. Humphries, Jr., "Status of the Los Alamos Heavy Ion Injector," High-Power Electron & Ion Beam Research, Osaka, Japan, June 9–12, 1986, Los Alamos National Laboratory document LA-UR-86-1987.

R. G. H. Robertson, T. J. Bowles, D. A. Knapp, J. F. Wilkerson, M. P. Maley, and J. C. Browne, "The Los Alamos Experiment on the Beta Decay of Free Molecular Tritium," International Symposium on Beta Decays and Neutrino, Osaka, Japan; 12th International Conference on Neutrino Physics and Astrophysics, Sendai, Japan, June 2–8, 1986, Los Alamos National Laboratory document LA-UR-86-1804.

R. G. H. Robertson, "Measurements of Neutrino Mass," Congress of the Canadian Association of Physicists, Calgary, Canada, June 23–25, 1986, Los Alamos National Laboratory document LA-UR-86-1059.

R. G. H. Robertson, "Neutrinos—Weighting to Close the Universe?" McMaster University, Canada, March 5, 1986; Princeton University, March 6, 1986; California Institute of Technology, Pasadena, April 25, 1986; Los Alamos National Laboratory document LA-UR-86-737.

R. G. H. Robertson, "Status of the U.S.-Canadian Gallium Solar Neutrino Experiment," VI Moriond Workshop on Massive Neutrinos in Particle Physics and Astrophysics, Tignes, France, January 25–February 1, 1986, Los Alamos National Laboratory document LA-UR-85-4116.

R. A. Robinson, R. Pynn, J. Eckert, and J. A. Goldstone, "Los Alamos Constant-Q Spectrometer," 8th Meeting of International Collaboration on Advanced Neutron Sources, Oxford, England, July 7–12, 1985, Los Alamos National Laboratory document LA-UR-85-2070.

H. Robinson, G. J. Russell, E. D. Tucker, E. R. Whitaker, K. D. Williamson, Jr., and F. J. Edeskuty, "LANSCE Liquid Hydrogen Moderator System Hardware-Characteristics-Operation," 8th Meeting of International Collaboration on Advanced Neutron Sources, Oxford, England, July 7–12, 1985, Los Alamos National Laboratory document LA-UR-85-2857.

S. H. Rokni, H. W. Baer, J. D. Bowman, F. Irom, M. J. Leitch, J. Alster, E. Piasetzky, J. R. Comfort, J. N. Knudson, B. L. Clausen, R. A. Loveman, R. J. Peterson, J. L. Ullman, A. G. Bergmann, C. J. Seftor, and U. Sennhauser, "Systematics of High-Energy-Pion Single Charge Exchange Reactions," American Physical Society Meeting, Washington, D.C., April 29–May 1, 1986, Los Alamos National Laboratory document LA-UR-86-470.

L. A. Rosocha, "Aurora—A Short-Pulse Multikilojoule KrF Inertial Fusion Laser System," CLEO '85 on Lasers and Electro-Optics, Baltimore, Maryland, May 21–24, 1985, Los Alamos National Laboratory document LA-UR-84-3933.

L. A. Rosocha, "Short Pulse Multikilojoule KrF Inertial Fusion Laser System," CLEO '85 on Lasers and Electro-Optics, Baltimore, Maryland, May 21–24, 1985, Los Alamos National Laboratory document LA-UR-85-1506.

L. A. Rosocha, P. S. Bowling, M. D. Burrows, J. A. Hanlon, M. Kang, J. McLeod, J. Ratliff, D. O. Whitcomb, and G. W. York, "Aurora Multi-Kilojoule KrF Laser System for ICF Studies," American Institute of Physics International Laser Science Conference, Dallas, Texas, November 18–22, 1985, Los Alamos National Laboratory document LA-UR-86-90.

L. A. Rosocha, P. D. Goldstone, and R. Kristal, "Status of the Aurora Laser System Angular-Multiplexed Multi-Kilojoule Krypton Fluoride Prototype for Inertial Fusion," CLEO '86, San Francisco, California, June 9–13, 1986, Los Alamos National Laboratory document LA-UR-85-4473.

L. A. Rosocha, J. A. Hanlon, and J. Mcleod, "Beam Propagation Problems in the Aurora Laser System," Lasers '85, Las Vegas, Nevada, December 2–6, 1985, Los Alamos National Laboratory document LA-UR-85-2132.

G. J. Russell, C. D. Bowman, E. R. Whitaker, and H. Robinson, "LANSCE High Power (200 Micro Angstrom) Target-Moderator-Reflector-Shield," 8th Meeting of the International Collaboration on Advanced Neutron Sources, Oxford, England, July 7–12, 1985, Los Alamos National Laboratory document LA-UR-85-2487.

G. J. Russell and J. S. Gilmore, "Some Results of Applied Spallation Physics Research at Los Alamos," Accelerator Breeder Workshop, Chalk River, September 19–20, 1984, Los Alamos National Laboratory document LA-UR-84-778.

G. J. Russell, M. M. Meier, D. B. Holtkamp, G. L. Morgan, H. Robinson, E. R. Whitaker, W. Amian, and N. Paul, "Inclusive (p,xn) Cross Section Measurements at WNR," American Physical Society Meeting, Washington, D.C., April 28–May 1, 1986, Los Alamos National Laboratory document LA-UR-86-374.

H. L. Rutowski, A. W. Ehler, L. S. Engelhardt, and S. J. Humphries, "Development of an Ion Source for the Heavy Ion Fusion MBE Injector," American Physical Society, Division of Plasma Physics, Boston, Massachusetts, October 29–November 1, 1984, Los Alamos National Laboratory document LA-UR-84-2274.

H. L. Rutkowski, H. Oona, E. A. Meyer, R. P. Shurter, R. S. Engelhardt, and S. Humphries, Jr., "Ion Source Development for the Los Alamos Heavy Ion Fusion Injector," Particle Accelerator Conference, Vancouver, Canada, May 13–16, 1985, Los Alamos National Laboratory document LA-UR-85-1584.

A. M. Sabbas, P. Dyer, and S. A. Wender, "Laser Spectroscopy of the Transition Nucleus ^{151}Sm," American Physical Society, Washington, D.C., April 23–26, 1984, Los Alamos National Laboratory document LA-UR-84-293.

E. T. Salesky, "Analysis of the Breakdown of the Long-Range Interaction Model for Pressure Broadening by Noble Gases," Spectral Lineshapes, Aussois, France, June 11–14, 1984, Los Alamos National Laboratory document LA-UR-84-945.

E. T. Salesky, "Calculation of Pressure Broadened Linewidths of CO_2 Due to Self-Broadening," Spectral Lineshapes, Aussois, France, June 11–14, 1984, Los Alamos National Laboratory document LA-UR-84-970.

E. T. Salesky, "Calculation of Pressure Broadened Linewidths of HCl(1-0) Perturbed by N_2, O_2 and CO Using the Semiclassical Theory of Leavitt and Korff," Spectral Lineshapes, Aussois, France, June 11–15, 1984, Los Alamos National Laboratory document LA-UR-84-969.

E. T. Salesky and W. D. Kimura, "Gain and Absorption Measurements of KrF Mixtures with High Kr Concentration," CLEO '85 on Lasers and Electro-Optics, Baltimore, Maryland, May 21–24, 1985, Los Alamos National Laboratory document LA-UR-84-3991.

E. T. Salesky and W. D. Kimura, "KrF Laser Extraction Measurements for High Kr Concentration Gas Mixtures," International Quantum Electronics Conference, Los Angeles, California, June 18–21, 1984, Los Alamos National Laboratory document LA-UR-84-1629.

E. T. Salesky and J. Kilkenny, "A Torodially Curved Crystal Spectrograph for Laser Plasma Measurement," 5th Topical Conference on High Temperature Plasma Diagnostics, Tahoe City, California, September 16–20, 1984.

D. Schiferl, A. I. Katz, R. L. Mills, L. C. Schmidt, C. A. Vanderborgh, E. F. Skelton, W. T. Elam, A. W. Webb, S. B. Qadri, and M. Schaefer, "Novel Instrument for High-Pressure Research at Ultra-High Temperatures," Xth AIRAPT High Pressure, Amsterdam, The Netherlands, July 8 11, 1985, Los Alamos National Laboratory document LA-UR-85-2362.

D. Schiferl, R. L. Mills, L. C. Schmidt, C. A. Vanderborgh, E. F. Skelton, W. T. Elam, A. W. Webb, L. C. Ming, J. Balogh, and M. H. Manghnani, "High-Pressure/High Temperature Diamond-Anvil Cell Capable of Uniform, Well-Characterized P-T Conditions with Pressures over 50 kbar at Temperatures up to 1200 C," Xth AIRAPT High Pressure, Amsterdam, The Netherlands, July 8 11, 1985, Los Alamos National Laboratory document LA-UR-85-781.

G. G. Schmitt and R. D. Dick, "Use of Corrtex to Measure Explosive Performance and Stem Behavior in Oil Shale Fragmentation Tests," Explosives & Blasting Technique, San Diego, California, January 28 February 1, 1985, Los Alamos National Laboratory document LA-UR-85-321.

T. J. Sedillo, J. C. Cobble, P. D. Goldstone, A. Hauer, G. Stradling, J. J. Chmielewski, G. E. Eden, I. V. Johnson, M. Richardson, and G. Gregory, "Transmission-Grating Spectrograph for 0.1-5 keV," American Physical Society, Division of Plasma Physics, San Diego, California, November 3 8, 1985, Los Alamos National Laboratory document LA-UR-85-3888.

P. A. Seeger, "An Overview of the Los Alamos Neutron Scattering Center," University of Texas, El Paso, April 7, 1986, Los Alamos National Laboratory document LA-UR-86-1214.

P. A. Seeger and M. J. Nutter, "Status of the Los Alamos Anger Camera," 8th Meeting of International Collaboration on Advanced Neutron Sources, Oxford, England, July 7 12, 1985, Los Alamos National Laboratory document LA-UR-85-2402.

P. A. Seeger, A. Williams, and J. Trewhella, "Design of the Low Q Diffractometer at Los Alamos," 8th Meeting of International Collaboration on Advanced Neutron Sources, Oxford, England, July 7 12, 1985, Los Alamos National Laboratory document LA-UR-85-2458.

R. L. Sheffield, J. S. Fraser, and A. H. Lumpkin, "Electron Beam Diagnostics for the Los Alamos FEL Oscillator Experiment," Linear Accelerator Conference, Darmstadt, West Germany, May 7 11, 1984, Los Alamos National Laboratory document LA-UR-84-92.

R. L. Shepherd, D. R. Kania, L. A. Jones, and M. D. Maestas, "Characteristics of a High Density Plasma Formed in a 20 μm-Diameter Capillary," American Physical Society, Division of Plasma Physics, San Diego, California, November 4 8, 1985, Los Alamos National Laboratory document LA-UR-85-2592.

R. L. Shepherd, D. R. Kania, L. A. Jones, and M. D. Maestas, "Experimental Studies of 10 μm-Diameter High Current Capillary Discharges in Polyurethane," American Physical Society, Division of Plasma Physics, Boston, Massachusetts, October 29 November 1, 1984, Los Alamos National Laboratory document LA-UR-84-2161.

R. L. Shepherd, D. R. Kania, L. A. Jones, M. D. Maestas, and K. A. Stetler, "Strongly Coupled Plasma Formed in a Polyurethane Capillary Discharge," Strongly Coupled Plasma Physics, Santa Cruz, California, August 4 9, 1986, Los Alamos National Laboratory document LA-UR-86-2115.

E. B. Shera, "Probing Nuclear Structure with Muons," 7th International Conference on Atomic Masses and Fundamental Constants, Darmstadt, West Germany, September 3 7, 1984.

E. B. Shera, V. M. Hoehn, P. Bergem, M. Boschung, T. Q. Phan, G. Piller, A. Ruetschi, L. A. Schaller, L. Schellenberg, and H. Schneuwly, "New Evaluation of Muonic X-Ray Energies in ^{208}Pb," International Conference on Particles and Nuclei, Heidelberg, Germany, July 30 August 3, 1984, Los Alamos National Laboratory document LA-UR-84-2013.

S. S. Shiah and J. K. Hoffer, "Optical Effects of the Gravitationally Induced Concentration Gradient in Tricritical ^{3}He^{4}He," Low Temperature Physics, Karlsruhe, West Germany, August 15 22, 1984, Los Alamos National Laboratory document LA-UR-84-944.

R. E. Siemon, W. T. Armstrong, R. R. Bartsch, R. E. Chrien, J. C. Cochrane, W. N. Hugrass, K. F. McKenna, D. J. Rej, J. L. Schwarzmeier, D. C. Barnes, R. W. Kewish, R. K. Linford, R. D. Milroy, C. E. Seyler, Jr., and R. L. Spencer, "Review of the Los Alamos FRX-C Experiment," IAEA Advances in Compact Toroid Research, Sidney, Australia, May 1985, Los Alamos National Laboratory document LA-UR-85-1706.

R. N. Silver, "Neutron Scattering Research at the WNR/PSR Facility," Neutron Scattering in the 90's, Juelich, Germany, January 14–17, 1985, Los Alamos National Laboratory document LA-UR-84-2330.

R. N. Silver, R. M. Brugger, A. Taylor, and G. Reiter, "Lattice Dynamical Information for Graphite Obtained from Deep Inelastic Neutron Scattering (DINS)," Materials Research Society, Boston, Massachusetts, November 26–30, 1984, Los Alamos National Laboratory document LA-UR-84-2710.

H. N. Simpson, J. A. Goldstone, and J. W. Hemsky, "Initial Increase, 'Peaking Effect,' in the Internal Friction of Copper Following Pulsed Neutron and Electron Irradiation," 8th International Conference on Internal Friction and Ultrasonic Attenuation in Solids, Urbana, Illinois, June 3–6, 1985, Los Alamos National Laboratory document LA-UR-85-1829.

S. Singer, "Excimer Lasers for Inertial Confinement Fusion," American Nuclear Society, New Orleans, Louisiana, June 3–8, 1984, Los Alamos National Laboratory document LA-UR-84-442.

S. Singer, "Recent Advances in Excimer Laser Systems for Inertial Confinement Fusion," CLEO '84, Anaheim, California, June 19–22, 1984, Los Alamos National Laboratory document LA-UR-84-2522.

S. Singer, "Recent Advances in KrF Systems Technology," CLEO '84, Anaheim, California, June 19–22, 1984, Los Alamos National Laboratory document LA-UR-84-738.

D. N. Sinha and J. K. Hoffer, "Maximum Supercooling in Liquid ^{3}He^{4}He Mixtures Near the Tricritical Point," Low Temperature Physics, Karlsruhe, West Germany, August 15–22, 1984, Los Alamos National Laboratory document LA-UR-84-904.

E. F. Skelton, W. T. Elam, T. L. Francavilla, S. B. Qadri, A. W. Webb, S. A. Wolf, and C.-Y. Huang, "High Pressure Studies of First and Second Order Transition at Cryogenic Temperature Using Synchrotron Radiation," Low Temperature Physics, Karlsruhe, West Germany, August 6–8, 1984, Los Alamos National Laboratory document LA-UR-84-1476.

I. Slaus, J. M. Lambert, P. A. Treado, T. A. Treado, F. D. Correll, R. E. Brown, and N. Jarmie, "Some Quasifree and Final-State Interactions in ^{2}H(t,pt)n Reactions at 18 and 24 MeV," American Physical Society, Washington, D.C., April 23–26, 1984, Los Alamos National Laboratory document LA-UR-84-249.

V. Smiley, B. M. Whitcomb, C. W. Colburn, L. Woo, and J. W. Ogle, "Multi-Mode Connector Evaluations," OFC/IGWO, Atlanta, Georgia, February 26–28, 1986, Los Alamos National Laboratory document LA-UR-85-3450.

J. L. Smith, Z. Fisk, J. D. Thompson, and J. O. Willis, "Actinides and Their Heavy Electrons," American Chemical Society, Anaheim, California, September 7–13, 1986, Los Alamos National Laboratory document LA-UR-86-1400.

J. C. Solem, L. C. Biedenharn, G. C. Baldwin, and K. Boyer, "Nuclear Excitation by Laser Driven Coherent Outer Shell Electron Oscillations," Laser Science, Dallas, Texas, October 1985, Los Alamos National Laboratory document LA-UR-85-2846.

J. E. Sollid and W. H. Reichelt, "Large Optical Components for 10.6 Micrometer Lasers," Optical Society of America, Monterey, California, April 16–20, 1984, Los Alamos National Laboratory document LA-UR-84-55.

S. H. Southworth, A. C. Parr, J. E. Hardis, and J. L. Dehmer, "Resonance Structure in the Vibrationally Resolved Photoelectron Branching Ratios and Angular Distributions of the $2\pi^{-1}$ Channel of NO," VUV Radiation Physics, Lund, Sweden, August 4–8, 1986, Los Alamos National Laboratory document LA-UR-86-1213.

K. P. Staudhammer, K. A. Johnson, G. A. Reeves, and L. R. Veeser, "Microstructural Analysis of Vapor Deposited Multilayer Laser Targets," American Vacuum Society, Albuquerque, New Mexico, April 12–19, 1984, Los Alamos National Laboratory document LA-UR-84-1064.

M. L. Stelts and P. J. Bendt, "24 KeV Neutron Beam at the Omega West Reactor," American Physical Society, Crystal Springs, Virginia, Spring 1985, Los Alamos National Laboratory document LA-UR-85-187.

G. J. Stephenson, Jr. and T. J. Goldman, "Color-Flavor-Spin-Space Correlations in Nuclei," American Physical Society, Washington, D.C., April 1984, Los Alamos National Laboratory document LA-UR-85-1263.

G. J. Stephenson, Jr. and T. J. Goldman, "Quark Tunnelling in Nuclei," American Physical Society, Washington, D.C., April 23–26, 1984, Los Alamos National Laboratory document LA-UR-84-251.

W. F. Stewart, "Refueling Considerations for Liquid-Hydrogen Fueled Vehicles," 5th Intersociety Cryogenics Symposium, New Orleans, Louisiana, December 9–13, 1984, Los Alamos National Laboratory document LA-UR-84-1490.

W. F. Stewart and J. A. Barclay, "Cryogen Liquefaction Using Magnetic Refrigeration," Hydrogen Storage Conversion and Safety, International Energy Agency Task VII Workshop, Toronto, Canada, July 12–13, 1984, Los Alamos National Laboratory document LA-UR-84-1600.

G. L. Stradling and J. Chmielewski, "X-Ray Transmission Grating Calibrations," 3rd Topical Meeting on Short Wavelength Coherent Radiation: Generation and Applications, Monterey, California, March 24–27, 1986; Optical Society of America, Washington, D.C., October 14–18, 1985, Los Alamos National Laboratory document LA-UR-85-4242.

R. Stringfield, R. R. Bartsch, H. A. Davis, and E. G. Sherwood, "Vacuum Pulse Conditioning and Risetime Sharpening on a Low ν/γ Multi-MeV Electron Beam Accelerator," 13th IEEE Conference on Plasma Science, Saskatoon, Canada, May 9–13, 1986, Los Alamos National Laboratory document LA-UR-86-535.

R. Stringfield, J. C. Cochrane, L. A. Jones, D. R. Kania, P. H. Y. Lee, R. Price, L. R. Veeser, R. J. Trainor, and E. Zimmermann, "Research in High Current Density Vacuum Opening Switches for Inductively Driven Imploding Plasma Experiments," Discharges & Electrical Insulation in Vacuum, Berlin, East Germany, September 24–28, 1984, Los Alamos National Laboratory document LA-UR-84-967.

R. Stringfield, J. C. Cochrane, P. H. Y. Lee, R. Price, J. D. Seagrave, R. J. Trainor, and L. R. Veeser, "Rail-Gun Opening Switch for Inductive Energy Storage and Power Multiplication for the HEDP Facility," American Physical Society, Division of Plasma Physics, Boston, Massachusetts, October 29–November 1, 1984, Los Alamos National Laboratory document LA-UR-84-2190.

J. K. Studebaker, D. W. Forslund, G. R. Magelssen, and D. R. Bach, "Low-Z Exploding Pusher Cylinders," American Physical Society, Division of Plasma Physics, San Diego, California, November 4–8, 1985, Los Alamos National Laboratory document LA-UR-85-2655.

D. M. Stupin, J. M. Williams, and G. T. Schappert, "X-Ray Measurement of Concentration of Metallic Atoms in Low Density Materials," 4th Target Fabrication Specialists, St. Petersburg, Florida, March 26–28, 1985, Los Alamos National Laboratory document LA-UR-85-359.

J. W. Sunier, M. R. Clover, R. M. DeVries, N. J. Digiacomo, J. S. Kapustinsky, P. L. McGaughey, and W. E. Sondheim, "Search for Antiproton-Nucleus States with the (p^-,p) Reaction Over ^{28}Si," American Physical Society, Washington, D.C., April 23–28, 1984, Los Alamos National Laboratory document LA-UR-84-352.

G. W. Swift, A. Migliori, T. Hofler, and J. C. Wheatley, "Intrinsically Irreversible Acoustic Heat Engines," Workshop on Solar Applications of Direct Energy Conversion Technology, Lakewood, Colorado, February 19, 1985, Los Alamos National Laboratory document LA-UR-85-634.

G. W. Swift, A. Migliori, and J. C. Wheatley, "Liquid Metal Thermoacoustic Engine," Acoustical Society of America, Cleveland, Ohio, May 13, 1986; 21st Intersociety Energy Conversion Engineering Conference, San Diego, California, August 25–29, 1986, Los Alamos National Laboratory document LA-UR-86-1548.

T. Tajima, W. Horton, K. Witte, and S. Singer, "Pump Depletion and Laser Staging for Beat-Wave Accelerator," Particle Accelerator Conference, Vancouver, Canada, May 13–16, 1985, Los Alamos National Laboratory document LA-UR-85-2361.

T. Tajima, K. H. Witte, and S. Singer, "Laser Staging for Beat Wave Accelerator," Particle Accelerator, Vancouver, Canada, May 5, 1985, Los Alamos National Laboratory document LA-UR-85-550.

R. L. Talage, D. A. Krakauer, R. C. Allen, Jr., V. Bharadwaz, G. A. Brooks, H. H. Chen, P. J. Doe, R. Hausammann, H. J. Mahler, A. M. Rushton, K. C. Wang, T. J. Bowles, R. L. Burman, R. D. Carlini, D. R. F. Cochran, J. S. Frank, E. Piasetzky, and V. D. Sandberg, "Observation of Electron Neutrino-Electron Elastic Scattering," American Physical Society, Santa Fe, New Mexico, October 31–November 3, 1984, Los Alamos National Laboratory document LA-UR-84-2780.

R. D. Taylor, "Diamond Anvil Cells A New Tool for High Pressure Studies," Lectures at Tel Aviv University, Israel, May 5, 1985, Los Alamos National Laboratory document LA-UR-85-1529.

R. D. Taylor, "Metastable Complexes of Helium-Hydrogen Isotopes," Low Temperature Physics, Karlsruhe, West Germany, August 15 22, 1984, Los Alamos National Laboratory document LA-UR-84-1088.

R. D. Taylor, "Mössbauer Effect Studies at Pressures to 300 kbar," Lectures at Tel Aviv University, Israel, May 2, 1985, Los Alamos National Laboratory document LA-UR-85-1569.

R. D. Taylor and J. N. Farrell, "Pressure Induced Valence Shift and Reduced Magnetic Moment in Europium Metal," Gordon Research Conference, Research at High Pressure, Meriden, New Hampshire, June 23–27, 1986, Los Alamos National Laboratory document LA-UR-86-2185.

D. R. Thayer, M. Graser, Jr., C. F. Virchow, C. Gallegos, R. Becker, and F. J. Leonberger, "Use of Ti-Indiffused Linbo 3 Interferometric Modulators for High Voltage Transient Measurements," OFC/IGWO '86, Atlanta, Georgia, February 26–28, 1986, Los Alamos National Laboratory document LA-UR-85-3336.

J. D. Thompson, "Effect of Pressure on Heavy-Fermion Systems," University of California, Irvine, November 17, 1984, Los Alamos National Laboratory document LA-UR-84-3510.

J. D. Thompson, "High Pressure Experiments on Heavy-Fermion/Mixed-Valence Compounds," Anomalous Rare Earths and Actinides, Grenoble, France, July 7 11, 1986, Los Alamos National Laboratory document LA-UR-86-2085.

J. D. Thompson, H. Borges, S. Horn, and R. D. Parks, "Evolution of the Structural Phase Transition in CeAg in the Low Pressure Range," International Conference on Magnetism, San Francisco, California, August 25–30, 1985, Los Alamos National Laboratory document LA-UR-85-986.

J. D. Thompson, H. Borges, and R. D. Parks, "Effect of Pressure on Neel Temperature of Kondo Lattice Systems," International Conference on Magnetism, San Francisco, California, August 25–30, 1985, Los Alamos National Laboratory document LA-UR-85-985.

J. D. Thompson, Y. Chen, Z. Fisk, and J. M. Lawrence, "Pressure Investigation of the New Kondo Lattice Systems Ce_3Sn, Ce_3In, Ce_3Al," Rare Earth Research Conference, Hamilton, Ontario, Canada, June 18–22, 1986, Los Alamos National Laboratory document LA-UR-86-1159.

J. D. Thompson, M. A. Edwards, S. Horn, and R. D. Parks, "Interplay of Crystal Field Effects and Fluctuations in $CeCu_2Si_2$ and Related Alloys," Crystalline Field and Anomalous Mixing Effects In f-Electron Systems, Sendai, Japan, April 15–18, 1985, Los Alamos National Laboratory document LA-UR-85-1015.

J. D. Thompson and Z. Fisk, "Relative Stability of Heavy-Fermion Ground States with Respect to Moderate Hydrostatic Pressure," Heavy Fermions, Argonne, Illinois, August 19–20, 1985, Los Alamos National Laboratory document LA-UR-85-2790.

J. D. Thompson, Z. Fisk, M. W. McElfresh, and J. O. Willis, "Electrical Resistivity and Magneto-Resistivity of UBe_{13} at Elevated Pressures," American Physical Society, Las Vegas, Nevada, March 31–April 4, 1986, Los Alamos National Laboratory document LA-UR-85-4122.

J. D. Thompson, Z. Fisk, and H. R. Ott, "Response of Uranium-Based Heavy-Fermion Magnets to Hydrostatic Pressure," Magnetism, San Francisco, California, August 26–30, 1985, Los Alamos National Laboratory document LA-UR-85-2162.

J. D. Thompson, Z. Fisk, and J. O. Willis, "Pressure-Dependent Resistive Behaviour of $YbBe_{13}$," 17th International Conference on Low Temperature Physics, Karlsruhe, West Germany, August 15–22, 1984.

J. D. Thompson and G. P. Meisner, "Pressure Dependence of the Electrical Resistivity and T_c of the Nearly-Heavy Fermion Superconductor U_2PtC_2," EPS— Electronic Structure and Properties of Rare Earth and Actinide Intermetallics, St. Polten, Austria, September 3–6, 1984, Los Alamos National Laboratory document LA-UR-84-1092.

J. W. Toevs, P. J. Kruse, and B. L. Freeman, "Fast, Simple DB/DT Probe," 4th International Conference on Megagauss Magnetic Field Generation, Santa Fe, New Mexico, July 14–17, 1986, Los Alamos National Laboratory document LA-UR-86-2413.

R. Varma, J. Eckert, J. A. Goldstone, V. A. Maroni, and C. Giordano, "Inelastic Neutron Scattering Study of β-PbO^2 Recent Results," International Society of Electrochemistry, Berkeley, California, August 5–10, 1984, Los Alamos National Laboratory document LA-UR-84-798.

R. Varma, J. Eckert, V. A. Maroni, J. A. Goldstone, C. Giardono, T. Cehelnik, R. Kumar, S. Siegel, and B. Tani, "Structural Studies on Lead Oxides," Electrochemical Society, New Orleans, Louisiana, October 7–12, 1984, Los Alamos National Laboratory document LA-UR-84-2729.

L. R. Veeser and G. W. Day, "Fiber Optic, Faraday Rotation Current Sensor," 4th International Conference on Megagauss Magnetic Field Generation, Santa Fe, New Mexico, July 14–17, 1986, Los Alamos National Laboratory document LA-UR-86-2084.

L. R. Veeser, R. S. Caird, Jr., D. J. Erickson, and C. M. Fowler, "Fiber Optic Sensor for Measuring Multimegampere Currents from Flux Compression Generators," SPIE Symposium & Instrument Exhibit, San Diego, California, August 22–24, 1985, Los Alamos National Laboratory document LA-UR-84-2344.

L. R. Veeser, G. I. Chandler, and G. W. Day, "Fiber Optic Sensing of Pulsed Currents," SPIE Advanced Institute Series on Broadband Photonic Sensors, Howey in the Hills, Florida, April 7–11, 1986, Los Alamos National Laboratory document LA-UR-86-1212.

L. R. Veeser, G. I. Chandler, G. W. Day, J. D. McFadden, and R. W. Cernosek, "Optical Fiber Sensors for the Measurement of Pulsed Electric Currents," AGARD, Ankara, Turkey, September 9–12, 1985, Los Alamos National Laboratory document LA-UR-84-3401.

P. J. Vergamini and H. R. Wenk, "Texture Analysis by TOF of Pulsed Neutrons," American Geophysical Union, San Francisco, California, December 3–7, 1984, Los Alamos National Laboratory document LA-UR-85-247.

V. K. Viswanathan, I. O. Bohachevsky, and T. P. Cotter, "Attempt to Develop an 'Intelligent' Lens Design Program," International Lens Design Conference, Cherry Hill, New Jersey, June 10–14, 1985, Los Alamos National Laboratory document LA-UR-85-2035.

V. K. Viswanathan, A. C. Saxman, and G. L. Woodfin, "Resonator Optical Designs for the High Energy Free Electron Lasers (FELS)," Quantum Electronics (IQEC), Anaheim, California, June 18–21, 1984, Los Alamos National Laboratory document LA-UR-84-514.

V. K. Viswanathan, G. Woodfin, P. Wolfe, V. Zeigner, and T. A. Swann, "Antares Reference Telescope System Results," SPIE Symposium East '84/Optical Alignment II, Arlington, Virginia, April 29–May 4, 1984.

P. Vorderwisch, F. Mezei, J. Eckert, and J. A. Goldstone, "Analysis of Inelastic Neutron Scattering Spectra from a Time-of-Flight Spectrometer with Filter Detector," Workshop on Neutron Scattering Data Analysis, Rutherford Appleton Laboratory, Didcot, England, March 13–14, 1986, Los Alamos National Laboratory document LA-UR-86-193.

R. F. Walter, P. D. Tannen, P. S. Laybourne, D. C. Gardner, and E. T. Salesky, "Staging Analysis of a 20-Kilojoule Krypton Fluoride Laser Amplifier System," Lasers '84, San Francisco, California, November 26–30, 1984, Los Alamos National Laboratory document LA-UR-84-2552.

W. K. Wang, S. A. He, P. Beijing, J. D. Boyer, and C.-Y. Huang, "Superconductivity and Phase Compositions in Annealed Amorphous Niobium-Silicon Alloys Under High Pressure," American Physical Society, Detroit, Michigan, March 26–30, 1984.

J. S. Wark, A. Hauer, and J. D. Kilkenny, "Studies of Subnanosecond X-Ray Switching and Shuttering Techniques," 6th Topical Conference on High-Temperature Plasma Diagnostics, Hilton Head Island, South Carolina, March 9–13, 1986, Los Alamos National Laboratory document LA-UR-86-67.

R. W. Warren, D. W. Feldman, W. E. Stein, B. E. Newnam, S. C. Bender, A. H. Lumpkin, R. A. Lohsen, B. D. McVey, J. C. Goldstein, and D. Chan, "Recent Results from the Los Alamos Free-Electron Laser," 8th International Free Electron Laser Conference, Glasgow, Scotland, September 1–5, 1986, Los Alamos National Laboratory document LA-UR-86-3009.

D. L. Weiss, R. A. Oliphant, Jr., J. D. Seagrave, R. Stringfield, and A. Wilson, "Ablative Closure in the Pioneer Series of Experiments at Los Alamos," 5th IEEE Pulsed Power Conference, Arlington, Virginia, June 10–12, 1985, Los Alamos National Laboratory document LA-UR-84-3896.

P. B. Weiss and L. Walling, "Comparison of Several Large Photocathode Electronic Streak Tubes," SPIE 30th Annual International Technical Symposium, San Diego, California, August 17–22, 1986, Los Alamos National Laboratory document LA-UR-86-921.

S. A. Wender, "White Neutron Source at WNR (Target-4) Construction Update," Nuclear Physics Laboratory Workshop, Los Alamos Meson Physics Facility, December 1985.

S. A. Wender and G. F. Auchampaugh, "Fast Neutron Capture with a White Neutron Source," 5th International Symposium on Capture Gamma-Ray Spectroscopy and Related Topics, Knoxville, Tennessee, September 10–15, 1984, Los Alamos National Laboratory document LA-UR-84-2711.

S. A. Wender, G. C. Baldwin, W. L. Talbert, and H. R. Reiss, "Predicted Changes in the Internal Conversion Rates of ^{119}Sn Due to Admixtures of Lower Multipole Order," International Conference on Laser Science, Dallas, Texas, November 18–22, 1985.

J. C. Wheatley, "Intrinsically Irreversible Acoustic Engines I," Frontiers in Physical Acoustics, Varenna, Italy, July 10–20, 1984, Los Alamos National Laboratory document LA-UR-84-2270.

J. C. Wheatley, "Intrinsically Irreversible Acoustic Engines II," Frontiers in Physical Acoustics, Varenna, Italy, July 10–20, 1984, Los Alamos National Laboratory document LA-UR-84-2271.

J. C. Wheatley, "Natural Engines," London Lecture Series, Duke University, Durham, North Carolina, March 13–14, 1984, Los Alamos National Laboratory document LA-UR-84-723.

J. C. Wheatley, "Natural Engines (Lecture 3)," Frontiers in Physical Acoustics, Varenna, Italy, July 10–20, 1984, Los Alamos National Laboratory document LA-UR-84-2272.

J. C. Wheatley, "Natural Engines—With Demonstrations," Ohio State University, November 27, 1984; University of Illinois, November 29, 1984, Los Alamos National Laboratory document LA-UR-84-3707.

J. C. Wheatley, "Nonlinear Natural Engines (Lecture 4)," Frontiers in Physical Acoustics, Varenna, Italy, July 10–20, 1984, Los Alamos National Laboratory document LA-UR-84-2273.

B. M. Whitcomb, R. L. Flurer, L. Woo, K. W. Toms, and J. W. Ogle, "Calibration System for Sub-100 ps Relative Timing," SPIE Optoelectronics and Fiber Optic Applications, Cambridge, Massachusetts, September 21–26, 1986, Los Alamos National Laboratory document LA-UR-86-1211.

J. B. Wilhelmy, C. Albiston, J. P. Bocquet, J. G. Boissevain, H. C. Britt, Y. D. Chan, R. L. Ferguson, A. Guessous, B. V. Jacak, P. Lysaght, G. Mamane, F. E. Obenshain, F. Plasil, C. Ristori, R. Schmidt, R. G. Stokstad, S. Wald, M. M. Fowler, A. I. Gavron, A. Gayer, and S. Gazes, "Saddle to Scission—Time Scales and Dissipative Mechanisms," American Chemical Society, Chicago, Illinois, September 1985, Los Alamos National Laboratory document LA-UR-85-1109.

J. F. Wilkerson, "Results from Tritium Beta Decay Experiments," Colloquium, Argonne National Laboratory, Chicago, Illinois, May 19, 1986.

J. F. Wilkerson, "The Determination of the Neutron Lifetime Using e-p Coincidence," Workshop on the Investigation of Fundamental Interactions with Cold Neutrons, National Bureau of Standards, Gaithersburg, Maryland, November 14–15, 1985.

J. F. Wilkerson, T. J. Bowles, J. C. Browne, T. H. Burritt, J. A. Helffrich, D. A. Knapp, M. P. Maley, R. G. H. Robertson, and M. L. Stelts, "Status of the Los Alamos National Laboratory Free Atomic Tritium Beta-Decay Experiment," American Physical Society, Washington, D.C., April 23–26, 1984, Los Alamos National Laboratory document LA-UR-84-187.

J. F. Wilkerson, T. J. Bowles, D. A. Knapp, M. P. Maley, and R. G. H. Robertson, "Los Alamos Free Molecular and Atomic Tritium Beta Decay Experiment," VIth Moriond Workshop on Massive Neutrinos in Particle Physics and Astrophysics, Tignes, France, January 25–February 1, 1986; International Conference on High Energy Physics, Berkeley, California, July 16–23, 1986, Los Alamos National Laboratory document LA-UR-86-1674.

A. Williams, "Amorphous/Liquids Diffraction—Can a General Purpose Powder Diffractometer Satisfy the Needs of the Glass Diffraction Community or Is a Dedicated Instrument Required?" Workshop on Advanced Neutron Powder Diffraction, Session 4, Amorphous/Liquids Diffraction, Los Alamos National Laboratory, May 19–21, 1986, Los Alamos National Laboratory document LA-UR-86-2580.

A. Williams, "Future Prospects for Powder Diffraction at LANSCE—How Far Can We Push the State of the Art at the Proposed Facility at LANL?" Workshop on Advanced Neutron Power

Diffraction, Session 4, Los Alamos, New Mexico. May 19–21, 1986, Los Alamos National Laboratory document LA-UR-86-2579.

J. O. Willis, Z. Fisk, and J. D. Thompson, "Effect of Pressure on the Heavy Fermion Superconductor UPt_3," 1984 Gordon Conference—Research at High Pressure, Meriden, New Hampshire, June 25–29, 1984, Los Alamos National Laboratory document LA-UR-84-1742.

J. O. Willis, J. D. Thompson, J. L. Smith, and Z. Fisk, "Magnetoresistance and Upper Critical Magnetic Field of Uranium Beryllium (13) Under Pressure," Anomalous Rare Earths & Actinides, Grenoble, France, July 7–11, 1986, Los Alamos National Laboratory document LA-UR-86-2137.

D. C. Wilson, K. B. Riepe, E. O. Ballard, E. A. Meyer, R. P. Shurter, F. W. Van Haaften, and S. Humphries, Jr., "Progress on the Los Alamos Heavy-Ion Injector," Heavy Ion Fusion, Washington, D.C., May 27–29, 1986, Los Alamos National Laboratory document LA-UR-86-1867.

M. S. Wire, J. D. Thompson, and Z. Fisk, "Electrical Resistivity at High Pressures and Low Temperatures of UAl_2 and UPt_3," American Physical Society, Detroit, Michigan, March 26–30, 1984.

S. A. Wolf, C.-Y. Huang, P. M. Chaikin, W. W. Fuller, R. C. Lacoe, and H. L. Luo, "Role of Pressure in Understanding the Anomalous Superconductivity in $EuMo_6S_8$," AIME, Los Angeles, California, February 29–March 1, 1985, Los Alamos National Laboratory document LA-UR-84-450.

G. L. Woodfin, V. K. Viswanathan, and J. R. Parker, "Performance Evaluation of the Antares Reference Telescope System," Southwest Conference on Optics, Albuquerque, New Mexico, March 4–8, 1985, Los Alamos National Laboratory document LA-UR-84-3263.

G. J. Yates, J. J. Bujnosek, S. A. Jarmillo, R. B. Walton, T. M. Martinez, and J. P. Black, "Radiation Effects on Video Imagers," IEEE Nuclear Science Symposium, San Francisco, California, October 23–25, 1985, Los Alamos National Laboratory document LA-UR-85-3803.

G. J. Yates, D. L. Dunbar, S. A. Jaramillo, P. Nedrow, and D. Esquibel, "Gated SIT Vidicon Streak Tube," SPIE Technical Symposium, San Diego, California, August 18–23, 1985, Los Alamos National Laboratory document LA-UR-85-675.

M. A. Yates, S. C. Evans, and J. D. Gallagher, "Nuclear Activation Proton Calorimeter," American Physcial Society, Division of Plasma Physics, San Diego, California, November 3–8, 1985, Los Alamos National Laboratory document LA-UR-85-2689.

G. J. Yates, S. A. Jarmillo, T. S. Pagano, and J. P. Black, "Shuttering Efficiencies of Nanosecond-Gated Photoemissive Shutter Tubes," SPIE's 29th Annual International Technical Symposium, San Diego, California, August 18–23, 1985, Los Alamos National Laboratory document LA-UR-85-2743.

G. J. Yates, S. A. Jaramillo, M. Thomas, and P. A. Zagarino, "Stripline MCPTs for Subnanosecond Optical Gating Applications," SPIE International Technical Symposium, San Diego, California, August 18–23, 1985, Los Alamos National Laboratory document LA-UR-86-1735.

G. W. York, S. J. Czuchlewski, L. A. Rosocha, and E. T. Salesky, "Energy Extraction and Gain Measurements on the Los Alamos Large Aperture Krypton Fluoride Laser," Lasers '84, McLean, Virginia, November 27–29, 1984, Los Alamos National Laboratory document LA-UR-84-3346.

G. W. York, S. J. Czuchlewski, L. A. Rosocha, and E. T. Salesky, "Performance of the Large Aperture Module of the Aurora KrF Laser System," CLEO '85 on Lasers and Electro-Optics, Baltimore, Maryland, May 21–24, 1985, Los Alamos National Laboratory document LA-UR-84-3938.

G. W. York and F. D. Feiock, "Physics of Large Aperture KrF Lasers," Lasers '85 Conference, Las Vegas, Nevada, December 1985, Los Alamos National Laboratory document LA-UR-85-4424.

C. B. Zimm and J. A. Barclay, "Measurement of the Adiabatic Temperature Change in Ferromagnetic Intermetallic Compounds," Magnetism and Magnetic Materials, San Diego, California, November 27–30, 1984, Los Alamos National Laboratory document LA-UR-84-2155.

J. D. Zumbro, C. E. Bemis, M. V. Hoehn, R. A. Naumann, W. Reuter, E. B. Shera, and Y. Tanaka, "Precision Muonic-Atom Determinations of the Charge Parameters for $^{233,234,235,238}U$," American Physical Society, Washington D.C., April 23–26, 1984, Los Alamos National Laboratory document LA-UR-84-284.

J. D. Zumbro, M. V. Hoehn, A. R. Kunselman, and E. B. Shera, "Measurement of the Pionic 3D 2P X-Ray Transition in $^{54,56}Fe$, ^{59}CO, and $^{38,60,61,62,64}Ni$," American Physical Society, Washington, D.C., April 24–27, 1985, Los Alamos National Laboratory document LA-UR-85-893.

J. D. Zumbro, M. V. Hoehn, R. A. Naumann, W. Reuter, E. B. Shera, and Y. Tanaka, "Precision Muonic-Atom Determinations of the Charge Parameters for ^{232}Th and ^{239,240,242}Pu," American Physical Society, Washington, D.C., April 24–27, 1985, Los Alamos National Laboratory document LA-UR-85-202.

PATENTS

H. L. Anderson, W. W. Kinnison, and J. W. Lillberg, "Apparatus for Reading Two-Dimensional Electrophoretograms Containing β-Ray-Emitting Labeled Compounds," filed April 30, 1985; allowed January 14, 1987.

E. O. Ballard, "Purged Window Apparatus Utilizing Heated Purge Gas," U.S. Patent No. 4,443,072, April 17, 1984.

J. A. Barclay, "Low-Temperature, Magnetic Refrigerator," U.S. Patent No. 4,507,927, April 2, 1985.

J. A. Barclay, "Magnetic Refrigeration Apparatus with Heat Pipes," filed October 25, 1985.

J. A. Barclay, "Rotary Multiposition Valve," U.S. Patent No. 4,553,566, November 19, 1985.

C. A. Ekdahl, "Capacitively-Coupled Inductive Sensors," U.S. Patent No. 4,438,394, March 20, 1984.

C. A. Ekdahl, "High Power Microwave Generator," U.S. Patent No. 4,596,967, June 24, 1986.

T. Hofler, J. C. Wheatley, G. W. Swift, and A. Migliori, "Acoustic Cooling Engine," allowed September 1986.

C.-Y. Huang, "Four-Wave Light Mixing Gaussmeter," authorized November 21, 1985.

R. J. Jensen, "Apparatus and Method for Laser-Induced Isotope Separation," filed February 9, 1984.

R. J. Jensen, "Photochemical Isotope Separation," filed December 23, 1985.

D. R. Kania and E. L. Zimmermann, "Fast Shutter Apparatus," U.S. Patent No. 4,515,173, May 7, 1985.

A. Migliori and G. W. Swift, "Feedback Regulated Induction Heater for a Flowing Fluid," U.S. Patent No. 4,560,849, December 24, 1985.

A. Migliori, G. W. Swift, and S. L. Garrett, "Remotely Readable Fiber Optic Compass," U.S. Patent No. 4,577,414, March 25, 1986.

W. C. Overton, Jr., "Apparatus and Method for Detecting a Magnetic Anomaly Contiguous to Remote Location by SQUID Gradiometer and Magnetometer Systems," U.S. Patent No. 4,437,064, March 13, 1984.

W. C. Overton, Jr., W. F. Stewart, and J. A. Barclay, "Magnetic Refrigeration Apparatus and Method," U.S. Patent No. 4,459,811, July 17, 1984.

E. B. Shera, "Device to Resolve and Identify Proteins," reactivated October 15, 1984.

W. F. Stewart and J. A. Barclay, "Magnetic Refrigeration Apparatus with Belt of Ferro or Paramagnetic Material," filed April 3, 1986.

G. W. Swift, A. Migliori, and J. C. Wheatley, "Microchannel Crossflow Fluid Heat Exchanger and Method for its Fabrication," U.S. Patent No. 4,516,632, May 14, 1985.

T. H. Tan and A. H. Williams, "Apparatus for Recording Emissions from a Rapidly Generated Plasma from a Single Plasma Producing Event," U.S. Patent No. 4,542,290, September 17, 1985.

D. S. Warren and M. E. Thuot, "Prefire Identification for Pulse Power Systems," U.S. Patent No. 4,510,451, April 9, 1985.

J. C. Wheatley, G. W. Swift, A. Migliori, and T. Hofler, "Heat-Driven Acoustic Cooling Engine Having No Moving Parts," allowed September 1986.

J. C. Wheatley, G. W. Swift, and A. Migliori, "Intrinsically Irreversible Heat Engine," U.S. Patent No. 4,489,553, December 25, 1984.

J. C. Wheatley, G. W. Swift, and A. Migliori, "Method of Measuring Reactive Acoustic Power Density in a Fluid," U.S. Patent No. 4,538,464, September 30, 1985.

J. C. Wheatley, G. W. Swift, and A. Migliori, "Thermoacoustic Magnetohydrodynamic Electrical Generator," U.S. Patent No. 4,599,551, July 8, 1986.

S. K. Wilson, "Heat Sink Configuration for Printed Circuit Assembly," filed September 11, 1984.